THE DAMARA MOBILE BELT
IN THE
SOUTH-WESTERN KAOKOVELD
SOUTH WEST AFRICA

by

P. GUJ

Thesis submitted in fulfilment of the requirements
for the degree of Ph.D.

University of Cape Town
1970

THE DAMARA MOBILE BELT IN THE SOUTH-WESTERN KAOKOVELD

ABSTRACT

After the establishment of the N-S Andib-Ganamub trough, the ubiquitous Lower Nosib subarkose was succeeded in the west by the Upper Nosib greywacke which indicates that orthogeosynclinal subsidence was already active in pre-Damara times.

A pulse of NNE folding (F_1N) concluded this sedimentary cycle and was accompanied by amphibolite-grade metamorphism (M_1), occasional migmatisation (A_1), and later feldspar blastesis. This episode was most intense in the west, so that the overlying Damara rocks paraconformable in the east, are unconformable there.

Martin's (1965) separation of the succeeding Damara basin into a western eugeosyncline and an eastern miogeosyncline applies very well to this area, though the separating hinge-line appears to have been located farther to the west (±80 Km) of the Kamanjab inlier, along the western flank of a N-S geanticlinal belt.

The Lower Hakos semipelite and lenticular carbonate, thinning out against the eastern flank of this positive element controlling the deposition, may, prior to deformation, have created a transition between the western eugeosynclinal greywacke and the eastern miogeosynclinal Lower Otari carbonates.

The fractured hinge-zone provided channels for the ascent of syndepositional intrusions and volcanics.

Regional erosion following upwarping in the east caused a large influx of detritus into the Khomas furrow prior to the disconformable deposition of the Tillite Substage, which is the only reliable chronostratigraphic link between the base of the Upper Otavi and that of the Upper Hakos Series, the latter partially intertongueing with the succeeding Khomas Series.

Gravitational creeping of the miogeosynclinal carbonates down the western slope of the upwarped Kamanjab inlier towards the sinking basin, produced the first folding (F_2O) in the east. Almost contemporaneously, buoyant uplifting forces, related to anatexis (A_2) along the axis of the eugeosyncline, created slopes sufficient to convey nappes (F_2S) of scarcely metamorphosed Damara schists towards the eastern foreland, overriding the miogeosyncline along the N-S Sesfontein Thrust. Eastern foredeeps were rapidly filled by the Mulden molasse. Steep slip folding (F_2S and F_4) in the cores and roots, and the formation of scattered domes at depth, controlled the successive structural evolution of the nappes. Large-scale axial undulations were later produced by orthogonally superposed F_3 folds striking east.

The Damaran metamorphism (M_2), which outlasted deformation, has a Barrovian character and grades in the Damara sediments from amphibolite (sillimanite) grade in the west to greenschist (sericite-chlorite) grade in the east.

In the previously dehydrated, deformed and metamorphosed,

polymetamorphic (M_1/M_2) Nosib terrains, retrograde parageneses and transition granulites developed to the east and to the west of the Damaran hornblende-oligoclase isograd respectively.

The Damaran tectono-thermal episode culminated in advanced migmatisation of the Khomas greywacke (possibly equivalent to the Salem granite-gneiss) and final anatexis (A_2) in the late-kinematic Ganias -Uhima (possibly equivalent to the Donkerhoek) granite, followed by widespread feldspar blastesis.

The drop in rheomorphism in the deformed mass at the margin of the migmatite zone induced intense shearing and produced belts of mylonite and cataclastic gneiss.

At a later stage, the Sesfontein Thrust was buffered against the Otavi dolomite relief and its speed of advancement reduced to match that of the erosion of its frontal toe, which now separates two completely different structural-stratigraphic domains:

i) an eastern miogeosynclinal, feebly metamorphosed and volcanic-free domain (Damara System, Outjo Facies) deformed into non-basement-involving tectonites, overridden by

ii) a western domain of suprastructural nappes and metamorphosed eugeosynclinal sediments (Damara System, Swakop Facies) deformed in response to basement-involving tectonic processes promoted by deeply seated anatexis along the axis of the former eugeosyncline.

The present model involves many stratigraphic revisions, one of the most important being that no rocks older than the Nosib Formation outcrop in the area and possibly along most of the Damara mobile belt in the western Kaokoveld.

CONTENTS

CONTENTS OF POCKET

Sheet 1913A (Hoanib)
Sheet 1913B (Sesfontein)
Sheet 1813C (Gomatum)
Stratigraphic Legend
Structural Sections

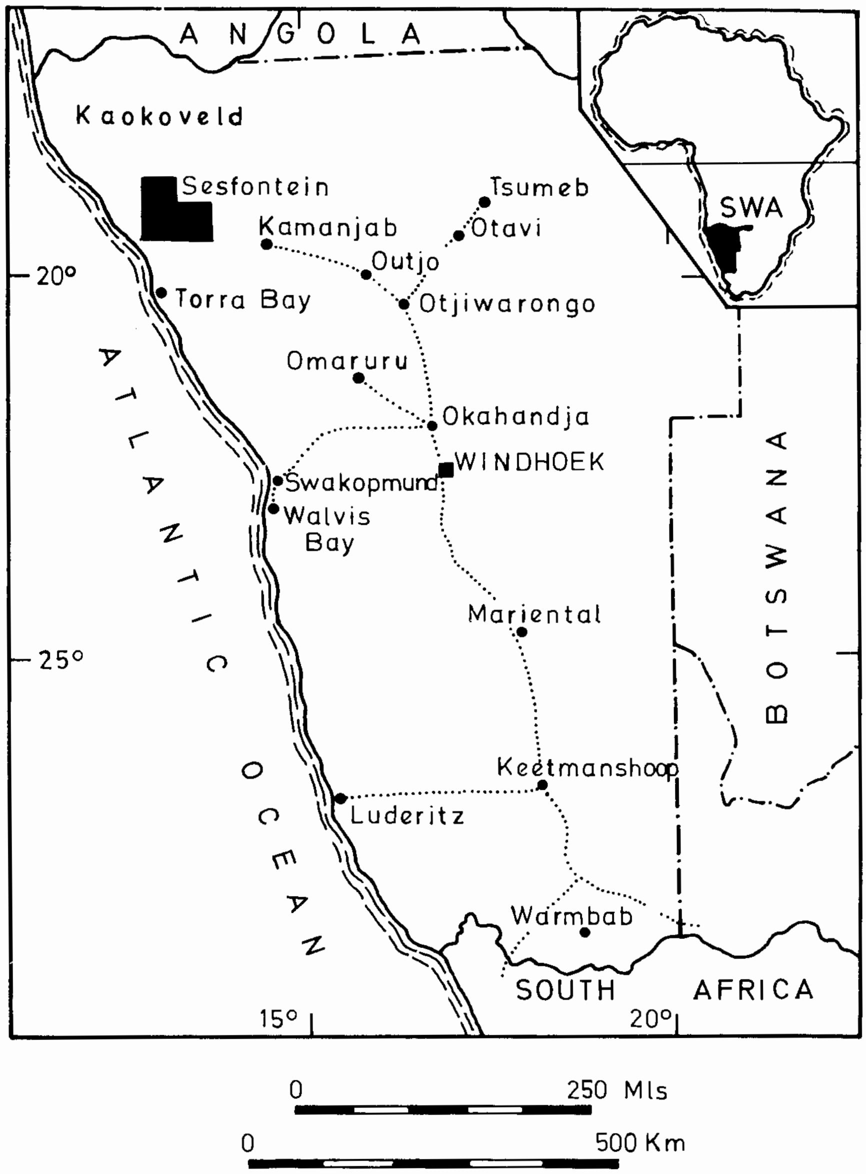

Figure 1. Location and extent of the area investigated

THE DAMARA MOBILE BELT IN THE SOUTH-WESTERN KAOKOVELD

SOUTH WEST AFRICA

I. INTRODUCTION

A. GENERAL

Mineral exploration, so intense over the rest of South West Africa during the last two decades, has not spread to the Kaokoveld, due to a variety of geographical, historical and climatic factors. As a result, fundamental unsolved regional problems are still numerous in this wild and scarcely populated region. The present research is intended to bridge one of these gaps, namely the extent and structural evolution of the Damara mobile belt in the south-western Kaokoveld.

Logistic difficulties were encountered due to scarcity of roads or tracks, which hampered fieldwork, whereas the extremely arid landscape and the scarce mountain or riverine savanna vegetation created ideal conditions for preliminary photogeological interpretation.

During three years of fieldwork, carried out for the Geological Survey (South West Africa Administration), approximately 8,000 Km^2 of the territory surrounding the village of Sesfontein were mapped at a scale of 1:125,000. This area covers the western part of the Etosha Game Reserve from the coastal Namib Desert (longitude 13°00'E) to the Hundskopf Hills (longitude 14°00'E) between latitude 18°45' and 19°30'S (fig. 1).

Data compilation and final preparation of the manuscript for publication were completed during one year spent in the Precambrian Research Unit attached to the Geology Department of the University of Cape Town, where the author had the privilege of being granted a post-graduate scholarship.

B. PREVIOUS WORK

No specific publication deals with any aspect of the geology of the area and adjoining territories. The regional interpretation, appearing on the Geological Map of South West Africa at a scale of 1:1,000,000 (1963), is essentially based on the unpublished reports of the Kaokoveld Exploration Company (Rabie et al., 1949) and Bethlehem Steel Corporation (Rabie, 1954), integrated by reconnaissance traverses by Martin (1965).

Since the beginning of the century, a substantial distinction has been made between the calcareous and feebly metamorphic Otavi System (Bembe System of Angola) and the unconformably underlying, undifferentiated primitive or fundamental crystalline complex (Hermann, 1908; Kuntz, 1913; Stahl, 1926, 1940). Only later was the Damara System (Chella System of Angola) delineated within the basement (Gevers, 1932; Beetz, 1933) as a separate and possibly younger entity, locally named the Andib System (Rabie et al., 1949).

After the Second World War, Martin (1950) discovered a lateral transition between the Damara and the Otavi System. The implication of synchronous deposition deprived the "Archaean Basement" of its Damara episode. Damara System is now a well-accepted term indicating these two heteropic facies in general. The western, highly deformed and metamorphosed clastic sequence, called the Swakop Facies (formerly the Damara System sensu stricto) represents the thick filling of a eugeosyncline. The calcareous, gently folded, practically unmetamorphosed, eastern Outjo Facies (formerly the Otavi System) is deemed to be formed in the adjoining miogeosyncline. Gevers and Frommurze (1929), Smith (1965) and Martin (1965) in disagreement with the Geological Survey (Nel, 1954), postulated uninterrupted sedimentation between the Damara System and the underlying Nosib Formation, which they regarded as the basal clastics of the sequence.

C. THE PROBLEM

Reconnaissance traverses carried out in the western Kaokoveld between 1963 and 1966 by Martin and de Villiers, and by the author accompanying the latter, revealed problematic antiforms of Nosib rocks completely surrounded by gneiss, traditionally accepted as basement. Only extremely involved structural explanations could account for the obvious stratigraphic paradox.

Sparse, apparently anomalous K/A radiometric dating along the Hoanib and Hoarusib Rivers (Clifford, 1967) also did not seem to fit easily with the previous interpretation of this granitised belt (Official Geological Map of South West Africa, 1963), based of necessity on insufficient field-evidence. Dating diastrophisms, however, might not clarify the stratigraphy of extensive polymetamorphic terrains. Basement rocks can be positively identified only if complete "welding" or "cratonisation" has, as to the east of the area, prevented successive deformation during following orogenies. The Damaran (550-450 My) isotopic age of some of the metamorphites west of Sesfontein might be the stigma of the last "homogenising" (Newton, 1968) tectono-thermal episode on rocks bearing completely different geological histories. A world-wide "shrinking" of elastic and undefined "Archaean

Complexes", with the possible exception of the Lewisian metasediments at Scardroy, Ross-shire, Scottish Highlands (Sutton, in Clifford, 1960), seems to have followed the detailed structural analyses of previously misinterpreted granitised belts.

The Sesfontein region was selected as the most suitable to unravel the structural-stratigraphic setting in the Kaokoveld because a transition from slightly metamorphosed and stratigraphically well-defined Damara terrains into granitised metasediments, traditionally accepted as basement, occurs here. As Martin (1965, p.9) commented: "This area with its excellent exposures could form a rewarding subject for a structural study".

The first approach was to define the geometry of these tectonites, purposely avoiding any geochronologic or lithostratigraphic preconceptions. The detail and scale of investigation were adapted to the complexity of the various problems, which can be grouped as follows:

i) Substantial revision of the stratigraphy of the western Kaokoveld.
ii) Distinction of the various phases of deformation and metamorphism, their chronological relation and mechanical characteristics.
iii) Combination of all available evidence into a model of evolution of the Damara mobile belt.

The validity of the proposed interpretation was then tentatively extended by means of reconnaissance traverses in more northerly regions, as far as the Kunene River (de Villiers, 1968), where additional evidence is at present being gathered by other members of the Geological Survey.

D. THE STRUCTURAL-STRATIGRAPHIC DOMAINS

An extensive, low-angle thrust with NNW strike, (hereinafter called the Sesfontein Thrust) bisects the study-area, giving two distinct structural-stratigraphic domains:

<u>The eastern domain</u> (sheet 1913B (Sesfontein)) is occupied by the Outjo (miogeosynclinal) Facies of the Damara System, which is not to be found west of the Sesfontein Thrust.

<u>The western domain</u> which is composed of metasediments belonging to the Swakop (eugeosynclinal) Facies of the Damara System, occupies sheets 1813C (Gomatum); 1913A (Hoanib) and part of 1913B (Sesfontein). No rocks related to this sequence outcrop east of the thrust.

This conspicuous natural subdivision is retained in the description. The evolution of both these structural-stratigraphic domains and of the Sesfontein Thrust will be discussed in the concluding chapters since the events involved were geologically synchronous and interacting.

The South African stratigraphic classification, as reviewed by Verwoerd (1964), is retained for the sake of uniformity. The ambiguous term "Formation" has been interposed between "System" and "Series" in the stratigraphic column, so as to advocate its substitution with either of them, once a satisfactory stratigraphy has been established in South West Africa.

E. ACKNOWLEDGMENTS

The writer is indebted to Dr. W.L. van Wyk, who in his capacity as Assistant Director of the Geological Survey at Windhoek suggested this project in the first instance and made it possible through generous technical and financial support.

Deep gratitude is due to: Prof. J. de Villiers, Director of the Precambrian Research Unit of the University of Cape Town, for his guidance, constructive criticism, for a Chamber of Mines postgraduate scholarship and for having edited the present paper; Dr. F.C.M. Mathias and Mr. J.H.W. Ward for suggestions and critical review of the section on metamorphism; Dr. J.J. Gurney and Mr. J.P. Willis for the chemical analysis and Mr. R.V. Danchin for the Fe determinations; Mr. A.R. Newton for his suggestions and constructive criticisms throughout the preparation of the manuscript; finally to my wife Luisa for many tedious hours of typing of the first draft and to Mrs. P. Rand for the final typescript.

II. THE EASTERN STRUCTURAL-STRATIGRAPHIC DOMAIN

A. GEOGRAPHIC DISTRIBUTION

The domain covers two distinct physiographic regions:

i) A massive karst mountainland exceeding 1600 m above m.s.l., which bounds the area to the north and the east. Limitation of superficial drainage and consequent erosion due to rain "swallowing" in solution fretworks, channels and sinkholes (Guj, 1968) enhanced the massiveness of this highland which greatly contrasts with the intensely degraded

ii) southern lowveld dissected by dendritic drainage into scattered hills with a summit level 700-900 m above m.s.l..

To the south, the Precambrian sediments are concealed below the Lower Cretaceous (Siedner and Miller, 1968) Etendeka Basaltic Plateau, extending uninterruptedly over more than 160 Km with a summit level exceeding 1400 m above m.s.l.. Scattered isolated mesas provide a record of its original extension.

All the surface water drains to the Atlantic Ocean by the Hoanib River, which occupies deep superposed gorges across the karst highveld and is bedded on its own extensive alluvial plains (third order of terraces (Guj, 1969)) through the southern lowveld.

B. STRATIGRAPHY AND LITHOLOGY

A typical later Precambrian, feebly metamorphosed and locally volcanic-free, miogeosynclinal sequence is developed in the area east of the Sesfontein Thrust. This is composed of three major sedimentation cycles, characterised by extremely different and regionally persistent lithostratigraphic associations (Krumbein and Sloss, 1963), which are from the top:

iii) The Mulden greywacke association : Mulden Formation (Mn)

ii) The Otavi carbonate association : Otavi Series (D_1) (Outjo Facies, Damara System)

i) The Nosib arkosic association : Nosib Formation (Ns)

1. The Nosib Arkosic Association (NsQ)

This massive, rather homogeneous, psammitic succession unconformably overlies the basement metasedimentary and granitoid rocks of the Kamanjab inlier in the Hundskopf Hills to the east of the area. Its extremely variable thickness locally exceeds 1000 m. A rather thick, even bedding is normally found in its basal blanket (Krumbein and Sloss, 1963). Stratification, however, becomes coarser upwards or is replaced by cross-bedding. Pink to brownish weathered, pale-brown to grey, generally feldspathic quartzite, arkose and grit constitute its bulk. Moderately sorted, well rounded monogenetic vein-quartz and quartzite pebbles commonly form bands and lenses or are dispersed throughout this arkosic wedge.

2. The Otavi Carbonate Association (D_1)

A full development of over 1500 m in thickness is attained only in the north-eastern corner of the area, where these sediments follow the Nosib clastics paraconformably. Southwards the lowermost members either progressively pinch out in a transgressive overlap (Martin, 1965) or have been eroded. The highest members can, therefore, lie on any of the older ones, on the Nosib and farther east directly on the basement.

Where sedimentation was continuous, the Otavi Series can be farther subdivided into two stages.

The Lower Stage (D_1l) is composed of whitish shale and siltstone (D_1lS) intercalated with increasingly frequent, light-coloured finely crystalline, intraclastic dolomite (Folk, 1959). This, eventually, forms a persistent and rather thick, occasionally cherty member (D_1lC). Some of the thinly laminated rocks, however, proved to be phyllonites.

The Upper Stage (D_1u) follows discordantly. Its base is marked by reddish-brown or grey feldspathic quartzite, grit and polygenetic puddingstone, showing ripple marks and cross-bedding. The lithoclasts and grains are poorly to moderately sorted, but, as a rule, well rounded. These are topped by unsorted and angular polygenetic, rudaceous material of glacio-marine derivation (Martin, 1965), embedded in a ferruginous marly or shaly matrix. Iron is occasionally concentrated in scattered lenses of low-grade ore. This coarse Tillite Substage (D_1uG) was preceded by the development of rare isolated bioherms and followed by coalescent dolomitic stromatolite reefs (D_1uC_1). Dark, percussion-fetid, massive dolomitic biolithite (Folk, 1959) and coarse, angular, dolomitic sedimentary breccia compose this member. Decreasingly frequent heteropic bodies of dark bluish, unstratified biolithite are intercalated at the base of the overlying light-coloured biostromal dolomite, to disappear completely higher in the sedimentary sequence. Several hundred metres of thinly and evenly bedded, grey cherty dolomitic micrite (D_1uC_3) (Folk, op. cit.), resting on a ubiquitous marker of white or pale rose calcareous or dolomitic micrite (D_1uC_2), completes the stage. Subordinate thin intercalations of light grey siltstone or fine-grained sandstone were observed toward the top of the succession in the Khowarib area.

3. The Mulden Greywacke Association (Mn)

The bulk of this monotonous succession, which overlies the Otavi Series unconformably, is composed of greenish-grey (rarely purplish) phyllite and silty phyllite (MnS), grading into, intertongueing with or overlain towards the south-west by occasionally cross-bedded feldspathic quartzite and greywacke. Thin intraformational bands or lenses of monogenetic, poorly sorted and rounded dolomitic conglomerate (MnR) and dolomite (MnC) are interbedded within the phyllite.

The original thickness cannot be evaluated because of folding, thrusting and concealment of the topmost members under the Etendeka plateau-basalt to the south. Several hundred metres (>600 m) of clastics, however, are still exposed in the area south of Sesfontein and Warmquelle.

The stratigraphic succession for the eastern domain is shown schematically in folder 1.

C. STRATIGRAPHIC ANALYSIS OF THE DAMARA MIOGEOSYNCLINE

There is no particular problem in establishing regional correlations with similar lithostratigraphic units developed over most of the crescent forming the eastern Damara (Outjo Facies) miogeosynclinal belt (Söhnge, 1961; Smit, 1962; Rabie, in Martin, 1965). The Tillite Substage, however, is possibly the only isochronous marker, because this unit results from paleoclimatic conditions which are likely to have affected very large areas contemporaneously.

On a smaller scale, significant changes in depositional environments (i.e. at the base of the Otavi Series and of the Mulden Formation) cause major isopic associations to diversify into minor, generally heteropic members diagrammatically summarised in folder 1.

1. The Nosib Sedimentary Cycle

In proximal (cratonic) margins, the thickness and geometry of the Nosib clastics are extremely variable due (Martin, 1965) to the progressive filling of discontinuous basins in the encroached pre-Nosib landscape, with the creation of the major (U^1) unconformity exposed all over the country. In more distal areas, however, thickness differences in the order of 5000 m (Rabie, 1954, in Martin, 1965) would correspond to an excessive pre-Nosib topographic relief for what, 150 Km to the south-east in the Huab-Welwitschia area (Frets, 1969), appears as an intensely degraded landform approaching peneplanation. Consequently some of the embayments flooded and sand-filled by the transgressing Nosib sea must have started subsiding actively and independently at quite an early stage to justify the high thickness-gradient (Beloussov, 1963).

During this process embryonic basins located increasingly farther east were probably successively "captured" into the developing miogeosyncline. From folder 1 it is obvious that during this marine incursion the Nosib-basement (U^1) unconformity underwent a progressive westward tilt generated by the difference in subsidence between two points along the roughly east-west line of section.

The original lenticular shape of most of the Nosib and basal Damara members could have been enhanced by differential compaction along the western flank of the crystalline and uncompressible, "buried" Kamanjab inlier (Powers, 1926; Nevin, 1936; Beloussov, 1963).

Moreover, if the lenticular shape were exclusively a landform cast, as is the case at the Ruacana Falls occurrence described by Martin (1965, p.27), conspicuous cross-bedding would be expected in the lowermost members and even stratification towards the top when infilling was almost complete. Opposite features, however, are exposed to the east of the area along the Otjovasandu-Sesfontein road. Thickly but evenly bedded psammites form the basal blanket, followed by a more massive or strongly cross-bedded, conglomeratic arkosic wedge.

2. The Lower Otavi Sedimentary Cycle

As islands became smaller or distant and a veneer of sediment was laid over most of the elevated pre-Nosib landforms (e.g. the Kamanjab inlier) coarse clastics became extremely scarce. Pelitic sedimentation in lagunal basins, probably bordered by the first biohermal reefs accompanied locally a pause in subsidence. Calcarenitic intercalations, exposing allochemical ghosts of intraclasts (Folk, 1959) and oölites, indicate a subsequent slow or oscillatory subsidence and deepening leading to gradual transgression. Intense winnowing of the sediments and rapid removal of H_2S are suggested also by the whitish colour typical of many back-reef environments (Ginsburg, 1957).

The undisturbed sedimentation of the well-stratified,

DIAGRAMMATIC STRATIGRAPHIC ANALYSIS OF THE EASTERN (OUTJO FACIES) DOMAIN

MULDEN	700 m	GREYWACKE ASSOCIATION	Non- marine (molasse)	Well-stratified, rarely cross- or current-bedded, chloritic, feldspathic quartzite, greywacke and phyllite
			marine shallow burial (flysch)	Greenish or purplish phyllite and silty phyllite with intercalations of conglomeratic and detrital dolomite bands
?				Unconformity = Deposition and re-working of Otavi phyllite (?)
OTAVI – Upper	900 m	CARBONATE ASSOCIATION	Biomicrite Blanket	Well and evenly stratified, light-grey, cherty (grey or blue) dolomite micrite Well stratified, white or rose, dolomite micrite
			Biostrome Blanket	Well stratified, light or dark grey, cherty dolomite micrite. Thinly laminated darkgreenish-grey, marly dolomite. Massive, bluish, dolomite biolithite
	0-250		Barrier Reef	Massive, or coarsely bedded, bluish, fetid stromatolitic dolomite, biolithite and calcirudite
	0-250		Tillite	Poorly bedded or massive, brownish, unsorted and extremely angular, polygenetic breccia, cemented by ferruginous marly or shaly matrix - scattered itabirite
			Unconformity sand	Thickly or cross-bedded, often ripple-marked, brown or grey, feldspathic sandstone, grit and polygenetic pudding-stone. Clastic elements always well rounded
OTAVI – Lower	0-200-300	CARBONATE ASS.	RANDOM BIOHERM *	Well stratified, grey or whitish, seldom cherty intraclastic dolomite. Subordinate, reddish or greenish marly dolomite and calcirudite Massive bluish dolomite biolithite *
			BLANKET BIOSTROME	Thinly laminated, whitish shale and siltstone with intraclastic dolomite intercalations
NOSIB	1000 m	ARKOSE CLASTIC ASSOCIATION	WEDGE	Coarsely, unevenly or cross-bedded, cream-coloured or grey, feldspathic quartzite, arkose and grit Bands and lenses of conglomerate or scattered, well rounded, monogenetic (vein-quartz and quartzite) pebbles
			BASAL	Thickly but fairly evenly bedded pale brown or grey feldspathic quartzite, arkose and grit

↓ Rate of Supply (Su) / Rate of subsidence (Sb) = Sedimentation Ratio (in feet or m/My)

$Sb^W - Sb^E$ Subsidence in the west minus Subsidence in the east = T^W westwards pre-diastrophic tilt.

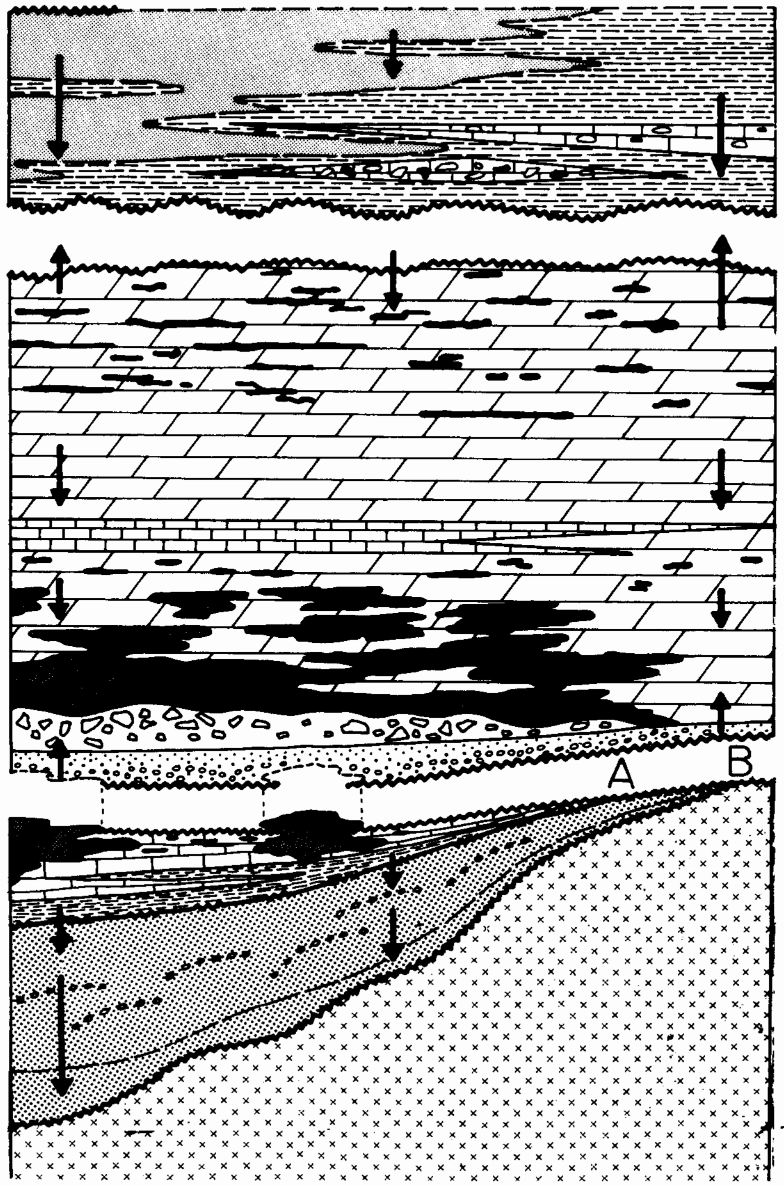

Su/Sb > 1 Sb^W-Sb^E ≶ 0 Su/Sb < 1 Su/Sb ≶ 1	Progressive filling of the basin Advance of Western Sesfontein thrust -- mass isolation of basin Regional flexure to the SW (along NW axis) = intense subsidence Folding with creation of large synclinoria = exogeosyncline	Coarse immature detritus flow Western crystalline nappes Fine or extremely coarse detritus from Otavi Series (phyllite (?) and cherty dolomite)	SYN- TO POST-OROGENIC SEDIMENTATION	Metamorphism (M_2)
	Initial phase of Damara Orogeny			
Su/Sp < 1 Sb^W-Sb^E ≥ 0 = Low	Faster subsidence, slow deposition Deepening of basin Moderate westerly gradient	Endogenetic Carbonate	UPPER OTAVI TRANSGRESSION	II Anadiagenetic cycle
Su/Sb ≤ 1 Sb^W-Sb^E ≥ 0 Low	Slow subsidence, slow deposition Moderate westerly gradient			
Su/Sb < 1 Sb^W-Sb^E > 0 Fair	Active subsidence, slow deposition Gradual deepening of basin Sensible westerly gradient			
Su/Sb = 1	Pause or slow deepening of basin			
Su/Sb < 1 Su/Sb ≫ 1	Stasis + Slight deepening of basin due to negative eustasis (?) Uplift (not necessarily tilt) + positive eustasis (?)	Immature, polygenetic detritus from glacial exaration erosion Mature, re-worked detritus from Lower Otavi and Nosib	NOSIB - LOWER OTAVI TRANSGRESSION	
Su/Sb < 1 Sb^W-Sb^E > 0 Medium	Active subsidence, medium deposition Slight deepening of basin Sensible to Medium westerly gradient	Fine detritus + Endogenetic Carbonate		I Anadiagenetic cycle
Su/Sb ≫ 1 Su/Sb < 1 Sb^W-Sb^E > 0 Su/Sb ≪ 1 Sb^W-Sb^E ≶ 0	Stasis or slight uplift Fast negative regional epeirogenesis + progressive coalescence of embryonic basins into common Western miogeosynclinal subsidence + Extreme Westerly gradient = warping Slow Negative regional epeirogenesis + localised subsidence of submerged pre-Nosib landforms = formation of embryonic basins	Coarse immature detritus; local or short transport from polygenetic crystalline sources (basement)		

Su/Sb = 1 Constant sedimentation environments

Su/Sb 1 Deepening of sedimentation environments

Su/Sb 1 Gradual filling of sedimentation basin.

occasionally, cherty, dolomitic Lower Otavi Stage which follows, is likely to have occurred in neritic environments grading to subpelagic.

On the basis of local evidence, the author is in agreement with Martin (1965, p.27) in minimising the stratigraphic significance of the paraconformity separating the Damara System from the Nosib Formation in the Hundskopf Hills. South-east of Otavi, however, a different relationship was observed by Smit (1962, p.72) who maintains that: "The present outcrop areas of the Nosib Formation were therefore presumably terrains of higher relief during the deposition of the Otavi Series". It is thus likely that the Kamanjab and Grootfontein basement inliers represented positive areas throughout the Nosib and Lower Otavi deposition. The positive movement must, however, be visualised as a relative phenomenon occurring against a background of intense regional subsidence or even as localised slower subsidence. Uplift during fast regional subsidence was accompanied by sedimentary thinning in crestal areas. Erosion and reworking followed upwarping during moderate regional subsidence. As a result steep thickness-gradients radiate from the western margin of the Kamanjab inlier, which is generally speaking an area of minimum Damara thickness. As sedimentation takes place subhorizontally such different thicknesses were accommodated by differential movement or adjustment of the basin-floor with the creation of a pre-diastrophic westward tilt of all major stratigraphic discontinuities.

3. The Tillite Disconformity

In pre-Tillite times a large-scale upwarping gradually reexposed the Nosib-Lower Otavi succession. Erosion occurred over very vast regions (most of South West Africa) and was accompanied by little or no deformation at all. The Kamanjab basement inlier was easily denuded of its inconsistent Nosib-Damara cover. The Damara-Nosib (P^2) paraconformity and Nosib-basement (U^1) unconformity were successively intersected by this new (D^3) disconformity surface, due to their pre-diastrophic westwards tilts. Their mutual intersections are shown as points A and B in folder 1. Such relationship is verified in the south-easternmost corner of sheet 1913B or on a broader regional scale in the Geological Map of South West Africa (1963) scale 1:1,000,000 modified in figure 2.

Coarse, rather mature, reworked detritus was again available and distributed by waves and currents, indicated by the presence of ripple marks and cross-bedding, along wide strand flats to form the disconformity blanket appearing at the base of the Tillite Substage. The brick-red colour of some of the matrices of the resulting grits and puddingstone is interpeted as a hematitic or bauxitic residual of chemical weathering of material of igneous derivation and impure carbonate rocks under oxidising epidiagenetic conditions or in fairly warm waters (McCarthy, 1926). Significiant contents of chert and occasional cherty dolomite lithoclasts (Plate 1) seem to confirm that a possibly considerable portion of the highest dolomitic members of the Lower Otavi was locally eroded, as chert is virtually absent in the Nosib and obviously in the basement. Similar pre-Tillite clastics were observed by Clifford (personal communication) between Outjo and Fransfontein.

Thick Lower Otavi sequences of cherty dolomite are preserved in the northern Kaokoveld (i.e. 2700 m; Rabie in Martin, 1965) and in the Otavi mountainland (i.e. 1900 m; Söhnge, 1961), where this phase of erosion may have been less severe. A comparison of these maximum thicknesses with the 0-500 m found in the Sesfontein area provides a rough indication of the possible amplitude of this upwarping.

A comparison between the textures of a typical Nosib grit (Plate 2) and an Upper Otavi disconformity grit (Plate 1) shows how absence of cement, interlocking of grains, anadiagenetic silicification and dolomitisation, and scarcity of lithoclasts are conspicuous in the former contrasting strongly with the abundance of shaly, often ferruginous, matrix, roundness of grains barely in mutual contact and number of lithoclasts (mainly chert and subordinate cherty dolomite) of the latter. Since to the south-east these two rock types come into direct sedimentary contact, it must be concluded that conspicuous anadiagenesis (Fairbridge, 1966) lithified the Nosib clastics prior to the deposition of the Upper Otavi Series.

All these considerations indicate that a considerable hiatus in sedimentation and intensive erosion, in spite of the modesty of angular unconformity, took place at this level. The stratigraphic significance of this (D^3) pre-Tillite disconformity may, therefore, locally exceed that of the Nosib-Damara paraconformity (P^2).

Heteropic bioherms (Plate 3) developed, although partially hindered by excessive terrigenous supply, during this long period of eustatic oscillations. Meanwhile considerable paleoclimatic changes were taking place with the advent of the regional late Precambrian glaciation, which may have involved most of the southern hemisphere (Haughton, 1969). Colder waters and overwhelming clastic sedimentation rapidly inhibited the growth of the algal colonies.

Angular, unsorted, polygenetic rudaceous material generally cemented by ferruginous carbonate-rich or shaly matrices follows concordantly. General agreement seems to exist (Gevers, 1931; Le Roex, 1941) on the glacial or more likely ice-drift depositional origin (Martin, 1965) for most of the synchronous and correlatable deposits in the Kaokoveld.

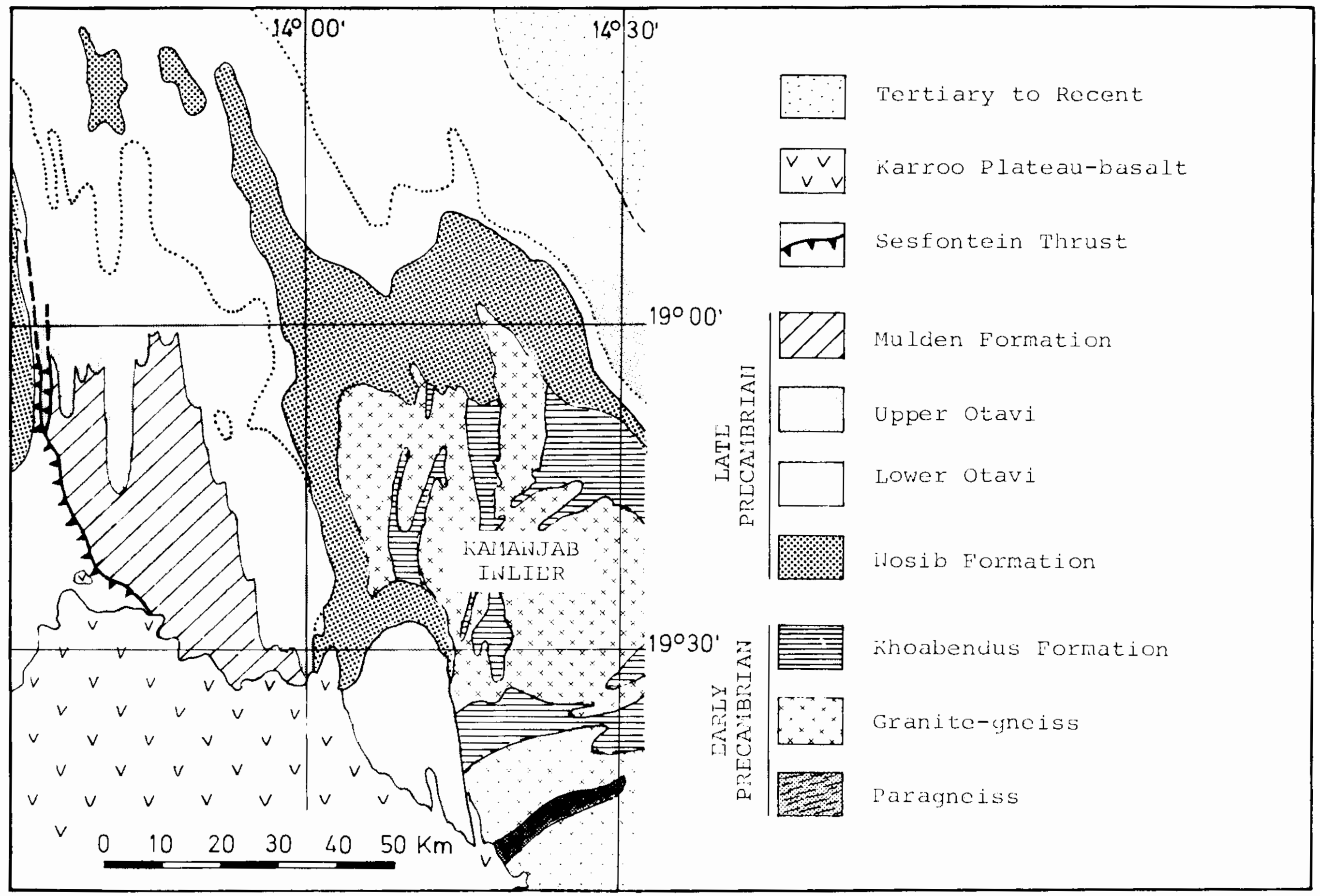

Figure 2. Geological map of the eastern structural-stratigraphic domain and its relationship to the Kamanjab inlier (modified after the Offical Geological Map of South West Africa, 1963)

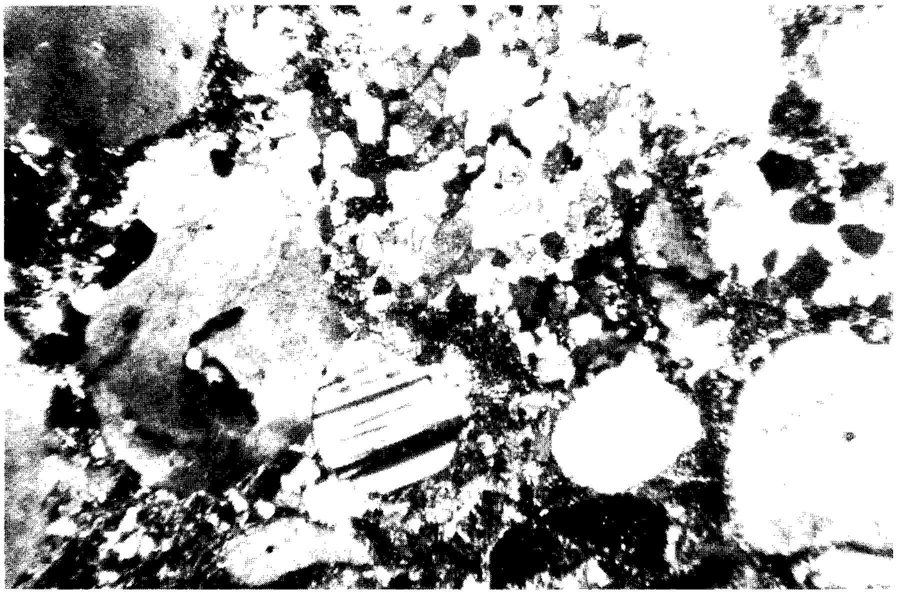

Plate 1. Roundness of grains and abundance of matrix in Upper Otavi disconformity grit (x35)

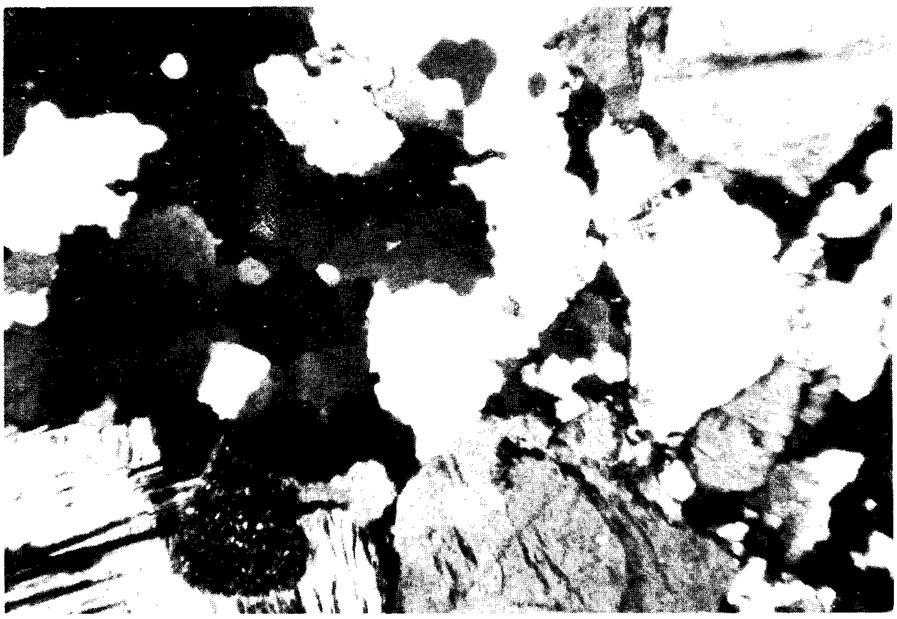

Plate 2. Interlocking grains and absence of cement in Nosib grit (x35)

The irregular geometry of the tillite deposit, ranging in thickness from 0 m in the south-eastern to more than 300 m in the northern parts of the study area, could be either inherent to the mechanism of deposition or the effect of a transgressive overlap on a tilted and eroded Lower Otavi-Nosib-basement succession bordering the Kamanjab Inlier.

4. The Upper Otavi Sedimentary Cycle

After the Tillite deposition the sea-floor must have been comparatively shallow and uneven. With the advent of warmer paleo-climates this was an ideal pedestal for the flourishment of biohermal algal colonies (Plate 4). Slow oscillatory subsidence enabled the light-dependent (Johnson, 1961) stromatolites to expand laterally. Bioherms grew to such an extent as to interfere mutually and to coalesce into massive reefs, which are preserved as a variably thick band of dark blue, fetid, vuggy, massive dolomitic biolithite (Folk, 1959). Discontinuous masses of coarse, angular, dolomitic sedimentary breccia (reef talus) and finely laminated (interreef) argillaceous micrite were heteropically developed. It is likely that barrier reefs bordered the western flank of the Kamanjab inlier, probably dying out to the south-east. Here thick masses of coarse dolomitic sedimentary breccia, possibly remains of forereef assemblages, are still exposed along one of the Hoanib tributaries. They disappear completely a few miles farther south, where stratigraphically higher biostromatic dolomite lies directly on the Nosib clastics with a veneer of reddish, conglomeratic, basal sand. A similar relationship would not have been possible if only a continuous transgressive overlap of progressively higher members of the Damara System onto the basement had taken place as postulated by Martin (1965, p.30), minimising the amount of erosion that occurred in pre-Tillite time. It would have been logical to expect the lowermost members, i.e. the Nosib quartzite, to pinch out before the overlapping Lower Otavi and Tillite Substage.

Progressive layering of the top of the reef indicates the inability of the algae to cope with the gradually deepening environment. The bioherms eventually separated and were replaced by heteropic thinly laminated biostromal micrite. Deeper sea finally transgressed once again onto the Kamanjab inlier, depositing a thick pile of evenly bedded Upper Otavi cherty dolomite. The relevant (>900 m) and even thickness of this typical nonclastic blanket micrite association together with the vertical and lateral facies persistence, reflect a very long span of slow regional subsidence and deepening, characterised by very low westwards gradients.

In the Otavi district (Söhnge, 1961; Smit, 1962) phyllite overlies and intertongues with this member. Sparse intercalations of fine-grained sandstone towards the top of the sequence

Plate 3. An isolated bioherm surrounded by heteropic clastics (Tillite Substage) along the eastern cliff of the karst highveld

Plate 4. A large stromatolite (Collenia?)

in the Khowarib valley seem to indicate impending clastic deposition. Whether a pelitic member comparable to the Otavi phyllite was locally and conformably deposited on top of the Upper Otavi dolomite is impossible to say, since relics of it are not preserved anywhere in the area. However, indirect observations in the overlying Mulden clastics point towards deposition followed by erosion, rather than non-deposition.

5. The Mulden Sedimentary Cycle

The rather immature Mulden clastics, which follow unconformably, comprise an eastern and northern mainly pelitic member (Sesfontein phyllite) with intercalated bands of monogenetic dolomitic conglomerate (Warmquelle conglomerate) and calcarenite. This grades into and is progressively overlain to the south-west by a mainly psammitic member composed of occasionally cross-bedded greywacke and chloritic feldspathic sandstone. An analogous distribution is reported for the Mulden sediments west of Welwitschia (Frets, 1969), where, however, the psammitic member is overwhelmingly developed.

The scarcely rounded dolomite and chert pebbles in the Warmquelle conglomerate and their distribution within the phyllite, which forms a rim around the dolomite highveld, suggest a local derivation from the north and the east i.e. from re-working of some high pelitic (Otavi phyllite?) member of the Otavi Series and part of the Otavi cherty dolomite.

The coarser lithotypes to the south-west cannot be similarly explained. One would, in fact, expect decreasing average grain-size and more regular bedding south-westwards, i.e. towards deeper sections of the basin. Moreover, the immaturity of the clastic grains, the abundance of feldspar, the great scarcity of chert in the westernmost members and the relative abundance of heavy minerals of metamorphic or igneous derivation exclude the Otavi Series as a possible parent source. Since only one alternative is left open, it is concluded, in agreement with Frets (1969, p.105), that the south-western psammitic assemblage originates from metasedimentary rocks belonging to the western Swakop Facies of the Damara System.

The discontinuous syn- or post-orogenetic character and the geometry of this shallow burial or non-marine greywacke association are typical of exogeosynclines (Kay, 1951) or rather of what alpine geologists would term molasse foredeeps (Aubouin, 1965).

Most of the original Mulden basin is either buried below the Karroo plateau-basalts or overridden by the Sesfontein thrust-mass and nappes. The marked deflection of the gravimetric contours on the Official Geological Map of South West Africa (1963) might possibly delineate its concealed shape and extension.

D. STRUCTURAL ANALYSIS

East of the Sesfontein Thrust the lithostratigraphic contacts have been progressively deformed into a general N-S direction (sheet 1913B), conforming with the average trend of the axial-plane traces of the folds.

This regional or longitudinal folding (Turner and Weiss, 1963), hereinafter symbolised F_2, locally common to all the late Precambrian sequences, is the tectonic element of homogeneity defining the eastern structural-stratigraphic domain. Capitalised symbols will be added to F_2 to denote related phases of folding in different domains or zones, whenever subtle differences might arise. Thus F_2O will mean F_2 in the Outjo Facies of the Damara System, F_2M in the Mulden Formation, and so on.

Fold size and geometry, attitude of axial-planes and general mechanism of deformation, on the other hand, vary greatly, determining zones of higher homogeneity:

1. the Damara dolomite highveld
2. the Mulden synclinorium, including the N-S belt of tectonites induced by the Sesfontein Thrust.

Their geographic distribution, shown in the structural map (folder 2) reveals a remarkable coincidence with the physiographic regions previously described.

The folds geometry in each zone will be discussed first, but for the purpose of kinematic interpretation and chronological evolution of the tectonites, the domain will be considered as a whole.

All the structural data were projected on the lower hemisphere of an equal-area (Schmidt) net and contoured using a new distortion-free and non-subjective technique conceived by the author and proposed in the structural Appendix A accompanying the present paper.

1. The Damara Dolomite Highveld

Although this zone covers about two-thirds of the eastern structural-stratigraphic domain (folder 2), it represents only the south-western fringe of an extensive, homogeneous and gently deformed outlier (Billings,1954) of carbonate rocks surrounding the northern nose of the Kamanjab inlier. This regional open folding, however, becomes increasingly complex towards the south-west.

Due to the physical properties and sedimentary geometry of the predominant rock-types (massive competent sandstone at the bottom and thinly bedded plastic dolomite at the top), and to the shallow supracrustal conditions and consequent absence of metamorphism under moderate confining pressure, flexural-slip folding (Whitten, 1966) is the main mechanism of deformation. Development of slaty cleavage and slip folding is confined to the subordinate pelitic members of the sequence (Lower Otavi phyllitic sandstone). The only other types of penetrative foliations are mechanical schistosities resulting from local shearing (basal slide and Sesfontein Thrust) or other dislocative processes.

Bedding (ss) or bedding-foliation (s_0), non-penetrative axial plane surfaces (s_2^*) and fold-axes (B_2) are the fundamental macroscopic fabric elements.

On the whole, zone 1 exhibits polyphase deformation, although only one phase of longitudinal folding (F_2O) and one of flexuring (R_5) have regional significiance, the others being either quantitatively subordinate (F_3 and R_4) or else confined to limited subareas (F_7).

Most of the F_2O folds can generally be subdivided into a limited number of meso- or macroscopic planar-cylindroidal (Clark and McIntyre, 1951) segments, geometrically generated by $B_2(B_{s_0}{}^{s_2})$ axes, symbolised with crosses on diagrams 1, 2 and 3 in folder 2.

On account of its advanced lithification at the time of deformation, the Nosib clastics must have acted as a semi-rigid buffer between the unfolded but intensely faulted basement and the extremely plastic overlying unconsolidated, water-saturated carbonate blanket undergoing the early burial stages of syndiagenesis (Bissell, 1959). Moreover, the absence or widely spaced bedding-planes, together with its lithological homogeneity and rarity of "lubricating" phyllitic minerals, limited the initial folding to a large-scale concentric type accomplished through intergranular (de Sitter, 1956, p.51) slip and re-cementation. Due to the lenticular shape of this formation, strain must have been inhomogeneously distributed and fracturing easily induced by the underlying brittle basement. The inherent irregularity of the Nosib-basement contact must have produced an interlocking effect between these geological bodies, reducing possible shearing or sliding along this surface.

Disharmony and décollement between the Nosib and the overlying Damara dolomites could, on the other hand, be concentrated along the basal Lower Otavi pelites. Indeed, some of these finely laminated rocks proved to be phyllonites. The existence of a slide, or better, of a bedding-plane thrust (Badgley, 1965; p.188) at this level is supported by conspicuous mesoscopic disharmonic folding, crenulation and shearing just above the Nosib-Damara contact at various localities along the eastern foothill of the karst highveld. Such tectonites, denoted by asterisks on

---

* An asterisk will hereinafter denote limited or non-penetrative development of the fabric element under consideration.

folder 2, do not appear higher in the sequence. Conspicuous differential movement was, therefore, concentrated along these minor but nevertheless tectonically important levels.

As the Lower Otavi Stage is exposed only in confined portions of the area and its preserved thickness is quantitatively negligible, most of the fabric elements were sampled in the younger, thick and widely distributed Upper Otavi Dolomite.

Except where later tectonic events obliterated it, a roughly perpendicular ($\sim$E-W) axial undulation F_3 accompanies the N-S longitudinal F_2O folding. This is a typical $B_2 \perp B_3$ penecontemporaneous superposed system as classified by Whitten (1966), reviewing Sander's original definition (1948). The B_3 axis is defined by the bimodal preferential distribution of B_2 poles (crosses) and by the E-W symmetry of the s_0 contour on diagram 1 in folder 2. B_3 can, therefore, be symbolised both as $B_{B_2} s_3^*$ or $B_{s_2^*} s_3^*$. F_3 is an open deformation of very large wavelength, consequently the B_2 plunges do not normally exceed 10° towards either north or south. A conspicuous example of interference pattern between the N-S F_2O and an F_3 anticline is to be found to the east of Warmquelle, where streams draining in opposite directions expose its tillite core. The northern and southern flanks dip so gently as to be within the spread of the central portion of the s_0 contouring of diagrams 1 and 2 in folder 2.

Geometrically and with respect to F_2O, zone 1 can be farther subdivided into three areas determined by symmetry criteria, longitudinal persistence of directional attributes of fabric elements, and fold wavelengths. From east to west these are:

a. The Proximal area : $F_2O \perp F_3$
b. The Transition area : $F_2O \perp F_3$
c. The Distal area : $(F_2O \perp F_3) \parallel R_4$ and
$[(F_2O \perp F_3) \parallel R_4] \wedge R_5$

Adjacent areas, however, are transitional and the whole zone must be regarded as the deeply modified western flank of a very large megastructure, implying a common, though complex genesis. The most relevant characteristics of these tectonic subdivisions have been summarised in Table 1, and their geographical distribution shown in folder 2.

a. The Proximal Area: $(F_2O \perp F_3)$

This eastern area of open folding (Billings, 1954) is characterised by low bedding-dips over relatively large extensions (unimodal peak in diagram 1 of folder 2) bordered to the west by steeper dips (rarely exceeding 45°). The F_2O folds exhibit steep

---

The symbols $\perp$, $\parallel$, $\wedge$ refer, if not otherwise specified, to the N-S F_2O longitudinal folding.

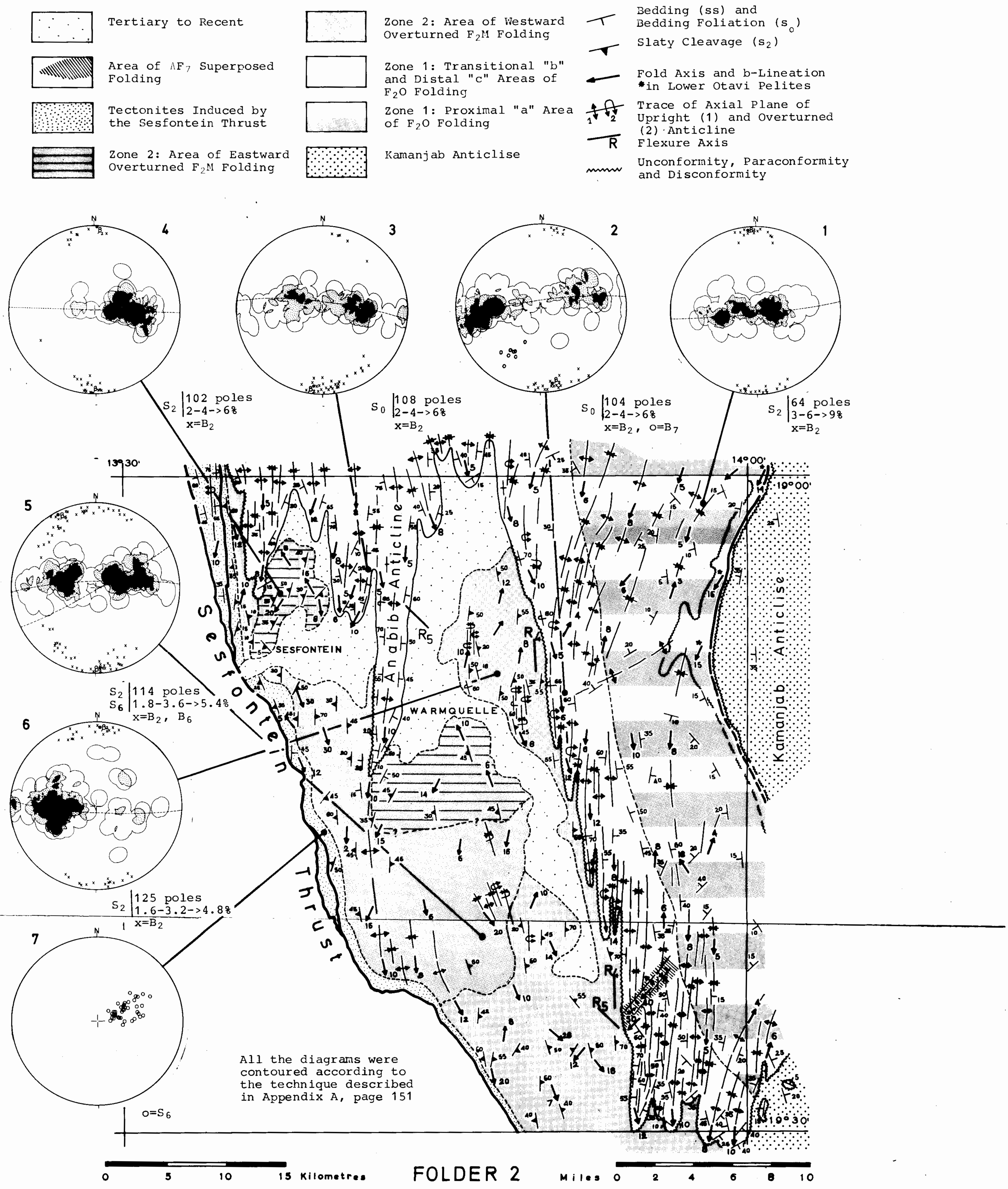

FOLDER 2

STRUCTURAL MAP OF THE EASTERN DOMAIN

axial planes with macroscopically curvilinear (horizontal) traces and large wavelengths (in the order of 3 to 5 Km).

The symmetry is triclinic but composed of a number of monoclinic or even orthorhombic segments (diagram 1 in folder 2). If the slightly curvilinear traces of the axial planes are regarded as a series of rectilinear elements, the folds can be reconstructed to a plane cylindroidal form (Turner and Weiss, 1963).

Due to the vertical or generally steep dip of the axial surfaces the B_2 fold axes trend sub-parallel to their traces (fig. 3) and are not deflected by the moderate axial undulation (bimodal distribution of fold axes and b-lineations in diagram 1 in folder 2) due to the F_3 cross-folding. The B_2 trend thus follows the swing of the curvilinear axial plane traces leading to a maximum variability of about 25^0 in the north (fig. 3), gradually decreasing to the south. The term sub-homoaxial is tentatively proposed for macroscopic structural complexes exhibiting such features.

This spreading and eastwards bending of the folding trend in the northern portion of the area is not a superposed feature, but seems to reflect the curvilinear shape of the Kamanjab inlier and possibly the thickness gradients radiating from it. The resulting open basins are normally distorted by minor mesoscopic heteroaxial, shallow folds and bounded to the west by relatively steep limbs of adjoining short wavelength anticlines. The longitudinal persistence of each fold is comparatively moderate.

The geometry of this discontinuous folding resembles the Caucasian "intermediate ridgelike folding" described by Russian authors (Beloussov, 1963) typical of areas situated between platforms or positive areas and zones of subsidence.

A N-S and NW framework of normal faults and joints accompanies the F_2O folding along the margin of the Kamanjab inlier becoming gradually attenuated to the west. The genetic implications of these dislocations will be stressed later.

b. The Transition Area: ($F_2O \perp F_3$)

In this area, which grades into area 'a' to the east and area 'c' to the west, the bedding-dips can exceed 45^0, while the axial planes of the F_2O folds retain their sub-vertical or steeply dipping attitude. Their horizontal traces, however, straighten into the N-S direction. The B_2 trends coincide with the trace of the axial planes in spite of a more or less pronounced pene-contemporaneous axial undulation. Since the trend is roughly rectilinear, the area is typically homoaxial (Hills, 1963) (average directional variations $<10^0$).

Much shorter wavelengths (of the order of 1 to 2 Km) and marked longitudinal persistence of F_2O folds differentiate this from area 'a'.

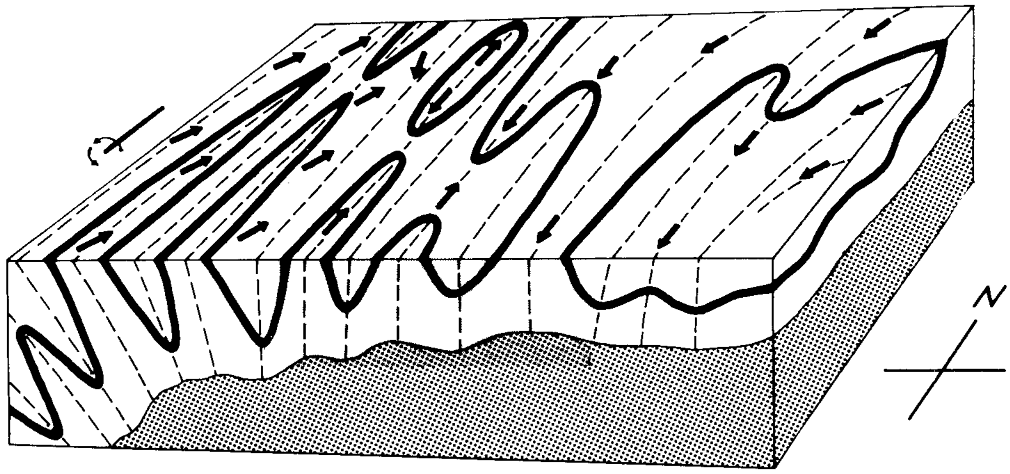

Distal Area "c" | Transition Area "b" | Proximal Area "a"

Figure 3. Progressive deflection of the B_2 trend from the trace of the axial plane as an effect of R_4 rotation. Shaded area enlarged in figure 7

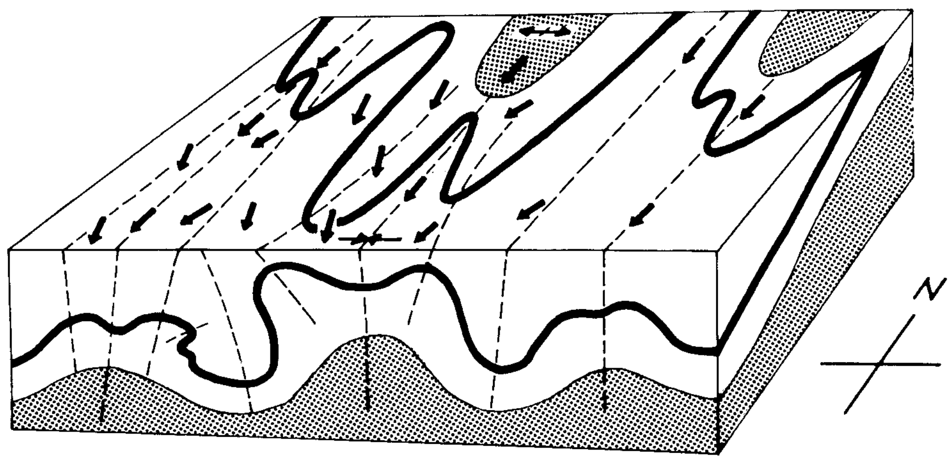

Collapse structures (Anabib anticline) | Transition Area "b"

Figure 4. B_2 trend deflection in box-folds. Note transition of a synform into an anticline in crestal areas

The local tectonites usually exhibit monoclinic or orthorombic symmetry.

The transverse profiles of F_2O folds are upright or slightly inclined, tight, symmetric or slightly asymmetric and show flank thinning and hinge thickening due to flattening.

The large synclinal basins, typical of area 'a', are here replaced by well-defined elongated synclines, locally still subordinate to the anticlinal ridges.

The faults and joints, so common in area 'a', are less frequent, while the basal slide is concealed due to insufficient erosion.

Particularly outstanding F_2O anticlines exhibit peculiar modification of their crests which flatten, broaden and even invert into more or less shallow synforms (Bailey and McCallien, 1937). When the flank dips steepen and overturn to maintain continuity with the crest, the fold assumes a fan-like (Billings, 1954) or mushroom-like shape; whereas, when the steepening of the limbs does not exceed the vertical, a box-like shape (de Sitter, 1959) is most common. The transverse profile normally changes along the fold (block-diagrams 2 a, b, c and d in folder 3) and the various types can grade into one another. The trace of the axial plane varies generally from rectilinear to curvilinear as the crestal flattening increases. When overturning of both flanks or when the formation of a crestal synform takes place, it splits into two auxiliary traces defining the two lobes (see idealised block diagram in fig. 4). As the flattening proceeds from an upright similar fold to a box- or mushroom-like fold the B_2 fold axis also loses its individuality and splits into a set of gradually diverging (synclinal) or converging (anticlinal) axes generating the two crestal lobes. It is significant that these modifications occur invariably in the topographically most elevated structures, as for instance the Anabib anticline.

A similar disharmonic overturning of the bedding plane was also observed on a mesoscopic scale at the noses of some of the anticlines, where slip-sheets (Harrison and Falcon, 1934 and 1936) of Otavi dolomite overlie the Mulden phyllite anomalously.

c. The Distal Area: $(F_2O \perp F_3) \| R_4$ and $[(F_2O \perp F_3) \| R_4] \wedge R_5$

The bedding dips vary from rather steep (over 60° on both flanks) to overturned to the west (maximum 50°E), as shown in diagram 2 in folder 2.

Folding accordingly changes from upright to increasingly westwards overturned. The strike of the s_2^* axial planes remains N-S, but due to their increasing eastwards dips (minimum 55°E) a deflection (trend-strike angle of Elliott, 1965, p.872) appears on the map between these N-S traces and the trend of the B_2 fold

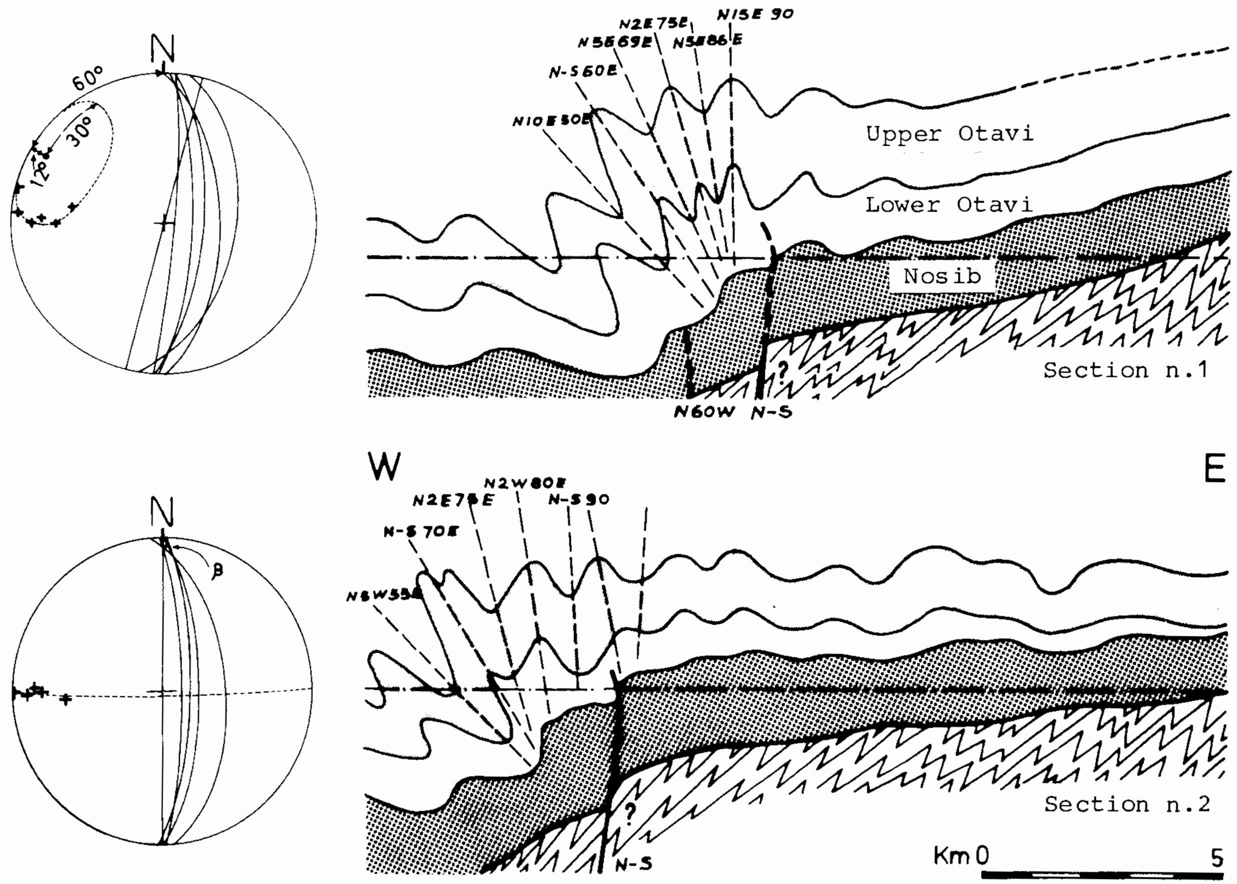

Figure 5. Variation in attitude of s_2 in the complex flexure west of Warmquelle (1) and Khowaris (2)

axes. This relationship is shown graphically in figure 3, while some related geometric extrapolations will be discussed in the structural Appendix B accompanying the present paper. The area is, therefore, homogeneous with respect to the N-S axial plane traces and inhomogeneous with respect to the deflected B_2 axes. The term sub-heteroaxial is tentatively proposed for areas exposing similar geometry.

The macroscopic symmetry of these tectonites is normally monoclinic, but can, in some instances, be brought back to rhombic symmetry by means of relatively simple rotations. The rotational modifications of the transitional b pattern are of two genetically related types:

i) The N-S belt of fan-like cascade folding or complex flexures (diagram 2 in folder 2).

ii) The NW en echelon alignment of southwards plunging nose structures (diagram 3 in folder 2).

Some of the non-parallel, macroscopic s_2^* axial planes of these complex flexures are plotted on combined π and β diagrams in figure 5. South-east of Khowarib (diagram and section n.1 in fig. 5) the poles of the fanning axial planes s_2^* are roughly aligned along a great circle defining a N-S sub-horizontal or slightly northwards plunging R_4 rotation axis $(B_{s_2^*} s_4^*)$ approximately coaxial with B_2. On account of this intimate connection R_4 could be included together with F_3 as a local penecontemporaneous modification of F_2O sensu lato.

East of Warmquelle, however, the s_2^* poles are distributed along a minor circle (diagram and section n.2 in fig. 5), defining a second non-coaxial R_5 rotation axis $(B_{s_2^*} s_5^*)$ trending N 60°W and with a slight (±12°) plunge to the NW. This direction coincides with the NW en echelon alignment of southwards plunging nose structures (Plate 5).

To establish what modifications of a typical 'b' pattern can result from rotation in R_5, a selected portion, shaded in block-diagram of figure 3, has been enlarged in figure 7 and average angular values attributed to the various fold elements (block-diagram n.1 in fig. 7). Progressive flexuring to the south-west along a NW trending R_5 axis is then applied (fig. 6), displacing the bedding plane poles a-g to new positions $a^1 \rightarrow g^1$ after a rotation of 30°.

The new values were subsequently plotted in block-diagram n.2 of figure 7 with respect to a geographic coordinate system. It is significant to note that:

i) the western flanks increase in dip, whereas those to the east decrease;

ii) for an adequate rotation each of the western flanks can successively be overturned;

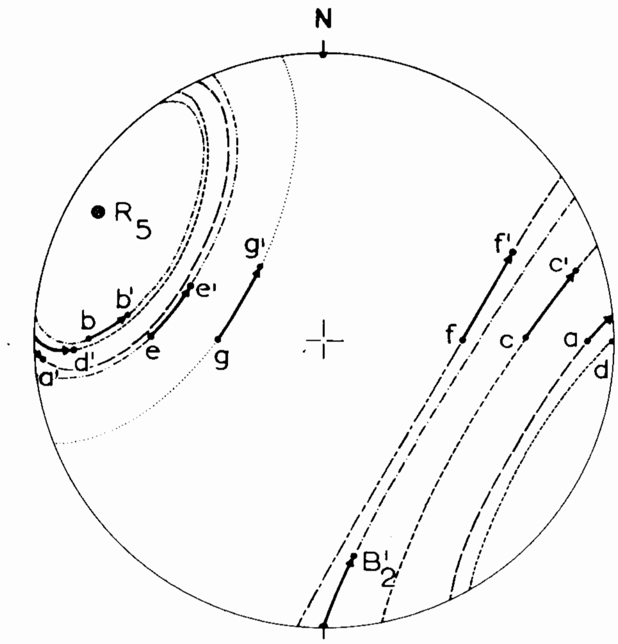

Figure 6. Diagram showing attitude of F_2O fold elements after R_5 flexuring.

iii) all the axial planes become inclined to the west (dipping to the east) at the same angle irrespective of the original steepness of the fold flanks;

iv) a definite southwards plunge develops;

v) rather moderate deflection (strike-trend angle) is induced by such rotation; and

vi) change in strike of the flanks is inversely proportional to their original dips.

Westwards overturning of fold flanks and axial planes and southward plunges of the B_2 fold axes are simultaneously achieved through only one rotation. A common parental derivation for plunges and overturning could be advanced and the necessity of the R_4 rotation could be excluded, but for the implication of the third point (iii) which does not account for the commonly observed s_2^* fanning. The magnitude of the rotation around these two completely different and independent axes (R_4 and R_5) may, however, have been proportionally larger in different areas.

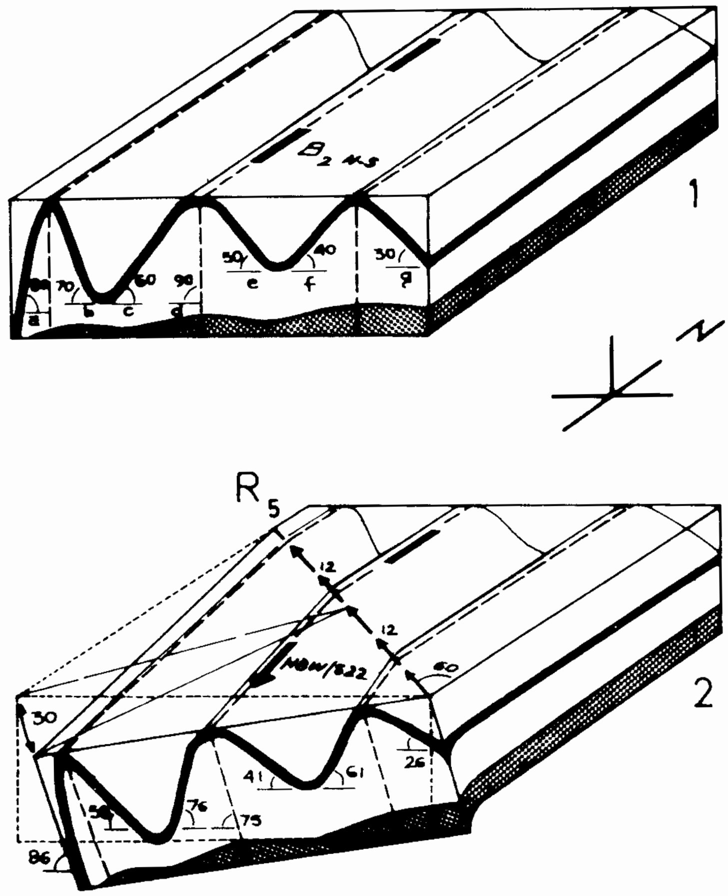

Figure 7. Simultaneous westwards fold overturning and southwards B_2 plunges induced by a 30° rotation in R_5

North-east of Numas-Ugams a narrow belt of NE trending F_7 folds intersects area c with the creation of a definite interference pattern: $\{[(F_2O \perp F_3) \| R_4] \wedge R_5\} \wedge F_7$. Two sharp kink folds of moderate (500 m) wavelength are developed close to the eastern margin of the Mulden basin, merging eastwards into a subvertical transcurrent or wrench fault. As the fault plane seems to represent the axial plane ($s_7^{\bullet}$) of these kink folds, their axis can, therefore, be defined as $B_{s_0} s_7^{\bullet}$ or $B_{s_2^{\bullet}} s_7^{\bullet}$. The B_7 fold axes appearing on diagram 2 of folder 2 plunge steeply south-west because they were measured mainly on the westwards dipping flanks of F_2O folds, due to the inaccessibility and consequent scarcity of measurements along the east-dipping flanks. That F_7 folding and shearing are late features, is proved by their superposition on structures younger than F_2O (i.e. the Sesfontein Thrust).

2. The Mulden Synclinorium

Slip-folding and gradual modifications towards mixed flexural-slip and slip folding (Whitten, 1966) at a mesoscopic scale are the main agents of deformation in this structural zone.

Lithostructural (Hartnady, 1969) differences account for the dissimilarity in mechanism of deformation with the parallel trending F_2O folding in the adjoining areas b and c of the Otavi dolomite highveld.

A generally well-developed slaty-cleavage is the most conspicuous penetrative s-surface in the zone. This is either a s_0 bedding foliation, possibly inherited from an original ss fine lamination enhanced by initial flexural-slip folding, or else s_2 axial planar foliation. Near the Sesfontein Thrust both these s-surfaces were transposed into an s_6 mechanical schistosity. Mesoscopic b-axes, crenulations and b-lineations are discontinuously exposed on all these lineation surfaces (Elliot, 1965).

With the exception of a late F_6 "Gleitbretter" (Sander, 1948) folding induced by the Sesfontein Thrust, zone 2 has essentially undergone only one phase of deformation. This can be broadly related to phase F_2O (inclusive of F_3 and R_4).

A characteristic of the Mulden Synclinorium mesoscopic folds is their inclined and generally overturned attitude (Plate 6). Concomitant deflection of fold axes is found all over the structural zone, while most of the axial planes strike concordantly. Following the definition introduced in area 'c' (p.23), the whole zone could be classified as sub-heteroaxial. The sub-parallel regional attitude of F_2M and F_2O is the tectonic element of homogeneity which links the Mulden Synclinorium to the eastern structural-stratigraphic domain.

A glance at folder 2 will show how the s_2 fabric elements are distributed into roughly N-S elongated homoclinal belts,

Table 1. Synopsis of Deformation in the Karst Highveld

Location of structural areas	F_2 O LONGITUDINAL FOLDING				Average SS and So dips	F_2O PENECONTEMPORANEOUS MODIFICATIONS			LATER SUPERPOSED PHASES		Style of folding and interference patterns
	Geometry and altitude of S_2^* axial planes	B_2 axis trend and plunge	Average wavelength (λ) and amplitude (A)	Longitudinal persistence		$\perp F_3$ (NE to NNE)	Faulting and sliding	Coaxial $\parallel R_4$ rotation ($\sim$N-S)	$\wedge R_5$ rotation (68N 12°NW)	$\wedge F_7$ wrench faulting or kink folding ($\sim$NE)	
(a) PROXIMAL AREA Western flank of the Kamanjab inlier	Macroscopically curviplanar, mesoscopically planar, sub-vertical or steeply dipping, N-S to N 30° E striking (variance ±30°)	Sub-parallel to the axial plane strike: ± 30° spread. Plunge to the N and S not exceeding 5°	Very large wavelength (λ up to 5 Km) decreasing westwards Shallow amplitude ($A < \frac{1}{2}\lambda$) increasing westwards	Regionally limited to moderate $< 10\lambda$	Largely shallow dipping Maximum dips in western margins 45 - 50°	Upright, large wavelength gentle E-W or ENE trending axial undulation. Maximum induced B_2 plunges 5-10° N or S	Rather intense N-S and NW trending normal faults. Extensive sliding along Lower Otavi basal pelites (phyllonites)	Absent	Absent	Two NE trending wrench faults in southern sector	Large open basins limited by steeper anticlines to the west. Discontinuous or intermediate ridge-like folding (Beloussov, 1963) $F_2O \perp F_3$ interference pattern
grading	SUB-HOMOAXIAL			DISCONTINUOUS							
into (b) TRANSITIONAL AREA	Planar, sub-vertical or steeply dipping N-S to N 10° E striking (variance ± 10°)	Sub-parallel to the axial plane strike homogeneously N-S trending (± 10° spread)	Moderate wavelength (λ up to 2 Km) decreasing westwards. Larger amplitude ($\frac{1}{2}\lambda < A < 1\lambda$) increasing westwards	Considerable $> 10\lambda$	Steep dips between 45° and 70°. Exceptional vertical or overturned strata in box- or mushroom-like folds	Same as above when not obscured by $\wedge R_5$ flexuring	Moderate normal faulting. Slide concealed at present erosion level	Absent	Developed west and south-west of Warmquelle	Same as above	Moderately tight, upright, continuous similar folding. Box- or mushroom-like folds (de Sitter, 1956) occasionally developed $F_2O \perp F_3$ interference pattern
grading	HOMOAXIAL			CONTINUOUS LONGITUDINAL							
into (c) DISTAL AREA Northern and western margin of Mulden exogeosyncline	Planar, progressively fanning from vertical to westwards overturned dips (minimum 50° E)	Progressive deflection from axial plane strike with change in S_2^* dip	Rather short wavelength ($\lambda < 1.5$ Km) Larger amplitude than areas a and b ($1\lambda < A < 1\frac{1}{2}\lambda$)	Considerable $> 10\lambda$	Very steep sub-vertical or westwards overturned dips (minimum 50-60°E)	Same as above	Same as above	Causes S_2 westwards overturning and fanning and related B_2 deflection	Causes S_2^* westwards overturning and creation of en echelon belt of southwards plunging B_2 structures	NE trending kink folding grading into wrench faulting eastwards	Fan-like, westwards overturned, cascade folding or complex flexures. En echelon belts of southwards plunging B_2 structures $\{(F_2 O \perp F_3) \parallel R_4\} \wedge R_5$ $\{[(F_2 O \perp F_3) \parallel R_4] \wedge R_5\} \wedge F_7$
	SUB-HETEROAXIAL			CONTINUOUS LONGITUDINAL							

Location with respect to F_2O dolomite anticlines	F_2M LONGITUDINAL FOLDING					PENECONTEMPORANEOUS F_2 M MODIFICATION	LATER SUPERPOSED PHASES		
	Geometry and altitude of S_2 axial planes	B_2 axis trend and plunge	Average wavelength (λ) and amplitude (A)	Longitudinal persistence	Average SS and So dips	$\perp F_3$ (NE to ENE)	$\wedge F_6$ ($\sim$ NNW)	$\wedge F_7$ ($\sim$NE)	Style of folding and interference patterns
(1) Along eastern flanks (2) Along western flanks (3) Above either flank of concealed (plunging) F_2O structures	Planar, homogeneously N-S striking (variance $\pm$ 10°) eastward inclined or overturned westward inclined or overturned	Noticeable* deflections and plunges towards either N or S not exceeding 30°	Moderate* wavelength (λ = few metres to few hundred metres). Moderate to large amplitude ($\frac{1}{2}\lambda < A < 3\lambda$)	* Considerable 10	Medium to* shallow dips in both normal and overturned flanks. Occasionally subparallel to S_2	Upright * large wavelength, gentle E-W or ENE trending axial undulation. Maximum induced B_2 plunges 10-15°	NNW * trending, eastwards recumbent, "Gleitbretter" folding induced by shearing below the Sesfontein thrust, transposing SS, So and S_2 into S_6	NE * trending crenulation cleavage on S_o and S_2	Belts of east-* wards or westwards overturned, mesoscopic, almost isoclinal, slip and flexural-slip folding with moderate axial undulations. "Gleitbretter" folds. Crenulations and kink bands
	SUB-HETEROAXIAL			CONTINUOUS LONGITUDINAL					

* Applicable to all three areas

Table 2. Synopsis of Deformation in the Mulden Synclinorium

Plate 5. The southward plunging closure of the Anabib anticline.

Plate 6. Westward overturned, similar, almost isoclinal folding in the Mulden synclinorium

bordering the Otavi dolomite highland. Eastwards inclined or overturned folding (axial planes dipping westwards) seems to be confined to the eastern flanks of outstanding F_2O anticlines in the Otavi dolomite (diagram 4 in folder 2). A conjugate orientation of F_2M folds (diagram 6) formed along opposite flanks. Most of the eastern margins of these elevated structures are, unfortunately, bordered by a thick cover of Tertiary to Recent sediments (sheet 1913B) concealing the attitude of the underlying Mulden phyllite, with the exception of two areas, located at the very nose of the Anabib anticline and north of Sesfontein village, denoted by horizontal ruling in the structural map of folder 2.

Towards the centre of the basin, where the geometric relation to F_2O is not too obvious, the diagrams (5 in folder 2) exhibit a bimodal girdle. It is possible, however, that by trial and error zone 5 could be split into several homoclinal areas similar to 4 and 6, once detailed sampling is carried out in a greater number of crucially located stations.

Many of the westwards dipping planes plotted on diagram 5 may also be s_6 schistosity planes of late shearing related to the Sesfontein Thrust, which are difficult to distinguish from s_2. Their pattern of orientation defines a late superposed "Gleitbretter" folding ($F_2M\Lambda F_6$) on diagrams 4 and 5 in folder 2. The l_6 lineations and crenulations parallel to the S_2/S_6 intersection seem to be distributed along a great circle defining the average orientation of this late s_6 schistosity. Distinction between B_2 and l_6 lineaments becomes somewhat uncertain for low values of plunge. If s_6 poles (the preferred orientation of which is shown in diagram 7 of folder 2) were hypothetically eliminated from diagram 5, the resulting pattern would become essentially westward inclined.

North of Numas-Ugams a markedly later NE trending l_7 intersection lineation and subordinate crenulation cleavage were superposed on F_2M. Sparce l_7 lineations are encountered elsewhere in the Mulden basin and correspond to similarly orientated late wrench or transcurrent faults. The distribution of this last phase of deformation is extremely limited and subordinate, by analogy to the distal area c of the Otavi dolomite highveld.

3. Kinematic Interpretation

Westwards pre-tectonic dips developed along the margin of the Kamanjab inlier as a cumulative effect of:

i) westwards subsidence and thickness gradients in the miogeosyncline,

ii) relative, discontinuous, oscillatory uplift or moderate subsidence taking place in the Kamanjab inlier against a background of intense and variable regional subsidence, influencing both sedimentary thickness and re-working in the Nosib-Damara succession, and

iii) differential compaction of these sediments along the western flank of the crystalline incompressible "buried" inlier.

The resulting geometry is, therefore, characterised by decreasing values of pre-tectonic dips and more tabular shapes towards the top of the sequence (folder 1). A rough estimate of the tilt at the base of the Otavi Series can be obtained along the thick Nosib-Damara succession exposed over a short distance along the lofty eastern cliff of the karst highveld. The average bedding-dips gradually decrease from 25-35° in the Nosib to values as low as 15-30° in the Upper Otavi dolomite. As a negligible angular paraconformity marks the base of the Damara rocks, most of the 5-10° difference must be explained as a pre-orogenic feature. Syn-depositional differential movement, however, must have concentrated along the flank of the Kamanjab inlier to compensate for the relatively rapid subsidence in the adjoining miogeosynclinal furrow producing a belt of anomalously high dips, while noticeable flattening is likely to have occurred more distally.

Similar, large wavelength upwarping accompanied by upwards decrease of pre-diastrophic dips are typical of supratenuous (Hills, 1953) megascopic elevations forming in platform or proximal areas, termed anticlises (Shatski and Bogdanov, 1959; Potapov, 1960).

The summit level in the karst highveld slopes sensibly westwards. This is the erosional product of a much steeper "level of flexure" (Beloussov, 1963) megascopically enveloping the top of the Otavi Series along the western flank of the Kamanjab anticlise (fig. 8). The top of the Tillite Substage in the northeast of sheet 1913B, for instance, lies at approximately the same altitude as the top of the Upper Otavi dolomite in the Anabib anticline. The difference in elevation would in this case exceed 1400 m, even disregarding the intense uplift (>500 m) in the Anabib anticline.

In addition, the anticlines show a tendency not to exceed set average altitudes by flattening of their crests into box-like or mushroom profiles elsewhere similar or open (compare diagrams 2c and 2d with 2b in folder 3).

The swing of the longitudinal F_2O folds around the northern nose of the Kamanjab anticlise and the accompanying joints and faults indicate that a definite tensional stress-field acted along a wide aureole bordering this positive area. At lower levels of folding (close to the Damara-Nosib contact), on the other hand, tight disharmonic folding, crenulation and shearing (phyllonites),

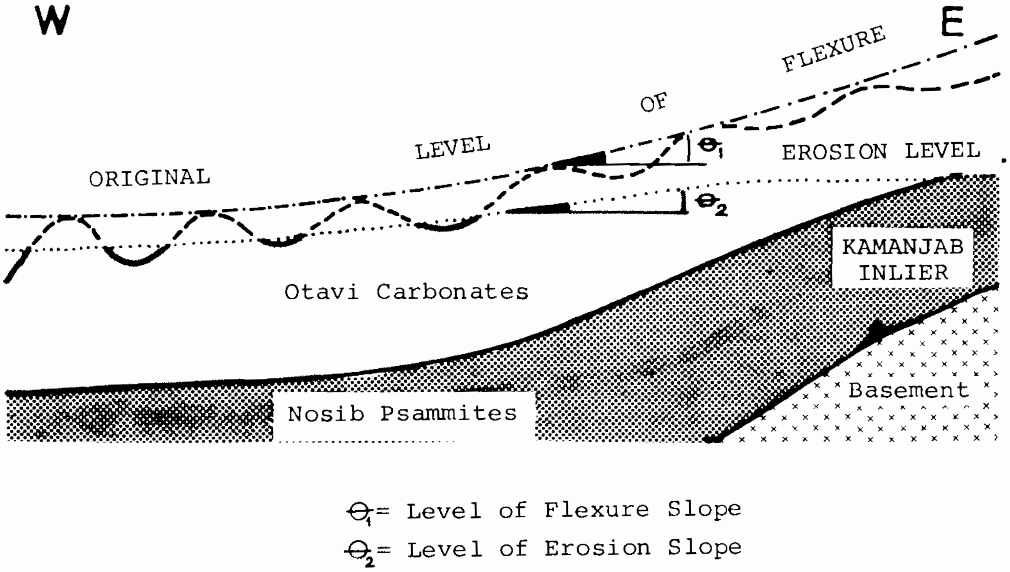

Figure 8. Relationship between level of flexure and summit level in the karst highveld.

all features which could form only within a compressive stress-field, are ubiquitously developed. Dragging and sliding have evidently acted along this easily flowing basal pelitic member to compensate for a slow radiating movement of the overlying dolomite blanket away from the westerly slope of the Kamanjab anticlise.

The thick pile of unconsolidated, water-saturated Damara calcareous mud and ooze must, already during sedimentation, have been resting on this "basal slope" in a condition of precarious balance. However, no movement took place until:

i) A sufficiently thick (z_1= 2500-3000 m) sedimentary pile was deposited.

ii) Subsidence in the geosyncline or relative uplift in the craton (acceleration of subsidence of Aubouin (1965)) tilted the basal slope above the critical angle (θ_C) sufficient to initiate gliding under the action of gravity alone (Hsü, 1969).

iii) Pore fluid migration during compaction of loosely packed underlying clastics produced abnormally high fluid pressure along the basal Lower Otavi pelites acting as "cap" rock.

iv) A possible increase in bulk density (ρ_b) was brought about by progressive volume-by-volume diagenetic replacement of calcite by denser dolomite, which is accepted as the most common process of dolomitisation (Friedman and Sanders, 1967) and is accompanied by a density increase of up to 12-13%. The basal clays could, in this instance, have behaved both as a source of additional Mg and as ion-exchange membranes for the upwards migrating fluids (Kahle, 1965).

It is easily accepted that no catastrophic or exceptionally intense compressive stress-field need be introduced to initiate movement along the clay-carbonate basal member forming an ideal plane of potential failure.

The strata folded with increasing intensity towards the west. The gradual change from tensional to compressional features resulted from the pressure exerted by the advancing mass against "risers" (Raleigh and Griggs, 1963) in the basal slope or other "hindering effects" (e.g. upwarping in the west; progressive lithification of the gliding-mass, or negative changes in sea-level). The enormous energy supplied by actively sliding undeformed masses pushing from higher eastern positions must have induced folding wherever the advancement was accidentally slowed down or stopped. Deformation should have lasted until equilibrium was reached and the whole mass became stationary. However, weight redistribution by erosion and sedimentation could have gradually affected equilibrium and resulted in the gliding blanket resuming its slow creep.

As progress was accomplished through flowing and shearing of the "lubricating" basal member, where, as in the south-east, this pinches out, movement was severely impeded with the production of tight, undifferentiated upright folds.

Under hydrostatic conditions, the carbonate ooze was competent enough to transmit lateral pressure and to generate anticlines (e.g. Anabib anticline), but its competency was insufficient to sustain such structures, when they emerged above sea level, due to the greater effective action of gravity on the laterally unsupported mass. This could explain the collapse structures (box-like or mushroom folds) developed almost exclusively in topographically elevated areas (i.e. northern portion of the Anabib anticline, block-diagram 2a in folder 3). With progressive lithification the effect of gravity on the shape of the folds was greatly reduced.

The difference between the maximum height potentially attainable at any point and the highest elevation of the sliding-mass on the basal slope could tentatively be called the "potential drop" and depends on the magnitude of the hindering effects.

FOLDER 3. THE MAJOR STRUCTURES OF THE EASTERN DOMAIN

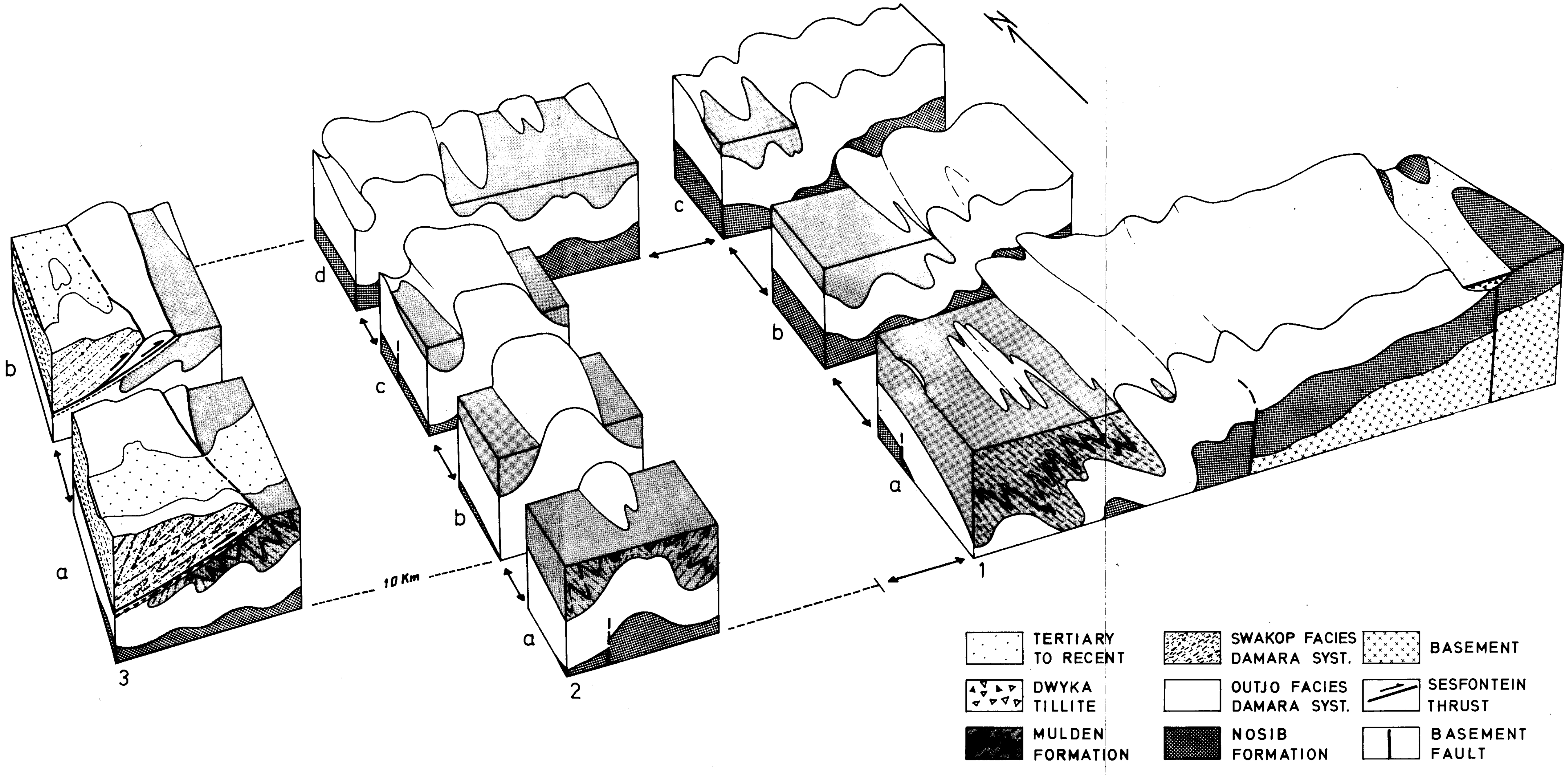

The surface forming the locus of all the maximum potential heights forms the level of flexure (Beloussov, 1963) enveloping the megascopic tectonite which would result if deformation were carried to final equilibrium with no variation of any parameter involved.

Under normal circumstances the trend and inclination or overturning of folds is a function of the dip of basal slope and of the thickness-gradient. Maximum overturning is to be expected where the slope steepens, upright folds on flattish areas, and antithetic inclination on risers. A drop of several hundred metres in the basal slope can be easily inferred along the N-S margin of the Warmquelle plains (block-diagram 1a in folder 3) and parallel to the NW en echelon belt of nose structures.

The N-S and NW framework of subvertical normal faults and joints developed in the proximal area 'a' at the north-eastern corner of sheet 1913B could bear two diametrically opposite interpretations:

i) It could be superficial and limited to the carbonate blanket as an effect of "radial stretching" at the edges of the Kamanjab anticlise, while gradually creeping down the basal slope, by analogy with observations made by Badgley et al. (1960) and Kelley et al. (1960); or else

ii) it could represent the upward propagation of larger rejuvenated fractures affecting the underlying rigid basement. A similar mechanism was observed by Hodgson (1961) in his regional study of jointing in Arizona and Utah.

The first interpretation could apply only in tensional areas of open folding, whereas it does not fit too easily where, as in the transitional area 'b', comparatively tight compressive folding is exposed. Frets (1969) reports intensive N-S poly-phase block-faulting within the basement in the Huab area 80 Km to the SE. These dislocations, rejuvenated during Damara time (Frets, 1969, p.221) could meet, if extended below the Etendeka plateau-basalt, the N-S fault valley delineating the western flank of the Kamanjab anticlise in sheet 1913B (block-diagram 1a in folder 3). Deep fracturing could thus have affected the basal slope both during and after the gliding had been completed. The downthrow of these brittle dislocations, which seems always to be to the west (i.e. towards the Damara eugeosyncline first and the Mulden exogeosyncline later), induced analogously orientated plastic deformation in the overlying unconfined, supracrustal sedimentary blanket (block-diagram 1a and 2a in folder 3). A similar mechanism of folding by vertical block uplift and consequent lateral spreading was conceived by Beloussov (1959) and reviewed by Billings (1960).

Analogous processes were successively active at different scales. Thus upwarping or horst-faulting in the Kamanjab anticlise initiated macroscopic F_2O folding in the Otavi dolomite on a regional scale on an extensive "first generation" basal slope. Later, the progressively steepening flanks of the F_2O anticlines acted as sets of "second generation" antithetic basal slopes along which F_2M mesoscopic folding took place in the accumulating Mulden pelites. Westerly slopes induced westerly inclined or overturned folds, while easterly slopes produced the opposite (i.e. eastern flank of the Anabib and Sesfontein anticlines, block-diagram 2a in folder 3). Where no outstanding dolomite folds were developed, with the consequent absence of second generation basal slopes (central or southern portions of the Mulden basin), a definite influence was still exerted by the Kamanjab anticlise and westward overturning was generally retained. The main macroscopic longitudinal F_2O folding in the dolomite and the subparallel mesoscopic F_2M folding in the Mulden pelite have thus a definite genetic relation, being products of the same tectonic phase which started deforming the older rocks, generated the younger ones and proceeded to deform both contemporaneously along a similar trend but on different scales and according to different mechanisms, depending upon bulk lithological dissimilarities. The Mulden pelites were, therefore, deposited initially in F_2O synclines developing in the Otavi dolomite as an effect of erosion proceeding in more elevated anticlinal areas. As the topmost members of the Otavi Series may have been pelitic (Otavi phyllite) and thereby easily and completely disaggregated, no basal conglomerate was initially deposited.

Lithification, dolomitisation and chertification must have been proceeding while the folding was taking place, with consequent steadily decreasing plasticity of the rock-mass undergoing deformation. Directed pressure in the sliding-sheet could be transmitted laterally allowing the rise of anticlines close to or even above sea level. Only then did intense erosion attack the carbonate anticlinal crests and produce coarse, immature rudaceous materials, deposited after very short transport into synclinal basins to form the Warmquelle conglomerate (block-diagram 1a in folder 3).

It is possible that appreciable deformation could have been induced in the underlying Nosib clastics due to the enhanced competency of the gliding-blanket. The extent of structural involvement is, however, difficult to evaluate because this formation never outcrops again to the west of the Kamanjab anticlise in the eastern domain. The closest occurrence, exhibiting noticeable deformation, is a small inlier of Nosib rocks along the approximate axis of the Anabib anticline 50 Km north of the area (fig. 2). A definite, though less intense, deformation has been, therefore, assumed on most of the deep, inferred portions of the structural sections.

The advance of the Sesfontein Thrust and nappes isolated the Mulden exogeosyncline towards the close of the Damara orogeny, whereas intense subsidence may have been antithetic to uplift and granitisation taking place at that time to the west.

It must also be noted that none of the afore-mentioned processes imply crustal shortening and that compressive stress-fields are localised and derived from regional vertical fault displacements in the rigid infrastructure.

4. A Mechanical Basis for the Sliding Hypothesis

The pressure exerted by the sedimentary blanket on the basal slope under the action of gravity was $G=g\rho_b z^1$; where g is the gravitational acceleration, ρ_b is the bulk density and z^1 is the vertical thickness (fig. 9). Where a pre-diastrophic dip θ of about 5-10^0 was developed, G can be split into two components, i.e. S and τ, respectively normal and tangential to the slope along the direction of maximum dip. The shear component $\tau=G\sin\theta$ is much smaller than the normal stress $S=G\cos\theta$ (fig. 9). Thus τ is well below the critical shear stress τ_c capable of producing failure at the base of the potential gliding sheet. This is defined by the Coulomb-Mohr criterion: $\tau_c=\tau_0+S\tan\phi$, which agrees with the physical constants for various rock-materials obtained by triaxial tests (Handin and Hager, 1957). The "initial shear strength" (Hubbert and Rubey, 1959) or "cohesive strength" τ_0 (Hsu, 1969) is an empirical constant depending upon the physical nature of the rock undergoing deformation. The angle of internal friction ϕ is defined as $\tan\phi=\frac{\tau}{S}$.

Failure could not be achieved by increasing the τ component alone through progressive tectonic tilt of the basal slope θ, as this would reach unrealistic values.

The vertical migration of the interstitial fluids, on the other hand, may have been "capped" by the inherently impermeable Lower Otavi pelites, building up abnormally high pore fluid pressure (p) (Hubbert and Rubey, 1959) lowering the effect of S to σ (effective normal stress)=S-p. With increase in pressure (better expressed as pressure/overburden ratio λ_1) at the base of this potential thrust-plane, the mass was more and more sustained by the fluids (λ_1 close to 1). The failure threshold τ_c can thus increasingly approach the initial shear strength τ_0:

$$\tau_c=\tau_0+(1-\lambda_1)\rho_b g z^1\cos\theta\tan\phi$$

as the second member of the equation is drastically reduced (fig. 9). The tilt $\Delta\theta$ to be applied to the basal slope to initiate movement is much smaller, yet many known thrusts and slides, as well as deformation in the Sesfontein karst highveld, could not easily have taken place.

Experiments carried out by Handin et al. (1963), Laubscher

(1961) and Heard and Rubey (1966) have provided increasingly lower values of τ_0 for various rock-materials. Values in the order of 30 bars followed the dehydration of gypsum in evaporitic or lagunal sediments. Physico-chemical changes in clay minerals (Ramsey, 1967), filtration of migrating fluids (Werner, 1961) and ion-exchanges seem to be particularly active in clay-limestone intercalations (Von Engelhardt, 1961), for which (Krsmanovic and Langhof, 1964) very low orders of magnitude of τ_0 ($\pm$2 bars) were recently experimentally obtained. The τ_0 of the Lower Otavi clay-carbonate intercalations cannot have possibly exceeded 30 bars and was likely in the order of 2-5 bars as large amounts of limestone were sheared within the clay-sericite-chlorite intergrowth and the silt-size quartz cataclasts in the phyllonite zone.

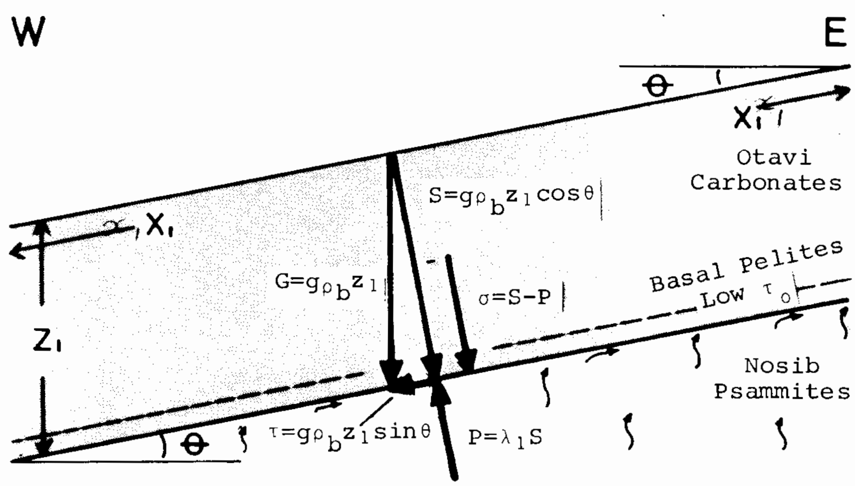

Figure 9. Physical factors acting on the potential plane of failure.

Vugs partially refilled by drusy calcite may formerly have lodged gypsum crystals. In the light of these considerations (i.e. λ_1 tending to 1 and very low values of τ_0, probably between 30 and 2 bars) large overthrusts and slides are no longer a paradox.

Hubbert and Rubey (1959) also postulated that failure is not simultaneous along the base of a slide-block, but propagates as a dislocation along an advancing line of high fluid pressure, leaving a virtually cohesionless mass behind. So once τ_c is overcome and the fracture is initiated, slippage could proceed according to "the law of frictional sliding", which regards τ_0 as numerically negligible:

$$\tau=\sigma\tan\phi.$$

Hsu (1969) disagrees with this assumption, already criticised by Birch (1961). Cohesionless movement, he argues, would lead to catastrophically large overthrusts and slides moving at very high speeds (in the order of 100 m/sec) along infinitesimal slopes. Eye-witnessed high-speed slides, however, are generally limited in extension and extremely shattered (Heim, 1932; Shreve, 1966, 1968). On the contrary, most of the large, practically unshattered overthrusts offer evidence of slow creep while still largely cohesively or rather adhesively attached to their footwalls. Trümpy and Herb (1962), for instance, suggested that the Glarus overthrust in the Helvetian Alps was completed over a period of 10^5-10^6 years, that is at speeds of centimetres or fractions of a centimetre per year. Analogous rates were obtained by Gilluly et al. (1958). As the pelitic and calcirruditic members of the Mulden Formation are the product of erosion and deposition generated by deformation of the Otavi sedimentary blanket, the ratio between their total thickness and the approximate rate of deposition provides a rough estimate of the time elapsed. Even assuming a rather high rate of deposition of 300-600 m/My and a total thickness of autochthonous clastics of 500-600 m at least, 1-2 My would have elapsed during this syn-Mulden phase of deformation.

The average horizontal translation (x_1) as an effect of folding, estimated from the structural sections, seems to be ±30% of the E-W width of the sliding-mass (±65 Km), i.e. less than 20 Km. It can thus be appreciated that the average speed of advancement must have been in the order of one to two centimetres per year. This figure is of necessity purely speculative, but it fits Hsü's opinion (1969 and 1969$_a$) that movement remains throughout somewhat adhesively bound along the detachment surface. It is, however, logical to assume, as both Hubbert and Rubey (discussion, 1969) and Hsu (1969$_a$) agree, that the magnitude of the cohesive forces (τ_0) bounding hanging wall to footwall in an unsheared rock-mass is likely to be larger than that (τ_a) necessary to maintain movement along pre-existing slippage-planes in a material already sheared. This means that dimensional and critical slope values for potential slide-masses, computed by Hsu (1969) for τ_0=30 bars (Table 3) might largely exceed the natural values.

In the case under consideration the preserved thickness of the sliding blanket is about 2000 metres in the north and possibly increases to the west, neglecting the topmost eroded members including part of the Otavi dolomite and an unknown thickness of Otavi phyllite. The original thickness, resting along

Table 3. Angle of Critical Slope (θ_c) and Maximum Translation (x_1) (in Km) of a Gliding-mass under the Action of Gravity, as a Function of z_1 and λ_1, assuming τ_0=30 bars (modified after Hsu, 1969)

	Pressure - overburden Ratio λ_1											
z_1	0.5		0.6		0.7		0.8		0.9		1.0	
(Km)	θ_c	x_1	θ_c	x_1	θ_c	x_1	θ_c	x_1	θ_c	x_1	θ_c	x_1
1.0	23	9.7	20	11	17	13	14	15	11	19	7.5	27
2.0	20	14	17	16	14	19	10	25	7.0	35	3.7	62
3.0	18	18	15	21	12	25	9.1	32	5.8	48	2.5	105
4.0	18	22	15	25	12	30	8.4	39	5.2	60	1.9	155

The underlined figures are in the range of the tectonite under consideration

the western margin of the Kamanjab anticlise on a basal slope of 5-10°, might have ranged in a conservative estimate from 2500 to 3000 m. It has been shown how an anomalously high (possibly not less than 0.8) pressure-overburden ratio (λ_1) was reached along the detachment surface. The length (y_1) of the gliding-blanket extends from the south-east, where the movement hinged due to the pinch out of the Lower Otavi pelites, to roughly 70 Km north of the study area, where the Official Geological Map of South West Africa (1963) reveals a change in the strike around a large, eastward protruding basement inlier. The total length (y_1) could then be ±1° of latitude, i.e. 110-120 Km. In the light of these values an examination of Table 3 shows conclusively the feasibility of the proposed model for any value of τ_0 lower than 30 bars and disregarding hindering effects, overcome by the energy surplus derived from the excess in angular slope $\theta-\theta_c$ and in the τ_0 values used in the computation.

Experimental data on the mechanics of deformation of rock materials at present can provide accurate predictions on laboratory experiments, but only orders of magnitude when applied to nature, due to the multiplicity of elements escaping control. Some of them are worth being summarised again:

i) erosion and sedimentation altering the loads along the basal slope and in toe areas;

ii) relative fluctuation of sea-level influencing the effective weight and lateral support by varying the submerged/emerged ratio in the sliding-mass and controlling erosion and deposition;

iii) progressive lithification with consequent increasing energy absorbed by permanent plastic deformation; and a possible increase in bulk density (ρ_b) in the gliding-sheet due to concomitant volume-by-volume diagenetic dolomitisation;

iv) migration and partial escape of pore fluids with time and consequent release of pressure;

v) positive or negative tilts in the basal slope (θ) due to synchronous upwards propagation of basement faults; and

vi) T-P changes induced by advancing metamorphic fronts.

The shear-components (τ_e) of each of these elements calculated along the direction of sliding can be either positive or negative with respect to the movement. As some components may be of opposite sign and could neutralise reciprocally, only the vectoral balance is meaningful as a final additional hindering or pushing effect.

E. SUMMARY OF THE GEOLOGICAL EVOLUTION OF THE EASTERN DOMAIN

Three major deposition cycles, marked by extremely different sedimentary associations and geometries, compose the volcanic-free, feebly-metamorphosed, later Precambrian succession overlying unconformably the basement gneisses of the Kamanjab inlier. From the oldest these are:

i) Nosib arkose association	: Nosib Formation (Ns)
ii) Otavi carbonate association	: Otavi Series (Outjo Facies) Damara System (D_1)
iii) Mulden greywacke association	: Mulden Formation (Mn)

A westwards thickness-gradient characterises the first two sequences. Pre-diastrophic dips of about 5-10°W were consequently developed at the base of the Otavi Series along a belt bordering the western flank of the Kamanjab inlier. Repeated epeirogenic fluctuation and a related erosion-deposition episode acting on these inclined sequences generated a paraconformity (P^2) at the base of the Otavi Series and the ubiquitous disconformity (D^3) preceeding the deposition of the Tillite Substage around the Kamanjab anticlise. Here, attenuated subsidence or relative uplift seem to have acted constantly against a background of intense regional subsidence.

Due to its marked anadiagenesis and to the interlocking geometry of its basal members the Nosib Formation was structurally more adherent to the basement than to the overlying Otavi carbonate muds and ooze. Upward propagation of deep crustal fractures from a rejuvenated framework in the basement induced comparatively brittle deformation in the Nosib and extremely plastic effects in the Otavi carbonate blanket. Moreover differential compaction, fracturing and uplift at the western edge of the rigid Kamanjab inlier accentuated the western dip of the Otavi-Nosib contact in pre-Mulden times, until it exceeded the critical value θ_c for which slow westwards creeping of the overlying carbonate blanket became possible under the action of gravity alone. Detachment occurred along the pelitic base of the Otavi Series just above the Nosib clastics on account of the locally very low inherent cohesive strength (τ_0) and of the possible action of abnormal pore fluid pressure.

Movement must always have been extremely slow (i.e. completed over $\pm$1-2 My, at speeds less than 1-2 cm/year) and somewhat adhesively bound to this first generation basal slope. Deformation into longitudinal F_2O flexural-slip folds occurred as a consequence of slowing down or stopping of the advancing mass to the west. This was reflected in a marked increase in intensity of deformation towards the west.

Typical box- or mushroom-like anticlines in elevated areas reflect the initial inability of the incompletely consolidated sediments to be lifted above sea-level by lateral compression due to the larger effective weight in non-hydrostatic environments. Towards the end, however, progressive lithification increased the competency, allowing definite lateral vectoral stresses to push major anticlines above sea-level, inducing, at the same time, partial deformation of the underlying Nosib.

At a later stage, the basal slope must again have undergone deep faulting and consequent localised steepening along NS and NW belts. At high levels of folding this was matched by plastic overturning and macroscopic fanning of the pre-existing or developing F_2O structures.

Exogeosynclinal basins or foredeeps were initially filled by the products of erosion of the Upper Otavi members, forming the syn- to post-orogenic Mulden pelites which are the ultimate results of this deformation. These clastics, deposited in F_2O synclinal basins, underwent F_2M slip folding on a mesoscopic scale due to the action of gravity along the steepening flanks of outstanding Otavi dolomite anticlines. Both sets of structures were subsequently transgressed by the Sesfontein Thrust (D_6) advancing from the west and largely contributing to the deposition of the uppermost Mulden molasse and later by quantitatively subordinate kink folds (F_7) related to NE striking wrench faults.

In conclusion, it must be remarked:

i) that no exceptionally intense tectonic event was necessary to generate the folding as conditions of precarious balance were initially produced in the sedimentary basin;

ii) that compressional stress-fields locally developed as a consequence of initial tension generated by gravity alone; and

iii) that no crustal shortening, only vertical displacements, are involved in the whole deformative process.

III. THE WESTERN STRUCTURAL-STRATIGRAPHIC DOMAIN

A. GEOGRAPHIC DISTRIBUTION

This domain extends from west of Sesfontein to the Atlantic Ocean across three successive physiographic regions:

i) An eastern, homoclinal mountainland (Hills, 1963), controlled by a dominant westerly foliation, culminating in a few peaks exceeding 1200 m above m.s.l.; which grades westwards into

ii) N-S aligned inselbergen-pediplain belts, gradually losing their individuality and fading into the

iii) Namib Desert Plain (Gevers, 1936), a gently rolling hammada along which the Precambrian rocks are progressively concealed below isolated or coalescent barkans moving before the prevalent south-westerly wind. The resulting 10 to 15 Km wide dune belt along the Atlantic coast has obstructed the Hoanib River mouth, forming the Ausis Swamps at the western limit of the area investigated. The ephemeral Hoanib River, crossing the domain from east to west, therefore, differs from the adjoining Hoarusib and Unjab drainages in its endoreic (de Martonne, 1929) character.

B. STRATIGRAPHY AND LITHOLOGY

Only rocks belonging to the Nosib Formation and the Swakop Facies of the Damara System occur west of the Sesfontein Thrust. The bulk of the sequence is composed of clastics and only very subordinately of lenticular carbonates.

Intense metamorphism and deformation have obscured and in certain instances completely obliterated the sedimentary structures of this eugoesynclinal succession (Martin, 1965). Metavolcanics appear to be typically interbedded within the sediments.

Lithostratigraphic equivalents of the depositional cycles of the eastern domain can be established, with the exception of the Mulden Formation, which possibly was not deposited locally.

An isochronous horizon, connecting the two facies, probably lies within the Tillite Substage (see Stratigraphic Legend in pocket).

Neither the base, nor the top of the late Precambrian Nosib-Damara sequence is exposed anywhere in the area.

The preserved stratigraphic succession can be subdivided into two major sedimentation cycles, which are from the bottom:

i) The Nosib arenite-greywacke association : Nosib Formation (Ns)

ii) The Damara shale-greywacke association : Swakop Facies of the Damara System (D).

1. The Nosib Formation (Ns)

Two successive and partially intertongueing stages were distinguished.

The base of the essentially psammitic <u>Lower Stage</u> (Nsl) is not exposed locally. More than 2000 m of thickly to thinly bedded, occasionally cross-bedded, poorly to moderately sorted quartzite or arkosic quartzite (NslQ) (average feldspar content ±27%), grit and local intraformational conglomerate form its bulk. Lenses of this conglomerate are discontinuously developed in the Aub-Nunarus area where its thickness exceeds 200 m. The poorly sorted and moderately rounded boulders and pebbles are substantially monogenetic, as quartzite and vein-quartz compose most of them, while leucocratic gneiss and amphibolite are rare. The matrix is always pelitic (mica schist). Subordinate pelitic members (now mica schist) and interbedded basic lavas and intrusions (now concordant and discordant orthoamphibolite (Au_1) are confined to the top of the stage).

The <u>Upper Stage</u> (Nsu), which follows concordantly, is essentially pelitic. Evenly and rather thinly bedded shale and greywacke (now biotite schist and gneiss (NsuGn)), intercalated with occasional arkosic arenite (feldspathic metaquartzite (NsuQ)) must have composed the bulk of this stage which locally exceeds 1500 m in thickness.

2. The Damara System (D) (Swakop Facies)

This sequence overlies the Nosib clastics paraconformably over most of the area (P^2 in sheet 1913A and Stratigraphic Legend).

A marked angular unconformity is, however, developed along two N-S belts running along the Andib and Ganamub Rivers and to the south of the Hoanib-Murodib confluence.

The sequence can be subdivided into the Hakos Series (D_1) and the Khomas Series (D_2). Westwards sedimentary thinning and eventual disappearance of all the Lower Hakos and most of the Upper Hakos members (including the Tillite Substage) takes place over the eastern half of sheet 1913A. The stratigraphic succession described below must therefore be regarded as a composite sequence.

Thicknesses were evaluated with difficulty because of their inconsistency and of tectonic repetition. The values supplied must be considered as approximate.

a. The Hakos Series (D_1)

A discontinuous (up to 10 m thick) band of dark polygenetic conglomerate or grit ($D_1 lR$) cemented by a calcareous or pelitic, ferruginous matrix marks the base of its Lower Stage ($D_1 l$). The unsorted and poorly rounded pebbles are composed of quartzite, gneiss and amphibolite. Boudined pseudo-pebbles of light-coloured carbonates are of common occurrence. A variable thickness (60-100 m) of a very dark coloured ferruginous, pelitic member ($D_1 lS_1$) follows concordantly. At the southern nose of the Andib anticlinorium and along the western margin of the Aub plains the iron content increases and the rock becomes a layered ironstone. Elsewhere the pelitic fraction is predominant, and a dense, very dark sericite-chlorite-biotite schist is then developed. The light to dark grey phyllitic or sandy schist ($D_1 lS_2$) which follows, has extremely variable thickness (several hundred metres) and is occasionally graphitic. Itabirite and siliceous carbonate ($D_1 lC_1$) intercalations are scattered throughout the sequence, becoming dominantly developed at the southern nose of the Andib anticlinorium, where they stand out topographically from the easily eroded schist. Higher up infrequent carbonate bands ($D_1 lC_2$) accompany increasingly coarser grained schists ($D_1 lS_3$). Several concordant and discordant generally coarse-grained amphibolite bodies, emplaced within these sediments, seem related to the pre-Tillite Khankhaib Gabbroid Complex (A Ng) (p. 58) and must be regarded as sills and stocks. The highest member contains numerous bands of comparatively pure sericitic quartzite ($D_1 lQ$). In the Khankhaib-Mudorib area (sheets 1913A and B) a fine-grained quartz-amphibole schist ($D_1 lAm$) is concordantly intercalated towards the top of this sequence. Textural considerations and development of this meta-amphibolite over more than a thousand square kilometres suggest that it must be regarded as an integral part of the sedimentary succession. Lentiform basinal carbonates ($D_1 lC_3$) (Krumbein and Sloss, 1963) reappear towards the top of the sequence.

The Upper Hakos Stage ($D_1 u$) is marked at its base by the Tillite Substage ($D_1 uG$). This is composed of an extremely thick sequence of poorly and unevenly bedded black, brown or grey biotite-sericite-chlorite schists ($D_1 uS_1$) containing siliceous carbonate and iron ore intercalations. Densely or loosely packed, extremely unsorted and angular, polygenetic rudaceous material is to be found embedded in the schist almost everywhere. The size of the boulders, of leucocratic or granodioritic gneiss, amphibolite, quartzite, vein-quartz and subordinate carbonate rocks, is extremely variable and ranges from rare 80-100 cm blocks to an average common size of 5-10 cm. Light or cream coloured pseudo-pebbles, derived from boudinage of carbonate lenses, are very common.

A variable thickness of phyllitic, occasionally (Mudorib area) graphitic schist (D_1uS_2) containing calcareous intercalations (D_1uC) is then developed. These carbonate bands, though relatively thin (0.50-10.0 m), are remarkably persistent throughout some of the highly metamorphosed areas, where they provide reliable information on the stratigraphy and the attitude of the bedding-planes. Progressive change in their mineral paragenesis gives a valuable indication of the metamorphic gradient in the area.

b. The Khomas Series (D_2)

The Khomas Series is an extremely thick (more than 4000 m) and monotonous, essentially semi-pelitic schistose greywacke association. Psammitic intercalations are locally very limited if compared with the characteristic sequence south of Windhoek (Gevers, 1934; Schalk and Hälbich, 1965; Guj, 1967) and in western Damaraland. Rare, fairly well-rounded pebbles of quartzite, vein-quartz and leucocratic gneiss are dispersed throughout the sequence in the lower Mudorib area. Discontinuous pure quartzite intercalations were observed south of Mt. Sima, where they provide one of the few relics of sedimentary stratification in highly deformed environments. The base of the sequence was set above the last significant calcareous band (Hakos Marble) and related pelitic schist by analogy with the stratigraphy established by Smith (1965) in the Khan and Swakop River area, which most closely resembles the terrain under discussion. Such a subdivision fits the Hoanib and Mudorib area (sheet 1913A) unambiguously. In the northern Hoarusib and Gomatum area (sheet 1813C) this contact becomes somewhat arbitrary, as schistose greywacke typical of the Khomas Series interfingers with the Hakos schist well below the same carbonate band, which can be traced all the way northwards from the definite contact established along the Hoanib River. The top of the sequence is not exposed anywhere in the area.

C. SEDIMENTARY ANALYSIS OF THE DAMARA EUGEOSYNCLINE

No direct transition between the eastern (Outjo) and western (Swakop) Facies of the Nosib-Damara succession was observed in the area, as the contact is tectonic (Sesfontein Thrust).

As already stated, the proposed stratigraphic column must be regarded as a composite succession. This implies that:

i) Not all the members were developed everywhere.

ii) Lithostratigraphically similar members are not necessarily synchronous all over the area. A probable exception to this rule is the Tillite Substage which, due to paleoclimatic implications, is likely to be the only chronostratigraphic link between the mio- and the eugeosynclinal facies.

1. The Nosib Sedimentary Cycle

The basement-Nosib unconformity (U^1) is not exposed in the area. That the eugeosynclinal facies of the Nosib Formation rests unconformably on the basement rocks, however, has been observed in several areas (Martin, 1965; Smith, 1965; Schalk and Hälbich, 1965). Locally the lowermost stratigraphic level reached by erosion in the core of the Khudobib brachyanticline still lies within the Lower Nosib psammites approximately 2000 m below the Upper-Lower Nosib contact i.e. ± 3500 m below the base of the Damara System. What thickness of Nosib clastics still underlies that point is unknown.

All the differences between the eastern and western psammitic members are essentially due to the metamorphic and deformational history, with the possible exception of a slightly higher maturity (better sorting and lower feldspar content) and more arenitic character in the west. The depositional environments must therefore have been very similar and there is no doubt that these two lithosomes can be regarded as lithostratigraphic equivalents. They are likely, however, to be somewhat asynchronous. As the craton was progressively engulfed from the west, the Nosib clastic association must have migrated with the transgressive sea (fig.10) towards the eastern source of subaerial denudation and coarse feldspathic debris supply.

Farther from the shoreline (i.e. in the west) the only sediment available was of a much finer grain. Upper Nosib shale and greywacke then started to intertongue with the arkose and arenite, to become prevalent as the Nosib transgression proceeded. In spite of metamorphism the Upper Nosib metasediments have preserved something of their original rhythmic cycles grading from subordinate feldspathic wacke and arenite into greywacke and shale over a thickness in the order of 10-20 m or more. It is conceivable that the basin had already undergone considerable subsidence towards the close of the Upper Nosib cycle and was rapidly filled by turbidites.

Generalising, both the basement-Nosib and Lower Nosib-Upper Nosib contacts are "migratory" and have only lithostratigraphic, non-isochronous significance. It may also be presumed that the Nosib coarse arkosic sedimentation occurred in the miogeosyncline concomitantly with the Upper Nosib finer pelite and greywacke deposition in the eugeosyncline (eg. points A and B in fig.10), which results from the different (pelagic) environment and transport (turbidites). What difference in sedimentation age may exist between the base of the late Precambrian sequence in the eugeosynclinal trough and on the platform is difficult to estimate as it depends upon two variables (i.e. rate of sedimentation and maximum

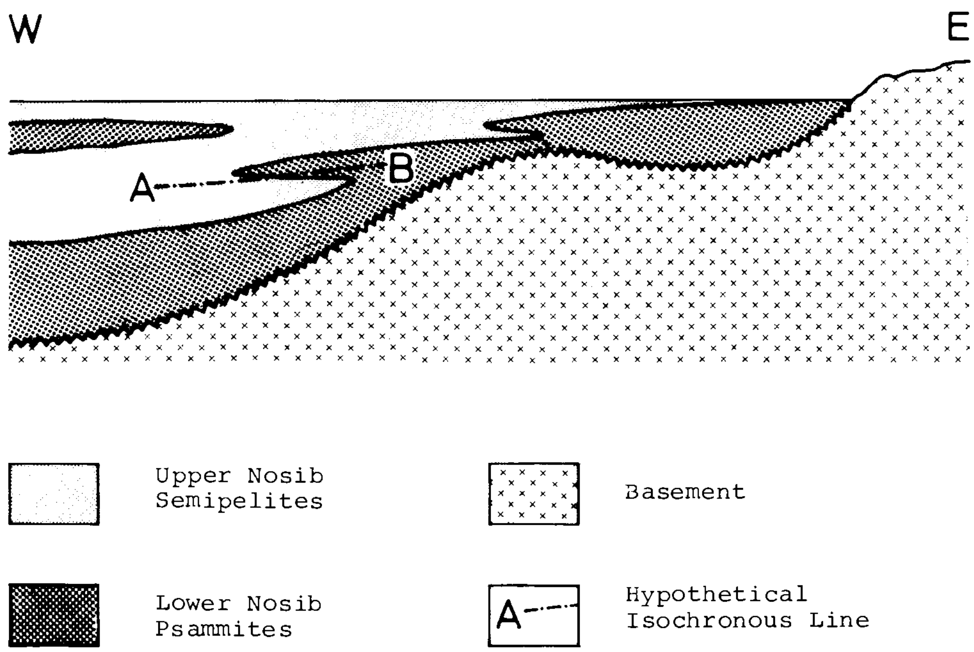

Figure 10. Diagrammatic section showing the possible stratigraphic relation between Lower and Upper Nosib clastics.

thickness) which are both unknown. Locally, over a distance of 100 Km the difference in thickness exceeds 2500 m. As neither the base of the Nosib clastics nor the centre of the original basin is exposed, the difference could be much larger and even assuming a rather high sedimentation rate, the Nosib transgression might have lasted several million years.

The limit between eu- and miogeosyncline is traditionally marked by the appearance of volcanicity (Kay, 1951) along the hinge-belt where deep fractures have been induced by the intense differential subsidence necessary to accommodate the extremely rapid clastic accumulation. These syn-depositional igneous occurrences will be described briefly in the following chapter D.

2. The Damara Sedimentary Cycle

The marked U^2 angular unconformity, detected along two N-S elongated belts, extends over about 16% (i.e. 155 Km) of the

Plate 7. The overturned Nosib-Damara U^2 unconformity west of the Aub Plains.

950 Km of Nosib-Damara contact exposed in the study area. This is in contrast to the eastern structural-stratigraphic domain, where the Nosib-Damara contact is everywhere paraconformable. The first and more extensive unconformity belt runs just to the west of the Aub Plains (Plate 7) and can be followed throughout the area from the Andib valley to the northern Ganamub River (sheet 1913B and U^2 in fig.11). The second starts imperceptibly south-west of the Hoanib-Mudorib confluence to attain obvious angular values at the southern margin of sheet 1913A (U^2/D^3in fig.11). Along the eastern (Andib-Ganamub) ridge the Damara-Nosib U^2 unconformity is overlain by a variable thickness (more than 2000 m maximum) of Lower Hakos schists, resting on a basal conglomerate, and followed by tillite. The Nosib sediments, therefore, were here deformed (F_1N) and concomitantly (M_1) metamorphosed prior to the Lower Hakos sedimentation.

The basal Hakos members are generally highly ferruginous, Mn-rich and occasionally graphitic, all elements pointing towards initially shallow, possibly non-marine environments characterised by low energy and Eh, established while the tectonised belt was again partially transformed into an actively subsiding furrow. The undoubtedly sedimentary, progressive pinching out of the Lower Hakos-Tillite succession if followed westwards across the Mudorib Syncline towards the second belt (structural section JK and fig.

11), indicates that this must have developed as a positive area complementary to the subsiding Andib-Ganamub trough during most of the Lower Hakos sedimentation. The Upper Nosib rocks were here eroded and the unconformity created during the regional uplift, preceding or accompanying the deposition of the Damara tillite, which impressed its imprint also on the eastern structural stratigraphic domain (p.9), creating the (D^3) disconformity. Along the second belt the Upper Hakos marble and related schists rest above the unconformity surface on a discontinuous veneer of reddish metagrit. The geological setting is similar to that observed by Smith (1965, p.22) in the Khan and Swakop River area, and conceivably over most of the Damara geosyncline.

The presence of Lower Hakos sediments above the eastern unconformity belt and their thinning westwards followed by complete disappearance above the second unconformity belt indicate that the basal U^2 Damara-Nosib unconformity has locally migrated westwards.

It can be concluded that, prior to Upper Hakos times, westwards shifting, wave-like tectonic pulses created positive geanticlinal ridges, rising or subsiding at a much lower rate than the rapidly sinking troughs. This process influenced the thickness and type of sedimentation over a very long span of time, and induced progressive pinching out of some of the basal members and intensive reworking of large masses of sediments, leading to a gradual transition from evident angular unconformity to paraconformity observed at the base of the Damara System. The unfolded or slightly tilted Damara sequence was then upwarped jointly over the deformed and metamorphosed ("pseudo-cratonised") Nosib substratum during pre-Tillite or Tillite times. Consequently, a regional uplift of considerable amplitude was accompanied by only very moderate angular deformation. However, as in the Hoanib-Mudorib belt, where the deformed Nosib metasediments were reached by the consequent erosion, a definite angular unconformity was "inherited" (point A in fig. 11).

The debris resulting from erosion of the Lower Hakos cover and of the underlying Nosib was transported westwards and redistributed by turbidites into actively subsiding portions of the eugeosyncline, where the Khomas greywacke association was being deposited.

The upwarped area was by now fairly well levelled and possibly again rather shallowly submerged. The Upper Hakos pelite-carbonate assemblage was thus deposited under slow regional subsidence in this neritic to sub-pelagic, high-energy environment, as the extreme areal persistence of its carbonate member seems to confirm.

The hinge-line and belt of rapid subsidence were concomitantly shifted westwards where, judging by the thicknesses and thickness-gradients involved, immature sediments must have been

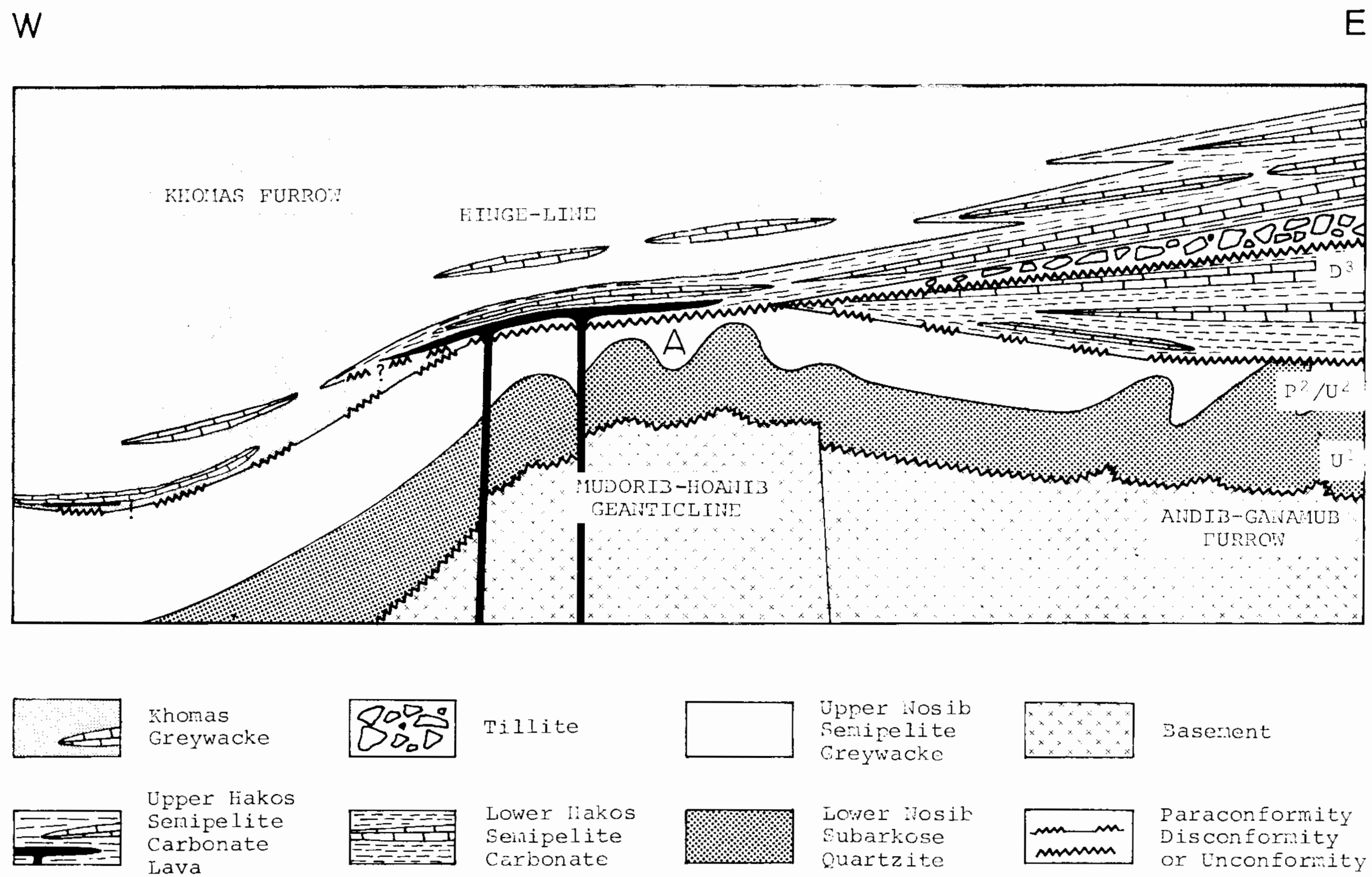

Figure 11. Facies distribution in late Khomas time in the western domain

literally poured into this collapsing "Khomas" furrow, while the areas of early Damara deformation followed the subsidence sluggishly.

Effusion of lava of intermediate to acid composition (Noeroep metavolcanics, p.56 and fig. 11) seems to be associated with the crustal fractures generated by such an intense differential subsidence.

No less than 4000 m of shale and greywacke accumulated locally. Subsidence, however, must have taken place in successive "pulses" because in the hinge belt comparatively rapid accumulation of a typical Khomas schistose greywacke intertongued with a more mature and slowly accumulated pelitic-carbonate assemblage. When the influence of the downwarping became more extensive, greywacke was deposited in areas underlain by thin Lower Hakos and Tillite rocks, e.g. Mudorib and Otjihue synclines (sections ABC and JK). Only here is the full "possible" Damara succession developed and minor thicknesses of Khomas schistose greywacke were observed to overlie the Upper Hakos schist-carbonate suite and the Tillite. This seems to confirm Gevers' (1963, p.208) and Martin's (1965, p.40) views that the Upper Hakos-Khomas contact may be stratigraphically somewhat unwarranted. This distinction should be applied, bearing in mind its non-chronological value in the north-western Kaokoveld, as the Damara stratigraphic sequence may turn out to be largely or exclusively composed of Khomas gneisses.

The inversion of relief, which in late Precambrian or early Cambrian times followed the collapse of the Khomas furrow, was reflected in the polyphase deformation, metamorphism and anatexis known as the Damaran Orogeny (Martin, 1965) or the Damaran tectono-thermal episode (Clifford, 1967) of sub-continental extent.

The top of the Khomas sequence is not exposed anywhere in the area, nor does the Mulden Formation come into contact with it. Their possible genetic relationship, however, has already been discussed in a previous chapter (p.15).

Analysing the problem of the great thickness of the Khomas Series, Martin (1965, p.41) maintains that: "The area or areas from which the erosion products were derived must have been extensive and must have undergone rapid erosion of the pre-Damara basement, for an erosion of the Lower Damara sequence alone would probably not have yielded such a large volume of generally badly sorted materials". He adds: "In the northern part of the geosyncline both the Kamanjab inlier and the Grootfontein inlier.... may have filled this role". So far as the western Kaokoveld branch of the Damara geosyncline is concerned, the present author is inclined to disagree partially with these deductions. There is no doubt that a considerable amount of detritus was derived from the Kamanjab inlier, though stratigraphic considerations suggest that during at least part of the Damara sedimentation most of the inlier must have been concealed below a veneer of Nosib-Otavi sediments (p.13). However, even assuming that all the present extent of the Kaokoveld basement inliers was a source area during Khomas times, several difficulties arise:

i) The conveyance of the finest fractions of the erosional products of the granitoid Kamanjab inlier towards the eugeosyncline, bypassing the miogeosynclinal trough, should have left behind large amounts of coarse, possibly arkosic material. No coarse clastic sequence is exposed around the inlier with the exception of the Mulden Formation, for which a post-Khomas age has been postulated by Frets (1969, p.110). In places (i.e. west of Fransfontein), this overlies the basement directly, suggesting that it could not easily have originated from its local erosion.

ii) Considering only the western Kaokoveld branch of the Damara geosyncline (i.e. north of 21° latitude S and west of 15° longitude E), the surface of exposed basement inliers is $\pm 15,000$ Km^2, i.e. one-fifth of the area underlain by eugeosynclinal (Swakop Facies) metasediments ($\pm 70,000$ Km^2). If all the sediments composing the Khomas Series (>4000 m in thickness) were to be derived from the basement inliers, uplift should have been very much faster in the inlier than subsidence in the basin to provide sufficient material. Even taking a conservative average thickness of 3 Km for the Khomas Series over the known eugeosyncline, neglecting the unknown western extension and assuming no crustal shortening, 280,000 Km^3 of sediments deposited would imply an unrealistic uplift in the basement inliers of the order of several thousand metres during Khomas time only. It is true that the structural-stratigraphic analysis of the eastern domain (p.16) has shown that considerable differential movement was concentrated along the western margin of the Kamanjab inlier throughout the Damara sedimentation, but the disconformable relation and transgressive overlapping attitude of all the post-Tillite formations (Martin, 1965) indicates that most of the effective uplift exposing the inliers to subaerial erosion occurred prior to, or concomitantly with, the creation of the Tillite disconformity. Whereas, after the deposition of the Damara tillite, while gradually covered by the Otavi dolomite, the positive tectonic character of the inliers, relative to the adjoining more rapidly subsiding miogeosyncline, can be better expressed in terms of slower subsidence rather than of proper uplift.

Some other source areas and/or processes must, therefore, be sought after to justify at least partially the extreme thickness of the Khomas Series.

Four factors, in the present author's opinion, play an important role:

i) The evidence that the Khomas Series was not deposited everywhere in the N-S eugeosyncline or at least not with the same thickness. If deposition had taken place only in the westernmost "Khomas" furrow, prior to relative stabilisation and uplift of the Andib-Ganamub and Hoanib-Mudorib belts, the area of effective sedimentation would be greatly reduced and the erosion/sedimentation balance more closely approached.

ii) The regional extent and so far scarcely appreciated amplitude of the pre-Tillite discordance, developed over most of the country with the exception of typical high-thickness Khomas areas, which must have produced an enormous amount of clastics with a minimum of vertical displacement.

iii) It has also been assumed so far that the Khomas clastics were derived exclusively from the east, possibly as a result of the lack of information about the western edge of the Khomas furrow. However, as no detailed sedimentological investigation of the Khomas greywacke association has as yet been undertaken, a partial sediment supply from the west, though unlikely cannot be totally excluded.

iv) The syn-depositional Noeroep volcanism, so far unknown or scarcely investigated, might have produced intercalations of pyroclastics within the Khomas schistose greywacke, which escaped detection on account of their advanced metamorphism.

In conclusion the anomalous thickness of the Khomas Series could be the result of a westwards migration of the lines of maximum subsidence (eugeosynclinal furrow) and subsidence-gradient (hinge-line) in front of oscillatory tectonic pulses propagating from the craton and pushing forward a wave of reworked clastics. This process might have induced concentration and rapid accumulation of the available detritus and at the same time narrowing of the belt of intensive subsidence with consequent increase in sedimentation rates. When subsidence became deep enough to generate metamorphism and metatexis (Andib-Ganamub and Hoanib-Mudorib belts) the deformed areas were "pseudo-cratonised" and jointly upwarped in pre-Tillite times. Large amounts of clastics were thus generated by positive movements of comparatively small amplitude over extremely extensive areas and literally poured as turbidites into a finally well-established distal "Khomas" furrow. Subsidence then reached its climax as the basin floor was sinking to

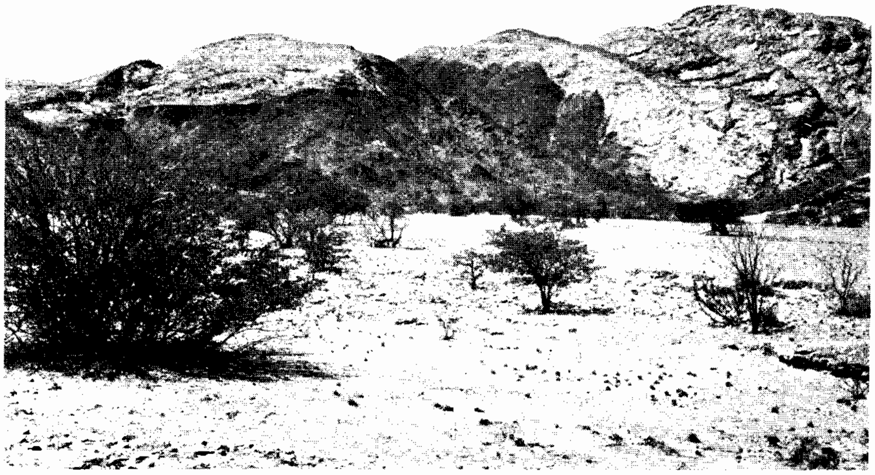

Plate 8. The Khankhaib Gabbroic Complex (dark) intruding the Lower Hakos metasediments

Plate 9. A roof pendant of "resisters" (marble and quartzite) in the metagabbro

levels of migmatisation and anatexis.

It was only with the consequent major inversion of relief (Damara orogeny) that this westwards migration was interrupted and then reversed. The bulging of the granitic/granodioritic infrastructure created slopes sufficient to convey nappes towards the craton (chapter E), isolating large non-marine exogeosynclines which were progressively filled by the Mulden molasse.

D. SYNDEPOSITIONAL IGNEOUS ACTIVITY OF NOSIB OR EARLY-DAMARA AGE

Both concordant and discordant orthoamphibolites are rather uncommon within the Lower Nosib psammites, but become very frequent within the Upper Nosib and Lower Hakos semipelites. Metamorphism has generally obscured or even completely obliterated their original igneous structures and textures, as well as their mineralogy (p. 103), while deformation has often transposed their geometric attitude with respect to the bedding foliation of the invaded sediments. Nevertheless, three major subdivisions can be made on a regional scale on the basis of their geometry and of a few palimpsest textures:

i) Early- to late-Nosib basic (doleritic) and ultrabasic hypabyssal sills, dykes and possibly lavas (AU_1)
ii) Late-Nosib to early-Damara intermediate to acid lavas: Noeroep metavolcanics (ML)
iii) Early-Damara (pre-Tillite) gabbroid intrusions, with basic and ultrabasic satellite stocks and sills: Khankhaib Gabbroic Complex (ANg)

Suite (i) accompanies the Nosib metasediments ubiquitously and can be distinguished from suite (iii) as it normally bears the imprint of a pre-Damara phase of deformation (F_1N) and metamorphism (M_1), absent in the latter. Intersections of the two successive generations of basic intrusions, though not too common, were observed in the high Andib valley.

The igneous origin of suite (i) is proved by occasionally preserved blastophitic textures (specimen 23) clearly inherited from a parent rock belonging to the gabbroic clan. Rare trachytoid blastoporphyritic textures (specimen 125), obviously derived from an original lava, were also observed. As such textures are relatively rare, especially in concordant bodies, distinction from the para-amphibolites, derived from recrystallisation and metamorphic differentiation of marly pelites, becomes rather difficult in the field. A finer grain, and variable amounts of quartz and biotite, normally subordinate or absent in orthoamphibolites, characterise the latter. The metamorphic texture and mineral parageneses of these rocks, however, will be described in some detail in

Plate 10. An undeformed and unmetamorphosed soda-aplite dyke cutting foliated metagabbro

the section devoted to the metamorphism.

The Noeroep metavolcanics (ii) are developed only to the west of the Noeroep brachyanticline, where volcanicity must have been relatively intense during early-Damara times. It is likely, in fact, that a great deal of the dark fine-grained schists, commonly encountered just above the Damara-Nosib contact in the western half of sheet 1913A, may prove to be of metavolcanic origin if petrographically and geochemically investigated in proper detail. For the purpose of the present paper the emphasis is placed essentially upon the most widespread lithotype in which the blastoporphyritic texture is undoubtedly derived from an original volcanic texture. Sample 4/107/7 represents a rather continuous flow along the Nosib-Damara contact across the Hoanib-Mudorib confluence, possibly developed over an area of several hundred square kilometres with extremely variable thickness normally not exceeding 100 m. Phenocrysts of calcic oligoclase and hornblende are set in a rather fine-grained groundmass, inhomogeneously devitrified and coarsened slightly by the relatively high-grade metamorphism undergone.

As the poor resolution due to the fine and uneven grain of the matrix hampered the microscopic volumetric determination of its mineral constituents, sample 4/107/7 has been chemically analysed. Its composition (Table 4) matches quite closely that of the average

	Sample	307	139	137	4/107/7	308
		Quartz-anorthosite	Anorthositic gabbro	Pyroxenitic gabbro	Dacite	Soda-aplite
CHEMICAL ANALYSES	SiO_2	67.76	49.00	48.35	65.14	74.67
	TiO_2	0.31	2.11	1.68	0.81	0.25
	Al_2O_3	12.78	18.63	13.77	14.86	13.04
	Fe_2O_3	4.92	2.25	2.52	2.42	0.48
	FeO	1.26	8.70	9.41	3.86	1.58
	MnO	0.06	0.13	0.04	0.11	0.03
	MgO	0.22	3.19	9.02	1.96	0.36
	CaO	11.72	8.59	12.98	2.77	1.79
	Na_2O	0.01	4.81	1.73	3.99	7.18
	K_2O	0.03	0.42	0.25	2.58	0.11
	P_2O_5	0.16	0.34	-	0.22	0.04
	L.o.i.	1.16	0.82	0.20	1.13	0.11
	H_2O	0.18	0.08	0.26	0.12	0.48
	Total	100.57	99.07	100.21	99.97	100.12
CATION PROPORTIONS	Si	67.12	46.34	56.27	61.73	68.82
	Ti	0.23	1.50	0.47	0.58	0.17
	Al	14.93	20.77	18.44	16.60	14.17
	Fe^{3}	3.67	1.60	2.31	1.73	0.33
	Fe^{2}	1.04	6.88	2.79	3.06	1.22
	Mn	0.05	0.10	-	0.09	0.02
	Mg	0.32	4.50	4.57	2.77	0.49
	Ca	12.44	8.70	5.81	2.81	1.77
	Na	0.02	8.82	6.71	7.33	12.83
	K	0.04	0.51	2.64	3.12	0.13
	P	0.13	0.27	-	0.18	0.03
	Total	100.00	100.00	100.00	100.00	100.00
KATANORMS	Q	46.93	-	-	-	26.22
	Or	0.19	2.53	1.50	-	0.65
	Lc	-	-	-	-	-
	Ab	0.10	40.42	15.73	-	64.17
	Ne	-	2.21	-	-	-
	An	37.18	28.61	29.45	-	3.02
	C	-	-	-	-	-
	Di	1.50	10.11	28.61	-	4.45
	Wo	8.81	-	-	-	-
	Hy	-	-	14.14	-	0.57
	Ol	-	9.98	5.54	-	-
	Mt	2.44	2.40	2.67	-	0.50
	He	2.04	-	-	-	-
	Il	0.46	3.00	2.37	-	0.35
	Ap	0.36	0.73	-	-	0.08
	Total	100.01	99.99	100.01	-	100.01

Loss at 950°C

All analyses executed in the Geochemistry Department of the University of Cape Town by Mr. J.P. Willis and Dr. J.J. Gurney using the method of Norrish and Hutton (1969)

Table 4. Chemical Analyses, Cation Proportions and Katanorms of Metamorphosed Syndepositional Intrusives and Lavas

dacite (Johannsen, 1948).

The volcanism occurring during the Hakos sedimentation along the hinge-line of the "Khomas" eugeosynclinal furrow has thus rather acid character and might be considered as a "subsequent" extrusion (Stille, 1940), which followed the tectonic unrest of late-Nosib and pre-Tillite age along the Andib-Ganamub furrow and Mudorib geanticline as shown in figure 11.

The Khankhaib Gabbroic Complex (iii) includes several basic bodies intruding all the Precambrian metasediments older than the Damara Tillite, by which it is overlain nonconformably.

The bulk of most of the occurrences in the high Andib Valley and along the eastern flank of the Mudorib syncline is a rather undifferentiated fine- or medium-grained nematoblastic amphibolite. A relatively large intrusion exposed SW of the Khankhaib Plains, in contrast, exhibits a rather differentiated character. This complex, roughly 1 Km in diameter, forms a conspicuously dark mass unambiguously intrusive into the Lower Hakos metasediments (Plate 8). Relatively large xenoliths and roof pendants (Plate 9) of country rocks and resisters in particular (i.e. quartzite and marble) "floating" in the gabbro are not uncommon. At or near the contact a peculiar whitish fine-grained rock with glomeroblasts of biotite, chlorite, actinolite and occasional garnet set in a leucocratic fine-grained plagioclase- and epidote-rich matrix is likely to be a relic of an original hybrid contact metamorphic aureole which has survived the subsequent Damaran regional dynamothermal metamorphism (p. 97). Occasional masses of yellowish-brown, coarse-grained, leucocratic feldspar-quartz-epidote rock (sample 307) may also be a metamorphosed contaminated quartz-anorthositic member belonging to the contact zone.

No rhythmic layering was observed either in the massive intrusive body or in the associated sills, which are essentially composed of:

i) Coarse- to very coarse-grained and massive, strongly deformed meta-anorthositic gabbro (sample 139) intruded by

ii) a fine- to medium-grained, deformed and metamorphosed amphibolite, derived possibly from a parent pyroxenitic gabbro (sample 137) or pyroxenite. Both suites are transgressed by

iii) later, subordinate, undeformed and unmetamorphosed dykes of soda-aplite (sample 308) (Plate 10).

As the Khankhaib Complex falls within one of the lowest-grade zones of the Damaran metamorphic front (p. 97) and as there is no field or microscopic evidence of potash-metasomatism over a very large area, it seemed justified to analyse four specimens representative of the most common suites to obtain some indication of their pre-metamorphic mineralogy by means of kata-norms calculated according to Barth's method (1959). The absence of potash-metasomatism was later substantiated by the low K_2O content of all the rocks analysed, which ranges between 0.03 and 0.42% (Table 4).

The Damaran metamorphism has radically transformed the mineralogical composition of all the samples except sample 308. The similarity between the modal and normative mineralogy of this dyke together with its undeformed attitude confirm that this third phase of intrusion is later than the Damaran tectono-thermal episode and must, therefore, be excluded from the Khankhaib Complex <u>sensu stricto</u>.

There seems to be a gradual transition in the field from gabbros through gabbroic anorthosites to true anorthosites, marginally contaminated by the country rocks, similarly to what was observed by Mathias (1956; p.9) in the Messum Complex. The discordant intrusion of plagioclase-poor amphibolites (originally melanogabbros or pyroxenites) might correspond to the uprise of the melanocratic counterpart essentially concentrated at lower levels in the intrusive body and injected later into the gabbro-anorthositic mass and country rock.

E. STRUCTURAL ANALYSIS

The structural element common to all the western domain is a ubiquitously developed and generally NNW trending regional F_2S folding, with a tendency to be eastwards inclined, overturned or recumbent. The scale, style and mechanism of deformation gradually change towards the west due to a multiplicity of factors among which are:

i) The position with respect to the cratonic edge of the geosyncline, implying broad facies and therefore lithological changes

ii) The varying influence of the westward Damaran metamorphic gradient (p. 96) and the migmatisation radiating from the axial zone

iii) The westward increase in the magnitude of the orogenetic uplift and the consequent increase in the depth of erosion.

Accordingly the western structural domain can be subdivided into three successive zones, shown in folders 4 and 6(b), which from the east are:

i) The nappe zone, composed of large eastwards recumbent folds of weakly metamorphosed (greenschist facies), inhomogeneous metasediments.

ii) The root zone of steep eastward overturned isoclinal folds and domal structures of highly metamorphosed (amphibolite-granulite facies), inhomogeneous metasediments.

iii) The axial uplift composed of highly metamorphosed (amphibolite facies) and migmatised, homogeneous metasediments.

In all three zones deformation has been polyphase, but, with the exception of phase F_2S, not all the phases of folding are penetrative (Turner and Weiss, 1963) or even present everywhere.

Mixed flexural-slip folding and slip folding (Whitten, 1966) is the main mechanism of deformation in the nappe zone (i), whereas slip folding is predominant in the other two zones.

Folds are both cylindroidal planar and non-planar, occasionally non-cylindroidal (Whitten, 1966). The overall symmetry of these tectonites is generally monoclinic or triclinic.

The successive phases of folding are progressively numbered by analogy with the eastern domain. However, successive phases may have lasted long enough as to overlap in time and be active contemporaneously as will be advanced in page 86 (fig.13).

1. The Nappe Zone

The nappe zone covers an approximately 35 Km wide belt immediately west of the Sesfontein Thrust. A number of extremely large and complex F_2S structures occur in this zone, which can be broadly subdivided (see folder 4) from the east into:

i) The Khankhaib synclinorium
ii) The Aub anticlinorium
iii) The Aub and Otjihue synclines
iv) The Andib-Ganamub and Tomakas nappe
v) The Geinas synclinorium
vi) The Gomatum nappe and synform

These folds, however, are not strictly successive in an east-west direction, but merge somewhat into one another due to well developed plunges.

The Sesfontein Thrust (p. 75) is genetically related to these F_2S megastructures and bounds the two easternmost ones (i.e. the Khankhaib synclinorium to the south and the Aub anticlinorium to the north of sheet 1913B).

The style and mechanism of deformation differ greatly between the core, the carapace and the front of any nappe. The core is composed of massive and psammitic Nosib rocks (eg. Aub anticlinorium), which having been deeply buried and previously metamorphosed (eg. Andib nappe) during a pre-Damaran (M_1) episode (p. 97), behaved more competently than the overlying unconsolidated, unconfined and water-rich Damara schists, which at the time of deformation were

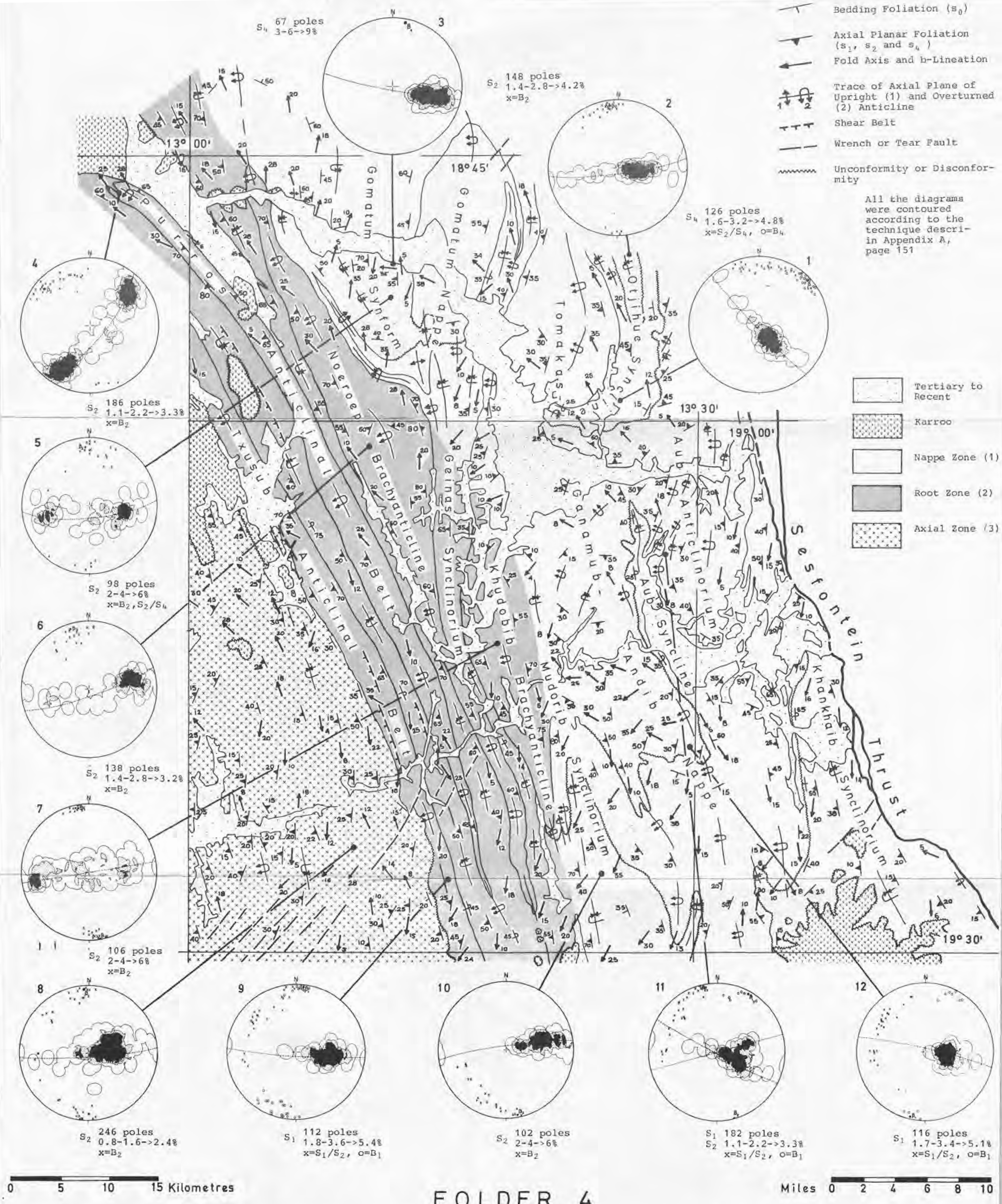

FOLDER 4

STRUCTURAL MAP OF THE WESTERN DOMAIN

undergoing their first substantial cycle of metamorphism (M_2) (p. 97).

As the behaviour of a rock-mass undergoing deformation (structural regime) depends largely upon the metamorphic grade and amounts of fluids thereby produced (Holland and Lambert, 1969), the difference in style and mechanism of deformation between the polymetamorphic Nosib cores and the shallow supracrustal Damara schists in the Sesfontein nappes is easily explained. For this purpose three areas were selected, where the tectonic fabrics obtained in the Nosib cores could easily be compared with those of the adjacent Damara tectonites.

In all three localities, namely the Andib valley and the Otjihue and Ganamub areas, the Damara-Nosib (U^2) unconformity attains its maximum angular values. The Upper Nosib granodioritic paragneiss is here penetratively foliated along NNE striking, normally westwards (10^o-50^o) dipping, biotite/muscovite s_1 surfaces. These can be either subparallel to a compositional banding or bedding foliation (s_0) (Knill, 1960) enhanced by metamorphic differentiation, or intersect it at a rather low angle in hinges of mesoscopic, eastwards overturned, cylindroidal, symmetric or isoclinal folds (Plate 11). The occasional s_0/s_1 intersection lineations (l_1) thus coincide with B_1; or, using Turner and Weiss (1963) symbols, $B^{s_1}_{s_0}$ axes. The folding, responsible for the creation of the observed fabrics and of the (U^2) unconformity, occurred concomitantly with or just preceded the first phase of metamorphism (M_1) which emphasised s_1 by the preferred orientation of its phyllitic minerals.

The B_1 axis was also statistically obtained using the spread of s_1 poles on π diagrams. The distribution of the measured B_1 linear elements and β is quite close on all three diagrams. If, on the other hand, these B_1 fabrics are compared with any of those obtained in the Damara schists in the area it can be easily seen that the fit is rather poor. Two apparent exceptions, however, seem to exist. One is the southernmost nose of the Otjihue syncline and the other is a small syncline dying out just to the west of the Sesfontein topographic beacon. The possible explanation for this apparent anomaly will be advanced in due course.

A number of different linear elements (l_2), normally crenulation cleavages, also appear on s_1, while occasionally the gneisses seem to part more easily along a different weakly penetrative NNW striking, s_2 foliation. A best-fitting great circle drawn through a Schmidt-diagram plot of l_2 is very close to the average s_2. This geometry suggests their genetic relationship. If this (l_2/s_2) array of data is compared with the fabrics of folds in the adjoining Damara schists a satisfactory correspondence seems to exist.

It is concluded in general that the Nosib cores of the nappes

Plate 11. Tight, recumbent F_1N slip folding in biotite paragneiss grading into flexural-slip folding in metapsammitic bands

include one set of s-surfaces and lineations more than those normally observed in the carapaces and digitation fronts. Thus the Nosib gneisses underwent one phase of deformation prior to that (F_2S) which formed the nappes and imparted the fissility to the overlying Damara schists. As this phase of deformation is the oldest in the area and is invariably related to the Nosib terrains, it will be symbolised F_1N. This is, however, inhomogeneously developed on a regional scale and in some places it has been obscured or even completely obliterated by later deformative and metamorphic episodes, while elsewhere it did not occur at all. Moreover, F_1N seems to be confined to the Upper Nosib semipelitic gneiss and occurs only subordinately in the Lower Nosib psammites, where the F_2S pattern is more strongly developed.

Where interference patterns were observed, F_2S is superposed at an angle ($\pm 35^{\circ}$) and it is not penecontemporaneous to F_1N but definitely later, i.e. the superposed folding is of the $B_1 \wedge B_2$ (3rd category) type as defined by Whitten (1966; p.358).

The F_2S folding is ubiquitously developed in the nappe zone. It is normally subdivisible into the macroscopic structures listed in page 60 and a variety of mesoscopic folds, in general concordant (Martin, 1965; plate IV, fig.1) and only occasionally discordant with the major structures, forming the carapace and digitation front of the nappes. In most cases F_2S folding is similar, isoclinal and overturned or recumbent to the east. In some of the digitations (Plate 12) the s_2 axial planar foliation can reach the horizontal or even be dipping eastward, i.e. in the direction (a) of advance of the nappe. As the amplitude (A) of the major nappes is extreme (more than 6 Km), their recumbent attitude over the miogeosynclinal basin gives a rather impressive order of the magnitude for the overthrust of allochthonous Swakop Facies metasediments on the autochthonous Outjo Facies Damara sequence to the east, even disregarding the effective, possibly equally large, disruptive translation effected along the Sesfontein Thrust during the latest stages of the nappes development. The $\lambda/_A$ ratio is normally rather low. On a mesoscopic scale, the ratio seems to be very variable and dependent on the lithology of the rocks undergoing deformation and their relative position in the stratigraphic sequence. Extremes were observed in some persistent carbonate bands south of Aub, such as that reproduced in Plate 12, which formed a disharmonic digitation with $\lambda/_A < 1/15$, i.e. a fold more than 150 m in amplitude and only 10 m wide. The surrounding pelitic schists are folded into much smaller mesoscopic folds with $\lambda/_A$ normally not less than $1/5$.

Strikingly disharmonic folds were also observed in the Gomatum synform where even more convolute folds multiply the original thickness of a single carbonate band in a crumpled cascade of virtually the same horizon (Plate 13).

A similar, though subdued, style of folding is not confined to the carbonate only, but can also be observed in the psammitic members and quartz veins, as in the sequence of schists belonging to the Tillite Substage appearing in the Khankhaib synclinorium to the north-west of the Orowau Peak (Plate 14). Concentric flexural-slip folding in the boudined competent beds and veins on a scale of a few metres is accompanied by small-scale slip-folds in the pelitic members, where s_2 is penetratively developed. It should be noted that the normal limbs and axial planes of these F_2S folds are very often horizontal, implying that the main stress responsible for deformation must have been subvertical, the tangential stresses being subordinate. All the elements seem thus to point towards gravity as one of the main factors in the structural evolution of these supracrustal tectonites.

On a very large scale the Damara nappes exhibit definite northward plunges to the north and southward plunges to the south of the Hoanib River respectively. This regular pattern seems related to a regional ENE superposed F_3 folding. The large-scale interference pattern created by this $F_2S \perp F_3$ penecontemporaneous superposition (Whitten, 1966; p.327) is evident from a cursory examination of sheets 1813C, 1913A and B, supported by the block-diagrams of folder 5.

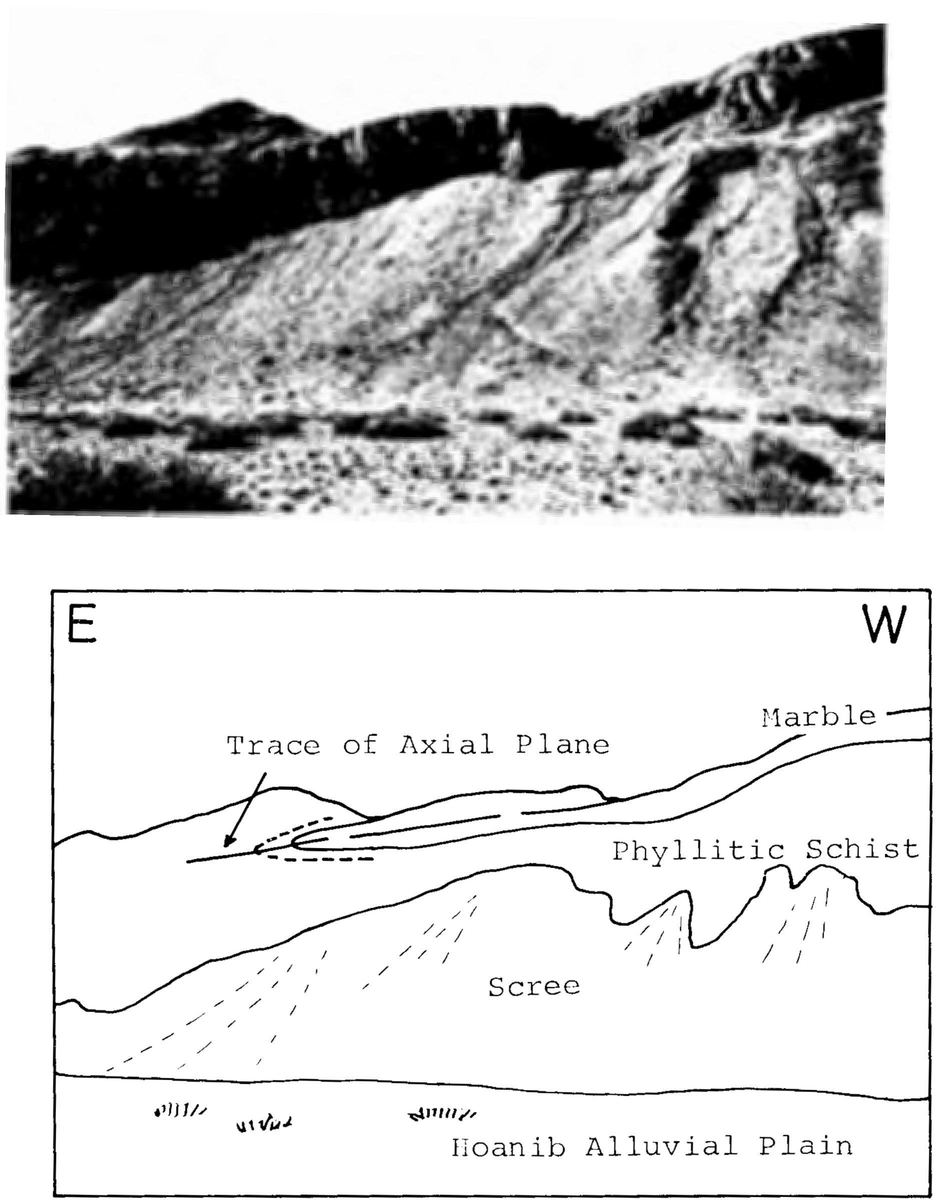

Plate 12. A high-amplitude, low-wavelength digitation in the Andib nappe front

On a mesoscopic scale the development of F_3 tectonites was extremely inhomogeneous and subordinate, particularly so as most of the study area occupies a crossfolding anticlinal region, i.e. an area of tensional structural regimes. Nevertheless ENE trending, weakly penetrative l_3 lineations, normally crenulation-cleavages, can occasionally be observed on s_1 and s_2. In particularly well exposed tectonites, the subvertical and undeformed attitude of the s_3 planes of slippage is evident, producing the crenulation as an intersection with any of the previous planar elements (i.e. s_3/s_1 and s_3/s_2). F_3 is thus locally mainly an upright fold with extremely large wavelength (λ=30-40 Km) and comparatively small amplitude ($A<1/30\lambda$) and is defined by the opposite regional plunges induced in the B_2 axes on either sides of the Hoanib River. The ENE trending B_3 axis can thus be defined as B^{S3}_{B2}. At a few localities, as for instance east of the Khudobib brachyanticline, the F_3 folding developed into small kinks. It is possible, though difficult to prove positively, that folding and/or differential movement along this ENE (B_3) trend may have been active over a long span of time, being feebly repeated till very late-kinematic stages.

In the Gomatum nappe s_2 is rather weakly penetrative at places, while a new strongly penetrative (s_4) chlorite/biotite foliation is often discontinuously developed. This normally intersects s_0 and s_2 at a considerable angle (up to 50°-60°) (Plate 15), though in general there is not much difference in strike between s_4 and the previous s-surfaces. Thus, they produce similarly oriented β axes if plotted on a Schmidt diagram. The F_4 mesoscopic slip-folding seems thus to be generally coaxial with F_2S but much more steeply inclined eastwards (Plate 15). Another peculiarity of this s_4 foliation is that it is mainly developed, in areas such as west of Tomakas, where the B_2 axes are deflected in the eastern lobe of the Gomatum nappe to a trend similar to that of F_1N in the Nosib infrastructure (i.e. N10-15°E). The superposition of F_4 can thus be regarded as $F_2 \| F_4$ pattern.

Considering now the regional distribution of the various structural elements (folder 4) analysed so far, it will be noted that F_1N is directionally relatively homogeneous in trend and inclination wherever developed, whereas F_2S is extremely variable. It is important to establish whether this directional variability of the F_2S elements is a primary feature or whether it is related to the interference of a yet later phase of folding. For this purpose the Otjihue syncline, a structure which is developed along the eastern front of the Tomakas nappe and which exhibits the widest variation of B_2 trends (i.e. from N 8°W in the north to approximately E-W in the southern nose) was examined in some detail. No compelling evidence of a hypothetical NW trending superposed phase of folding which could be responsible for such a macroscopic deflection, could be detected within the Damara schists. However, as previously mentioned, the F_2S fabric elements in the

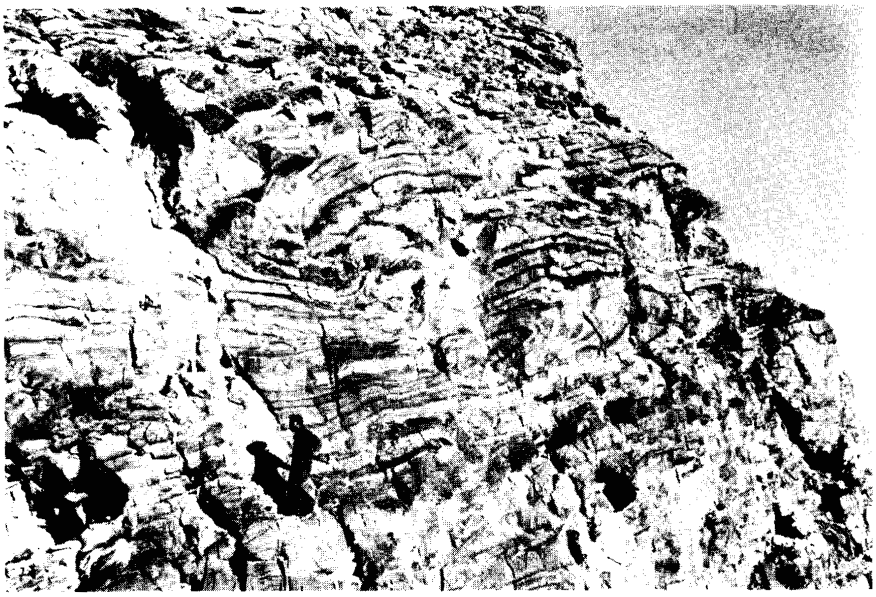

Plate 13. Convolute F_2S folding in Hakos marble in the Gomatum synform

Plate 14. Mixed F_2S flexural-slip and slip folding in the Khankhaib synclinorium

southernmost nose of the Otjihue syncline (diagram 1 in folder 4) are remarkably concordant with the underlying F_1N elements, and in fact, the U^2 unconformity is not geometrically detectable in the E-W branch, whereas to the north-east where the syncline straightens to the N-S direction it is very conspicuous. Study of the metamorphism above and below the Damara-Nosib contact in the area (p. 113) indicates, however, that the Nosib gneiss reached a much higher grade (middle amphibolite facies) than the overlying Damara schists (greenschist facies). The contact is therefore extremely sharp even where, as in the southernmost nose of the Otjihue syncline, an apparent parallelism exists between the two formations. Analogous circumstances were encountered to the west of the Sesfontein beacon, where a small, southwards plunging nose of a syncline of Damara carbonate, overturned to the east, conforms closely to the underlying F_1N pattern, no more than 2 Km away from an evidently unconformable contact. It is significant that this syncline merges with and is in fact overridden by the NNW trending remains of the recumbent Andib-Ganamub nappe and Aub syncline (see block-diagram 2 in folder 5). This geometric relationship clearly indicates that this NNE folding has a Damara age though it appears to have started somewhat earlier than the development of the (F_2S) Damara nappes. A feasible explanation is that the NNE striking s_1 foliation of the underlying Nosib metasediments may initially have concentrated the shear-stresses at depth during the early Damara deformation, controlling the orientation of the plastic flexural-slip folding in the overlying Damara sediments. Renewed slippage along the pre-existing s_1 foliation occurred because its geometrical orientation was in general not particularly different from that of the potential s-surfaces which the stresses would have created if they were to overcome the cohesive strength (τ_0) anew in a homogeneous, non-foliated rock-mass of similar mechanical properties. In other words, the stresses required to redistribute the movement along s_1 were lower than those necessary to produce a new set of failure planes in spite of their more or less oblique application. It is for this reason that s_1 is still not only fairly well preserved but even enhanced in places in the Nosib metasediments, in spite of the exceptional intensity of the later Damara deformation. Once it is accepted that each phase of deformation may have been active over a long span of time and in several pulses, as advanced in page 86, the F_4 slip folding is also easily explained as induced by the foliation of the Nosib gneisses. Movement recurring along the same slippage planes in an older tectonite (eg. Nosib substratum) is called "renewed or posthumous" movement in B_1 by Whitten (1966; p.327).

As already mentioned, most of the nappes have a definite eastwards recumbent attitude. The Gomatum nappe seems to be an exception to the rule. Viewed in its complexity in an E-W section (DE section and block-diagram 4 in folder 5), the anticlinal nature of the Gomatum nappe is not at all obvious, as this structure is

Plate 15. Large (circa 60^0) angle between the dip of s_0 (white marble band) and that of s_4 (dipping steeply to the right) in the Gomatum synform

remarkably lobate. The eastern lobe is regularly recumbent eastwards, and conforms to the usual style whereas the western lobe is overturned backwards to the west. They converge to the south, merging into the narrow and complexly folded Geinas synclinorium of Damara schists to the west of the Giribes plains (block-diagram 3 in folder 5), stretching uninterruptedly across the area from north to south. To the north, on the other hand, the anticlinal lobes diverge and their Nosib cores plunge below the Damara schist forming a fanning synclinorium or rather a synform, named after the Gomatum River which cuts an extremely well exposed section across it. A spread of at least 40^0 on the map (sheet 1813C) is exhibited by the meso- and macroscopic B_2 axial trends in the Gomatum nappe. In section (BC) this is accompanied by a fanning or conjugate attitude of the s_2 foliation which from preponderantly westerly dipping ($\pm$20^0) in the east ranges to steeply ($\pm$60^0) easterly dipping in the west.

Apart from the western edge of the Gomatum nappe, easterly dips are not common, reappearing only in some fan-like complex structures (section AB) along the Hoarusib River at and beyond the north-western margin of the study area. The Gomatum section (DE) itself is somewhat of an oversimplification of the natural geo-

FOLDER 5. THE MAJOR STRUCTURES OF THE WESTERN DOMAIN

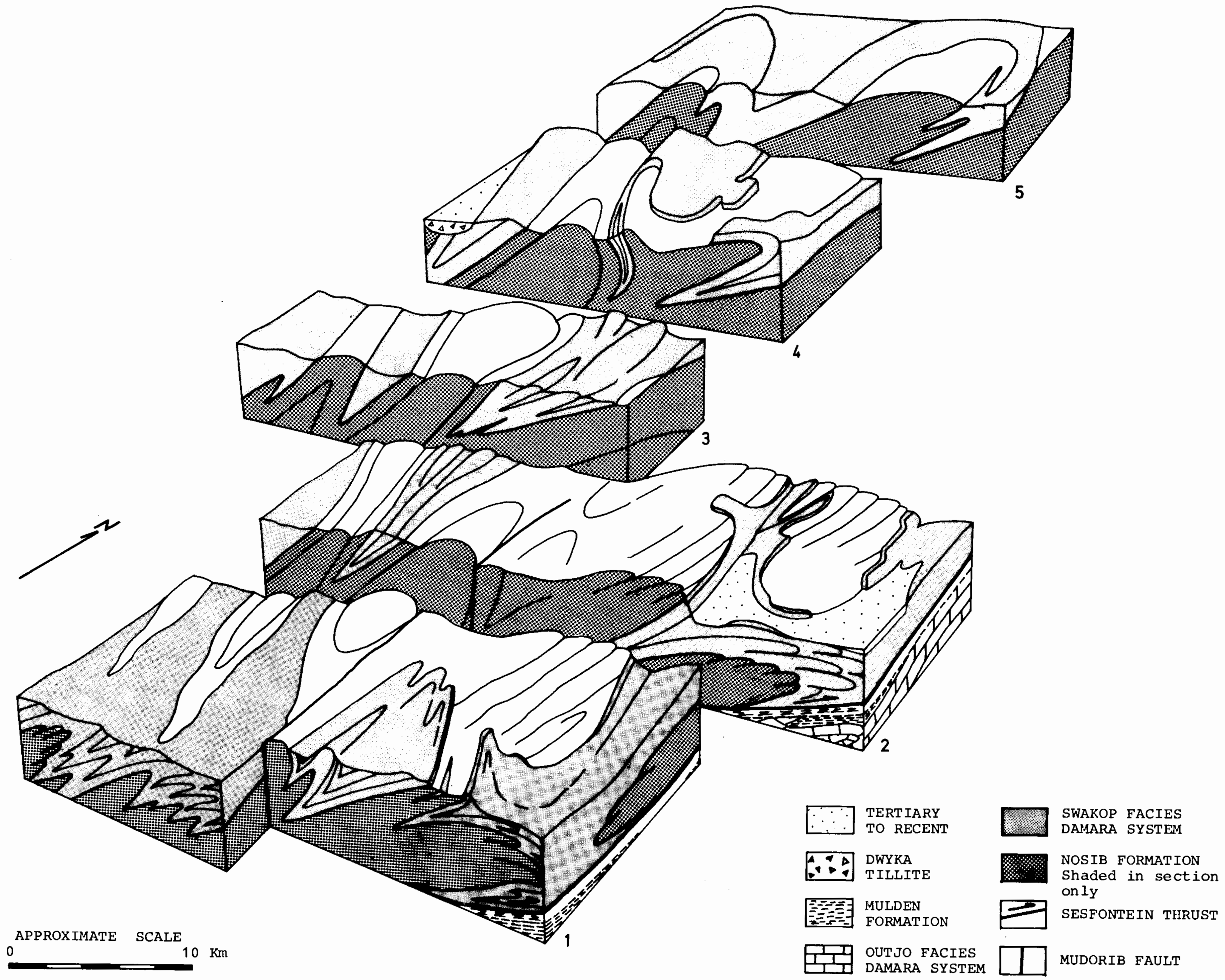

metry which at a mesoscopic scale is likely to contain more than one such lobate repetition piled up in the Damara schist synform. Finally, the Damara nappes south of the Hoanib River seem less complex and have a more concordantly eastwards recumbent geometry when compared to their northern counterparts.

2. The Root Zone

The Damara nappes are followed and partially underlain to the west by very steep, elongated anticlinal belts composed of granulitic Nosib metasediments separated by extremely narrow but uninterrupted synclinal belts of Damara schists and gneisses. The anticlinal belts normally trend N 10-15°W in sheet 1913A but swing gradually westwards across sheet 1813C so that along the Hoarusib River the fold trend changes to N 65°W in a wide, westwards concave arc.

Two megascopic domal or rather brachyanticlinal structures, namely the Noeroep anticlinorium and the Khudobib brachyanticline, are developed in this zone just west of the nappes. Both structures are terminated by rather steep antithetic plunges, so that their N-S longitudinal geometrical axes are approximately 3-4 times their E-W width. The core of the Noeroep brachyanticlinorium is composed of Nosib granulites, the Khudobib's of Lower Nosib psammites, i.e. of extremely competent lithotypes in general. This massive character is in contrast to the plastic overlying pelitic and semipelitic gneisses which extend northwards and southwards forming relatively narrow anticlinal belts, similar to those (eg. Purros and Txusub) commonly developed to the west, where no domal structures are present. The width of the anticlinal cores rarely exceeds 4 Km against a longitudinal persistence of over 80 Km (see folder 4).

Deformation in the domal structures is a relatively simple interference of the $F_2S \perp F_3$ phases alone as F_1N is in most cases developed very weakly or not at all. These brachyanticlines are normally inclined eastwards, though their axial planes dip westwards very steeply (±75°W). The exposed eastern flanks of the granulite and psammite cores are never overturned, whereas vertical or inverted dips were found as a rule in the adjoining gneisses. Observations along the eastern flank of the Khudobib brachyanticline, however, suggest that a vertical or slightly overturned (no more than 80°W) attitude may be attained at depth and that the structural relief exposed by erosion is not exactly the hinge-line of this large structure, but only part of the westward curving normal flank. The maximum structural elevation reached by the competent beds at the top of these structures must have been great, as topographic altitudes exceeding 1000 and 800 m above m.s.l. are still preserved in the Noeroep and Khudobib brachyanticlines respectively, in spite of the intensive erosion that they have experienced. This in turn seems to indicate extremely localised

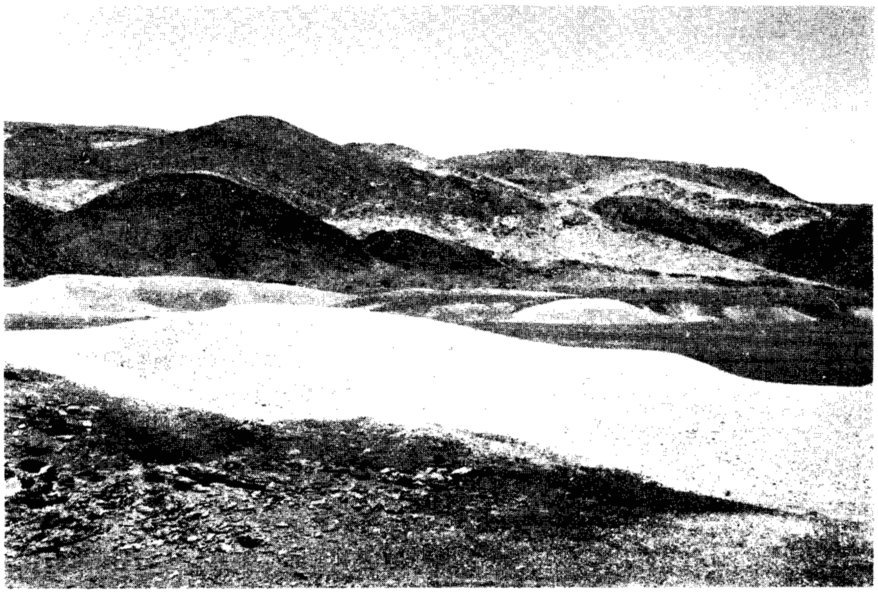

Plate 16. Closure in Hakos marble resister in migmatitic environments near Purros. Terraced Tertiary and Dwyka fluvioglacials in the foreground

Plate 17. F_2SAF_3 interference pattern in the Mudorib valley

uplift, a hypothesis supported by the fact that the cores of these domal structures contain the lowest stratigraphic levels, never exposed elsewhere in the area. The genetic relationship between these upwarped structures and the adjoining nappes will be discussed in due course.

A large subvertical or steeply westward dipping ($\pm 80^{\circ}$) normal fault with a downthrow of several hundred metres to the west, named the Mudorib fault, displaces the eastern flank of the Khudobib brachyanticline, dying out at the edge of the Giribes Plains. To the south of sheet 1913A, however, this fault has displaced the Etendeka (Karroo) plateau-basalt (Guj, 1968) and has, therefore, a definite post-Karroo (late-Cretaceous) age.

The two successive anticlinal belts, to the west of the Noeroep brachyanticline, are normally composed of steep, eastwards overturned (50-70°W), often isoclinal, similar slip folds. Only exceptionally in hinges or nose areas is the original, uninverted bedding-foliation detectable, as in the Purros nose structure where the second-last anticlinal belt plunges northwards below the migmatitic Damara gneiss. This contact and related structural setting would have been extremely difficult to detect were it not for the rather conspicuous development and tectonic thickening of the Upper Hakos marble resister overlying the Nosib metasediments (Plate 16). Strict parallelism of the main penetrative foliation in Nosib and Damara tectonites was observed in most of these anticlinal belts and it is, therefore, concluded that s_1 was generally either originally weakly developed or has been completely transposed in s_2.

In the southern portion of the westernmost belt, however, to the south of the Hoanib-Mudorib confluence, NNE trending, eastwards inclined F_1N folding reappears in the Nosib granodioritic gneisses (diagram 9 in folder 4). The conspicuous NNE trending fabrics were not observed within the overlying Damara gneisses where the NNW trending F_2S remains predominant. Under these circumstances the U^2 unconformity can again be detected on a regional scale at the base of the Damara System in spite of the relatively high metamorphic grade. It was also noted that this relationship becomes more and more obvious to the south of sheet 1913A.

The steeply overturned attitude of the folds in this zone (average s_2 dip $\pm 50^{\circ}$W), however, seems to depend to a certain extent upon the depth of erosion. If, for instance, the narrow extension of the Noeroep anticlinal belt is followed across the Hoanib River until it plunges southwards below the Damara metagreywacke, a substantial change in style of deformation can be observed. The structural pattern is here evident on account of several minor carbonate bands outlining the attitude of s_0. The dip of the highest members flattens noticeably, so that in places the attitude of the folds again becomes recumbent. The anticlinal structure, well defined at depth, diversifies again into

Plate 18. Recumbent F_2S flow folding in the migmatised zone

numerous disharmonic digitations. The style and mechanism of folding at high levels are, therefore, similar to those encountered to the east in the Andib nappe. It is thus likely that this zone of steep, elongated anticlinal belts is the area where other minor nappes (now eroded) originated, piling up against the major frontal nappes which have just been discussed. This view could possibly be substantiated by the structural analysis of sheet 1913C because, as a result of the southern regional plunge, the sequence of structures observed in the root zone will be exposed there at increasingly higher tectonic levels.

At depth in high metamorphic terrains, particularly away from areas of tensional anticlinal cross-folding which produced the domal structures, F_3 is much more pronounced at a mesoscopic scale. It gradually loses the upright attitude observed in the nappe zone and reclines southwards (concordantly with the regional plunge). Spectacular, though relatively rare, $F_2S \perp F_3$ interference tectonites were observed along the Mudorib River (Plate 17) in banded biotite-hornblende gneisses derived from Nosib sediments.

The western boundary of this zone is marked by intense shearing, often producing belts of mylonitic or cataclastic gneisses (folder 4). This line of dislocation seems to correspond to the

Table 5. Synopsis of Deformation in the Western Structural-Stratigraphic Domain

Location of structural zone in the mobile belt	F_1 N PRE-DAMARAN FOLDING				F_2 S DAMARAN LONGITUDINAL FOLDING				PENECONTEMPORANEOUS FOLDING PHASES		LATER DEFORMATIONS		Style of folding and interference patterns
	Geometry and altitude of S_1 axial planes	B_2 trend and plunge	Wave length (λ) and amplitude (A)	Longitudinal persistence	Geometry and altitude of S_2 axial planes	B_2 trend and plunge	Average wavelength (λ) and amplitude (A)	Longitudinal persistence	F_3 ($\sim$ NE)	F_4 ($\sim$NNE)	D_6 ($\sim$NNW)	D_7 ($\sim$NE)	
(1) NAPPE ZONE Overthrust on eastern areas of discontinuous folding	Planar, NNE striking, westwards dipping 20-40^o	N 15^o E to N 80^o E (variance: $\pm$ 65^o) Plunges: NW in the Aub-Ganamub area SW in the Andib area	Maximum λ = 500-1000m but usually in a range of 1-2m. Amplitude normally A = 2 -4	Moderate to considerable: Several (up to 15)Km Discontinuously developed in the Aub-Otjihue and Andib-Ganamub areas	Planar or curviplanar N-S to NW striking, gently westward rarely (Gomatum nappe) eastward dipping or horizontal. Variance $\pm$ 50^o	NNW or SSW, rarely (Gomatum Nappe) NNE trends N and S plunge north or south of the Hoanib River respectively	Very large wavelength (λ = several Km) Extremely large and variable amplitude (A=2-15 λ)	Large > 10 λ (i.e. > 20 Km)	Upright, extremely gentle, large (several Km) wavelength axial undulation creating the major B_2 regional plunges	Posthumous slip-folding in B_1, inducing coaxial (II) or inclined (Λ) superposed pattern with F_2S. Some movement is extremely early	NNW striking westwards dipping low-angle (Sesfontein) thrust and related "Gleitbretter" (F_6) folding	NE striking subvertical, wrench faults, kink bands or crenulations (F_7)	Large, eastwards recumbent nappes, with schistose digitated carapaces and slip folded gneissic cores, exhibiting definite plunges (F_2 S$\perp$$F_3$). Coaxial or angularly superposed F_4 slip folding (F_2S $\parallel$ F_4) and (F_2 S Λ F_4) Transposition of F_2S folds along the (D_6) Sesfontein thrust
(2) ROOT ZONE Between the hinge-line and the axial migmatised uplift	Same as above	Trend: N 10^o E variance: negligible Plunge: obscured	Not determinable but likely to be in the same range as above	Not determinable but likely to be in the same range as above Discontinuously developed S of the Mudorib-Hoanib confluence	Planar NNW striking, steeply westward, rarely eastward (Hoarusib fan-like folds) dipping (average 50-70^o) Customarily subparallel to So	NNW or SSW trends N and S plunges on either side of the Hoanib River respectively	Relatively large wavelength (λ = 1-4 Km) Amplitude much greater than (A =3-5λ)	Extreme 10 Many folds extend over more than 80 Km	Same as above Occasional southwards inclined slip folds at deep tectonic levels	Not observed	NNW striking, steeply, westward dipping, mylonite belts at or close to the boundary with the axial zone	Same as above	Large or mesoscopic, eastward inclined, almost isodinal, slip folds, forming N-S elongated (> 80Km) anticlinal belts, containing domal or brachyanticlinal structures contiguous to the nappes (F_2 S$\perp$ F_3) Rare (Hoarusib area) fan-like complex folds.
(3) AXIAL ZONE Migmatised uplift, inverted Khomas eogeosynclinal furrow	NOT EXPOSED				Planar, NNW to NE striking, gently westwards dipping or recumbent (0-30^o W)	NE to SW trends Plunges roughly continued in the average S_2 plane	Relatively small wavelength (λ = few metres or tens of metres) Amplitude relatively large (A =4-8λ)	Moderate to large 6-8	Same as above	Not observed	Absent	Wrench faults invaded by pegmatitic (Uhima) late-kinematic granite	Mesoscopic, eastwards recumbent, slip folds Flexural-slip folds and/ or ptygmatic folds in neosomatic pegmatoid mobilisate in migmatites Flow folding

belt of highest thickness-gradients (hinge of the Khomas furrow in fig. 11) and also to be related to the margin of the migmatite zone, i.e. to a considerable drop in mobility of the rock-mass undergoing deformation.

3. The Axial Uplift or Migmatised Zone

The western limit of the root zone seems to coincide broadly with the hinge-line or line of maximum thickness-gradient, i.e. with the margin of the Khomas furrow where the Damara greywacke association sensu stricto is developed. This line in turn marks the "front of the Damaran migmatites" (folder 6). The local structural evolution must, therefore, be visualised in the light of several factors:

i) The extreme thickness and originally comparatively homogeneous mechanical characteristics of the lithotypes undergoing deformation.

ii) The great depth to which the competent and crystalline basement and Nosib substratum were depressed by the intense orthogeosynclinal subsidence, and consequently their slight or even non-existent controlling power on the evolution of the overlying tectonites due to the extreme changes in rheomorphic properties introduced at this stage by migmatisation concomitant with deformation.

East of the migmatite zone, reference to the stratigraphic position of the various elements of the large-scale structures could be maintained where the persistence of impure carbonate bands and of occasional Noeroep metavolcanics provided reliable information as to the attitude of s_0. Proceeding westwards into the higher but migmatised Khomas members, that reference is lost. Neither does the compositional banding, so characteristic of the root-zone metamorphites, persist into these homogeneous, high-grade amphibolite (sillimanite) gneisses (p. 122). The only information about the attitude of the bedding foliation (s_0) in the zone is fragmentarily preserved in rare dark-grey fine-grained quartzite resisters appearing within the migmatites south of Mt. Sima.

Again folding (F_2S) becomes as a rule highly overturned to the east and even recumbent (Plate 18). A strongly penetrative axial planar s_2 biotite foliation is ubiquitously developed.

Pegmatoid mobilisate (Mehnert, 1969) veins were observed to be both concordant with and discordant to s_2 by which they are often intersected at a rather low angle in hinges of ptygmatic folds. This and the boudined "pinch and swell" (Mehnert, 1969) appearance of these convolute leucosome veins indicates that migmatisation proceeded and lasted throughout deformation. The microscopic study of metamorphic textures in the adjoining

Plate 19. The Sesfontein Thrust separating gently dipping Lower Hakos from underlying more steeply dipping Mulden pelites.

Plate 20. The Nunarus tectonic wedge of dolomite (white) bounded by the two branches of the Sesfontein Thrust

sillimanite-garnet paleosome revealed that these high-temperature minerals crystallised at least partially during late- and post-kinematic stages (p. 123) of the main Damaran (F_2S/M_2) tectonothermal episode.

The β axis trend obtained by evaluating the pattern of preferred orientation of s_2 poles on a Schmidt diagram, does not exhibit a good fit with the average trend of B_2 axes and l_2 lineations directly measured on minor mesoscopic folds. The B_2 and l_2 development, however, seems to be roughly confined to a relatively narrow band including the plane of average s_2 foliation, thus showing a certain limitation in their otherwise rather unsystematic spread. This distribution may indicate synkinematic differential flowage along the (a-b) plane of slip, induced both by the semiviscous or rheomorphic conditions (Holland and Lambert, 1969) derived from the abundant hypercritical fluids and their temperature and pressure variations (gradients) brought about by the tectonic stresses. This process may have controlled the continuous delicate balance of partial melting and successive recrystallisation in the neosomatic veins at different times and places along the same sets of s-surfaces.

The s_2 foliation is very weakly developed within the fine-grained Ganias granite and altogether absent in the coarsely pegmatitic Uhima granite. The latter seems to be preferentially intruded along a set of NE striking subvertical or northwards dipping, tear or wrench faults that represent the latest phase (D_7) of brittle dislocation in the Sesfontein area in general, as they were observed to intersect all the previous tectonites including the Sesfontein Thrust (D_6) in both eastern and western structural domains. The presence of syn-, late- and post-kinematic migmatites and granites together with the high metamorphic grade of the gneisses suggests that the rheomorphic firmoviscous (Whitten, 1966; p. 141) mechanical behaviour of these rock materials under stress must have lasted for a considerable time at extremely high temperature and pressure.

F. THE SESFONTEIN THRUST

1. The Geological Significance

The Sesfontein Thrust is a NNW striking, large-scale, low-angle dislocation which separates the western Damara eugeosynclinal domain from the eastern miogeosyncline over an ascertained distance of more than 120 Km. It bisects the study area (sheet 1913B) from north to south about 1.5 Km west of Sesfontein, disappearing below the younger, undeformed, Karroo plateau-basalt.

The thrust-mass is mainly composed of metasediments belonging to the Lower Stage and Tillite Substage of the Hakos Series of the

Swakop Facies of the Damara System. The thrust-floor is essentially composed of Mulden phyllite and greywacke (Plate 19) to the south and of Otavi cherty dolomite to the north.

The thrust-plane dips everywhere westwards at a variable angle. The dips are normally moderate (10°-25°W) where the thrust-mass advanced on Mulden clastics. However, against the Otavi dolomite highveld (i.e. north of the Hoanib River) the thrust splits into two auxiliary planes and the dips increase considerably (20°-60°W). The westernmost branch dips generally more steeply than the eastern, although the latter appears to steepen noticeably farther northwards. An eastwards inclined antiformal mass (Nunarus anticline) of intensely deformed Otavi dolomite occupies the wedge-shaped space between the two thrust-planes, and is in turn thrust over the Mulden phyllite (Plate 20).

The limit between Swakop and Outjo Facies, therefore, runs along the western branch of the Sesfontein thrust, which can be traced much farther northwards, whereas the eastern branch appears to die out gradually a few kilometres north of the study area.

A peculiarity, common to many other thrusts, is the presence of a variable thickness (1-10 m) of light grey or cream-coloured, often limonitised, finely crystalline or mylonitic dolomite and/or impure limestone marking the full extension of the thrust-line.

This carbonate band, included for practical purposes within the Hakos metasediments on sheet 1913B, is discordant with the bedding-foliation (s_0) in both hanging and foot walls of the thrust. In the Khankhaib Plains its genesis is not sedimentary but related to essentially two factors:

i) Mechanical transposition and plastic flowing of occasional thin dolomitic intercalations within the Mulden phyllites, which a few tens of metres below the thrust-plane do not differ much in strike from the fault itself but dip rather steeply (40-70°E) in the opposite direction. Closer to the thrust-plane, however, they are gradually transposed and sheared until beds which were originally far apart flow together into an almost continuous carbonate band including the actual thrust-plane.

ii) Synkinematic dolomitisation (Spörli, 1969; p.1839) and calcification due to abundant CO_2-rich solutions released during dehydration and decarbonatisation brought about by low-grade metamorphism occurring in the Mulden clastics at the time (p. 100). Upward migration may easily have taken place along the steeply dipping slaty cleavage of the Mulden phyllites, but the flux is likely to have been capped or rather deflected and concentrated along the low-dipping thrust-plane by the impervious Hakos schists. The presence of carbonate-rich solutions during deformation can be deduced from

Plate 21. The recumbently and deeply folded alternations of dark and light dolomitic laminae are intersected by a vein of lighter carbonate folded to a much lesser extent. The light carbonate vein obviously crystallised in an oblique shear-joint formed across the laminated dolomite after an initial stage of folding. Successive dragging has enhanced the amplitude of the folds in the laminated dolomite, whereas the carbonate vein was strained proportionally by the last pulse alone. A similar mechanism was observed by Ramsay (1967; p. 344) in migmatitic terrains.

The 20 x 40 Km wide, 1 to 20 m thick, Lochseitenkalk limestone underlying the Glarus overthrust in the Swiss Alps (Oberholzer, 1933), which shows particular analogy with the Sesfontein Thrust, has recently been interpreted (Hsü, 1969; p. 941) as flowage and smearing out of ".... a block of mainly Upper Jurassic limestone caught under the thrust and spread out for about 20 Km from its place of origin, while its thickness was reduced to a hundredth or less of its original thickness during the shearing movement".

A local example of flowage along a carbonate sedimentary unit at the base of step-bedding-plane thrusts (Badgley, 1965; p. 189) could be the "unconformity dolomites" underlying the Naukluft nappes (Korn and Martin, 1959; p. 1056) in the Maltahöhe district of South West Africa. North (1964; p. 194) and Spörli (1969; p. 1844) have questioned their sedimentary nature suggesting that they might be the product of synkinematic dolomitisation only, by analogy with a similar carbonate septum developed at the base of the Helvetic nappes in Central Switzerland. The present author feels, however, that the two processes are in fact interacting rather than antithetic and that the starting point must always be the presence of suitably distributed sedimentary carbonate members in areas of potential failure. Deformation and flowage at low metamorphic levels (regime 2 of Holland and Lambert, 1969; p. 204) is accompanied by the expulsion of an abundant fluid phase, which in turn favours recrystallisation. This combines with intergranular and infragranular gliding (Spry, 1969) to produce a new translated and deformed final shape. Increasing solubility in areas of high pressure, frictional heat and intense grinding (higher specific surface) creates carbonate-rich solutions which migrate preferentially along the mechanically permeable shear-planes in the direction of negative pressure-gradients, gradually crystallising as the pressure and the temperature drop. Thus, the distance of migration is a function of the dynamic evolu-

Plate 21. A large-amplitude "drag" folding in marble intersected by a folded synkinematic carbonate vein, originally a planar joint-filling in the partially folded carbonate band

tion of the thrust and it is not possible to define a boundary between strictly tectonic and chemical processes.

The fundamental role of the carbonate-pelite intercalation in lowering the cohesive strength (τ_0) along potential planes of failure (Hsu, 1969) and of the pore-fluid pressure build-up (λ_1) in counteracting the normal stress in thrust mechanics (Hubbert and Rubey, 1959) have already been exhaustively discussed and cannot possibly be over-emphasised.

The low-angle Sesfontein Thrust intersects the Mulden F_2M fabric elements (bedding-foliation s_0 and slaty-cleavage s_2) almost orthogonally, with the creation of the eastwards recumbent slip or "Gleitbretter" superposed F_6 folds described in page 29. In a few instances south of the Hoanib River, mylonitisation and rodding are so intense that both fabrics are disrupted into a chaotic mass of pervasively sheared and mixed phyllite and dolomite, riddled with quartz veins.

In the thrust-mass, however, the geometrical attitude of the thrust-plane is subparallel with respect to the penetrative s_2 axial planar and s_0 bedding foliations. Shearing was here distributed through minor differential movements along each of these penetrative s-surfaces with no obvious disruption of the F_2S mesoscopic tectonites, which are rarely intersected at angles higher than a few degrees.

On a regional scale the F_2S folding developed in the nappe fronts seems to conform closely with the thrust and only one major stratigraphic boundary (i.e. the Lower Hakos-Tillite contact) is transgressed at a small angle (sheet 1913B). The Sesfontein Thrust must, therefore, be regarded as the latest evolution of the nappes'development (F_2S) as is illustrated by some of the mesoscopic recumbent folds which occasionally exhibit stretched limbs disrupted into thrusts as in the carbonate band of Plate 22.

Although the Sesfontein Thrust is one of the latest structural elements in the area, still later minor phases of deformation affected this tectonite. The thrust-plane, in fact, undulates gently where it overlies the Anabib anticlinal nose, as shown by the definite bend exposed by its trace on sheet 1913B south of the Hoanib River. This feature lends itself to two concurrent kinematic interpretations, i.e. that slight deformation might still have occurred along F_2O trends throughout the Damaran orogeny and that the Otavi dolomite structures acted at the same time as buffers controlling the thrust advancement. This buffering effect and the remote influence of the Kamanjab inlier were moderate to the south where the dolomite anticlines were buried below a variable thickness of Mulden molasse and the thrust advanced towards an actively subsiding basin (i.e. Mulden exogeosyncline). Thrusting was effectively hindered to the north in the Nunarus area, where the original sole thrust (Badgley, 1965) steepened in the attempt to overcome the massive dolomitic relief, with the development of an erosional toe (Raileigh and Griggs, 1963; Hsü, 1969). The stresses, concentrating on account of their application against a much steeper thrust-plane, sought release through differential movement along a new plane of failure (i.e. the eastern branch of the Sesfontein Thrust). The Nunarus F_2O dolomitic anticline was thus sheared at the base and thrust as a tectonic wedge or imbrication over the younger Mulden phyllites.

After an initial period of relatively rapid advancement the Andib-Ganamub and Gomatum nappes must then have reduced their speed along the thrust to balance that of erosion in these toes as there is no evidence of allochthonous material having progressed far beyond the present location of the Sesfontein Thrust.

Rapid progress could by now have only occurred following the removal of large masses from the toes by intense erosion due to unusually rapid subsidence in the Mulden exogeosyncline or else a further uplift in the Khomas furrow. This would have induced an enhancement of the gravitational effects on the nappes and thus overcome the resistence created by the antithetic action of gravity in the toe areas due to the local dip of the thrust-plane being contrary to the direction of advancement of the nappes.

Plate 22. Relationship between nappe folding and thrust in marble at the mesoscopic scale

At a later stage the Sesfontein Thrust was disrupted by a few NE wrench or tear faults belonging to the latest D_7/F_7 phase of deformation.

2. Mechanical Considerations on the Sesfontein Thrust Toes

Raileigh and Griggs'(1963; p. 821) thrusting model is based on the assumption that an unconfined sliding mass advances freely under the action of gravity over a slope θ_1, tectonically produced at the margins of central uplifts in eugeosynclines, until it is compelled to overcome some obstacle creating an antithetic slope θ_2. If the sliding mass can produce enough energy to override the obstacle (normally a structural element of the thrust-floor) and proceed to the opposite side, a riser is created (Raileigh and Griggs, 1963; p. 827). If on the contrary the thrust-mass were arrested against an obstacle which could not be overcome, equilibrium would theoretically be reached when the driving force along the slope concordant to the movement pushes a toe up the buffer (toe thrust-plane) along the slope θ_2 discordant with the movement until it reaches a volume V_2, such that the following relationship is satisfied:

$$\rho_b g V_1 \sin\theta_1 = \tau_0 A + (1-\lambda_1)\tan\phi_i(\rho_b g V_1 \cos\theta_1 + F_h \sin\theta_1) + F_h \cos\theta_2$$

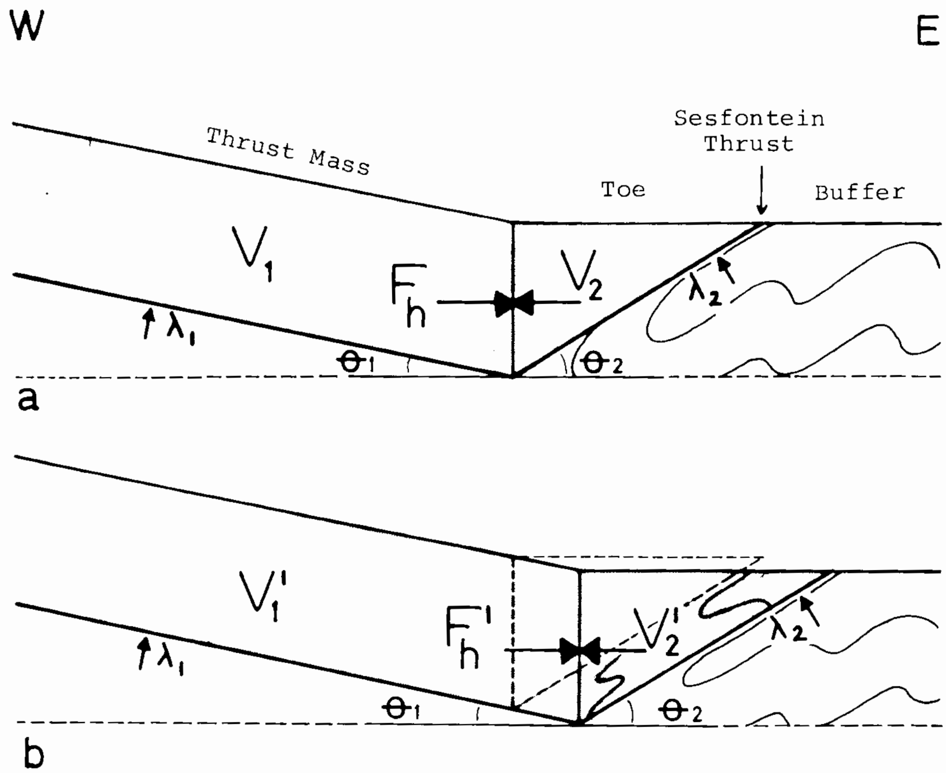

Figure 12. Physical factors acting in the toe area before (a) and after (b) the formation of an alternative toe-thrust (Modified after Hsu, 1969)

where V_1 and V_2 are the respective volumes of the sliding block and the toe and F_h is the horizontal force required to push the toe up the slope θ_2 (fig. 12(a)); the other terms having been already encountered in page 35. This formula, however, neglects for the sake of simplicity the unknown amount of energy absorbed by the bending of the thrust-mass where it changes dip.

Under these circumstances, movement depends entirely upon the speed of erosion in the toe which continuously alters equilibrium by reducing the toe-mass.

If, however, erosion in the toes fails (as normally happens) to keep abreast of the advancement of the thrust and the volume V_2 required for equilibrium is effectively reached, the thrust will stop only if the cohesive strength (τ_0) of the thrust-floor or buffer is large enough to hinder the formation of an alternative thrust-plane in the toe area below the previous one (Hsu, 1969; p.947). In this way (fig. 12(b)) the ratio volume of the thrust-block (V_1)/volume of the toe mass (V_2) is increased to V_1'/V_2' (where $V_1'>V_2'$) and consequently the left member of the equation becomes larger than the right:

$$\rho_b g V_1 \sin\theta_1 > \tau_0 A + (1-\lambda_1)\tan\phi i(\rho_b g V_1 \cos\theta_1 + F_h' \sin\theta_1) + F_h' \cos\theta_2$$

so that the thrust can resume its movement with the creation of an additional toe. This seems to be verified to the south of the Hoanib River, where several generally subparallel shear-planes were detected in the mélange of sheared phyllite and dolomite underlying the thrust north-west of Orowau Peak (area shaded by red ruling on sheet 1913B and section J-K). According to Hsu (1969, p.947) the "Wildflysch" of the Alps, the "Argille scagliose" of the Appennines and the "Franciscan" of the California Coast Range formed by an indefinite repetition of this process.

The same mechanism can apply to the Nunarus imbrication, which is, however, further complicated by a stress-couple possibly generated by different speeds of advancement of the thrust-mass above the Mulden phyllite to the south and its steep toeing or arrest against the Otavi dolomite highland to the north. This feature is suggested by the eastwards concave shape of the Thrust trace on sheet 1913B and by the gradual dying out of the eastern branch of the Sesfontein Thrust north of the study area.

The magnitude of the advancement of the western nappes over the miogeosynclinal basin is difficult to evaluate because of the absence of any point of reference, yet from the evaluated amplitude of the recumbent nappes and from the attitude of the toes this is likely to have exceeded 10-15 Km.

The close association of the Sesfontein Thrust with the formation of the Andib-Ganamub-Khankhaib and Gomatum nappes which proved to be largely gravity structures, the typical development of toes and the absence of basement cores in the structures of the western domain, seem to support the hypothesis that the thrust flattens at depth to the west into a sole or stretch thrust (Badgley, 1965). This would further support the possibility of a thin-skinned or non-basement-involving (Badgley, 1965) supra-crustal deformation as the most likely style of folding in the nappe zone bordering the mobile axial uplift (Carey, 1962) of the Damara geosyncline in the south-western Kaokoveld.

G. KINEMATIC INTERPRETATION AND COMPARISON WITH THE EASTERN DOMAIN

Several improved geotectonic theories, recently proposed, seem to share the concept that during the orogenic evolution of a mobile belt, extreme uplift occurs at some stage along elongated areas of previously abnormal subsidence (i.e. geosynclines), a phenomenon which has been deduced over and over again on conventional geological evidence. Phases of upwarping, resulting from deeply seated processes (convection currents, polymorphic inversion, etc.) possibly taking place in the upper mantle, are attained along the innermost migmatised belts and granitic/granodioritic massifs which have been referred to as "regurgitation or rising axial zones" by Carey (1958, 1962), "rising centres" by Haller (1956) and "buoyant meso-circuits" by van Bemmelen (1960).

Decreasing rate of uplift on either side of these axial zones of "infrastructural buoyancy forces" (Badgley, 1965) creates of necessity divergent slopes towards the cratonic edges, where static conditions or more often slight subsidence may exist during the orogenic cycle.

The study area lies between the eastern slope of one such large migmatised axial uplift zone (i.e. the N-S branch of the Damara orogeny, see folder 6(b)) and the margin of the stable Congo craton (de Villiers and Simpson, 1967). The action of gravity on the sedimentary masses lying on this slope supplied the deformational energy at supracrustal levels, to which the present research is mainly devoted and limited. The definite tendency towards lateral spreading is shown in the shallower and therefore unconfined levels by the eastwards overturned or recumbent regional style of folding.

Besides being a positive area, the axial uplift corresponds to a belt of anomalously high geothermal gradients, i.e. a localised elongated heat source. Uplift and consequent erosion have here been very much more intense than anywhere else, thus progressively deeper tectonic levels were exposed to the west. These need not necessarily be old in the stratigraphic sense (mainly Upper Hakos and Khomas metasediments), but on account of the previous anomalously high rate of subsidence, have undergone deformation at a much greater depth and under higher temperatures and pressures than those operative in the adjoining areas. In conclusion, temperature, load and tectonic overpressure, and amount of fluids available, all factors influencing the rheomorphism and therefore the mechanical behaviour of the rock-masses undergoing deformation, also exhibit a regional zonal distribution perpendicular to the axial uplift.

Against this background, the kinematic characteristics, which distinguished the western from the eastern domain, already discussed in page 29, can be analysed. These are essentially separate and yet related differences in:

i) the nature of the uplift generating deformation in the supra-structures in the east and west.

ii) the mechanical properties of the deformed rock-masses and the course of their respective changes with time.

The first difference concerns the degree of basement involvement, or to use Rodgers' (1953) term the transition between "thin- and thick-skinned" tectonics.

In the eastern domain a blanket of only 2000-3000 m of unmetamorphosed Damara sediments was plastically folded along the western slope of the Kamanjab anticlise, whereas the Nosib clastics were scarcely or only partially involved in late folding, being mostly affected by brittle block-faulting in the underlying basement (folder 6(b)). Deformation appears to have occurred here according to the mechanism conceived by Beloussov (1963; p.525), i.e. in a typical thin-skinned structural evolution.

West of the Sesfontein Thrust, however, things proceeded differently, as Nosib cores have been intimately involved in the Damara nappes in spite of their previous (M_1) mobilisation and metamorphism (pseudocratonisation) during the F_1N episode. Moreover, slip folding has to a large extent replaced the flexural-slip folding so typical in the east. However, as these metamorphosed nappes advanced for some distance over the unmetamorphosed Otavi and Mulden rocks along the Sesfontein Thrust, it must be assumed (as shown in folder 6(b)) that the eastern type of "non-mobilised" infrastructure extends farther west than the thrust-line itself. Block-fault subsidence below the Mulden exogeosyncline thus still controlled the final evolution of the front of this western allochthonous mass, generated initially in a completely different structural environment.

West of the Damaran hornblende-oligoclase isograd (folder 7), however, deeper erosion exposing progressive metamorphism westwards seems to indicate that all the major tectonic-stratigraphic units (i.e. Damara, Nosib and basement) have been re-involved in the Damara orogeny to a greater or lesser extent regardless of their previous metamorphic history. The massive Lower Nosib metapsammites and granulitic gneisses behaved more competently than the overlying Damara schists and, in addition, confined somewhat the surge of more mobilised masses at yet deeper levels (where temperature peaks were high enough to induce more partial melting), producing domal structures (i.e. Noeroep and Khudobib brachyanticlines). The irregular geometry of these competent masses also played an important part in the anisotropic redistribution of the deformative stresses.

An idea of the mechanical behaviour at depths greater than this root zone can be derived from the observation of the undifferentiated structures in the anatectic massif west of the study area,

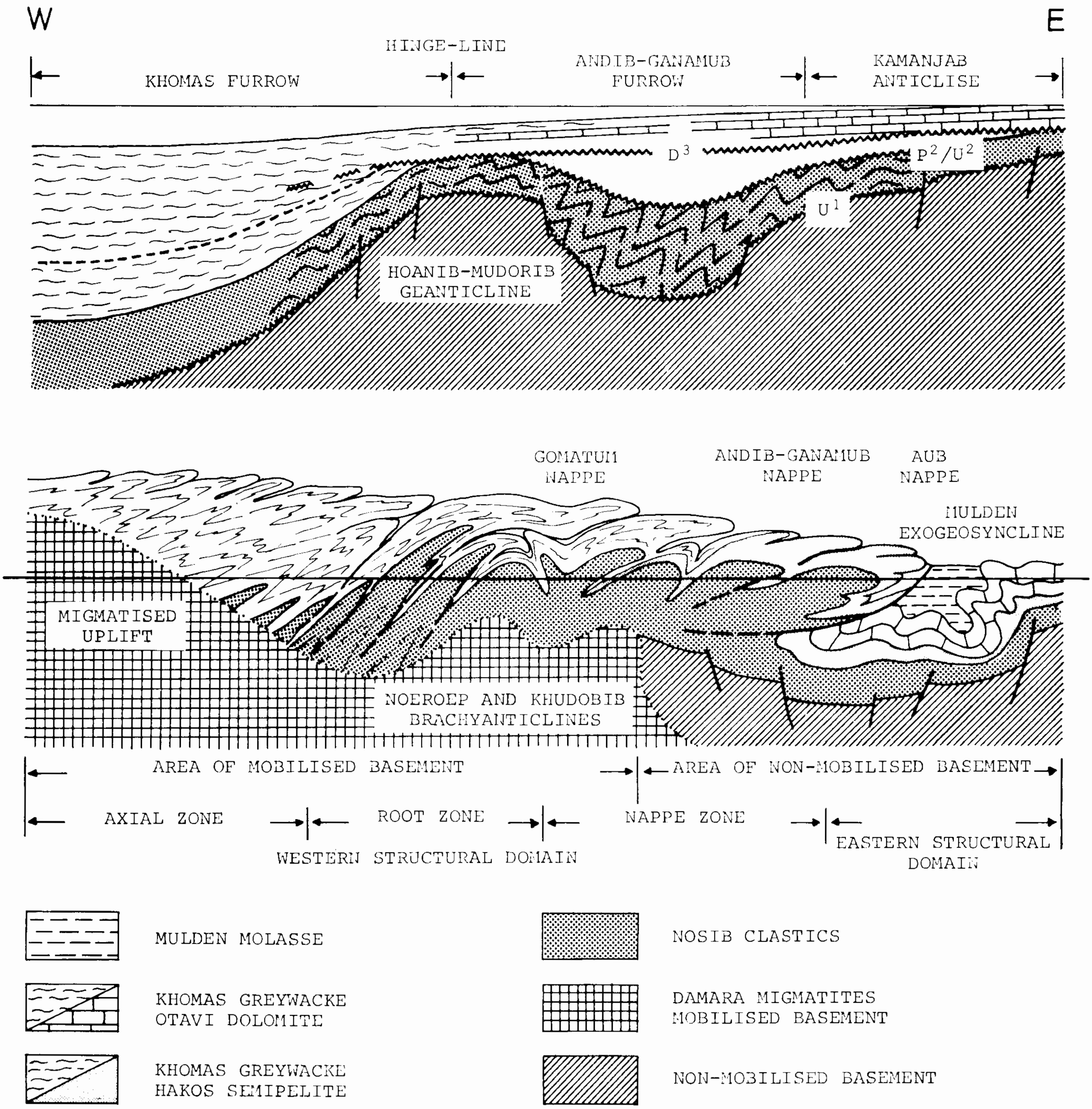

FOLDER 6. EVOLUTION OF THE DAMARA MOBILE BELT

where the Damara, Nosib and perhaps pre-Nosib mobilisates are no longer structurally distinguishable for lack of preservation of marker horizons, and consequently the masses lose their original stratigraphic identity, being transformed into a younger syn- to post-orogenetic Damara granitic/granodioritic body.

Summarising, the following conclusions seem to be warranted (folder 6(b)) for the three structural zones distinguished within the western domain:

i) In the nappe zone, the basement is unlikely to have been involved in folding, but was deformed only in an "eastern type" of block-faulting; the Nosib clastics were incorporated in cores of nappes and folded by both renewed slippage along s_1 and new slip folds in s_2, while the Damara suprastructures deformed plastically into mixed flexural-slip and slip folds in s_2 induced by the movement of the whole mass under gravitational stress.

ii) In the root zone, the basement and the lowermost Nosib metasediments were possibly partially mobilised, while the top of the Nosib was granulitised. Latent mobility at deep levels as compared to the relative competency at intermediate levels produced irregularly distributed domal structures (rising centres) providing additional local slopes for the nappes of zone (i) to be conveyed by gravity farther east towards the more stable or slightly subsiding foreland along the Sesfontein Thrust.

iii) In the zone of axial uplift, i.e. at greater depths in this area of anomalously high thermal gradients, all competence differences between the Nosib metapsammites and the overlying Damara metamorphites are progressively obliterated by advanced anatexis brought about, in spite of the relatively low water content, by extreme rises in temperature. Undifferentiated, often chaotically folded masses of mixed, more or less impure granites/granodiorites and unmelted relics of metasediments (restites) were thus formed. Long-lasting high temperatures and slowly-applied load and tectonic pressures, accompanied by relatively large amounts of pervasively distributed hypercritical solutions, enhanced the rheomorphic properties of these gneisses during deformation so that the rheidity (Carey, 1954; p. 115) may have been locally and temporarily exceeded in all three major tectonic-stratigraphic units and deformation was partially accomplished by flow into non-affine slip folds. The stresses were concentrated along the margin of this migmatite belt due to the extreme drop in rheomorphism with the consequent creation of shear-zones. The delicate balance between anatectic partial melt and subsequent recrystallisation was controlled on both meso- and macroscopic scales by local P-T gradients brought about by the dynamic variation of the tectonic stresses with time in the uprising mass. Crystallisation of leucocratic pegmatoid mobilisates at one place released large amounts of solutions which, in turn, may have promoted partial melting in adjoining masses (Mehnert, 1969). Shearing and flowage became deeply intermixed; thus slip folds in the paleosome are accompanied by flexural-slip folds in entirely crystallised pegmatoid veins and ptygmatic folds in the neosome which was possibly deformed under partially fluid conditions. It is therefore not surprising that folds in the viscous neosomatic veins may have flowed at different rates in the (a) direction, being on the whole contained in their movement within the (a-b) plane (axial plane) of penetrative schistosity formed by slip folding in the enclosing paleosomatic gneisses. The successive generation of high temperature metamorphic index minerals, the deformed pegmatoid mobilisate and the late- to post-kinematic development of sillimanite (p.123) indicate that deformation in the western domain was accomplished agains a background of increasing mobility (i.e. of decreasing viscosity). This mechanical behaviour also outlasted the last phase of D_7 wrench faulting, as is proved by the absence of a contact metamorphic aureole surrounding the Uhima granite emplaced along these dislocations in obviously extremely hot country rocks.

As for the concomitant changes in the mechanical properties of the rock-mass undergoing deformation in the eastern domain, a diametrically opposite course was followed. Diagenesis, dolomitisation etc., active during the tectonic evolution, gradually reduced the plasticity of the gliding carbonate blanket, with an increase of energy absorbed into permanent deformation (strain) progressively hindering folding.

H. TENTATIVE CORRELATION OF TECTONIC EVENTS IN THE EASTERN AND WESTERN DOMAINS

Figure 13 gives in an extremely diagrammatic fashion the regional distribution and trend of the different phases, while the accompanying diagram is an attempt to show the possible structure correlations between the eastern and the western domains.

The NNE trending F_1N folding in the Nosib clastics, so evident along the Andib-Ganamub and Hoanib-Mudorib unconformity belts, was not recorded in the east, where the only evidence of tectonic and metamorphic unrest at the time are a very slight angular difference and a marked anadiagenetic break in correspondence with the P^2 Nosib-Damara paraconformity.

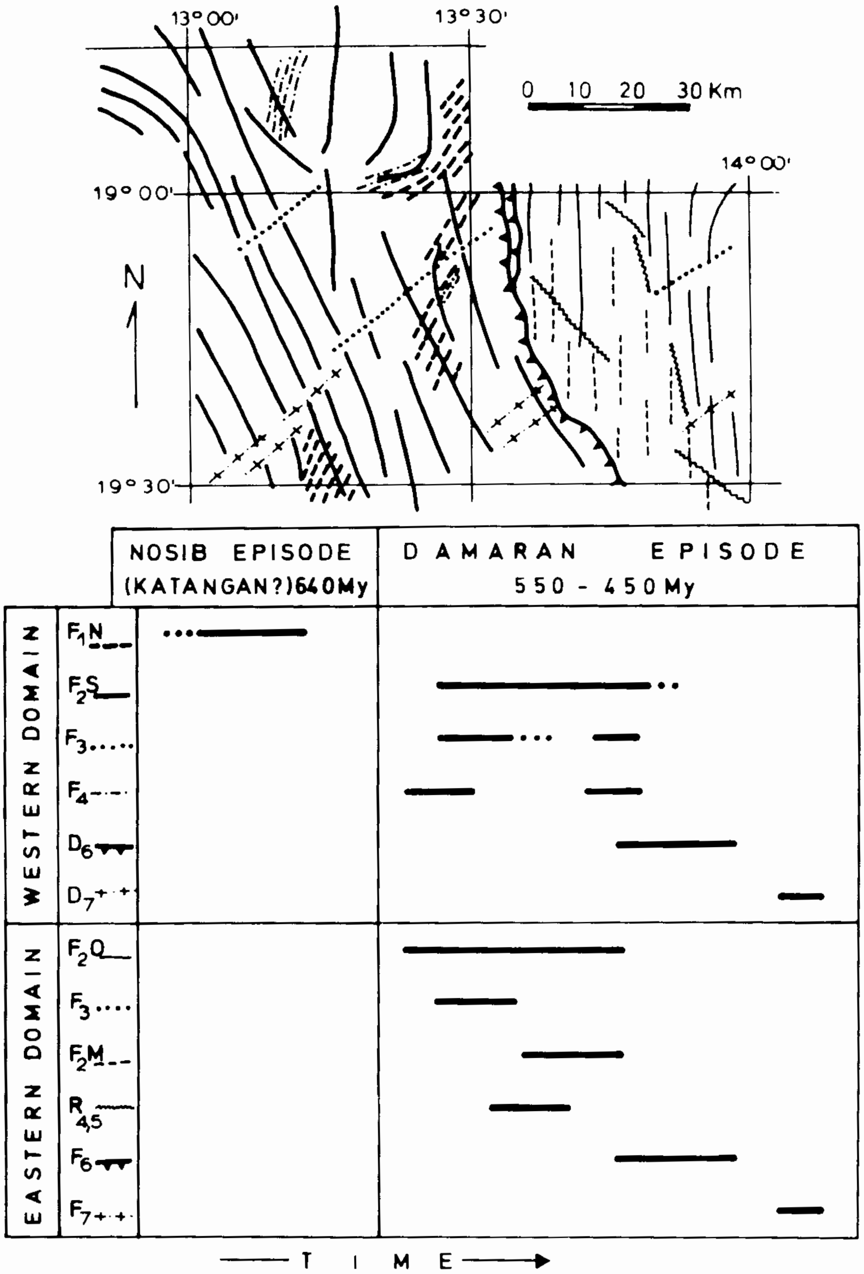

Figure 13. Distribution and time relationships of the different phases of folding

The following F_2O, F_2S, F_2M and F_3 phases of folding are generally speaking penecontemporaneous. F_2O, however, is likely to have preceded the others slightly because it appears to have controlled both the latest advancement of the F_2S nappes and the F_2M folding in the Mulden exogeosyncline. It is thus possible that gliding of the Otavi carbonate blanket away from the flanks of the rising Kamanjab anticlise towards the deeper miogeosynclinal trough may already have started during the latest sedimentation times, possibly induced by the high rate of subsidence in the western Khomas furrow. F_2S, though slightly later, must have outlasted F_2O and been active in successive pulses over a very long period, merging with the latest (D_6) Sesfontein overthrusting.

F_4, R_4 and R_5 were only local and rather limited events and cannot be strictly correlated. The F_4 trend, however, is likely to include repeated phases of movement, the first pulse (Otjihue and Sesfontein synclines) being very early, even preceding F_2S, the second pulse (coaxial superposed folding in the Gomatum synform) significantly later.

The NNW striking Sesfontein Thrust (D_6) and the belt of related "Gleitbretter" F_6M folding and transposition induced in the Mulden clastics, are obviously related and late.

The occasional NE striking, wrench or tear faults and related F_7 kinkfolds are much later, possibly post-orogenetic.

I. THE PROBLEM OF THE ARCHAEAN INLIERS IN THE WESTERN KAOKOVELD

The model of evolution of the western Kaokoveld branch of the Damara mobile belt appearing from the present research differs somewhat from the interpretation proposed in the Official Geological Map of South West Africa (1963). The consequent recommended stratigraphic revisions will be discussed in the following paragraphs.

1. The Khudobib Brachyanticline Paradox

Most of the metasedimentary gneisses west of Sesfontein were originally interpreted (Rabie et al., 1949, in Martin, 1965) as Archaean rocks "completely reconstituted and concordantly incorporated" in cores of large Damara nappes. Such an interpretation was based largely on a locally marked angular unconformity and definite textural-metamorphic step appearing at the base of the low grade schistose Andib System (Rabie, 1949) correctly correlated with the Damara System (Swakop Facies). It must be admitted that the initial impression which an observer receives when visiting the Andib area (Plate 7) is bound to influence his successive research. On a regional scale, however, the Damara- would be Archaean contact exposes an obvious angular unconformity only along less than 15%

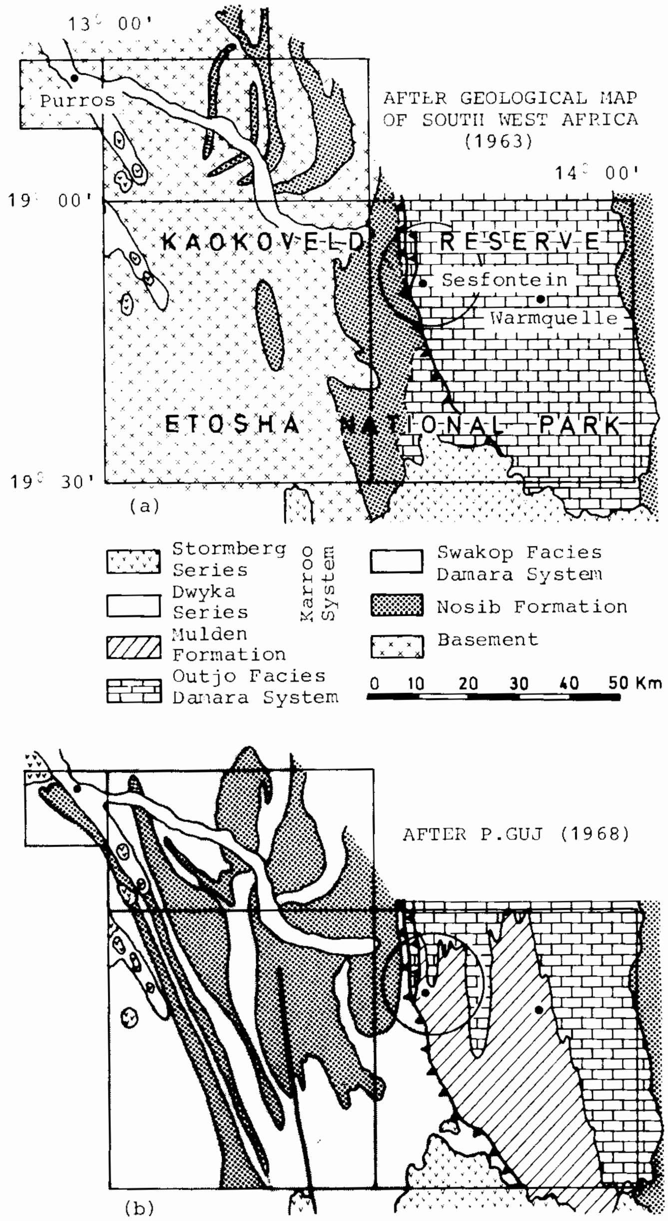

Figure 14. Recommended stratigraphic amendments to the Geological Map of South West Africa (1963)

(i.e. 155 Km) of its length (i.e. >950 Km), the major portion (85%) being paraconformable. The base of the late Precambrian sedimentary basins post-dating the 1000 My province of metamorphic and plutonic rocks (Martin, 1969; p.19), in contrast, should be characterised by an unconformity of regional if not subcontinental extent.

That local angular unconformities exist at the base of the Damara System in many parts of the country was already well known (Nel, 1954; Smit, 1962; Schalk and Hälbich, 1965). There has perhaps been a tendency in the past to attribute undue stratigraphic significance to unconformities, more on the basis of the degree of angular discordance than on their regional persistence and extension.

Approximately 12 Km to the west of the Andib valley, where the unconformity is best developed, however, the gneisses surround the impressive Khudobib brachyanticline (p. 69) of sericitic feldspathic quartzite, 10-15 Km in extent. The core of this structure has been traditionally accepted as being composed of late Precambrian Nosib quartzite and as such rightly appears on the Geological Map of South West Africa (1963), reproduced in figure 14(a). As no doubt existed at the time of compilation of this map about the antiformal nature of this fold, the existence of a stratigraphic paradox was tacitly acknowledged. A younger late Precambrian formation would in fact be encircled by older early Precambrian gneisses in an anticlinal structure. Three possible alternative solutions for the Khudobib stratigraphic paradox were analysed in the light of the new regional evidence and two of them eliminated:

a) To retain the interpretation, which appears on the Geological Map of South West Africa (1963), i.e. Nosib quartzite in the cores of antiforms surrounded by Archaean gneisses.

b) Retaining only the age of the gneisses as being Archaean and considering the quartzite in the antiform core as being older, excluding its Nosib age and therefore having a regular stratigraphic succession.

c) To maintain the Nosib age for the quartzite, but to consider the gneisses younger and in regular stratigraphic succession. Since they would be older than the basal Nosib, but younger than the Lower Hakos Damara metasediments, these gneisses could conceivably be correlated with the Upper Nosib pelitic gneisses in the Swakop and Khan Rivers area (Smith, 1965).

2. Discussion

To retain the present stratigraphic setting (alternative a), the only possible interpretation is that the Nosib rocks are ex-

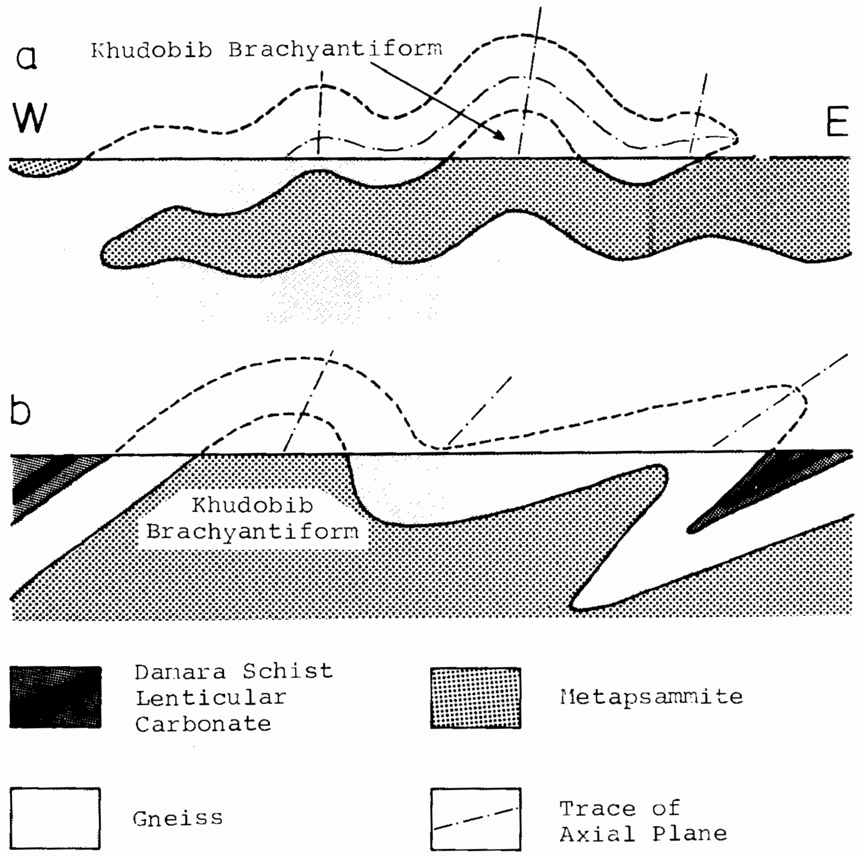

Figure 15. Hypothetical structural interpretations for the Khudobib stratigraphic paradox

posed by erosion on an antiform created by interference of a very steep domal deformation on a pre-existing, recumbent, very large-scale synclinal nappe or infold of basement gneisses, enveloping several thousand metres of Nosib quartzite, as represented in figure 15(a). This alternative must, however, be discarded because:

i) The western flank of the Khudobib antiform exposes an obvious regular succession from the Nosib psammites, throughout the gneiss, into the paraconformable base of the Damara System marked by a typical carbonate marker (fig. 15(b)), whereas if hypothesis (a) were sound no Damara rocks could possibly have appeared along the hypothetically overturned western flank.

ii) As it is obvious from figure 15(a) the Nosib-"Archaean" contact along the western flank of the Khudobib antiform should be inverted, whereas well-preserved upwards concave cross-stratification (Conybeare et al., 1968; p. 33) is exposed along it in the Obias river bed in a regular position.

iii) A basal unconformity, similar to the Andib unconformity, should be exposed at the contact between the Nosib quartzite and the "Archaean" gneiss, as there is no evidence of any re-foliation which might have obliterated it. This, however, is conspicuously absent over several kilometres of well exposed contact.

Alternative (b), whereby the psammites occupying the Khudobib antiform core would not be Nosib in age, but older than the alleged concordantly overlying "Archaean" gneiss and would therefore be interpreted as one of the numerous psammitic episodes within the basement (eg. the Huab Formation, Frets (1969), etc.), must also be discarded because:

iv) the structural history of these psammites appears to be extremely simple (one major F_2S period of deformation (N10°W) and one of later $F_2S \perp F_3S$ superposed folding.

v) if this were the case, the Damara succession would be deprived of its Nosib basal clastics, which a few kilometres to the east (i.e. in the Aub anticlinorium) are more than 3000 m thick.

vi) of the preservation of sedimentary structures likely to have been obliterated, if the apparent structural simplicity should be the effect of intense re-foliation and structural homogenisation of basement rocks during Damara times.

vii) along the western limb of the Khudobib brachyanticline, amphibolite bands concordant with the gneiss foliation are also essentially subparallel to the hypothetical Damara-"Archaean" contact. This suggests that no major cycle of deformation has occurred locally prior to the deposition of the Damara schists.

viii) this interpretation ignores the lithological similarities between the quartzite core and known Nosib sequences in adjoining areas.

Only one alternative (c) is left, which implies that the granodioritic paragneiss of the Pruwes, Andib and Ganamub area are not basement, but being stratigraphically between the Nosib psammites and the base of the Hakos Series (Damara System) must have a late Precambrian or Upper Nosib age. The hypothesis of a regular stratigraphic succession would solve points i, ii, iii, v, vii and viii quite well. A Nosib age would explain the structural simplicity and similarity to the Damara structures (point iv), and the preservation of sedimentary structures (point vi).

As a result a substantial revision of the stratigraphy which appears in the Geological Map of South West Africa (1963) is recommended. For the area investigated the amendments to be introduced are schematised in figure 14 in which the upper map (a) shows the previous interpretation and the lower one (b) is a reduction of the maps included in pocket to fit the same scale.

As for the large extension of "Archaean rocks", appearing between the study area in the south and the Kunene River (and beyond it) in the north on the Geological Map of South West Africa (1963), several reconnaissance traverses, carried out by the author along the Hoarusib, Khumib and Natas Rivers and by de Villiers (1968) in the Marienfluss-Hartmannberg area seem to point towards a structural-stratigraphic relationship very similar to that encountered west of Sesfontein. Additional reconnaissance work is recommended in order to determine whether any possible structural inlier of early Precambrian age is in fact present west of the N-S line connecting the Sesfontein Thrust to the van Zyl pass (de Villiers, 1968), where "no undoubted basement was seen..". Nosib and Damara metasedimentary and granitoid rocks could likely compose most, if not the whole of this so long insufficiently known mobile belt.

3. Possible Correlation of the Nosib and the Naauwpoort Formations

Large extensions of the territory west of Sesfontein, which were formerly believed to be basement, have thus been proved to be underlain by the arkosic or arenitic and greywacke clastic associations belonging to the Lower and Upper Nosib Stages respectively, including their accompanying and various syndepositional igneous suites. Some 100-150 Km to the south-east, near Welwitschia, another sequence of coarse clastics and associated differentiated volcanics and gabbroic intrusions, i.e. the Naauwpoort Formation, has been described by Leube (1963), Martin (1965) and recently by Frets (1969). The following striking analogies which seem to exist between the Nosib and the Naauwpoort Formations may not be accidental:

i) Both sedimentary successions are composed of arkosic quartzite, intraformational conglomerate and pelites in that order.

ii) The Naauwpoort sediments of Welwitschia are concordantly or paraconformably overlain by the Damara succession, as is normally the case with the Nosib in the Sesfontein area.

iii) Both sedimentary sequences are associated with volcanism (the Naauwpoort to a greater extent than the Nosib).

iv) In both areas pre-Tillite gabbroic intrusions (Bushöhe Complex of Welwitschia and Khankhaib Complex of Sesfontein) seem to be the latest related igneous activity.

Moreover, Frets (1969; p.51) discovered that a conglomerate, containing pebbles of Naauwpoort volcanics and resting concordantly at the base of the Damara sediments (therefore regarded by Martin (1965; p.8), possibly correctly, as the Damara basal conglomerate), is intersected by stocks of Bloukrans quartz bostonite related to the Naauwpoort volcano-magmatic episode. Frets included this rudite in the top of the Naauwpoort Formation as a product of local pre-Damara and at the same time pre-bostonite erosion, though it would appear simpler and perhaps more logical if, as Martin suggested, this is retained as the basal Damara conglomerate, implying only:

i) that the Naauwpoort clastics could be equivalent, as Leube (1963) proposed, to the Nosib Formation, which is otherwise conspicuously absent in the area, and consequently

ii) that the Nosib (i.e. Naauwpoort) igneous activity extended from Upper Nosib into Lower Damara times, as is the case in the Sesfontein area.

Moreover, the Naauwpoort Formation does not show any sign of deformation or metamorphism prior to the Damara episode and in contrast with any other pre-Damara formation in the area, is still substantially unmetamorphosed (Frets, 1969).

Frets (1969, p.88) adds that: "...the Naauwpoort igneous activity post-dates the basement complex and Fransfontein granite (1700 My) in age, but pre-dates the overlying Hakos Series of the Damara System (650-700 My). In the northern part of South West Africa only two other formations are known with an age in this time span: i.e. the Khoabendus and the Nosib(Hundskopf)Formation."

The Khoabendus, however, was severely folded during pre-Nosib time as it is separated from Nosib and Damara rocks by a marked angular unconformity (see fig. 2), whereas the Naauwpoort and the Nosib clastics seem to underlie the Damara sediments paraconformably along the whole western margin of the Kamanjab inlier.

Occurrences of lava in Nosib terrains in other northern areas of the country have been described by Smit (1962) and observed by Miller (personal communication).

Rb/Sr total rock age determinations of Naauwpoort felsite and porphyry yielded 557 ± 10 My (de Villiers, 1968). This age is certainly too low for the extrusive event, as similar ages have been obtained for granites, of intrusive or metamorphic origin, that are definitely younger than Khomas sediments, which in turn are demonstrably younger than either Naauwpoort or Nosib.

On the basis of these comparisons the present author advances the possibility that the Naauwpoort and the Nosib Formations may be correlated and included at the base of the Damara System, thus providing its basal clastics and volcanics, which are otherwise "poorly developed or conspicuously absent" (de Villiers and Simpson, 1968).

IV. METAMORPHISM AND ULTRAMETAMORPHISM

A. GENERAL

Regional dynamothermal metamorphism of variable intensity is widespread throughout most of the area studied. The metamorphic facies series is essentially Barrovian in character (Winkler, 1967).

Fairly homogeneous sampling coverage, due to the good exposure, allowed for the plotting of the regional distribution of the mineral parageneses into the isograd map of folder 7.

A selection of representative mineral parageneses, deriving from a few hundred metamorphosed lithotypes of siliceous-argillaceous, carbonate and basic igneous suites, are listed in table 6, 7 and 8. The minerals are tabulated in abscissa from right to left in order of increasing metamorphism or customary successive appearance. The different samples are listed from top to bottom in order of increasing metamorphic grade. The last column on the right provides the grid coordinates which will enable the reader to locate the various assemblages within reasonable limits on the isograd map of folder 7.

A cursory examination of folder 7 supported by tables 6, 7 and 8 will immediately reveal that:

i) A gradual progression takes place from low-grade metamorphic assemblages in the east to very high grades in the west. This feature, underlined by the appearance of successive index minerals, is the result of the latest metamorphic recrystallisation brought about by the youngest (M_2) Damaran tectono-thermal episode. Such a regional zoning will, therefore, hereinafter be referred to as the "Damaran metamorphic gradient".

ii) The highest-grade metamorphic zone (i.e. the sillimanite zone (J)) is duly accompanied by anatexis and migmatisation (A_2), broadly delimited by the line marked "front of the Damaran migmatites" in folder 7.

When the previous illustrations are analysed in parallel with the regional maps (in pocket) it will easily be noticed that the Nosib-Damara stratigraphic contact seems to:

iii) delimit very large extensions of retrograde metamorphism in the area east of the Damaran hornblende-oligoclase isograd (continuous bold line in folder 7).

iv) suggest a substantial textural difference between the two formations. This is particularly obvious in the field to the east of the above-mentioned Damaran hornblende-

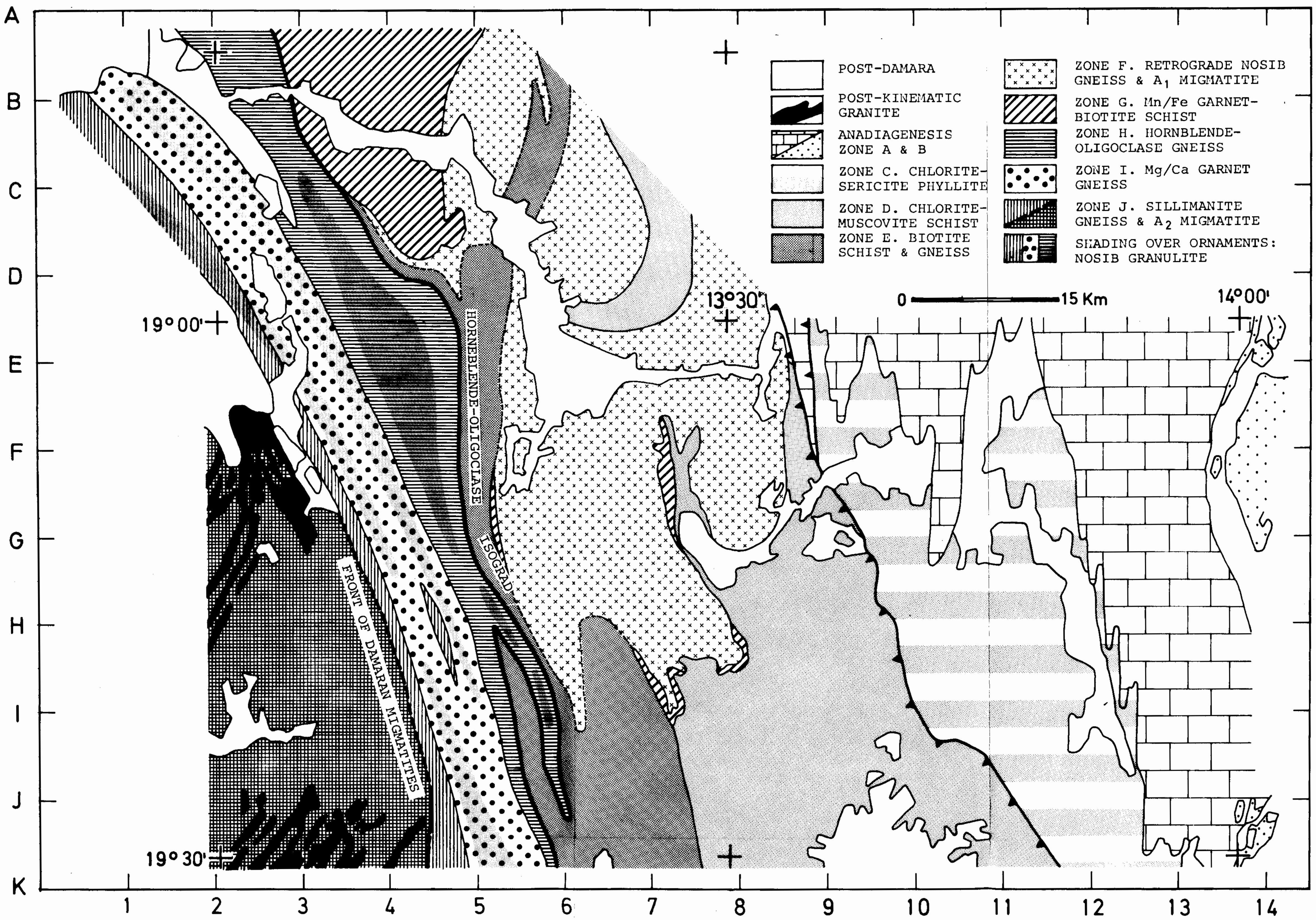

FOLDER 7. DISTRIBUTION OF METAMORPHIC ZONES IN THE SESFONTEIN AREA

Table 6. Representative Mineral Parageneses in Metamorphosed Siliceous-argillaceous Suite

SAMPLE NO.	Silliman.	Pyrox.	Garnet High T.	Ca-Plag.	Hornbl.	K-Feld.	Garnet Low T.	Epidote/ zoisite	Biot.	Trem./ Actin.	Ser. Musc.	Chlor.	Na-Plag.	Q	Location on map
6									x		X	X	x	X	E 10
46									x		X	X	x	X	F 10
126								x	x		x	X	x	X	H 11
54											X	X	X	X	G 10
70									x		X	X	X	X	J 9
75									x			X	X	X	J 8
71									X		X	X	X	X	J 8
59								X	x	x		X		x	J 8
52									X		X	X		X	G 9
60									X		X	X	X	X	I 10
58									X		X	x	X	X	I 9
68								X	X		X		X	X	J 9
74									X		X			X	J 8
5/125/2									X		X		X	X	I 7
5/125/1				Olig.				X	X		X		X	X	I 7
104									X	X	X	x_r	X	X	H 6
238								X	X		X		X	X	F 6
224				Olig.		X		X	X		X			X	F 5
225				Olig.		X		X		X	X			X	F 5
124								X	X		X	X	X	X	D 8
170								X	X	X_r	X_r	X_r	X	X	E 7
18/729/9B							X					X		X	B 5
18/729/4B							X		x			X		X	B 5
18/729/19							X		X			X	x	X	B 4
18/729/22							X		X			x	x	X	B 4
40							X		X			x		X	F 8
18/729/5							X		X				x	X	B 5
18/729/11+21							X		X		X			X	B 4
223				Olig.			X		X					X	F 5
92				Olig.				X	X		X	X	X	X	G 7
94/96				Olig.				X_a	X		X	X	X	X	G 6
18/729/1				Olig.				X	X		X			X	B 5
107				Olig.				X_a	X_r	X_r		X_r		X	H 7
44+44A				Olig.				X	X	X_r		X_r		X	F 7
212				Olig.				X_a	X_r	X_r		x	X	X	G 6
114				Olig.		X		X_a		X_r	x			X	H 6
19/865/1				And.		X		X	X		X_r	X_r	X	X	C 8
33				Olig. - And.		X			X		X		X	X	E 8
122				Olig.		X		X_a	X		X_r	X_r		X	D 8
123				Olig.		X		X	X		X_r	X_r		X	D 8
108				Olig.	X			X_a	X			X_r		X	H 7
164				Olig.	X			X	X					X	D 5
158B				Olig.	X	X		X_a	X				X	X	D 5
113				Olig.	X	X		X_a	X			X_r	X	X	G 5
5/125/3+4				Olig.	X	X		X_a	X			X_r	X	X	I 6
121				Olig.	X	X		X_a	X	X_r	X_r	X_r	X	X	F 5
168 A				Olig.	X	X		X_a	X					X	E 5
156				Olig.	X	X							x	X	E 4
153			X						X		X	X_r	X	X	F 4
3/68/4			X	Olig.					X				x	X	G 5
3/68/2			X	Olig.		X			X				x	X	H 5
5/123/2			X	Olig.					X				x	X	J 6
4/107/2			X	Olig.					X			X_r		X	H 5
4/108/1			X	Olig.					X		x			X	H 5
18/733/3			X	Olig.					X					X	A 2
4/110/6		X		Lab.						X_r		X_r		X	I 3
145A		X	X	Lab.						X_r	X_r	X_r		X	H 3
143		X		Lab.		X			X	X_r	X	X_r		X	H 3
146	X			Olig.		X			X					X	H 3
3/66/6	X		X	Olig.		X			X		x			X	G 3
5/126/3	X			Olig.		X			X					X	J 5
152 A	X			Olig.		X			X					X	E 4

X = Major constituent
x = Accessory
r = Retrograde
a = Allanite

oligoclase isograd, and is perhaps more deceptive to the west in the high amphibolite facies, where the mineral parageneses above and below the Nosib-Damara stratigraphic contact indicates with extremely rare exceptions, substantially the same metamorphic grade.

v) enclose areas (zone F) where migmatitic metatexis (A_1) occurred east of the Damaran hornblende-oligoclase isograd, i.e. where the Damaran tectono-thermal episode alone would not warrant its development. Migmatitic textures are here confined to metamorphic terrains of Nosib stratigraphic age.

vi) indicate that metamorphic textures and metamorphic grades inferred from the mineral parageneses are in full agreement only in metamorphites of Damara stratigraphic age.

vii) show that most of the metamorphic and migmatitic features which do not seem to be warranted by the Damaran episode alone are distributed in areas partially deformed by the F_1N phase of deformation (NNE), with which they are structurally associated.

It can be concluded, provisionally, that part of the study area underlain by rocks of Nosib age must have undergone polyphase metamorphism. The last Damaran tectono-thermal episode (M_2) (550-450 My) (Clifford, 1967) of end-Precambrian age (Martin, 1969; p.17) is thus superimposed on rocks which were discontinuously metamorphosed during a previous (post-Nosib/pre-Damara) episode, hereinafter symbolised M_1 (F_1N).

The various Damaran (M_2) and Nosib/Damaran (M_1/M_2) single- and poly-metamorphic terrains outlined in folder 7 can then be briefly described.

Apart from two successive and separate diagenetic cycles (described in p.10) determining an equal number of sub-metamorphic zones (A and B), seven progressive Damaran metamorphic zones (C to J) were established within the Precambrian metasediments over both western and eastern structural-stratigraphic domains. These were broadly subdivided into a greenschist and amphibolite facies in Table 9, while the symbols accompanying each zone in brackets are an attempt to correlate the present subdivision with Winkler's standard subfacies classification (1967; p.90) for Barrovian dynamothermal metamorphic facies series.

SAMPLE NO.	Wollas-tonite	Brucite	Spinel	Forster. + Serpent.	Diops.	Epidote	Trem. Actin.	Plag.	K-feld.	Biot.	Phlog. Musc.	Chlorite	Talc	Q	Calcite	Dolomite	Location on map
49										x	x	x	X	X	X 37.22	x	F 10
19/865/8								x	X		x		X	X	x 40.41	X	C 8
4/108/7				x	X	X	X	x	X					X	X 33.76		H 5
154 B,H,L					X		X	x	X					X	X 61.89		E 4
18/733/11					X			x	X	X	X			X	X 5.70		B 2
5/123/1				x	X		X_r	x			X				X 93.65	x	J 6
4/108/4				x	X		X_r	x	X		x			X	X 88.49		H 5
201				X	X		X_r	x	X					X	X 42.24		I 5
1/10/4		X*		X_s											X 82.08	x*	D 3
18/733/14	X			X_s							X				X 70.01	x	B 1
3/68/5	x	x		X							X				x 86.83	X	G 5
3/68/6	X		X	X_s							X				X 56.53	X	H 5

X = Major constituent
x = Accessory

* Total carbonate includes brucite
r = Retrograde s = Serpentine

Table 7. Representative Mineral Parageneses in Metamorphosed Siliceous Carbonate Suite

SAMPLE NO.	Silliman-ite	Pyrox.	Garn. High T.	Ca-Plag.	Horn.	K-Feld.	Garn. Low T.	Epidote Zoisite	Biot.	Trem. Actin.	Ser. Musc.	Chlor.	Na-Plag.	Q	Location on map
67									x	X			x	x	J 9
50								X	x	X			X	X	G 9
64								X	x	X			x	X	J 9
140/141				Olig. - And.				X	x	X			X		H 9
135/137								X	X	X		X	X		H 9
306				Olig. - And.		X		x		X_r		X		X	H 9
93				Olig. - And.		X			X	X_r				X	G 7
119				Lab.	X			X		X_r		X_r		X	H 6
168 C				Olig. - And.	X			x	x					X	E 4
207				Olig.	X			x						X	F 5
18/733/3A				Lab.	X				X	x_r	x_r			X	A 2
155				Lab.	X	X								X	E 4
18/731/1				Lab.	X	X								X	B 3
160		X_d		Olig.	X									X	D 4
202		X_d		Lab.	X	x			x	x_r		x_r		X	I 5
157		X_d		Lab.	X										D 4
17/862/1		X_d		Lab.	X										A 3
18/732/1		X_h		Lab.	X	x			x					x	B 2

X = Major constituent r = Retrograde d = Diopside
x = Accessory h = Hypersthene

Table 8. Representative Mineral Parageneses in Metamorphosed Igneous Basic Suite

B. THE GREENSCHIST FACIES IN THE EASTERN STRUCTURAL-STRATIGRAPHIC DOMAIN

1. Zone C

Zone C coincides with the Mulden clastic association east of the Sesfontein Thrust. It is bordered to the north and the east by diagenetic zone A, composed of rocks (carbonates) of uncongenial bulk chemical composition to react in low-grade metamorphic environments. The western limit is tectonic (Sesfontein Thrust). A definite discontinuity in metamorphic grade and texture marks the thrust line.

The predominant rock-type is a finely schistose phyllite and quartz phyllite.

Platy minerals are essentially sericite (illite to the east) and chlorite intergrowths. Albite is present but always subordinate to quartz in coarser lithotypes.

The most common paragenesis in the siliceous-argillaceous suite is therefore, quartz-sericite-chlorite.

A veneer of interstitial chlorite gives a dull greenish appearance to most of the feldspathic sandstone and wacke developed to the south-west of the Mulden basin.

The siliceous dolomite bands still unaffected in the eastern portion of zone C react in the west to produce the typical talc-calcite±dolomite±quartz paragenesis, depending on excess of quartz or dolomite in the original sediment.

Feldspar-free microsegregation banding and frequency of transgressive veinlets seem to increase westwards.

No biotite was recorded east of the Sesfontein Thrust, except for rather subordinate amounts along shear-zones.

Disregarding any other quantitatively insignificant phase, the reaction

$$3 \text{ dolomite} + 4 \text{ quartz} + H_2O \rightleftharpoons \text{talc} + 3 \text{ calcite} + 3CO_2$$

is bivariant (Metz et al., 1963) because of the gradual release of the new phase CO_2. In a closed system, i.e. in relatively thick carbonate successions the fluid pressure P_f would be equal to $P_{H_2O}+P_{CO_2}$ and the sum of the partial pressures could even exceed the load pressure P_l (Winkler, 1967; p.25), phenomenon bearing an important role in the mechanics of the Sesfontein Thrust (p.76).

In closed systems the equilibrium temperature of this reaction is directly proportional (Winkler, 1967; p.34 and Turner, 1968; p.136) to the mole fraction of CO_2 (X_{CO_2}). Thin (0.50-10.00 m thick) carbonate bands surrounded by inherently water-rich shales (pre-diagenetic H_2O content >70% (Larsen and Chilingar, 1967)) can-

Diagenesis	Zone A. Damaran anadiagenetic cycle	
	Zone B. Pre-Damaran anadiagenetic cycle	
Greenschist Facies Series (B1)	Zone C. Sericite-chlorite-talc	(B1.1)
	Zone D. Chlorite-muscovite-tremolite (sub. biotite)	(B1.1)
	Zone E. Biotite-epidote (prograde)	
	Zone F. Biotite-epidote (retrograde)	(B1.2)
	Zone G. Biotite-low temperature garnet	(B1.3)
Amphibolite Facies Series (B2)	Zone H. Hornblende-oligoclase	
	Zone I. High temperature garnet-biotite	(B2.1/2)
	Zone J. Sillimanite	(B2.3)

Table 9. Schematic subdivision of the Damaran Regional Dynamothermal Metamorphism in the Sesfontein Area

not be regarded as closed systems, as CO_2 is bound to escape and dissolve in the adjoining fluids.

Moreover a proportion of dolomite together with large amounts of calcite coexisting in paragenesis with excess of quartz (sample 49) proves that the reaction was not carried out to equilibrium. The equilibrium temperature of 400°C advanced by Winkler (1967; p.25) is, therefore, regarded as the maximum (possibly never attained) limit.

This would fit the pelitic paragenesis well, as heated illite-bearing clays with high Al/K ratio at P_{H_2O} of 2 Kb were experimentally converted into muscovite-chlorite-quartz at temperatures below 400°C (Winkler et al., 1957). Experiments by Velde (1964) on quartz-bearing montmorillonitic or illitic sediments have substantiated Fyfe, Turner and Verhoogen's (1958; p.173) view that the lower stability limit of the muscovite-chlorite assemblages of the greenschist facies is as low as T=300°C, or possibly somewhat lower, for P_{H_2O}=3 Kb. The natural value of hydrostatic pressure must if anything have been lower than this last figure as the Mulden pelites were the highest member of the sequence and their maximum recorded thickness does not exceed 3000 m (Frets, 1969; p.105) of which only 700 m are preserved locally. Pressure could, however, have been slightly increased by tectonic overpressure (Clark, 1961) due to the Sesfontein Thrust.

The P-T conditions which controlled the metamorphism of zone C are thus comparable with those characterising the lowest threshold of the chlorite subfacies (B1.1) of the greenschist facies of regional metamorphism as defined by Winkler (1967; p.95).

C. THE GREENSCHIST FACIES IN THE WESTERN STRUCTURAL-STRATIGRAPHIC DOMAIN

Most of the digitated front and carapace of the Andib-Khankhaib and Gomatum nappes (p.60) are composed of Hakos mica schist, and the cores comprise texturally extremely different paragneiss of Nosib age.

The whole allochthonous mass transgresses the Mulden phyllite along the Sesfontein Thrust. This line of dislocation marks a significant metamorphic boundary as biotite, virtually absent to the east, makes its first appearance here.

As the original sediments were ferruginous the common prochlorite-muscovite assemblage was in an ideal physico-chemical environment to start yielding biotite, conceivably at a somewhat lower temperature than that of the true biotite zone (B1.2 of Winkler, 1967). According to Turner (1968; p.118), under P_{H_2O} of a few kilobars and congenial chemical bulk composition the first biotite can appear at temperatures as low as 300-400°C. West of the Sesfontein Thrust the amount of biotite present grades from subordinate to significant (i.e. not less than 10% of all phyllitic minerals). The amount of this index mineral and its peculiar paragenetic, textural or structural associations define several metamorphic zones:

1. Zone D

Zone D of folder 7 is characterised by the persistence of muscovite and chlorite among the platy minerals, while biotite, though normally present, is limited to accessory quantity or confined to structurally-controlled areas of growth.

The appearance of weakly pleochroic (α=green, β=yellow, γ=yellowish green; $\gamma \wedge c=16^{\circ}$) tremolite/actinolite and epidote/zoisite (rarely clinozoisite) together with a generally much coarser lepidoblastic or nematoblastic texture in the resulting schists, makes the distinction from the Mulden phyllite (zone C) very easy in the field.

The typical paragenesis developed in the siliceous-argillaceous suite is: quartz-chlorite-sericite$\pm$albite$\pm$epidote/zoisite$\pm$biotite with calcite, iron ore and hematite as ubiquitous accessories.

In the siliceous carbonate suite, calcite is still a stable phase in the presence of quartz, as is, in most cases, dolomite. Similar sluggishness has been reported by Zen (1966) for carbonate assemblages of the greenschist facies of Vermont.

Most of the basic igneous suite parageneses comprise intrusive stocks and sills related to the pre-Tillite Khankhaib Gabbroic Complex (p.58) largely emplaced within the Lower Hakos metasediments. The typical mineral paragenesis is thus retrograde (or rather as it will be seen "apparently retrogressive" (Carpenter, 1969)) and composed of a certain number of mineral phases "stable" under the local Damaran physico-chemical conditions coexisting with a few "relics" of the parental high-temperature assemblage. The "stable" phases form the typical: albite-chlorite/actinolite-epidote/zoisite$\pm$sphene$\pm$biotite$\pm$quartz paragenesis. Relic phases are oligoclase and/or andesine (up to An_{36}) associated with albite ($<An_5$) as products of partial diaphthoresis of the more calcic plagioclase of the original gabbroid rocks, which from catanormal calculations (Barth, 1959) of chemical analyses seem to have ranged from calcic labradorite (An_{65}) in gabbros and pyroxenites to andesine (An_{41}) in more anorthositic differentiates (p.58). The amount of saussuritisation and replacement by albite seems to decrease in rocks exhibiting coarse blastophitic texture, due to preponderant grain-boundary diffusion of fluids, and consequently of heat, together with the lower specific reaction surface and consequent lower free energy of the system (Spry, 1969), lattice-diffusion being subordinate or even negligible.

The "feathered" (Carpenter, 1969) intergrowth of chlorite within the actinolite amphibole (α=bluish green, β=yellowish green, γ=yellow; $\gamma\wedge c=17^{\circ}$) (sample 306) supports its possible derivation from hornblende (partially a product of uralitisation of an original pyroxene) according to the reaction:

hornblende$\pm H_2O \rightleftarrows$chlorite+tremolite/actinolite+epidote+quartz

which although not yet thoroughly experimentally investigated is to be commonly expected in nature (Winkler, 1967; p.71). It must be appreciated that this reaction requires the presence of water, inherently scarce in typical "dry" metamorphism of gabbros and anorthosites (Spry, 1969).

Since the isograds intersect the structural boundaries, metamorphism is likely to have occurred at least partially in dynamic environments, i.e. concomitant with the formation of the Andib-Ganamub nappe front. The upward migration of aqueous solutions and volatiles must have been controlled by this dynamically changing system of pressure gradients and diffusion lines. Structurally controlled concentration of fluids towards zones of lower pressure and mechanical permeability (eg. shear-zones, axial planar zones of folds etc.) resulted in local mineral assemblages having a hydrous character customarily justified by T-P much lower than those actually operative. This "apparent retrograde metamorphism" was illustrated first by Carpenter (1969; p.185), who recognised that: "The role of structural deformation must be included in the interpretation of the paragenesis of a metamorphic rock. Pressure gradients created by folding and shearing are perhaps the most important factors in driving the chemical reactions of metamorphic differentiation". The role of pressure, chemical activity and fugacity of water (P_{H_2O}) and their variations with time have also been emphasised by Spry (1969; p.4), who stresses how the intermittent periods of deformation concomitant with metamorphism bring about independent variations of P_{H_2O} and P_l against the general rise in temperature.

In the light of these considerations the difference between zones D and E could only derive from the former's development in the low-pressure and therefore hydrous nappe front and not from effective lower operative temperature.

The drastic difference between the catanormative mineralogy (Table 4) calculated from the chemical analyses of metagabbroic rocks belonging to the Khankhaib Complex and their present metamorphic parageneses, just described, provides an impressive indication of the changes which an inherently anhydrous high-temperature (>800°C) assemblage underwent at low-grade metamorphic conditions due to the effect of water concentration and mechanically created permeability.

2. Zone E

The boundary with zone E, gradational to the west, is transitional over a fairly wide belt, as it is essentially based on the gradual increase of biotite to significant amounts. This is in turn strictly controlled by tight F_2S isoclinal or recumbent folding and therefore difficult to pinpoint in the field.

The textures are practically identical to those of zone D, but become slightly coarser and more banded in the west.

The most significant change is thus the appearance of biotite as an index mineral in the siliceous-argillaceous representative mineral paragenesis: quartz±albite-chlorite-biotite-muscovite-epidote/zoisite with iron ore, dolomite (ankerite) and sphene as common accessories. Biotite has normally a reddish-brown to yellowish-grey pleochroism, is associated with the iron ore and seems to coexist with chlorite in apparent equilibrium. This zone is thus likely to correspond to the quartz-albite-epidote-biotite B1.2 greenschist subfacies defined by Winkler (1967; p.98).

3. Zone F

Contrary to what has been observed so far, the boundary of zone F, forming the core of the Andib-Ganamub nappe, with zones D and E is not gradational but marked by significant textural differences. While in the carapace of the nappes the main rock-type is a lepidoblastic schist with moderate feldspar-free segregation banding enhancing an original lamination or layering, in zone F the metasediments have a definite gneissic texture ranging from coarse lepidoblastic to essentially granoblastic. Quartz-feldspathic segregation banding, metamorphic differentiation and localised migmatisation have been common processes in the zone during the Nosib (M_1) tectono-thermal episode. Plate 23 shows banding produced by metamorphic enhancement of an original compositional layering. The lighter bands are biotite-chlorite-actinolite (degraded hornblende) granodioritic gneiss, the darker are para-amphibolite. Metamorphic differentiation must still have been active during deformation as the high pressure-gradient interboudinage partition (Whitten, 1966; p.299) is occupied by rhomboid-shaped quartz and scarce feldspar at the top and, almost exclusively, actinolite/chlorite (degraded hornblende) at the bottom. A halo enriched in felsic components and therefore slightly paler than the adjacent para-amphibolite surrounds the interboudinage area.

Along the Andib-Ganamub unconformity belt and in the Giribes Plains, metamorphic differentiation and A_1 migmatisation coeval with the end of the F_1N phase of deformation has obscured the metasedimentary origin of some of these gneisses, which grade into igneous-looking foliated granodiorite (Pruwes granodiorite AG_1d) remarkably chemically and mineralogically homogeneous over a very large area as shown by the chemical analyses, and mesonorms of Table 10 supported by the modes of Table 11. It can be proved that for the most this was not mobilised and that its geometry is strictly structurally controlled. In the Aub anticlinorium, for instance, the granodiorite bodies are limited by, and never intersect, a band of metaconglomerate in which the bedding is still distinguishable. Its formation <u>in situ</u> is likely to be related to two fundamental factors, which in order of importance are:

i) A congenial bulk chemical composition of the sediments composing the original Upper Nosib greywacke association.

ii) Incipient to advanced (A_1) anatectic mobilisation of a partial melt of variable, generally leucocratic granitic/granodioritic composition, proportionally enriched in K-feldspar and quartz (Winkler, 1967; p.209). The conjugate depletion of the quartz/K-feldspar components in the non-mobilised gneiss may have induced slight granodioritisation (Marmo, 1967) and localised enrichment in mafics (restite of Mehnert, 1969). Plate 24 shows a network of pegmatoid mobilisates (Mehnert, 1969) crosscutting the Pruwes granodiorite.

Table 14 gives the modal mineralogical composition of 19 Upper Nosib granodioritic and granitic gneisses. Group A includes sam-

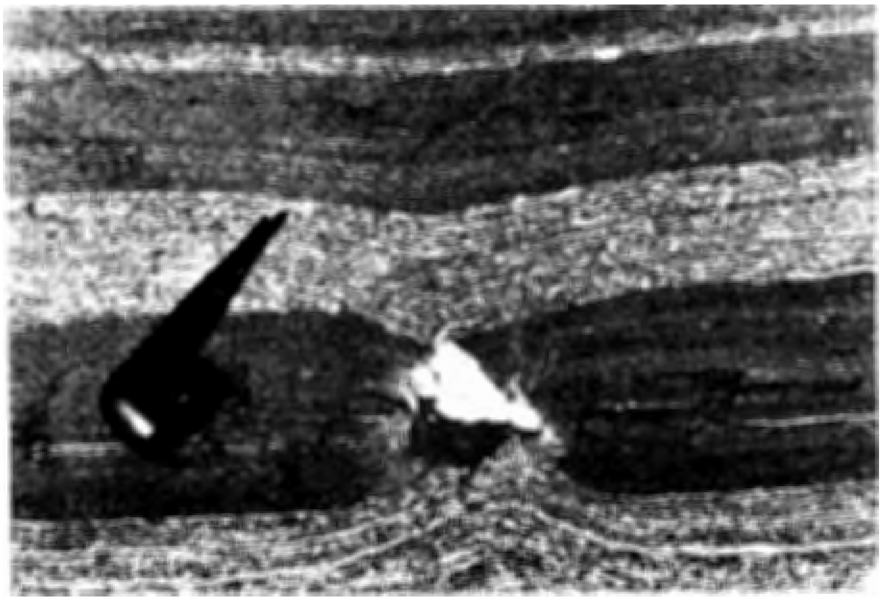

Plate 23. Metamorphic differentiation during boudin formation in banded Nosib paragneiss

ples which are not closely associated with leucocratic mobilisates whereas group B is composed of foliated grandiorites typically related to the mobilisates of group C.

That migmatisation is a local "venitic" phenomenon (Mehnert, 1969) and that no granitic "arteritic" (op.cit.) material was injected from below is proved by the absence of granitic/granodioritic dykes in the underlying Lower Nosib psammites, the modal mineralogical compositions of which is given in Table 12 (group A), together with those of a few (group B) Upper Nosib psammitic "resisters".

The "minimum melt" temperature is a function of the Ab/An ratio (Winkler, 1967; p.205) and is considerably lowered by the presence of volatiles (i.e. Cl, F, B etc.) in the fluid phase (von Platen, 1965). The normative Ab/An ratios calculated from the Pruwes granodiorite chemical analyses of Table 10 range between 1.5 and 5.8, which interpolating the experimental values at P_{H_2O}=2 Kb supplied by Winkler (1967; p.205) would give a "minimum melt" temperature range between 707° and 683°C respectively. Such a temperature range, however, must be regarded as maximum, since the boron silicate, axinite, found in a few samples (eg. 223) indicates a volatile-rich fluid phase. The amount of melt is a direct function of the T-increase and of the P_{H_2O} (Winkler,

	Sample	92	94	122
	Location	Audib Valley	Pruwes	Giribes Plains
CHEMICAL ANALYSES	SiO_2	63.85	59.06	61.25
	TiO_2	0.68	0.67	0.71
	Al_2O_3	16.79	16.62	16.12
	Fe_2O_3	2.29	2.88	1.50
	Feo	3.38	3.61	4.04
	MnO	tr.	0.11	0.08
	MgO	3.09	3.13	3.00
	CaO	2.18	5.72	4.49
	Na_2O	4.52	3.74	3.51
	K_2O	1.92	2.21	2.79
	P_2O_5	-	0.25	0.21
	L.o.i.	1.24	1.00	1.07
	H_2O^-	0.16	0.06	0.26
	Total	100.10	99.06	99.07
CATION PROPORTIONS	Si	59.75	55.97	58.22
	Ti	0.48	0.48	0.51
	Al	18.52	18.57	18.07
	Fe^3	1.61	2.05	1.07
	Fe^2	2.65	2.86	3.21
	Mn	-	0.09	0.06
	Mg	4.31	4.42	4.25
	Ca	2.19	5.81	4.57
	Na	8.20	6.87	6.47
	K	2.29	2.67	3.38
	P	-	0.20	0.17
	Total	100.00	100.00	100.00
MESONORMS	Q	24.37	15.90	20.59
	Or	1.21	4.80	5.26
	Ab	41.01	34.37	32.35
	An	8.54	22.56	18.92
	C	4.62	-	0.65
	Bi	16.40	13.70	18.65
	Act	-	3.63	-
	Sph	1.44	1.43	1.52
	Mt	2.42	3.08	1.61
	Ap	-	0.53	0.45
	Total	100.01	100.00	100.00

Loss at 950°C

Analyses by: Geochemistry Department, University of Cape Town

Table 10. Chemical Analyses, Cation Proportions and Mesonorms of Nosib (Pruwes) Granodiorites

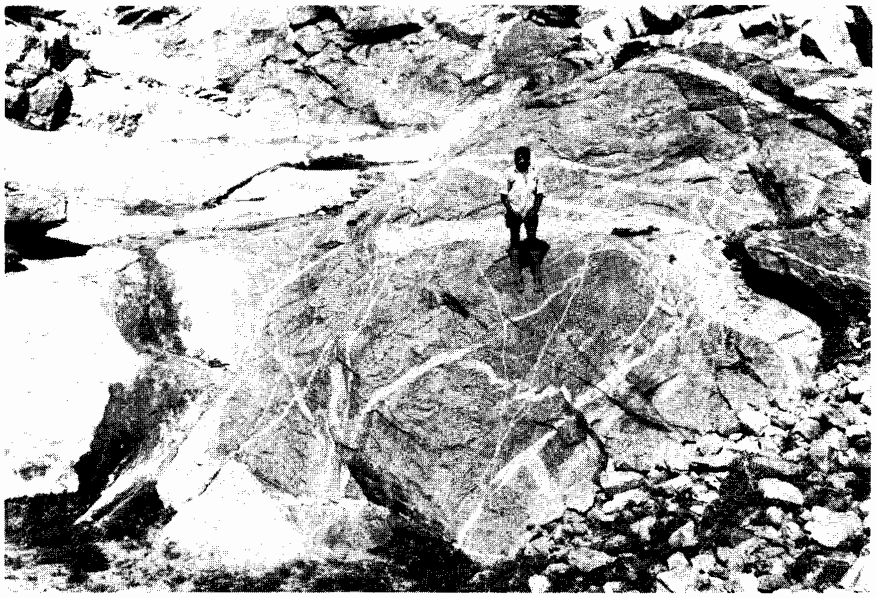

Plate 24. The Pruwes granodiorite and associated leucocratic mobilisate (white)

1967; Mehnert, 1969) which must have been extremely high as the sequence was then undergoing the first phase of deformation and metamorphism (M_1). Only the Ab/An ratio and the P-T conditions, possibly just reaching the threshold of "minimum melting", must account for the localised and comparatively scarce (regionally <15% by volume) amount of mobilisate in the migmatised area.

K-feldspar (microcline) blastesis and plagioclase replacement occurred along the s_1 foliation in limited areas of intense F_1N deformation. It is thus not excluded that regionally quantitatively subordinate syn- or post-kinematic potash metasomatism may have taken place as a result of concentration of residual fluids and their subsequent diffusion as an effect of extremely elevated pressure-gradients generated by folding. The relatively low K_2O concentrations, ranging between 1.91 and 2.79% (Table 10), however, seem to indicate that K-metasomatism could have occurred only on a very moderate scale.

Summarising, once the F_1N deformation and M_1 metamorphic phases were completed, the Nosib sequence consisted essentially of:

i) An extensive development of feldspathic quartzite in the Lower Nosib and irregular subordinate distribution of analogous lithotypes in bands throughout the Upper Nosib.

Sample	95	96	97	98	212	238	18/729/1	92	94	107	110	113	122	5/125/3	5/125/4	23	25	26	29
Q	32.50	36.04	27.92	43.67	17.58	28.71	27.90	26.93	15.86	26.89	36.07	33.99	19.85	27.38	22.51	16.21	45.54	44.20	35.16
K-feld	6.50	6.13	8.54	12.25	4.88	6.73	4.87	4.95	3.98	1.19	4.12	6.88	1.18	11.98	4.47	51.38	20.99	14.34	10.94
Plag.	37.28	26.49	25.42	22.53	33.59	11.88	32.96	38.45	54.64	29.28	23.72	25.93	47.13	28.52	36.08	23.52	21.78	36.74	43.16
Tot. feld.	43.78	32.62	33.96	34.78	38.47	18.61	37.83	43.40	58.62	30.47	27.84	32.81	47.31	40.50	40.55	74.90	42.77	51.08	54.10
Biot. Chlor.	19.50	28.65	21.46	9.29	33.59	36.83	15.36	22.79	15.58	21.12	27.68	15.72	23.11	22.24	24.57	-	-	-	-
Seric. Musc.	-	-	9.58	6.52	0.20	5.94	9.93	4.95	-	-	5.44	-	0.37	0.19	0.17	3.95	5.14	3.93	7.23
Horn.	-	-	-	-	4.10	-	-	-	-	5.78	0.49	8.25	-	7.98	6.70	-	-	-	-
Epid.	2.29	2.52	4.58	2.96	5.66	8.51	8.80	1.41	9.50	14.94	2.31	3.73	8.87	0.38	4.12	2.17	5.35	0.39	-
Acc.	1.91	0.18	2.50	2.77	0.39	1.39	0.19	0.53	0.44	0.80	0.16	5.50	1.48	1.33	1.37	2.77	1.19	0.39	3.52
Total	99.98	100.01	100.00	99.99	99.99	99.99	100.01	100.01	100.00	100.00	99.99	100.00	99.99	100.00	99.99	100.00	99.99	99.99	100.01

Group A (samples 95–18/729/1): Scarcely differentiated granodioritic paragneisses

Group B (samples 92–5/125/4): Non-mobilised Pruwes granodiorites

Group C (samples 23–29): Pegmatoid mobilisates

Table 11. Modal Mineralogical Composition of Nosib Granodioritic Paragneisses and Migmatites

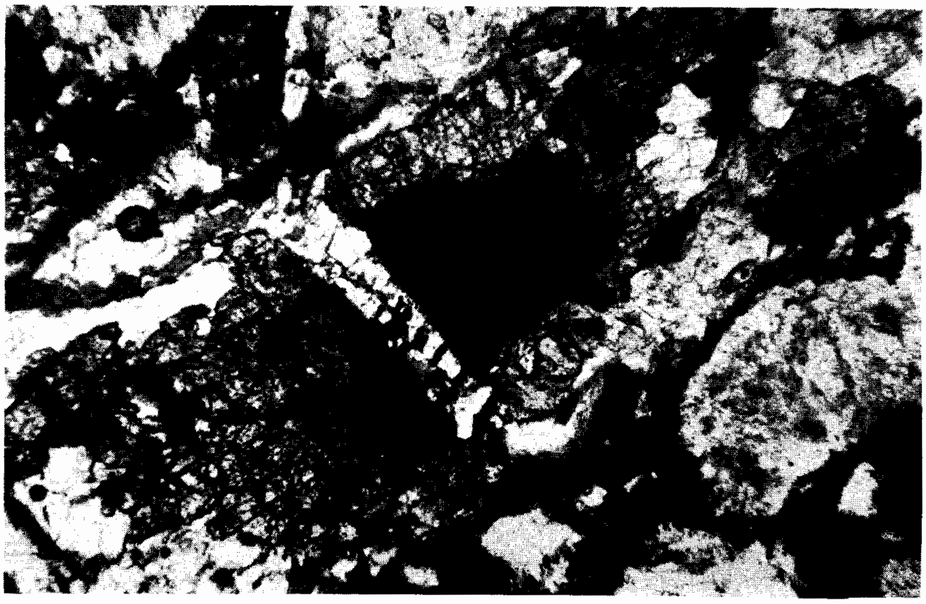

Plate 25. Zoisite/epidote-armoured allanite transgressed by Damaran micropegmatitic vein (x 50)

ii) A large mass of more or less differentiated Upper Nosib granodioritic paragneisses.

iii) Subordinate amounts of leucocratic granitic and granodioritic pegmatoid mobilisates.

iv) Subordinate amounts of orthoamphibolites.

Apart from textural evidence, the related M_1 mineral parageneses have been obscured by the succeeding M_2 Damaran tectonothermal episode, yet some indication of the metamorphic grade attained can be inferred from mineralogical "relics".

The M_1/M_2 interference metamorphic paragenesis of the siliceous-argillaceous suite is normally composed of: quartz-albite-(oligoclase)-epidote/zoisite/(allanite)-microcline-actinolite (degraded hornblende)-biotite-chlorite-muscovite with sphene, iron ore, apatite and calcite as common accessories.

The basic igneous suite paragenesis corresponds exactly to that of zone E and will therefore be deleted.

Three significant minerals appear (in brackets) in the paragenesis for the first time. Textural criteria indicate that they recrystallised first and that they are in obvious disequilibrium with the other "stable" phases, i.e. they form a "relic" para-

Sample	230	231	232	233	234	235	236	38	43	43A	43B
Q	72.54	69.71	55.82	56.35	66.79	65.97	70.69	60.59	64.75	56.48	61.68
K-feld.	20.64	22.33	31.53	16.75	25.28	21.99	24.52	2.75	5.35	6.49	5.79
Plag.	-	6.99	3.61	2.54	3.96	1.34	3.07	19.02	16.83	14.50	14.77
Tot. feld.	20.64	29.13	35.14	19.29	29.24	23.33	27.59	21.77	22.18	20.99	20.56
Biot. Chlor.	-	-	-	-	-	-	-	6.08	4.55	2.10	3.99
Seric. Musc.	6.81	0.97	7.83	21.83	2.45	10.52	0.19	10.98	7.13	18.89	11.78
Horn.	-	-	-	-	-	-	-	-	-	-	-
Epid.	-	-	-	-	-	-	-	-	-	-	0.80
Acc.	-	-	1.20	2.54	1.51	0.19	1.53	0.59	1.39	1.53	1.20
Total	99.99	100.02	99.99	100.01	99.99	100.01	100.00	100.01	100.00	99.99	100.01

Lower Nosib Group A (samples 230–236) — Upper Nosib Group B (samples 38–43B)

Table 12. Modal Mineralogical Composition of Nosib meta-psammites

Plate 26. "Chlorite-feathered" biotite in Pruwes granodiorite (x 35)

genesis.

The plagioclase crystals (occasionally porphyroblasts) show deeply saussuritised or sericitised cores. Alteration has normally obscured the original twinning, rendering an accurate identification extremely difficult under the microscope. Examination of several thin sections of specimens providing a fair coverage of zone F has proved that the original plagioclase was generally calcic oligoclase or, more rarely, andesine (An_{20-34}).

In some instances (especially in the coarse porphyroblastic gneiss) the plagioclase is surrounded by large unaltered microcline idioblasts, which can enclose several oligoclase-andesine patches together with characteristic (myrmekite-like) quartz blebs. The relation between oligoclase and K-feldspar is one of replacement.

Fresh albite with very low anorthite content ($An<5\%$) appears in peripheral positions in a few samples or, more rarely, in perthitic intergrowth within the microcline.

Allanite, though scarcely significant as a metamorphic index mineral, is worth mentioning as its occurrence is limited exclusively to granodioritic gneiss of Upper Nosib age. It is found in its normal and metamict modifications and is generally completely

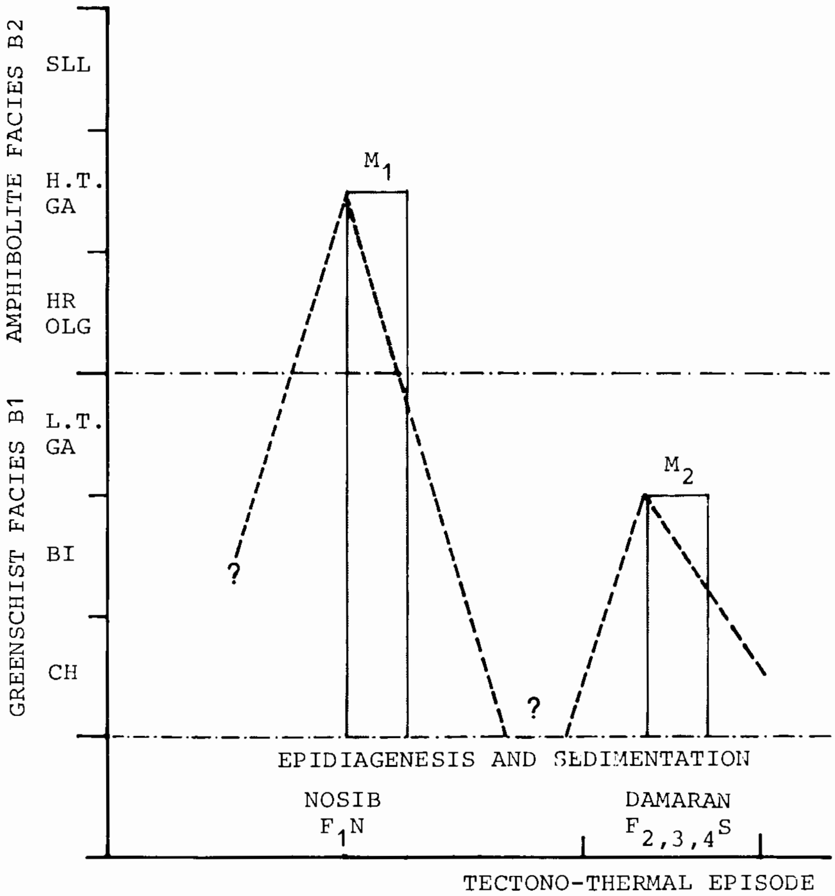

Figure 16. Graph of possible grade variation during polyphase M_1/M_2 interference metamorphism east of the Damaran hornblende-oligoclase isograd

surrounded by a rim of zoisite and/or patches of epidote. Its crystallisation predates the M_2 Damaran episode as rimmed crystals are often cracked and transgressed by leucocratic veinlets (Plate 25).

The amphibole is actinolite (α=brownish green, β=yellow, γ=yellowish green; $\gamma\wedge c=27^{\circ}$, in metasediments. α=bluish green, β= pale yellowish green, γ=pale green; $\gamma\wedge c=29^{\circ}$, in orthoamphibolites). Its close association with chlorite, by analogy with what has been observed in zone D, suggests hornblende as the parent mineral.

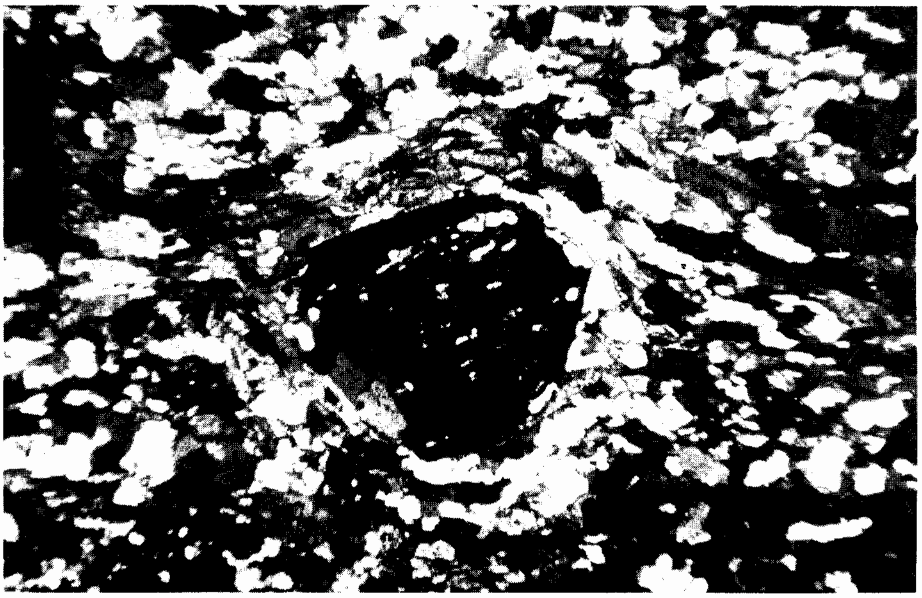

Plate 27. Rotated low temperature garnet porphyroblast containing straight trails of inclusions (s_i) discordant with the later chlorite/biotite s_4 foliation (x 35)

Indeed in the westernmost areas of this zone, unaltered hornblende gradually appears in the core of actinolitic idioblasts.

Unlike the brown biotite found in zone D, which coexists in apparent equilibrium with chlorite, biotite here is unstable and gradually replaced by chlorite (Plate 26). The olive green to dark greenish brown staining has been interpreted as being due to the release of an excess of ferric iron absorbed under different physico-chemical conditions (Barker, 1958; p.18).

It is concluded that the altered oligoclase-andesine, the chlorite-feathered actinolitic amphibole (degraded hornblende) and the green biotite, so characteristic of this zone, represent relics of an earlier (M_1) and higher-grade (middle to high-grade amphibolite facies) metamorphic assemblage, which has undergone a process of retrograde metamorphism. This justifies the obvious discrepancy existing between the gneissic and migmatitic texture of the metasediments composing zone F and the relatively low (B1.2 of Winkler, 1967) grade of the "stable" metamorphic paragenesis.

As zone F lies east of the M_2 Damaran greenschist-amphibolite boundary, the M_2 episode has locally been of a much lower grade than M_1 as schematised in figure 16 on the type of diagram introduced by Rast (1958), Ramsay (1963), Harte and Johnson (1969), Bowes (lecture at the University of Cape Town, 1969) and Spry (1963 and 1969). It must, however, be stressed now that such a graph has local but no regional validity as will be seen later.

Gradual transition into a strikingly similar yet unaltered M_1 paragenesis was commonly observed in the field west of zone F, where the M_2 Damaran episode reached higher grade, i.e. west of the Damaran hornblende-oligoclase isograd of folder 7.

4. Zone G

Where the sediments were particularly Fe- and Mn-rich under still higher M_2 regional temperature, or more likely in conjunction with structurally controlled thermal peaks (friction heat in the Aub and Andib syncline hinges or shearing along the Nosib-Damara contact), garnet makes its first appearance. X-ray diffraction indicates that this is a Fe-Mn-rich garnet of the ugrandite (uvarovite-grossularite-andradite) series of Winchell and Winchell (1927).

In the siliceous-argillaceous suite the typical paragenesis of this zone is: quartz±albite-biotite±chlorite-garnet-epidote/zoisite with iron ore, ankerite and apatite as common accessories.

The garnet porphyroblasts, which locally grew to a rather large size (over 5 mm in diameter), are embedded in a schistose lepidoblastic matrix which resembles very closely the average micaschist found in zones D and E.

It is peculiar how biotite may be subordinate in some samples (18/729/9B) leaving essentially a garnet-chlorite assemblage. That garnet with high MnO/FeO ratio could coexist with chlorite and little or no biotite (i.e. in low to middle greenschist facies) was first observed by Goldschmidt (1921) in the Stavanger district of Norway. Similar garnet in a paragenesis with ±25% biotite and little or no chlorite in Japan was deemed to have formed in a somewhat higher grade of the greenschist facies by Miyashiro (1953), who proposed an almandinious/non-almandinious subdivision within this type of metamorphism. MnO-rich garnet would crystallise under relatively high T and low P (non-Barrovian) controlled environments. This was, however, contested by Atherton (1965) and Clifford (1960), who demonstrated that the bulk chemical composition of a rock has as high a significance as the P-T conditions under which metamorphism occurs. Along the Gomatum valley the amount of garnet in subordinate lenses of congenial chemical composition can exceed 80% by volume (sample 18/729/4B).

The local evidence seems thus to substantiate Clifford's and Atherton's views.

Plate 28. Hornblende porphyroblast containing straight trails of inclusions (s_i) (x 35)

The porphyroblasts contain generally straight trails of inclusions (s_i)(samples 18/729/19 and 18/729/21). The average grain-size of these poikiloblastic inclusions is in the order of 0.1-0.2 mm, whereas that of the corresponding minerals in the matrix appears much coarser (i.e. ±1.5 mm). The garnet idioblasts are generally rotated. The internal foliation (s_i) remained straight and shows no continuity with the external (s_e) biotite and/or chlorite foliation (Plate 27), which flows around the porphyroblasts as a combined effect of flattening and gliding (Zwart, 1961). The angular value of rotation can be as high as 50-60°. It can thus be concluded that the garnet grew under relatively static conditions preceding the F_3 and F_4 tectono-thermal pulses which induced a "general matrix coarsening" (Harte and Johnson, 1969) and the establishment of a locally strongly penetrative biotite/chlorite s_4 foliation (s_e) accompanied by rotation of the porphyroblasts. Garnet blastesis on the other hand, must have followed the F_2S phase of folding which generated the Gomatum nappe and was accompanied by weak to moderately penetrative s_2 foliation, preserved as s_i in the porphyroblasts. As no marginal deformation of s_i was observed in several porphyroblasts examined it must be concluded that this ugrandite garnet is, following Zwart's (1962) terminology, interkinematic, i.e. crystallised between F_2S and F_3 phases of deformation.

No relevant change was observed in the parageneses of the siliceous-carbonate and basic igneous suites where the amphibole is still tremolite/actinolite. In the Gomatum area, however, this grades imperceptibly into hornblende to the west (zone H).

From these considerations it is obvious that the low temperature garnet developed over a wide P-T range, i.e. from the chlorite-biotite zone to the threshold of the amphibolite facies. The biotite and/or chlorite rich garnetiferous schists may, therefore, range from the middle to the highest subfacies (B1.3 of Winkler, 1967) of the greenschist facies or be the equivalent of Turner's (1968; p.271), Mason's (1962) and Brown's (1967) high-grade limit of the greenschist facies in the Southern Alps of New Zealand.

D. THE AMPHIBOLITE FACIES

1. Zone H

The appearance of hornblende (α=dark olive green, β=yellowish brown, γ=yellowish green, $\gamma \wedge c=30^\circ$) marks a NNW oriented belt on folder 7. This amphibole is generally associated with biotite, while the "stable" plagioclase changes from albite to oligoclase of progressively more calcic composition in prograde (Damara rocks) areas gradationally adjoining the biotite zone E. In areas adjacent to zone F, where the assemblage was essentially retrograde, the "unstable" oligoclase-andesine relics of the M_1 episode increasingly appear to be in equilibrium; so does the amphibole which gradually changes from "feathered" chlorite-actinolite into proper hornblende.

To the south, zone H interfingers with zone E (folder 7). As the hornblende-oligoclase appearance still seems to follow, at least initially, the Nosib-Damara contact, it must be assumed that here also an original difference in metamorphism existed between these two formations by analogy with what was observed in zone F. Part of the hornblende in the Nosib gneiss was possibly generated during the first M_1 metamorphic episode but not degraded during the successive M_2 pulse as the latter's grade was in the same range as that of the former. Hornblende generated during the M_2 pulse occasionally contains straight trails of poikilitic inclusions defining an internal foliation (s_i)(Plate 28)(sample 107). This is normally undeformed and exposes no continuity with the external (s_e) biotite and/or muscovite s_2 foliation. The s_i might, as in the case of the garnet of zone G, be a palimpsest of foliation created during a previous deformation phase preserved within the amphibole, which must then have grown at least partially, during an inter-kinematic period. Towards the western limit of the zone this mineralogical difference fades out completely, as does all sign of previous textural difference that may have

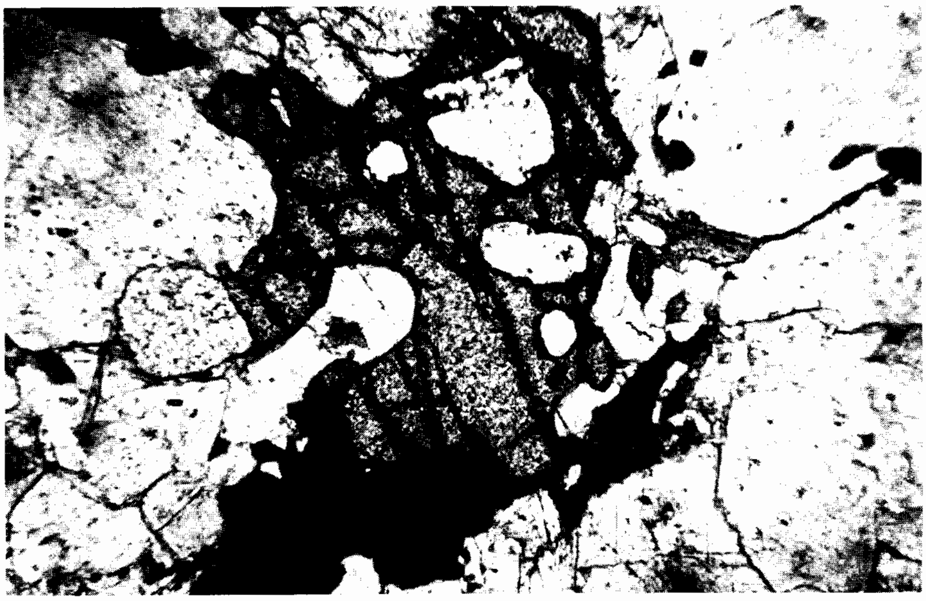

Plate 29. High temperature poikiloblastic garnet in Damara gneiss (x 35)

survived this far between the two Nosib and Damara metamorphites, because rocks which have undergone the second M_2 episode alone have by now acquired typical gneissic or granoblastic texture. The Nosib and Damara semipelitic metasediments cannot easily be distinguished any longer in the field by local cursory textural or mineralogical observations. Under the microscope, however, the presence of allanite allows an easy stratigraphic distinction of the Nosib metamorphites, as such a mineral is generally extremely rare, virtually absent, in the overlying Damara metasediments.

On a regional scale, however, pink streaked gneiss becomes increasingly frequent as intercalations within the hornblende-biotite semipelitic gneiss. Once the structural-stratigraphic setting was unravelled, it became evident that this lithotype was particularly abundant in the Upper Nosib Stage and rather scarce, and possibly only of mobilised origin, in the overlying Damara metasediments. West of the hornblende-oligoclase isograd the quartz-feldspathic content of these gneisses becomes preponderant over the mafics, while the texture soon grades into granulitic. At the moment it is sufficient to notice how the appearance of granulitic textures is limited to the metasediments of Nosib age and how it has subtly replaced the obscured contrast between the granoblastic Nosib gneiss and the lepidoblastic Damara schist, so obvious in the east. Attention must also be drawn to the fact that this textural change was brought about in areas where the maximum amphibolite grade of the M_1 episode has been reached or exceeded by the M_2 metamorphism. In other words, granulitic texture developed only in polymetamorphic Nosib terrains lying beyond (west of) the M_2 (Damaran) amphibolite isograd and never within the Damaran greenschist realm. The genetic significance of this observation will be discussed in page 140, while dealing with the hornblende (transition) granulite facies.

No typical alumino-silicate index mineral (eg. staurolite, kyanite or cordierite) was observed. The local Ca- and Mg-rich chemical composition of the original greywacke has possibly hindered their formation to the benefit of the development of plagioclase, epidote, biotite, etc. as commonly observed by Winkler (1967; p.194). Kyanite, however, was found previously in possibly more aluminous metasediments to the north of area 1813C as it appears on the Geological Map of South West Africa (1963).

The representative mineral paragenesis in the siliceous-argillaceous suite is thus:
quartz-oligoclase (rarely andesine)-K-feldspar-epidote/zoisite (allanite only in Nosib gneiss) -hornblende-biotite-muscovite with sphene, chlorite, apatite and iron ore as frequent and rather abundant accessories.

In the paragenesis of the igneous basic suite the plagioclase is slightly more calcic and ranges between common andesine and rare labradorite. The typical assemblage thus resulting is:
hornblende-andesine (rarely labradorite)±quartz±biotite±epidote/zoisite with iron ore, sphene, apatite and calcite as common accessories; clinopyroxene (diopside) is normally still absent.

2. Zone I

Farther to the west a second (late generation) garnet appears. X-ray diffraction indicates that this is normally a high temperature magnesium garnet, close to the pyrope member of the pyralspite (pyrope, almandine, spessartite) series of Winchell and Winchell (1927). The average size of the porphyroblasts ranges normally around 2 mm, while exceptional individuals can reach 8-10 mm in diameter. The garnet has commonly a skeletal, sieve or "fish-net" texture (Spry, 1969; p.27) and generally contains very large amounts of poikiloblastic inclusions (up to more than 50% by volume), a very common feature in post-tectonic garnets. The inclusions are randomly distributed or slightly aligned. Their grain-size is coarser (i.e. 0.4-0.6 mm) than that encountered in the low-temperature ugrandites (zone G, p.115) and compares closely with that of the granoblastic matrix, which is generally very slightly coarser (i.e. 0.8-1.0 mm). Under the microscope the garnet conveys the impression of having crystallised by accommodating itself along the intergranular boundaries (originally occupied by hornblende, mica and microgranulated quartz) with moderate or no disruption of the pre-existing texture. The final habit can be idioblastic or more rarely allotrioblastic (Plate 29). The s_2 biotite and/or muscovite regional foliation is not deflected around the garnet porphyroblasts, but transected sharply. Biotite flakes are often truncated or included poikilitically. There seems, therefore, to be continuity between the very weakly defined s_i and s_e while none of the garnet porphyroblasts examined showed any sign either of rotation or of wrapping by flattening in the matrix gneiss. It can then be safely concluded that the pyralspite idioblasts grew under relatively static conditions following the last significant tectonic pulses (F_3 and F_4) accompanied by M_2 metamorphism. The high-temperature garnet blastesis has, therefore, a definite post-kinematic character (Zwart, 1962).

The typical siliceous-argillaceous suite paragenesis becomes: quartz-K-feldspar-calcic oligoclase-biotite-muscovite-garnet with hornblende, iron ore, apatite, sphene and rutile as occasional accessories.

Under these physico-chemical conditions, the siliceous-carbonate suite yielded as a typical paragenesis:
calcite and/or dolomite$\pm$quartz-diopside$\pm$forsterite$\pm$phlogopite$\pm$ K-feldspar$\pm$oligoclase/andesine. Forsterite is, however, still comparatively scarce. Wollastonite is generally absent, with the exception of two samples (3/68/5 and 3/68/6) in which, due to the thinness (0.50-1.00 m) of the bands, P_{CO_2} escape may have occurred through the adjoining pelitic members, thus lowering the higher X_{CO_2} dependent (Winkler, 1967; p.36) equilibrium temperature of the diopside-calcite-quartz system. As there is no proof that the system may have been open, this high temperature island has been included in the following sillimanite zone (J) of folder 7.

As diopside alone or diopside-forsterite are encountered in paragenesis, the following two reactions are likely to have occurred (Winkler, 1967; p.30):
tremolite+3 calcite+2 quartz$\rightleftharpoons$5 diopside+3 CO_2+H_2O, or
3 tremolite+5 calcite$\rightleftharpoons$11 diopside+2 forsterite+5 CO_2+3 H_2O.

The equilibrium temperatures of both these reactions is almost independent of the X_{CO_2}% once the rather low value 0.2 is exceeded (Metz et al. 1964; Greenwood, 1962). Thus for pressures exceeding 1 Kb the temperature of $530^\circ\pm10^\circ$C must have been reached to obtain diopside from each of the two reactions (Winkler, 1967). As the natural pressure is likely to have greatly exceeded 1 Kb, this is a minimum temperature of metamorphism in zone I.

The diopside idioblasts, "armoured" by a rim of tremolite (sample 4/108/4) and the pseudomorphic serpentine replacing forsterite suggest that the M_2 Damaran metamorphic climax was locally followed by a still later metamorphic pulse of relatively lower middle greenschist grade inducing incipient diaphthoresis.

In the basic igneous suite the paragenesis remains unchanged except for the appearance of clinopyroxene (diopside) which is

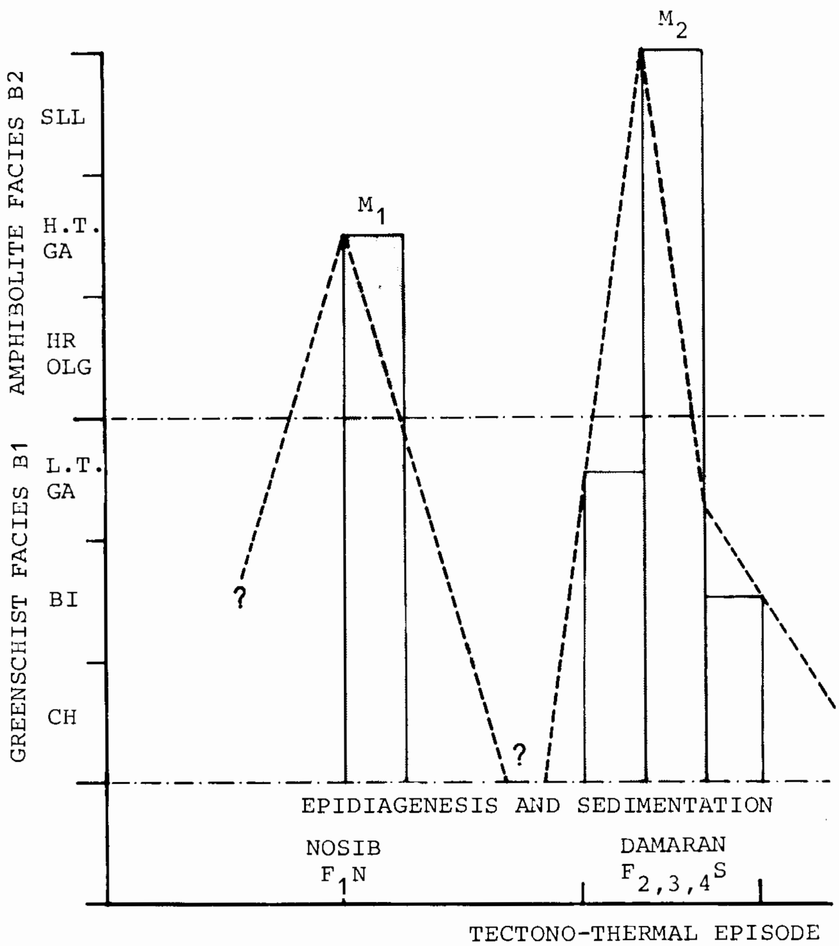

Figure 17. Graph of possible metamorphic grade variation during successive deformative events in localities west of the M_2 Damaran hornblende-oligoclase isograd

generally still in subordinate amounts.

If, as in figure 17, the inferred grade variations (M_1-M_2) were to be plotted against the successive phases of deformation (F_1N, F_2S, F_3S, etc.), by analogy with figure 16 a completely different succession of events would be obtained for zones H and D, i.e. west of the Damaran hornblende-oligoclase isograd, if compared to zone F. This indicates that a similar graph reflects only the "local" metamorphic history of a certain tectonite, whereas any

Plate 30. Irregularly seeded sillimanite (fibrolite) aggregates intersecting the undeformed s_2 biotite foliation (x 35)

regional extrapolation may be inadequate or even misleading.

3. Zone J

This zone is characterised by the appearance of the new index minerals:

i) sillimanite (fibrolite) in the siliceous-argillaceous suite, and

ii) wollastonite in the siliceous-carbonate suite parageneses.

Finely felted aggregates of fibrolite commonly form twisted layers intergrown with biotite and/or muscovite, while discrete trains of minute prismatic needles formed in K-feldspar or quartz. Regular spherulitic or rosette aggregates are less common (sample 152A). As the contorted fibrolite masses curve around older undeformed biotite crystals (s_2 foliation)(Plate 30), the twisting is not due to deformation but to "...irregular growth following irregularly seeded nucleation" (Spry, 1969; p.272 and Binns, 1964; p.304). The sillimanite of zone J post-dates the development of this regional and locally undeformed biotite foliation and is therefore, post-kinematic by analogy with the "fish-net" pyralspite garnet, which it often accompanies (sample 146).

Most of the minerals characterising the adjacent zone I remain unchanged with the possible exception of the plagioclase which generally becomes more calcic (oligoclase/andesine) and which, in rocks of suitable chemical bulk composition (i.e. carbonate-rich greywacke and marly shale), becomes as calcic as labradorite and is normally associated with clinopyroxene (diopside) showing faint greenish pleochroism.

Muscovite generally shows textural evidence of reaction with quartz, suggesting the production of K-feldspar (microcline). The resulting excess of alumina is only occasionally preserved as sillimanite. It is in fact conceivable that, in Mg- and Ca-rich environments, the high operative pressure might have promoted the formation of garnet.

Sometimes K-feldspar is associated with phlogopitic mica, corroded by quartz, and with plagioclase. In this case the corroded flakes are often surrounded by patches of dolomite (sample 151A), possibly fixing the released Ca and Mg in the presence of a CO_2-rich fluid phase.

Sphene, an ubiquitous accessory so far, becomes scarce or absent in the westernmost metamorphites.

The typical paragenesis in the metamorphosed siliceous-argillaceous suite thus is: quartz-oligoclase/andesine (rare labradorite)-K-feldspar-biotite$\pm$muscovite$\pm$garnet$\pm$sillimanite$\pm$ clinopyroxene with iron ore, rutile, apatite and spinel as common accessories. Sphene, calcite and tremolite on the contrary are normally deuteric and confined to the labradorite-clinopyroxene (diopside) paragenesis.

Metamorphism of the siliceous-carbonate suite produced the new phase wollastonite, while the previously formed calc-silicates such as diopside and/or tremolite become scarce or disappear in the presence of quartz and calcite. Wollastonite is normally associated with large amounts of forsterite (sometimes serpentinised) and occasionally spinel (pleonaste). In silica-free assemblages brucite is associated with forsterite (now serpentinised).

The typical paragenesis in the metamorphosed siliceous-carbonate suite is normally: calcite and/or dolomite (subordinate) $\pm$quartz$\pm$forsterite/serpentine$\pm$wollastonite$\pm$spinel$\pm$brucite$\pm$phlogopite with accessory iron ore and occasional sphene.

There are no substantial differences between the paragenesis of the metamorphosed basic igneous suite in this and the previous zone except that the quantity of clinopyroxene (diopside) seems to increase at the expense of hornblende.

The equilibrium temperature of the muscovite reaction in presence of quartz is noticeably pressure-dependent. Evans (1965) has obtained a temperature of 670°C at P=2 Kb. Though the natural pressure effective during the M_2 Damaran metamorphism is difficult to estimate, it is likely to have exceeded 2 Kb, and consequently the above temperature must be regarded as conservative.

The formation of wollastonite under regional metamorphic pressures ($P_f=P_{H_2O}+P_{CO_2}$) exceeding 2 Kb would imply unrealistic temperatures (Harker and Tuttle, 1955). However, as the thickness of the carbonate bands involved is only in the order of 1-2 m, P_{CO_2} may have escaped in the surrounding CO_2-free pelitic-psammitic layers thus hindering a pressure build-up and consequently lowering or rather maintaining the equilibrium temperature to more acceptable figures (Misch, 1964), possibly closer to those of the equilibrium curve computed by Danielsson (1950) corresponding to an average temperature of 700°C for P=2 Kb.

4. The A_2 Anatexis: the Front of Damaran Migmatites

Under these physico-chemical conditions the equilibrium curves of both the muscovite-quartz and the calcite-diopside-quartz systems intersect that of the beginning of anatexis (minimum and average)(Winkler, 1967; p.177). No wonder that the "front of Damaran migmatites" indicated on folder 7 runs subparallel and close to the sillimanite-wollastonite isograd and that anatexis and migmatisation become widespread phenomena in these high-amphibolite metamorphic terrains.

The Khomas greywacke association, which comprises the bulk of these migmatites, had a monotonous lithological composition; consequently the response to the anatectic conditions has been rather homogeneous.

Essentially two groups of parautochthonous mobilisates were observed in the sillimanite gneiss. In chronological order and scale of emplacement these can be divided into:

i) A synkinematic granite (migmatite neosome), which is normally concordant and deformed, and more occasionally discordant with the foliation of the enclosing gneisses. It can be distinguished by its whitish colour, medium to coarse grain and pegmatoid (rarely aplitic) texture. The synclinal structural position of these migmatites and coarse porphyroblastic Khomas gneisses was first discovered by Gevers and Frommurze (1929), who named these granitoid rocks the Salem granite. Later, Smith (1965) proved their parautochthonous metasedimentary origin. Both views seem to be supported by local evidence.

ii) A late- or post-kinematic granite which varies from subconcordant to the pre-existing structures (Ganias) to openly discordant and taphrogenetic (Uhima). A fine-grained, equigranular often aplitic texture together with a pale grey or pinkish colour characterise this intrusive, which for both structural and petrographic considerations could easily be compared with the Donkerhoek granite of Gevers (1963; p.215), developed along the north-western margin of the Khomas Highlands, and forming"the most extensive individual granite body in the whole of Central South West Africa." The associated, coarse-grained, inequigranular, generally pegmatoid Uhima granite has a consistent transgressive attitude to the Khomas gneisses and is one of the latest product of metamorphic differentiation and subsequent intrusion in the area.

The temperature of "minimum melt" inferred from the curve extrapolated from the experimental values supplied by Winkler (1967; p.205) should have ranged between 688 and 710°C, as the normative Ab/An ratios computed from the chemical analyses of two scarcely migmatised Khomas gneisses range in the order of 4.8, whereas those of the Ganias and Uhima late-and post-kinematic granites yielded ratios in the order of 1.0. It is assumed that the process was carried out under high P_{H_2O} because the inherently H_2O-rich Khomas greywacke and shale were undergoing the first phase of metamorphism. Thus it is likely that the amount of pegmatoid mobilisates is mainly a function of the rise in temperature. In the Uhima area over 30% by volume of partial melt was produced indicating that the inferred minimum melt temperature must have been somewhat exceeded, though an excess in the order of few degrees is sufficient to produce abundant partial melting (Winkler, 1967; p.215) in quartz-plagioclase-biotite rocks and a divariant melting interval of only 15°C is indicated for the $KAlSi_3O_8$-SiO_2-H_2O system by Lambert et al. (1969; p.617). A good agreement seems therefore to exist between these and the temperature obtained from the study of the metamorphic mineral parageneses.

Two sets of pegmatites are generally associated with the Ganias-Uhima granite.

The first is white, discordant and occasionally garnetiferous (sample 3/66/4). The second is generally pink and often intersects the white pegmatite, thus representing the latest intrusive in the area. The red or pink pegmatites can bear garnet and sillimanite (fibrolite)(sample 3/66/6). As these minerals are common to the paleosome gneisses and to the granitic mobilisates, there is additional evidence (Mehnert, 1969; p.234) that both suites might either have originated in situ or else have been mobilised over regionally moderate distances, across hot country rocks subjected to P-T conditions identical to those generating the granitic materials and for this reason did not develop a contact metamorphic aureole. That a relationship may exist between the parent metasediments, the synkinematic mobilisate and the Ganias-Uhima post-kinematic granite, seems to be indicated by the diagram of figure 18. The non-mobilised gneisses (open circles) are scattered due to the variable mineralogical composition which is a result of their sedimentary origin. The synkinematic mobilisates (full dots) reveal a much different spread, which appears to match closely the modal mineralogical composition of the Ganias-Uhima post-kinematic granite (crosses). It must also be noted how the post-kinematic granites are "encircled" by the synkinematic pegmatoid mobilisates, implying a much more homogeneous and differentiated mineralogical and chemical composition. This can be fully appreciated from a cursory comparison of their respective chemical compositions in Table 13 and their modes in Table 14.

Pairs of related gneisses and pegmatoid mobilisates, sampled together, are connected by interrupted lines in figure 18. Lines trending from right to left are likely to represent differentiated pairs in which (3/66/1-3/66/2; 151-151A; etc.) the neosome has migrated only slightly. Pairs aligned in the Q-Σfeld direction, i.e. with similar mafic content (samples 145-145A; 150-150A) represent parautochthonous neosomes which have migrated farther into areas of unrelated mineralogical composition.

Porphyroblastic paragneisses are by no means rare west of the hornblende-oligoclase isograd and particularly within the migmatite zone (D_2Gn in sheet 1913A). Two types of feldspar blastesis were observed:

i) a widespread "plagioclase blastesis"

ii) a localised "K-feldspar blastesis"

The first is ubiquitous. The size of the oligoclase (An_{20-30}) idioblasts reaches 5 cm in length. Both twinned and untwinned crystals occur, while antiperthite is common (sample 4/109/2). The porphyroblasts are rarely randomly oriented, more often they are aligned in the s_2 foliation. Their regional development does not seem to be related either to the synkinematic pegmatoid mobilisates or to the post-kinematic granite, as porphyroblasts are numerous both in areas devoid of, or riddled by, granitic material.

Though normally deformed (see bent twin lamellae and mortar texture in sample 4/109/2), somewhat rotated and "wrapped" by a film of mica, ophthalmitic ("augen") textures are not too common. The oligoclase blastesis has thus a late-kinematic character.

On the regional scale, the An component seems generally to increase westwards, i.e. concordantly with the Damaran metamorphic gradient, although the chemical bulk composition of certain parent lithotypes has, as it has been seen, affected the plagioclase composition irrespective of the metamorphic grade reached. Nevertheless, a certain analogy to the regional zoning of plagioclase Ca/Na component as observed by Wenk (1962) in the central Alps (where the growth and change in composition are attributed to the progressive achievement of internal chemical equilibrium in a Ca-rich rock-mass under progressive changes in T-P conditions) seems

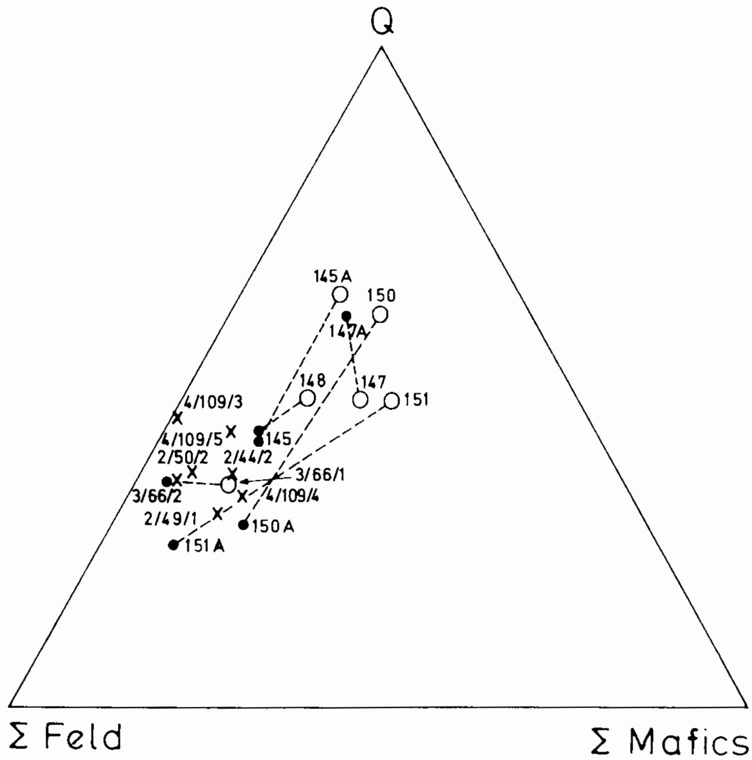

Figure 18. Mineral composition of Khomas migmatitic gneisses and late-/post-kinematic granites. Open circles: non-mobilised parent gneisses; full dots: synkinematic pegmatoid mobilisates; crosses: late- and post-kinematic granites. Interrupted lines connect related migmatitic pairs

to be present in the Sesfontein area too. The general picture thus appears to substantiate Mehnert's view (1969; p.127) that plagioclase blastesis "... is often of regional extent and hence not connected with particular magmatic intrusions" and that it "...resulted from a regional recrystallisation of rocks, not infrequently without any evidence of addition of matter or pathways of migrating substances".

The K-feldspar blastesis, on the other hand, is not regionally ubiquitous but limited to zones intruded by post-kinematic granites and pegmatites. The porphyroblasts are generally rather large (up to 8 cm in length) idioblastic individuals of pink microcline containing weakly developed plume perthite (sample 2/50/5) or microperthitic intergrowths. The K-feldspar idioblasts include

	Sample	4/109/2A	2/50/5	2/49/2	2/50/2	2/50/2A
		Salem gneiss	Salem gneiss	Hybrid Ganias granite	Ganias granite	Uhima granite
CHEMICAL ANALYSES	SiO_2	65.51	67.57	71.87	74.10	74.21
	TiO_2	0.93	0.72	0.38	0.20	0.25
	Al_2O_3	14.41	14.88	14.62	13.86	13.34
	Fe_2O_3	1.38	1.00	0.78	0.59	0.48
	FeO	4.34	3.18	1.23	0.80	0.94
	MnO	0.08	0.07	0.03	0.03	0.02
	MgO	1.84	1.40	0.55	0.42	0.31
	CaO	3.59	2.58	1.93	0.90	0.95
	Na_2O	2.93	3.31	4.38	3.50	3.01
	K_2O	3.16	3.55	2.73	4.80	6.38
	P_2O_5	0.26	0.30	0.07	0.12	0.10
	L.o.i.	0.64	0.76	1.10	0.41	0.37
	H_2O^-	0.01	0.03	0.05	0.20	0.03
	Total	99.08	99.35	99.72	99.93	100.39
CATION PROPORTIONS	Si	62.71	64.24	67.83	69.69	69.46
	Ti	0.67	0.52	0.27	0.14	0.18
	Al	6.27	16.68	16.27	15.37	14.72
	Fe^{3}	0.99	0.72	0.55	0.42	0.34
	Fe^{2}	3.48	2.53	0.97	0.63	0.74
	Mn	0.06	0.06	0.02	0.02	0.02
	Mg	2.63	1.98	0.77	0.59	0.43
	Ca	3.68	2.63	1.95	0.91	0.95
	Na	5.44	6.10	8.02	6.38	5.46
	K	3.86	4.31	3.29	5.76	7.62
	P	0.21	0.24	0.06	0.10	0.08
	Total	100.00	100.00	100.00	100.00	100.00
MESONORMS	Q	28.82	29.08	30.47	31.90	28.75
	Or	9.85	14.51	13.95	27.07	36.40
	Ab	27.20	30.51	40.08	31.92	27.32
	An	13.31	8.55	7.94	3.03	3.22
	C	1.64	2.85	1.79	2.01	0.35
	Bi	15.12	11.23	3.98	2.76	2.71
	Sp	2.01	1.55	0.81	0.42	0.53
	Mt	1.49	1.07	0.83	0.63	0.51
	Ap	0.56	0.64	0.15	0.25	0.21
	Total	100.00	99.99	100.00	99.99	100.00

Loss at 950°C

Analyses by: Geochemistry Department, University of Cape Town

Table 13. Chemical Analyses, Cation Proportions and Mesonorms of Damaran Migmatites and Granites

all the other minerals poikilitically, thus having a marked post-kinematic character. They are surrounded by a ring of rather fine-grained quartz, oligoclase which is often myrmekitic, and frequently by biotite and muscovite highly corroded by quartz.

Plagioclase and microcline porphyroblasts can coexist in the same rock and are readily identified in the field on the basis of their different colours (sample 2/50/5).

Non-porphyroblastic microcline normally found in minor amounts in most of the gneisses in the western domain has, on the contrary, a rather lighter colour and occurs irrespective of the presence of any mobilisate. It is also developed in non-migmatitic terrains, where it can be distinguished from oligoclase only under the microscope. It is thus possible that two successive generations of microcline are present. The white, non-porphyroblastic crystals might be the product of conservative or isochemical metamorphism, or migration limited to a micro- or mesoscopic scale. The porphyroblasts strictly associated with the Ganias and Uhima granite and pegmatite might have grown at least partially by later diffusion of fluids enhanced by mechanical flow along shear-zones fringing the intrusions. This hypothesis seems to be supported by the observation that the pegmatitic Uhima granite south-west of the Hoanib River is emplaced essentially along a system of late NE striking wrench or tear fractures (see folder 7). The plagioclase-microcline porphyroblastic gneiss would thus be similar to the blastomylonitic gneiss from Pfahl (Bavaria) ("palites") described by Mehnert (1969; p.127) in which potash migration was facilitated by shearing and high tectonic pressure-gradients. It may not be accidental, however, that the chemical analysis (Table 13) of sample 4/109/2 several kilometres away from the Ganias granite intrusions, and thus devoid of pink K-feldspar does not contain much less K_2O (3.39%) than sample 2/50/5 (3.68%) where the two types of microcline are developed. The regional existence and magnitude of a possible potash metasomatism cannot, however, be determined on a relatively limited scale, but should be considered in its petrological and geochemical complexity, starting from the Atlantic coast, where reconnaissance trips revealed a large axial granitic/granodioritic massif preceded by a belt of intensive microcline blastesis just S-W of the study area.

E. THE GRANULITE-AMPHIBOLITE TRANSITION FACIES

1. Distribution and Mineralogy

West of the Damaran oligoclase-hornblende isograd the proportion of leucocratic/melanocratic paragneisses seems to increase on a regional scale in the polymetamorphic Upper Nosib terrains, though an increase of the psammite/pelite ratio of the original

Sample	145A	147	148	150	151	3/66/1	145	147A	148A	150A	151A	3/66/2	2/44/2	4/110/5	4/109/4	2/50/2	2/50/2A	2/49/1	4/109/3
Q	62.33	46.47	46.67	59.20	46.24	33.59	40.00	59.01	41.45	27.59	24.13	34.00	35.27	41.43	31.74	30.27	34.21	29.16	43.56
K-feld.	-	6.71	6.25	6.90	8.86	15.18	6.24	2.14	1.54	19.73	21.42	35.09	14.92	23.21	25.60	27.03	28.62	18.45	32.77
Plag.	24.27	23.15	29.88	13.60	16.57	38.51	39.82	22.83	45.37	34.95	39.16	26.73	37.21	26.25	27.13	34.94	31.59	38.88	22.92
Tot. feld.	24.27	29.86	36.13	20.50	25.43	53.69	46.06	24.97	46.91	54.68	60.58	61.82	52.13	49.46	52.73	61.97	60.21	57.33	55.69
Biot. Chlor.	-	22.82	12.50	19.16	24.08	9.11	9.36	11.35	3.64	12.37	10.59	3.64	7.17	7.86	6.48	4.99	3.99	5.44	-
Seric. Musc.	0.58	-	2.93	-	4.05	3.61	2.57	0.53	5.88	4.01	2.83	-	4.65	1.25	6.48	2.59	1.60	5.93	0.57
Horn.	7.96	-	-	-	-	-	-	-	-	-	-	-	-	-	-	-	-	-	-
Epid.	-	-	-	-	-	-	-	-	-	-	-	-	-	-	-	-	-	-	-
Acc.	4.85	0.84	1.76	1.15	0.19	-	2.02	4.14	2.10	1.34	1.85	0.55	0.76	-	2.56	0.16	-	2.14	0.19
Total	99.99	99.99	99.99	100.01	99.99	100.00	100.01	100.00	99.98	99.99	99.98	100.01	99.98	100.00	99.99	99.98	100.01	100.00	100.01
	Non-mobilised gneisses Group A						Pegmatoid mobilisates Group B						Late-/post-kinematic granites Group C						

Table 14. Modal Mineralogical Composition of Damaran Migmatites and Granites

sedimentary sequence is rather unlikely. The colour of these felsic members is normally red or pink, due to relatively large amounts (generally more than 25% by volume) of pink microcline. Platy minerals (rarely exceeding 5-6% of the rock-volume) give a streaky appearance to some of these essentially quartzo-feldspathic members. The texture is granoblastic, with a faint foliation marked by the subparallel attitude of the phyllitic minerals, or else typically granulitic. The latter, denoted by dark shading over ornaments on folder 7, is comparable to the granulite *sensu stricto* from Rohrsdorf (Saxony) originally described by Tyrrell (1926), in which greatly flattened quartz lenticles and ribbons alternate with relatively fine-grained quartz and feldspar (ordinarily microcline and oligoclase) producing a definite foliation even in the absence of mica (hand specimens 111 and 152). Granulites are particularly well developed in the core of the Noeroep anticlinorium (sheet 1813C and 1913A) becoming subordinate towards the base of the Damara metasediments, while streaked granulitic gneiss is found for the first time overlying the Lower Nosib meta-psammites along the western limb of the Khudobib brachyanticline (centre of sheet 1913A). Alternate bands of melanocratic paragneiss and transition to amphibolite gneiss are, however, still common within these easternmost occurrences.

In Table 15 it can be noticed how a large proportion of the rock-volume (59.62% average of 17 modal analyses) is composed of feldspar, while quartz amounts to 34.16%, leaving only 6.22% by volume of mafics and accessories. In most (12) samples the K-feldspar/total feldspar ratio ranges between 1/3 and 2/3. The Nosib granulites have, therefore, mostly an adamellitic composition. In three samples the ratio is less than 1/3 and, only in two, more than 2/3, giving granodioritic and granitic compositions respectively.

Table 16 provides the chemical composition, cation proportions and mesonorms of two concordant (samples 164 and 167A) granulitic gneisses and of an associated mobilisate (sample 165A).

The typical mineral paragenesis in the Nosib granulites is composed of: quartz-K-feldspar-oligoclase$\pm$biotite$\pm$hornblende$\pm$ garnet with iron ore, rutile and allanite as occasional accessories. Hornblende is strongly pleochroic with α=dark bottle green, β=brownish and γ=yellowish green; $\gamma\wedge c=33^{\circ}$. Fair amounts of muscovite and/or sericite, epidote/zoisite and chlorite are derived from sericitisation of the K-feldspar, saussuritisation of the plagioclase and alteration of original hornblende. Similar typical olive or dull green chlorite-like pseudomorph alteration products after either hornblende or pyroxene, often in association with unaltered amphibole, were observed by Katz (1969; p.2026) in an analogous retrograde paragenesis in the granulite of Mont Tremblant Park (Quebec). High-temperature anhydrous assemblages, in fact, "...are particularly vulnerable to retrogressive metamorphism in the presence of pore fluids at lower temperatures, which are still high enough to permit relatively rapid chemical reactions" (Fyfe, Turner and Verhoogen, 1958).

Myrmekite of both K-feldspar and plagioclase, quartz bleb inclusions and antiperthites are relatively common, while braid or plume perthites (Spry, 1969; p.182) were occasionally observed.

Similar oligoclase-microcline-hornblende-quartz and microcline-oligoclase-quartz-hornblende and/or biotite assemblages are among the most common parageneses observed by Buddington (1963) in the transition to the granulite facies of the Adirondack Massif (N.Y. State).

The basic igneous sills and stocks associated with the granulite are generally rich in pale greenish or non-pleochroic clinopyroxene (diopside). Orthopyroxene (hypersthene, weakly pleochroic with α=very pale pink, β=very pale green and γ=colourless or very pale green) associated with hornblende (strongly pleochroic with α=yellowish brown, β=dark greenish brown and γ=yellowish brown; $\gamma \wedge c=30^{\circ}$) was observed only in one of the westernmost occurrences (sample 18/733/1). The increase in pyroxene seems to be followed by a substantial decrease and even disappearance of sphene. Nematoblastic textures grade into granoblastic as the intergranular boundaries straighten and form triple points (Spry, 1969). The mineral paragenesis of this hornblende-clinopyroxene granulite thus is: hornblende-clinopyroxene(diopside)-andesine/labradorite with minor amounts of quartz, K-feldspar, biotite, sphene, calcite and spinel. The last is synanthetically (Sederholm, 1916 in Spry, 1969; p.104) developed in the infragranular spaces by reaction of hornblende and plagioclase.

On strictly mineralogical grounds, and by the exclusion of one locality where orthopyroxene was recorded, the metamorphic assemblage of both these quartzo-feldspathic and hornblende-clinopyroxene granulites does not differ much from that of the Damaran zones H and I (i.e. oligoclase-hornblende and H.T. garnet) of folder 7 where they are enclosed in cores of anticlines.

The difficulty in deciding whether this assemblage belongs to the pyroxene or to the hornblende granulite subfacies, lies substantially in the recognition of whether hornblende and biotite are diaphthoretic or not (Fyfe, Turner and Verhoogen, 1958; p.233). In the case under consideration there is little or no doubt that in the quartzo-feldspathic granulites the biotite/chlorite derives from retrogressive alteration of hornblende, whereas no unaltered relic of pyroxene was found in the latter. On the contrary hornblende is always associated with biotite, microcline and plagioclase. This paragenesis, and the fact that xenoblastic hornblende crystallised in the intergranular spaces and not in large idioblasts typical of the biotite-hornblende gneiss of the amphibolite facies, supports the hypothesis of its prograde derivation from the reaction:

Sample	205	210	217	227	229	167A	165A	164	111	116	162	163	156A	114	209	106	168
Q	42.34	44.91	29.70	43.42	49.35	30.45	34.85	31.87	32.73	30.78	45.10	41.97	37.64	33.16	36.00	34.39	24.41
K-feld.	26.41	28.05	27.13	29.28	33.09	28.89	30.33	40.00	27.00	35.41	30.56	11.45	15.65	45.03	8.36	27.47	39.89
Plag.	27.62	24.85	30.98	25.66	11.65	31.43	29.11	24.13	34.86	29.98	18.40	29.12	44.90	16.75	51.09	26.88	21.86
Tot. feld.	54.03	52.90	58.11	54.94	44.74	60.32	59.44	64.13	61.86	65.39	48.96	40.57	60.55	61.78	59.45	54.35	61.75
Biot. Chlor.	1.01	-	4.01	0.49	2.77	5.53	4.23	2.95	0.16	1.41	-	15.86	1.59	-	-	-	0.56
Seric. Musc.	-	-	0.80	0.33	-	0.61	0.37	-	4.58	1.41	3.26	1.41	-	-	-	7.91	-
Horn.	-	-	-	-	-	-	-	-	-	-	-	-	-	3.66	3.27	-	11.66
Epid.	0.40	1.89	6.42	0.33	1.85	1.02	0.55	0.35	0.33	0.60	0.30	0.20	-	1.05	-	1.98	0.73
Acc.	2.42	0.29	0.96	0.49	1.29	2.05	0.55	0.70	0.33	0.40	2.37	-	0.23	0.35	1.27	1.38	0.91
Total	100.00	99.99	100.00	100.00	100.00	99.98	99.99	100.00	99.99	99.99	99.99	100.01	100.01	100.00	99.99	100.01	100.02
	Ad	Ad	Ad	Ad	Gr	Ad	Ad	Ad	Ad	Ad	Ad	Gd	Gd	Gr	Gd	Ad	Ad

Ad: adamellitic   Gr: granitic   Gd: granodioritic

Table 15. Modal Mineralogical Composition of Nosib Granulitic Gneisses

biotite+plagioclase+quartz±K-feldspar/albite component+hornblende, which in Fe and Ti rich biotites is accompanied by the formation of ore (ilmenite)(Winkler, 1967; p.214; Büsch, 1966).

Additional K-feldspar is produced by reaction of muscovite with quartz evidenced by the numerous relics of corroded muscovite and its consequent drastic reduction in volume.

It must also be noted how migmatites, pegmatites and cross-cutting mobilisates are in general relatively scarce, whereas the compositional banding normally conforms with the regional foliation.

In conclusion the Nosib metamorphic assemblage appearing in sheets 1913A and 1813C is similar to those described as hornblende (or biotite (Hsü, 1955; p.223)) granulite subfacies by Fyfe, Turner and Verhoogen (1958; p.232) or hornblende-clinopyroxene-almandine granulite subfacies of Winkler (1967; p.135).

Recently Fyfe and Turner (1966), in disagreement with Winkler (1967; p.20), recommended an abolition of all subfacies from metamorphic classifications. Meanwhile research carried out by Engel and Engel (1958, 1960) and Buddington (1963) in the north-western Adirondacks (N.Y.) and by Binns (1964, 1965) in Broken Hills (Central Australia) has shown that terrains grading from the amphibolite to the granulite facies offer parageneses typical of the hornblende-granulite subfacies. Turner (1968; p.186), therefore, has replaced this last classification with the better suited term of amphibolite-granulite transition facies, which applies well to the terrains under discussion.

The quoted occasional appearance of orthopyroxene to the west indicates a gradual transition towards the high-grade orthopyroxene subfacies, i.e. granulite facies proper. It is particularly unfortunate that this facies could not be followed throughout the full spectrum of Damaran metamorphism and in particular only marginally within its highest (sillimanite) zone J of folder 7, where erosion was not incisive enough to expose Nosib anticlinal cores.

2. Possible Antecedents of the Nosib Granulite

There has always been a tendency towards interpreting quartzofeldspathic <u>sensu stricto</u> granulites as the derivates of metapsammites of arkosic composition or siliceous igneous rocks (Williams, Turner and Gilbert, 1954; p.236). The possibility of their derivation from psammitic sedimentary antecedents was thus investigated first. Very simple petrographic calculations, however, discourage such possible parental relationship. Table 12 supplies the modal mineralogical composition of 11 arkosic quartzite and arkoses sampled throughout the massive Lower Nosib (samples 230-236) and in some of the sparse Upper Nosib psammitic intercalations. If the average total feldspar content (24.53% by volume) is compared with the average of 17 modal analyses of

Sample	164	167A	165A
	Pink streaked gneiss	Granulitic gneiss	Nosib (A_2) granite
CHEMICAL ANALYSES			
SiO_2	74.09	73.82	75.24
TiO_2	0.20	0.29	0.12
Al_2O_3	13.20	13.14	13.19
Fe_2O_3	0.50	0.96	0.61
FeO	0.57	0.59	0.37
MnO	0.02	0.05	0.02
MgO	0.24	0.29	0.29
CaO	0.91	0.83	1.00
Na_2O	2.92	4.02	3.11
K_2O	6.03	4.81	5.27
P_2O_5	0.08	0.07	0.10
L.o.i.	0.48	0.20	0.23
H_2O^-	0.01	0.11	0.02
Total	99.25	99.18	99.57
CATION PROPORTIONS			
Si	71.59	69.57	70.97
Ti	0.15	0.21	0.09
Al	15.04	14.60	14.67
Fe^3	0.36	0.68	0.43
Fe^2	0.46	0.47	0.29
Mn	0.02	0.04	0.02
Mg	0.35	0.41	0.41
Ca	0.94	0.84	1.01
Na	3.60	7.35	5.69
K	7.43	5.78	6.34
P	0.07	0.06	0.08
Total	100.00	100.00	100.00
MESONORMS			
Q	36.97	28.90	33.21
Or	36.10	27.97	30.88
Ab	17.99	36.74	28.45
An	3.44	2.70	3.96
C	2.63	0.39	1.05
Bi	1.71	1.53	1.33
Sph	0.44	0.62	0.26
Mt	0.55	1.02	0.65
Ap	0.17	0.15	0.21
Total	100.00	100.02	100.00

Loss at 950°C

Analyses by: Geochemistry Department, University of Cape Town

Table 16. Chemical Analyses, Cation Proportion and Mesonorms of Nosib Granulitic Gneisses and Mobilisates

Nosib granulites (56.37% by volume) it is obvious that no relation whatsoever could possibly exist between these two suites. Even if all the muscovite/sericite present were converted into mesonormative K-feldspar, the average figure would remain well below 50% of the respective quantity in the granulites. Moreover, the balance is almost entirely composed of plagioclase (calcic oligoclase), making an alternative metasomatic genesis extremely unlikely, as is obvious from the Q-ΣFeld - ΣMaf triangular graph of figure 19.

A possible parental relationship with the Upper Nosib greywacke association can then be sought in the light of the petrographic changes that the sequence had undergone during the pre-Damaran (F_1N/M_1) tectono-thermal episode, illustrated in page 105. Essentially two lithotypes were created during this episode, which in order of abundance are:

i) a large mass (more than 85%) of more or less differentiated but non-mobilised granodioritic paragneiss, the modal mineralogical composition of which was given in Table 11, plotted as open circles in the diagram of figure 19.

ii) subordinate (less than 15%) amounts of granitic/granodioritic pegmatoid mobilisates, the modal mineralogical composition of which was given in Table 11 group C, plotted as full circles in the diagram of figure 19.

Thus the following Damaran (M_2) tectono-thermal episode was impressed on large extensions of partially to deeply dehydrated schists and gneisses of high-greenschist to middle-amphibolite grade surrounding subordinate discontinuous migmatised areas.

The average total feldspar in the granodioritic suite reaches a much higher level (37.44% by volume) and approaches more closely that of the average granulite. However, a 20% difference in favour of the latter still exists, the balance being mainly composed of K-feldspar. On the other hand, a large quantity of potash, retained in hydrous or phyllitic minerals (biotite and muscovite), seems always to be paired with low K-feldspar contents in the granodioritic suite, whereas those minerals are extremely scarce or virtually absent in the granulites. The same applies, on a smaller scale, to the epidote/zoisite-plagioclase content. As both granodioritic and granulitic suites contain variable amounts of quartz of original clastic derivation, a large proportion of the granulite K-feldspar could have formed at P-T conditions exceeding the upper stability limit of the muscovite-quartz and biotite-plagioclase-quartz systems exemplified in the previous paragraph.

The alumina resulting from the destruction of muscovite was probably fixed as plagioclase in this Ca- and SiO_2-rich environment, and as Mg-rich garnet under high operative pressure. Free

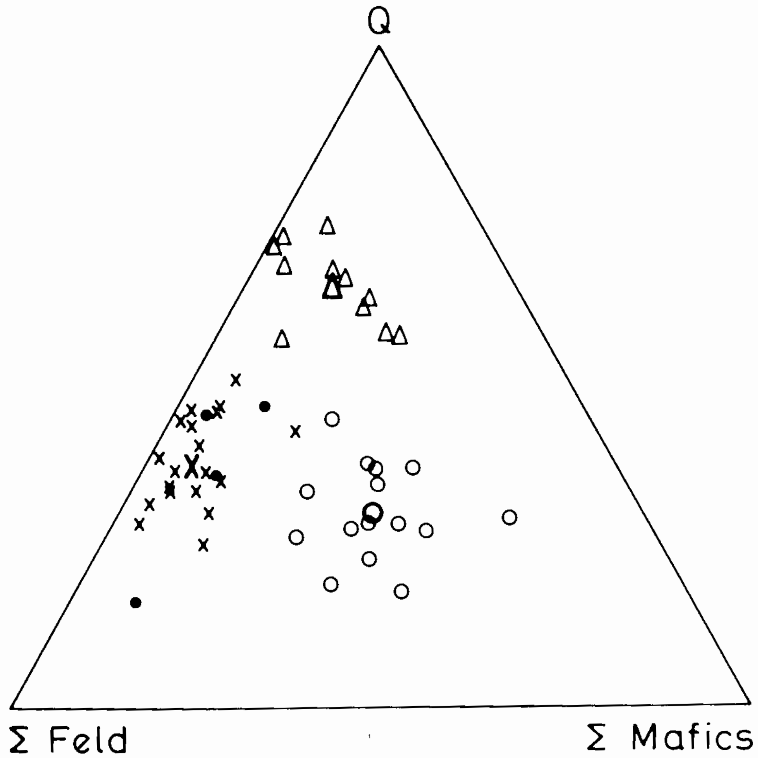

Figure 19. Mineral compositions of Nosib subarkoses (triangles), granodioritic paragneisses (open circles) and pegmatoid mobilisates (full circles) in comparison with that of Nosib leucocratic granulites (crosses). Bold symbols indicate respective average values

aluminosilicate was observed as sillimanite (fibrolite) only in minor mobilised portions or as discrete needles in feldspar or quartz. These considerations and the development of granulites in areas structurally underlying the Damaran garnet and adjoining sillimanite zones (I and J) indicate that temperatures in the order of 700°C must have been operative. At this temperature and relatively high P_{H_2O} the hornblende-granulite boundary plotted on a P-T diagram by Fyfe et al. (1958; p.237) intersects the "minimum melt" curve of granites; but, as has been mentioned, the amount of pegmatoid mobilisates in the pink gneiss/granulite is conspicuously subordinate when compared to that present during the formation of the overlying Damaran (A_2) migmatites (more than 30% by volume of mobilisates). Hence P_{H_2O} must have been extremely low in the former ($P_l >> P_{H_2O}$) and relatively high in the latter ($P_l = P_{H_2O}$) to justify the difference. However, Winkler and collaborators (1967; p.131) have experimentally shown how the survival of OH-bearing mineral phases at such temperature is impossible if the parental rock (i.e. the M_1 granodioritic gneiss) has undergone intense dehydration. At 700°C, for instance, a P_{H_2O}<1000 bars triggers the appearance of the first orthopyroxene, while at P_{H_2O}<500 bars no hornblende and biotite will survive. It is thus suggested that the majority of Nosib pink quartzo-feldspathic granulites and streaked gneisses appearing to the west of the Damaran hornblende-oligoclase isograd of folder 7, were derived by the superimposed effect of the Damaran (M_2) metamorphism on the Upper Nosib (M_1) deeply differentiated, biotitic granodioritic paragneisses and only subordinately on pegmatoid mobilisates (A_1) and related massive granodiorites. Previous and variable dehydration of the original greywacke and shale, metamorphosed into middle-amphibolite grade gneisses by the pre-Damaran (M_1) episode, has forced the course of the following (M_2) Damaran metamorphism towards a granulitic facies. The effect of relatively low P_{H_2O} under P_l and T similar to those operative in the high amphibolite zones of the advancing Damaran metamorphic front was sufficient to create this transition granulite facies.

The physico-chemical conditions were thus uncongenial for the production of an abundant anatectic melt but ideal to bring about the breakdown of most of the phyllitic minerals to produce albite-rich K-feldspar/hornblende and farther west, pyroxene.

Similar granulitic textures and analogous parageneses were described by Smith (1965; p.19-20) in the Khan and Swakop Rivers area. The polymetamorphic nature of these granulites, however, was then not recognised due to the local absence of an obvious P^2 or U^2 para- or unconformity at the base of the Damara System or to its tectonic obliteration. Discussions held with Gevers (October 1969) and subsequently with Smith (November 1969), however, have led to the conclusion that the proposed metamorphic history may satisfactorily apply also to the southernmost portion of the western branch of the Damara eugeosyncline. This hypothesis was later confirmed by orthopyroxene-hornblende granulites sampled in the area by Jacob (personal communication). A similar anomalously high metamorphic grade in Nosib pink granitic gneisses if compared with the overlying Damara schists in the Marienfluss-Hartmannberge area was observed by de Villiers (1968) during reconnaissance work along the Kunene River south of the Angolan border. Under his suggestion the present author visited the area during the same year and, after the local geological setting was kindly explained to him by Drs. Schalk, Porada and Hugo, who at present are carrying out extensive regional work in the area, satisfied himself that there also polymetamorphism has affected the Nosib terrains.

Figure 20, which is substantially an E-W section across the study area, shows the postulated interference of the M_1 and M_2 tectono-thermal episodes. The intersection of the Damaran metamorphic gradient curve with the Nosib curve delineates two fields of extremely different M_1/M_2 polymetamorphism. The western, where higher M_2 grades are superimposed on lower M_1 amphibolite grade, is the field of Nosib granulites and streaked gneisses. Under the opposite circumstances, i.e. where a lower greenschist Damaran (M_2) grade is superimposed on a higher amphibolite (M_1) grade, apparent retrograde metamorphism is generated during deformation with the formation of the parageneses described in zone F.

The Sesfontein area thus offers an example of a hornblende (transition) granulite assemblage overlapping the amphibolite facies (Fyfe, Turner and Verhoogen, 1958), rather than following it as a higher-grade facies. Similar temperatures, load and tectonic overpressures were accompanied by substantially different fluid contents in the rocks. Only to the west of the study area, where an orthopyroxene assemblage seems to be developed, can higher temperatures than those of the amphibolite facies ($>700^{\circ}C$) be inferred.

Holland and Lambert (1969) have shown how dehydration during metamorphism is a quantitatively discontinuous process. Maximum amounts of H_2O are released at low grades (regimes 1 and 2; op. cit., p.204), minimum amounts during middle grades (regime 3; op. cit., p.207) and a peak again in the high amphibolite grades (regime 4; op. cit., p.209). This seems to justify the granulite development from the superposed effect of relatively high (regime 4) M_2 Damaran metamorphism on comparatively low-grade (regime 2) M_1 Nosib metamorphites. The amount of water set free by the high amphibolite dehydration reaction of muscovite and biotite is relatively small, but is subjected to "processes of local migration and concentration" (Mehnert, 1969; p.243) and controlled by tectonic pressure-gradients. Concentration of H_2O content, in turn, is likely to have promoted the mobilisation of subordinate red, coarse pegmatitic granites occasionally encountered throughout the granulitic areas, whereas the successive release of water during their crystallisation may, under lower (still rather high) temperature, have induced retrograde transformations elsewhere. That the pink Nosib mobilisates are associated with structural lines of high pressure-gradients is proved by their common, if not invariable, cataclastic or mylonitic texture (sample 165A).

The present work, therefore, substantiates the polymetamorphic origin of granulites as described in the Lewisian of Scotland (Sutton and Watson, 1951) and in the San Gabriel Mountains of California (Hsü, 1955).

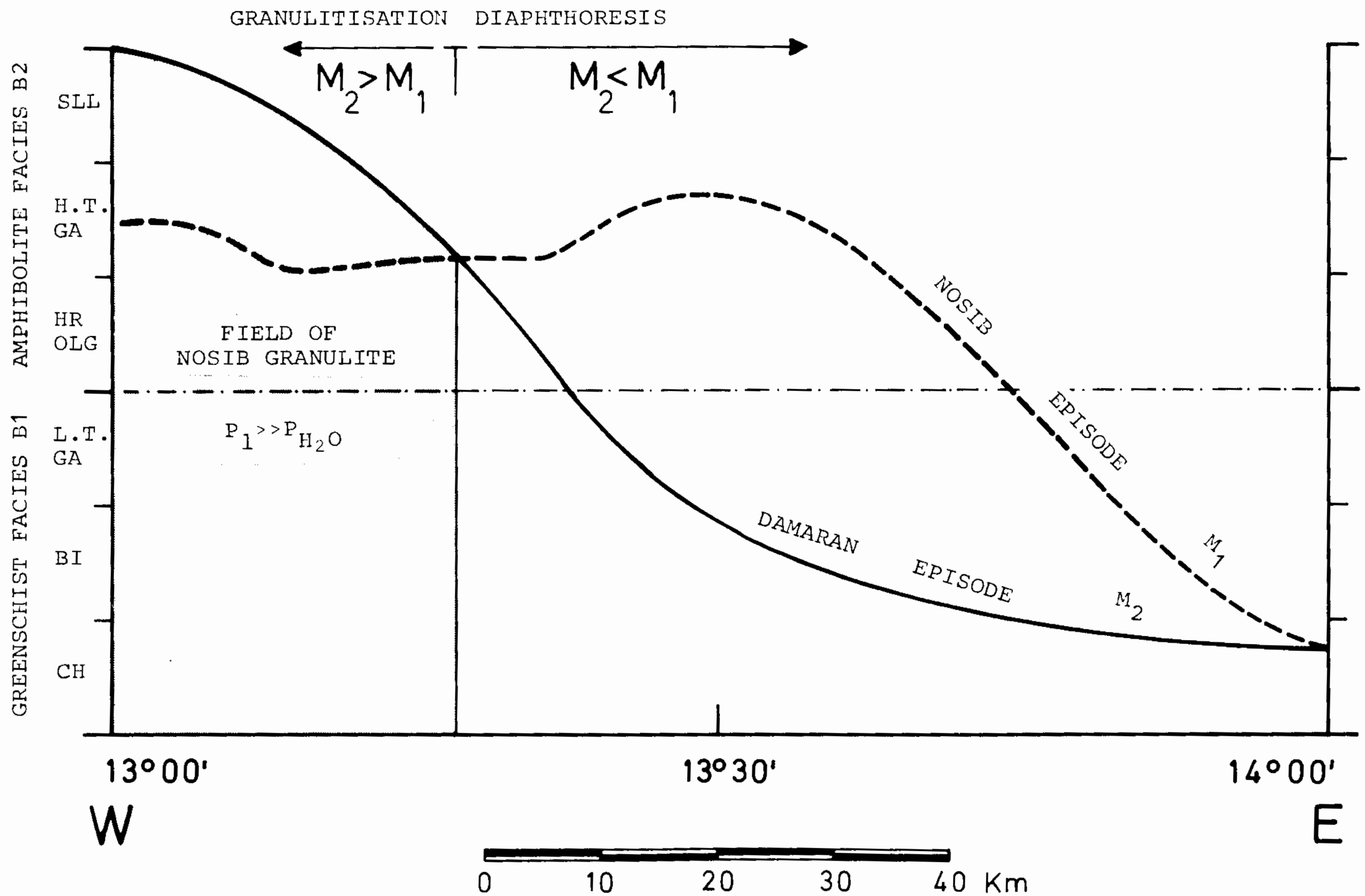

Figure 20. Different fields of M_1/M_2 polymetamorphism

F. CONCLUSIONS

Polymetamorphic assemblages observed within the Nosib terrains indicate that metamorphism in the Nosib-Damara geosyncline was active during at least two major episodes.

The first (M_1) accompanied the deformation of the Upper Nosib greywacke (F_1N) prior to the deposition of the Lower Hakos sediments. This pulse is thus unlikely to have occurred later than 600-700 My ago. Several radiometric ages in that span, obtained by various authors in central Africa for tectono-thermal events affecting the Katanga System of Zambia and the Lomagundi and associated rocks of Southern Rhodesia, have been reviewed by Clifford (1967; p.90-92). They were grouped into the Katangan episode, dated at 620±40 My, (hence of late Precambrian age as distinguished from the Kibaran episode dating back to 1100±200 My) and the early-Paleozoic Damaran episode, for which an age of 550-450 My has been postulated (op.cit.; p.3). Age determinations are at present being undertaken on behalf of the Precambrian Research Unit and it is thought that these may show that the F_1N/M_1, pre-Damaran episode has a Katangan age. As for the following $M_2/F_{2,3,4}S$ episode, its Damaran age has been structurally proved and this conclusion is supported by two K/A radiometric ages from the Hoanib and Hoarusib River gorges of 492±26 and 530±28/550±29 My respectively published by Clifford (1967; p.20).

Table 16 provides an idealised correlation of the chronologic succession of structural and metamorphic events for the south-western Kaokoveld.

Both episodes are characterised by the Barrovian metamorphic facies series.

The first (M_1) Nosib tectono-thermal episode must have reached middle-amphibolite facies grade and culminated in a few peaks of discontinuous metamorphic differentiation and minor (A_1) anatexis. The Lower Nosib arkosic sandstone was thus transformed into recrystallised feldspathic quartzite, whereas the Upper Nosib greywacke and shale were metamorphosed into a rather homogeneous mass of granodioritic gneiss transgressed by minor amounts of (A_1) pegmatoid mobilisates, amphibolites and subordinate alternations of psammitic resisters.

Once the successive sedimentation of the Damara System was completed, the following M_2 Damaran tectono-thermal episode was thus impressed with extremely different results over two completely different sets of rocks:

i) a basal, dehydrated, crystalline sequence of Nosib quartzite and gneiss

ii) a geosynclinal succession of unmetamorphosed, water-rich, Damara greywacke, shale and subordinate carbonate and basic igneous rocks.

A rather steep (M_2) Damaran, westwards metamorphic gradient is recorded in the prograde metamorphism of the Damara rocks, which ranges continuously from the lowest greenschist (chlorite-sericite) to the highest amphibolite subfacies (sillimanite) to the west. Final (A_2) anatexis accompanied this P-T increase with the formation of metatexitic gneisses, migmatites (synkinematic granites) and post-kinematic (Ganias-Uhima) granites, made possible by inherently large amounts of water and volatiles contained in these sediments undergoing their first metamorphism.

Where the M_2 Damaran gradient was superposed on the previously metamorphosed Nosib schist and gneiss the results were extremely different depending on the reciprocal grades of the two successive episodes. Thus where the M_2 episode reached a lower grade than the M_1 (i.e. east of the Damaran hornblende-oligoclase isograd), retrograde metamorphism was produced by concentration of fluids into high pressure-gradient zones. This was especially marked in axial cores of the Damara nappes where Nosib schists were infolded within water-rich Damara sediments.

In root zones or beyond the Damaran (M_2) hornblende-oligoclase isograd, where the M_2 episode reached higher grades than M_1, the interference metamorphism developed into a prograde anhydrous transition-granulite facies. Phyllitic minerals were destroyed in favour of K-feldspar and hornblende under T and P_1 similar to those operative in the highest amphibolite facies, but paired by anomalously low and variable P_{H_2O}. The low P_{H_2O} was due to dehydration of the Nosib metasediments during the previous M_1 episode. The scarcity of fluids hindered the formation of an abundant anatectic melt from the Nosib metamorphites. Subordinate pegmatoid mobilisates are limited to shear-zones, where scarce H_2O, derived from the breakdown of micas, is likely to have concentrated due to local high pressure-gradients and tectonic lines of diffusion.

Metamorphism, migmatisation and plagioclase blastesis are considered to have been conservative or isochemical on a regional scale. The possibility, not investigated thoroughly, of late- to post-kinematic potash metasomatism and related discontinuous K-feldspar blastesis cannot be excluded in the light of the limited geochemical evidence available.

			Deformation Phase		Metamorphism (M) and Anatexis (A)
NOSIB	1st Kinematic 620 ± 40 My?	F_1N	NNE trending, tight, eastwards overturned, regionally discontinuous slip folding. Penetrative S_1 foliation	M_1	Dynamothermal metamorphism reaching middle amphibolite grade
				A_1	Localised peaks of metamorphic differentiation and migmatisation Biotite-muscovite and hornblende S_1 foliation Moderate K-feldspar blastesis
		1st	Interkinematic phase		Erosion, sedimentation diagenesis
DAMARAN	2nd Kinematic	F_2S (initial)	NNW (wide variation) trending, eastwards overturned or recumbent (nappes), macro- and mesoscopic flexural-slip and slip folding. Weakly to strongly penetrative S_2 foliation	M_2 (1st pulse)	Moderate enhancement of bedding (S_0) and axial planar (S_2) foliations by chlorite, and biotite growth Conversion of pelites to fine-grained schists
		2nd	Interkinematic phase	M_2 (2nd pulse)	Development of low temperature garnet including straight trails (Si) of S_2 mineral foliation
	3rd Kinematic 450 - 550 My	F_2S	F_2S: Renewed movement of the nappes	M_2 (3rd pulse)	Metamorphic climax. Establishment of the Damaran gradient, with prograde chlorite and/or muscovite and/or biotite S_2 and S_4 foliation in Damara rocks Oligoclase blastesis.
		F_3	F_3: NE trending, upright, extremely large wavelength, axial undulation; rare southward overturned mesoscopic slip folding at very deep levels. Non penetrative S_3 foliation	A_2	Metatexitic banding and anatectic generation of Damaran syn kinematic pegmatoid mobilisate
		F_4	F_4: NNE trending, steeply eastwards inclined or overturned slip folding, coaxial or at an angle to F_2S Strongly penetrative S_4 foliation posthumous slippage in S_1 and S_2	$(M_2 > M_1)$	Granulitisation in M_1/M_2 Nosib poly metamorphic terrains west of the hornblende-oligoclase isograd
				$(M_2 < M_1)$	Diaphthoresis in M_1/M_2 Nosib poly metamorphic terrains east of the hornblende-oligoclase isograd
		D_6	Development of N-S striking, eastward directed, low-angle Sesfontein thrust		Late-kinematic growth of high temperature garnet and sillimanite (fibrolite) Formation of the late-kinematic Ganias granite
		D_7	Development of NE striking, subvertical wrench or tear faults		Emplacement of the coarse-grained pegmatoid Uhima granite and pegmatites K-feldspar blastesis

Table 17. Time Relationship between Deformation, Metamorphism and Migmatisation in the Nosib-Damara Mobile Belt

Plate 31. Isolated mesas of Etendeka plateau-basalt (Mt. Sima) resting over the re-exposed Mesozoic surface

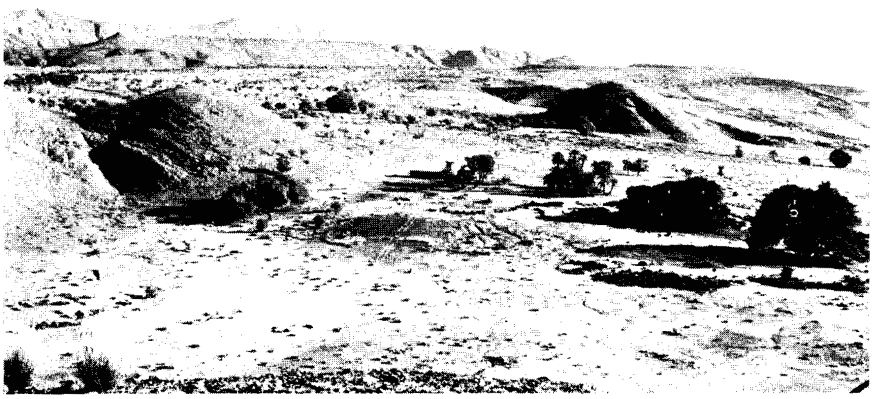

Plate 32. Successive orders of terraces north of the Sesfontein Plains

V. OUTLINES OF POST-OROGENIC GEOMORPHOLOGICAL EVOLUTION

Intensive degradation and energetic transport must have accompanied and followed the rise of the early-Paleozoic Damara orogen. The mass of new detritus collected in large intracontinental basins and foredeeps. A local example is the Etosha basin, where the gap between the top of the Mulden molasse and the post-orogenic sedimentation of the clastic non-marine Ovamboland Formation (revealed below the Dwyka tillite by several boreholes sunk by private enterprises and by the Geological Survey) could be very short or even uninterrupted.

The valleys of this Paleozoic relief were then re-modelled by the Dwyka glaciation and preserved under a thick pile of glacial and periglacial sediments (Martin, 1968). Re-excavated Dwyka valleys such as the Gomatum and the Purros valleys still show markedly U-shaped transverse profiles. Glacial over-deepening is also the most likely interpretation for the formation of the Giribes Plains, a peculiar, 12 Km wide endoreic basin about 15 Km west of Sesfontein. This has the shape of a triangle, from the apices of which, marked by shallow watersheds, large valleys radiate. None of these, however, drains the plains, where the occasional rain-water is conveyed to a pan which occupies its centre.

Later peneplanation was concluded with the evolution of a Mesozoic surface, shaped mainly in arid or desert environments (Martin, 1968), which was arrested at a late stage during the Lower Crataceous (Siedner and Miller, 1968) and preserved by fissure eruption of several hundred metres of plateau basalt. Erosion has again denuded this morphological surface, which is well preserved in the Ganias Plains where aeolian Cave sandstone (Martin, 1968) or volcanic agglomerate (Guj, 1968) appear at the base of a few plateau-basalt mesas (Plate 31). The summit level of this Mesozoic surface has been displaced by N-S striking, subvertical post-Etendeka (Stormberg) step-faults (eg. the Mudorib fault) marked by large westwards downthrows which break up the rather ill-defined "Great Escarpment".

Relics of at least four terraced aggradation surfaces (Plate 32) in the vicinity of Sesfontein represent the record of a number of cyclic epeirogenic tilts and consequent base-level fluctuations (Guj, 1969) of the order of several hundred metres. Wetter paleoclimatic conditions apparently accompanied this end-Tertiary to Pleistocene climax in the continental warping and marginal coastal flexuring (Mabbutt, 1952), inducing intense rejuvenation of the Hoanib drainage. The inherited Mesozoic surface was consequently farther regraded into several N-S aligned ranges of massive bastions and gneissic hills dissected by subsequent tributaries. Under later more arid climatic conditions these have been slowly exfoliated and wind abraded into groups or isolated inselbergen emerging from vast pediplains, derived from the rapidly decreasing transport power of the Hoanib tributaries. That more humid conditions must, at some stage, have controlled the morphological evolution is locally proved by the existence of karst features, unlikely to form under sub-arid climates. Striking similarity exists between the Hoanib terraces and those described by Mabbutt (1952) in the middle Ugab valley.

Summarising, the Hoanib and Gomatum valleys, west of Sesfontein, have conceivably overcome all the geological and geomorphological vicissitudes since the Paleozoic to be re-established along more or less the same lines during the Karroo glaciation and the Tertiary to Recent regradation (Martin, 1968). However, especially in the easternmost portion of the area where the Hoanib, entrenched in deep meandering gorges, intersects the karst highveld, the drainage system appears superimposed. Here the present pattern may possibly have been inherited from one previously established on the flat-lying Etendeka-plateau basalts which, prior to denudation, must have extended farther north covering at least part of the area. Analogous circumstances must have controlled the incision of the Ganamub River bed across the eastern apex of the Giribes Plains, because of its discordance with the trend of the pre-existing Dwyka glacial valley and of the absence of any structural control by the excavated Damaran gneiss.

In conclusion the Damaran tectono-thermal episode is the last orogenic cycle in the area, followed only by brittle dislocations and up- or downwarping of variable, occasionally extreme, amplitude during the Karroo and Tertiary to Recent geomorphological evolution.

VI. CONCLUSIONS

The conclusions of this study can best be stated in terms of a model of the evolution of the Nosib-Damara mobile belt. The main features of this model can be summarised as follows.

1. The encroachment upon the basement landscape was followed by the unconformable deposition of thick Lower Nosib arkosic wedges migrating towards the eastern sources of subaerial denudation and of coarse immature feldspathic debris. To the west, away from the shorelines, in pelagic environments, the successive Upper Nosib greywacke was rapidly deposited in response to the early establishment of the N-S trending Andib-Ganamub trough, while perhaps subarkoses were still being deposited farther to the east. Syndepositional intrusion and extrusion of basic igneous materials accompanied this first phase of rapid subsidence. A first pulse of tight pre-Damara folding along NNE trends (F_1N) and of metamorphism (M_1) reaching the middle amphibolite facies and culminating in a few peaks of migmatisation and anatexis (A_1), concluded this sedimentation cycle. The emplacement of a network of leucocratic pegmatoid mobilisates accompanied the granodioritisation in situ of part of the Upper Nosib greywacke and was in turn followed by moderate K-feldspar blastesis. In the western areas of maximum uplift and consequent intense erosion, a conspicuous angular unconformity (U^2) was thus created at the base of the following Damara sediments. This, however, fades eastwards into a paraconformity (P^2) towards the Kamanjab inlier, a positive area of slower subsidence, where the F_1N/M_1 tectono-thermal episode had insignificant intensity.

2. During the following Damara sedimentation a N-S hinge-line of westwards directed maximum subsidence gradients, separating a eugeosynclinal (Khomas) trough of essentially greywacke sedimentation from the transitional and miogeosynclinal regions, was established west of a geanticlinal ridge running through the present Hoanib-Mudorib confluence, and possibly due to the welding effect of the Nosib folding and metamorphism. This narrowed the original eugeosynclinal basin and produced a concentration of the available detritus with consequent increase in rate of sedimentation. The slow syndepositional rise of the geanticline controlled the sedimentary geometry of the Lower Hakos semipelites, lenticular carbonates and subordinate greywacke of the transitional zone, which thin out against its gentle eastern (proximal) flank, while an analogous influence was exerted by the Kamanjab inlier on the Lower Otavi carbonate sedimentation in the miogeosyncline. The intensive differential subsidence, necessary to accommodate the overwhelming mass of depositing greywacke, induced deep fractures along the steep western (distal) flank of the geanticline which provided chan-

nels for the ascent of the intermediate to acid Noeroep volcanics, and possibly later for the Khankhaib gabbro-anorthositic complexes.

3. The wide transitional and miogeosynclinal regions were then upwarped en bloc prior to the late Precambrian glaciation. A wave of re-worked clastics derived from the consequent ubiquitous erosion was poured into the Khomas furrow enhancing its practically uninterrupted subsidence. As uplift was accompanied by negligable angular deformation only, a disconformity marks the base of the following ubiquitous Tillite Substage of the Upper Hakos Series, in spite of a relatively long hiatus in sedimentation. However, where, as on the geanticline, erosion was so deep as to re-expose the folded Nosib substratum, a conspicuous angular unconformity was formed. The persistence of the Tillite Substage and the peculiar inherent paleoclimatic conditions, make this possibly the only truly isochronous link between the base of the Upper Otavi Series in the miogeosyncline and that of the Upper Hakos Series, partially intertongueing with the extremely thick, western Khomas greywacke succession.

4. Meanwhile, under the influence of intense subsidence to the west, the blanket of miogeosynclinal carbonates started creeping slowly down the western flank of the repeatedly upwarped Kamanjab inlier, under the action of gravity. Folding (F_2O) occurred whenever its advance was structurally hindered. Almost contemporaneously, paroxysmal subsidence along the axis of the eugeosyncline brought the base of the sequence to levels of migmatisation and anatexis. Resulting infrastructural buoyant forces pushed up a partially mobilised mass of granitic/granodioritic paragneisses preceded by the front of Damaran metamorphism. Decreasing rates of uplift towards the more stable or even slightly subsiding foreland, created slopes sufficient to convey large recumbent nappes (F_2S) of scarcely metamorphosed suprastructures eastwards to override the miogeosynclinal trough along the N-S striking, low-angle Sesfontein Thrust (D_6/F_6). Concomitant active erosion pushed forward an enormous mass of immature detritus rapidly deposited in the subsiding Mulden molasse foredeep or exogeosyncline, which was in turn overthrust. Movement was aided by shearing of clays and carbonates along the thrust-plane and by synkinematic dolomitisation. The root and cores of the Damara nappes, exposed by deep erosion, consist only in places of domal structures but more generally of extremely elongated (>80 Km) anticlinal belts of crystalline Nosib gneisses. Steeply or shallowly eastwards overturned slip folding at these deep levels (F_2S, F_4) has controlled the structural evolution of the suprastructural nappes. Renewed posthumous slippage along the s_1 foliation related to the previous pre-Damara F_1N phase of deformation was also impressed on part of the nappe carapaces. An orthogonally superposed, large wavelength F_3 folding produced megascopic

regional plunges (axial undulation) of the B_2 axes.

5. The Damaran (M_2) metamorphic spectrum grades from the highest (sillimanite:B2.3) amphibolite facies in the axial uplift area to the lowest (sericite-chlorite:B1.1) greenschist facies of the Barrovian dynamothermal series in the digitated front and carapace of the eastwards recumbent nappes of Damara schists, where these experienced their first phase of metamorphism. M_1/M_2 polyphase interference metamorphism induced by the Damaran episode on the previously metamorphosed and thus relatively dehydrated Nosib gneisses is exposed by deep erosion in the cores and roots of the nappes. East of the Damaran hornblende-oligoclase isograd, where the grade of the Damaran episode was lower than that attained during the Nosib pulse, retrograde parageneses are normally developed. Where, as to the west of the hornblende-oligoclase isograd, the latest Damaran episode reached the highest amphibolite grades, a granulite-amphibolite transition facies was developed in the polymetamorphic Nosib gneisses mainly on account of their dehydrated character, i.e. under the same T-P operative in the formation of the amphibolite-grade Damara gneiss and migmatite and not as a strictly higher temperature facies. Farther to the west, however, sparce hornblende-orthopyroxene granulites seem to indicate that a proper granulite facies is developed in the Nosib gneiss west of the area.

6. Rheomorphic conditions and therefore plasticity and mobility were at a maximum in the axial uplift on account of migmatisation and high-grade metamorphism, with the flowage into non-affine slip and ptygmatic folds. Mobility, however, dropped suddenly beyond the front of Damaran migmatisation. This sharp change in the mechanical properties of the rock-mass undergoing deformation induced intense shearing marked by belts of mylonite and cataclastic gneiss. Metamorphic textures indicate that the successive pulses progressively increased in grade and that sillimanite has a markedly late- or even post-kinematic character. It is thus understandable why no contact metamorphic aureole surrounds the fine-grained late-kinematic and structurally controlled Ganias granite (possibly equivalent to the Donkerhoek granite of Gevers (1963)), where it is intruded into the migmatised and often porphyroblastic Khomas paragneiss (possibly equivalent to the Salem granite of Smith (1965)), which seems to support its parautochthonous origin. Even the post-kinematic, pegmatoid Uhima granite, mostly emplaced along a system of NE tear fractures (D_7), does not show any obvious contact effect.

7. At a rather late stage, the eastward advancing Sesfontein thrust-mass impinged on the massive, folded Otavi dolomite relief, which it was unable to override. It therefore developed a frontal toe and its speed of advance was reduced to that of erosion of the toe. Where the thrust advanced on Mulden

phyllites, the stresses were released through the creation of alternative thrust-planes, with intense transposition and gleitbretter drag folding (D_6) of the footwall.

8. The Sesfontein Thrust now separates two extremely different structural-stratigraphic domains:
   i) an eastern miogeosynclinal, feebly metamorphosed and volcanic-free domain (Outjo Facies of the Damara System) deformed into thin-skinned or non-basement-involving tectonites, overridden by
   ii) a western domain of supracrustal nappes of transitional or eugeosynclinal metasediments (Swakop Facies of the Damara System), generated in response to thick-skinned or basement-involving anatexitic processes occurring at depth and creating buoyant uplifting forces along the axial zone of the former eugeosyncline.

9. The present model involves many stratigraphic revisions of the previous interpretation of this mobile belt. These are shown in figure 14(b) and herewith summarised:
   i) No basement rocks were found in the area and it is suggested that no undoubted basement exists in the western Kaokoveld beyond the van Zyl's pass- Sesfontein Thrust line.
   ii) The large western regions formerly deemed to be underlain by basement are composed of Nosib and Damara metasediments.
   iii) The Nosib Formation can be locally subdivided into a Lower subarkosic Stage and an Upper Stage (developed only in the eugeosyncline) composed of semipelites and greywacke. Both stages are accompanied in the west by syndepositional igneous activity which extends into lower Damara (pre-Tillite) times and ranges from basic and ultrabasic to intermediate or acid composition. This sequence is tentatively correlated with the Naauwpoort Formation of the Huab-Welwitschia area.
   iv) Emphasis is placed on the magnitude of the Tillite disconformity and its hitherto somewhat neglected stratigraphic importance.
   v) The clastic sequence developed to the south of Sesfontein and Warmquelle (former Sesfontein phyllite) is correlated with the Mulden Formation and considered to represent molasse-type sedimentation synkinematic with the formation of the Damara nappes.

APPENDIX

A. A TECHNIQUE FOR UNDISTORTED CONTOURING OF STRUCTURAL DIAGRAMS

1. General

Dissatisfaction with the present methods of contouring and counting of structural point-diagrams led the author to seek a more objective, distortion-free method.

Two graphic techniques are commonly used by most authors at present:

i) the Mellis or circle method, and

ii) the Schmidt or grid method

described by Turner and Weiss (1963; p.61). The first is suitable for point diagrams exposing a comparatively low (<150) number of readings, whereas the second is recommended for higher numbers.

Both methods make use of a circular unitary area (1% of the projection surface) counting device of constant dimension and shape for the counting of densities on every portion of the diagram. This circle should, in contrast, undergo distortion according to its position in the net, changing its area in the case of the Wulff net and its shape in the case of the Schmidt net as a direct function of the polar distance θ. In the stereographic (Wulff) projection the diameter of the circle is distorted equally both in the meridian (m) and parallel (n) directions by a factor of $m=n=\tan\theta/2$ (Vistelius, 1966; p.7). Thus a circle of unitary area is projected into a circle (Gallitelli, 1959; p.33), but of area 1.373 for $\theta=45^\circ$ or 4.00 for $\theta=90^\circ$. In the Schmidt projection the circular shape is lost as the deformation factor is different in the meridian (m) and parallel (n) directions and is related to the polar distance by equations $m=\cos\theta/2$ and $n=\sec\theta/2$ (Vistelius, 1966; p.9). The resulting figure is an ellipse, elongated in the direction of the parallels, with axes 0.924/1.082 and 0.707/1.414 times the original diameter for $\theta=45^\circ$ and 90° respectively.

In theory the diameter of a circle of 1% area on or tangential to the sphere of projection along the meridian is equivalent to a central angle of $\Delta\theta=360^\circ/31.4=11^\circ\ 27'\ 30''$. The circle in fact lies between θ_1 and $\theta_2=\theta_1+\Delta\theta$. As both m and n factors are subjected to variations as a function of the polar distance θ, the correct figure should not be an ellipse but an ellipsoid with a rectilinear (meridian) axis asymmetrically intersected by a symmetric curvilinear (parallel) axis as shown in figure 21.

For practical purposes distortion was calculated at the polar

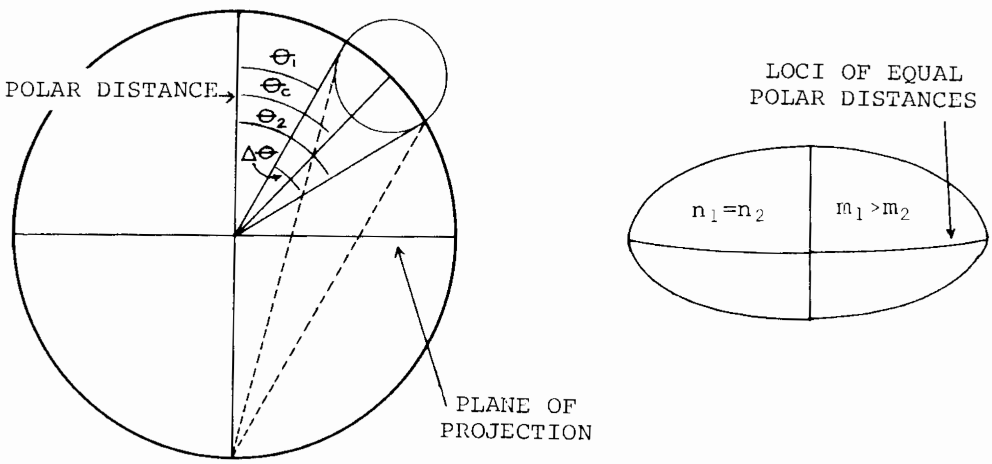

Figure 21

distance of the centre of the circle (θ_c) to be projected. Thus, the resulting figure becomes a regular ellipse. It is evident that if point-density is measured by overlapping an undeformed circle on an elliptically deformed equal area projection, a systematic error is introduced. This is also directly proportional to the polar distance θ and varies from 0% for a circle the centre of which coincides with the pole $\theta=0$ (centre of the net) to $\pm$ 33% (graphic calculation) for one lying along the equatorial major circle of the net i.e. $\theta=90^{o}$.

A number of ingenious attempts to obviate this difficulty have been produced in the past by Mellis (1942), Strand (1944, in Vistelius 1966) and Dimitrievič (1956, in Vistelius 1966). In all cases, however, only a limited number of deformed circles corresponding to 10^{o} θ polar intervals could be fitted in the limited space of a customary net on account of reciprocal overlapping. Counting and contouring could only be carried out using a modification of the Schmidt technique with relatively laborious and not very accurate results, while it was unfortunate that no use could be made of the non-subjective Mellis technique for low-number diagrams.

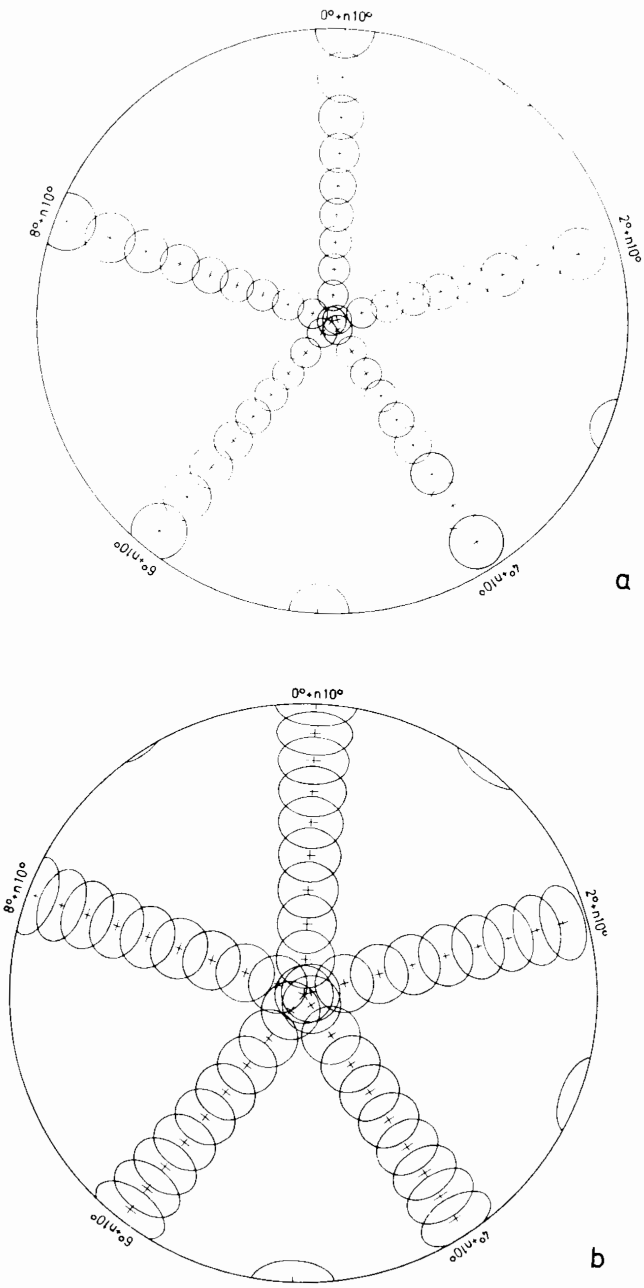

Figure. 22

In the following pages new counting and contouring nets and techniques, suitable for point diagrams irrespective of their measurements density, are proposed to eliminate the systematic error due to distortion. The non-subjective attributes of the Mellis method for diagrams of low to average (<150 points) number of measurements is retained.

2. The Nets

Wulff and Schmidt nets commercially available normally have a resolution of 2° and occasionally 1°. The accuracy of petrofabric and structural measurements is rarely contained within these limits (Kröner, 1968; p.24). The two prototypes of nets reproduced in figure 22 were, therefore, designed to match the resolution of ordinary nets, i.e. at 2° intervals. In both nets the distortion factor was calculated at the polar distance of the centre of the projection circle, i.e. for $\theta=\theta_c$.

In order to avoid extensive overlapping and facilitate the plotting of the deformed figures, series of circles (Wulff net) and ellipses (Schmidt net) corresponding to θ differences of 10° have been plotted starting from fixed θ values (multiples of 2°) on separate diameters of the net. Hence to achieve the same resolution of the ordinary Wulff and Schmidt nets, five diameters were used and the series of distorted circles plotted for 0°, 10°, 20°.....; 8°, 18°, 28°.....etc polar distances (fig. 22). The 46 figures plotted thus correspond to each of the polar distances indicated by meridian and parallel intersections on a customary Wulff or Schmidt net. The distorted figures were obtained by interpolation of several diameters and chords geometrically calculated and plotted at a very large scale. The area was provisionally checked by weighing and counting on a fine millimetre grid. More accurate prototypes will be available in the near future once a computer program for these calculations and their execution in a computer equipped with a graph plotting device has been finalised. Meanwhile, provisional specimens of the nets, in the customary 20 cm diameter size, will be available from the author on request.

3. The Counting and Contouring Method

Suitable modifications of both Mellis and Schmidt counting and contouring methods apply for use with the present nets.

a. The Modified Mellis Method

The transparent point-diagrams with a moderate or low (<150) number of measurements can be superposed on the counting net of figure 22(b) mounted on cardboard and equipped with a central pin to allow rotation. The diagram is then rotated so that each reading is in turn brought to coincide with the centre of an ellipse in the underlying net, which is duly traced on the diagram. As each reading represents a percentage (X%) of the total reading, the areas of overlapping of two ellipses will correspond to density 2X%, where three do so 3X%....or generally n overlaps will give n X%.

In practice while operating with the Mellis or circle method great and often unavoidable difficulty is experienced in determining the successive number of circle overlaps, thus the method was recommended for less than four contours (Turner and Weiss, 1963; p.64). The author found that the use of the following successive colours, given a light hue in areas of multiple overlapping, can obviate this difficulty and bring the number of contours obtainable to a recommended maximum of six (Turner and Weiss, 1963; p.61). A good sequence is:

		1	ellipse	:	pale yellow
overlap	of	2	ellipses	:	light orange
"	"	3	"	:	pea green
"	"	4	"	:	light red
"	"	5	"	:	light blue
"	"	6	"	:	dark brown

A cross-check can be obtained examining the curvilinear polygonal figures derived from the overlapping ellipses, because the number of overlaps is always equal to or greater than the number of convex sides.

It is also expedient to mark each point considered with a check to make sure that no reading is misread or plotted twice.

For point diagrams with marked preferred orientation it might save time to start from the densest areas, especially where more than one reading coincide. The initial ellipse will thus have the necessary "high density" colour at the start. When points are scattered it is quicker to proceed from areas of low density.

b. The Modified Schmidt Method

For point-diagrams with a rather high number of measurements (>150) the contouring procedure is a modification of the Schmidt technique. The diagram is stapled to a transparent 1 cm^2 grid, with one of the intersections in centre and the lines N-S and E-W aligned. Diagram and grid are then pinned on the counting net of figure 22(b), where by rotation each cross on the grid is brought to coincide with a centre of an ellipse on the underlying net. The number of readings contained in the ellipse is recorded on each intersection. Once this process is completed the combination of density values is converted into a contour pattern by tracing isolines by interpolation as described by Turner and Weiss (1963; p.62) and Whitten (1966; p.24). It should also be noted that this method does not "...comply with the probability theory. Thus it is not possible to apply any statistical treatment to the data obtained" (Vistelius, 1966; p.71). This stems from the fact that the same point can be simultaneously counted in "...two and sometimes as many as four overlapping circles" (Vistelius, 1966; p.71).

4. Conclusions

The proposed nets and contouring techniques offer the substantial advantage of eliminating the systematic error introduced by current counting or contouring using a circle of constant diameter and shape on a projection plane where the equivalent figure would be increasingly altered in size or portions at different polar distances.

When method "a" is used the advantage of non-subjectivity, inherent in the Mellis technique, is also achieved. The use of progressive colours further eliminates the difficulty in recognising the number of overlaps in a certain point, which is one of the practical limitations of the original Mellis method. As a consequence different operators contouring the same arrays of data should, if no accidental mistake is committed, reach "identical" contour patterns. Moreover, point diagrams with a very large number of readings (eg. 2000) contoured by method "b" (modified Schmidt) would not necessarily be more accurate or statistically sounder than a diagram with a lower number of readings (eg. 200) or composed of single or average measurements, contoured using method "a" (modified Mellis).

This technique is, if anything, less time-consuming than any other graphic contouring technique in current use. It is, therefore, recommended whenever circumstances allow for its use for the production of undistorted and directly comparable data.

B. A SAMPLING PROCEDURE TO IMPROVE THE ACCURACY OF STRUCTURAL MEASUREMENTS

The block-diagram of figure 3 illustrates the spatial distribution of the axial or lineation surface strike and dip, rake, trend and plunge of fold-axes and deflection.

The seven possible combinations of at least three of these directional parameters, unequivocally defining a lineation, are listed in table 18.

Combinations including two compass measurements (i.e. 1 and 4) are systematically less accurate and, thereby, inadvisable.

Rake is the most sensitive measure of variations of a lineation on the lineation surface (Elliot, 1965, p.874). Moreover it is the only angle which can be evaluated directly using a protractor and consequently independent of a magnetic needle. A

Table 18. Minimum Complete Specification of any Lineation on a Lineation Surface (after Elliot, 1965).

	Lineation Surface		Lineation
1)	Strike and dip	....	Trend
2)	" " "	....	Rake (r)
3)	" " "	....	Plunge (p)
4)	Strike (S)	....	Trend and Plunge
5)	" "	....	Plunge and Rake
6)	Dip	....	Trend and Plunge
7)	"	....	Trend and Rake

combination including rake (i.e. 2,5 and 7) is, therefore, most suitable. Moreover on well-exposed lineation surfaces, clinometer measurements, depending on a bubble-level horizontal reference line, are less subjective when operated by superimposing the instrument on a definite lineation than manually determining the position of maximum slope by trial and error. Plunge is, in this respect, preferable to dip thus limiting the ideal combinations to number 5 alone (i.e. Strike (S), plunge (p) and rake (r)).

An additional advantage is represented by the very simple trigonometrical law which links these parameters to the deflection (d), facilitating their successive plotting on a structural map. If a (i,j,k) ternary system of Cartesian coordinates is selected, so that the strike of the lineation-surface S coincides with the i axis (fig. 23) and in this the lineation L is plotted a unity vector, the following geometric relation will be verified:

$$\cos\ (\text{deflection}) = \frac{\cos\ (\text{rake})}{\cos\ (\text{plunge})}$$

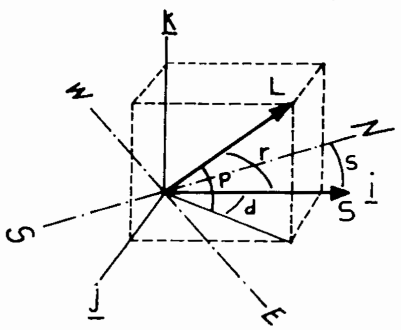

L = Lineation vector
S = Strike of lineation surface
s = Angle of Strike
p = " " plunge
r = " " rake or pitch
d = " " deflection
d±S= " " trend of lineation

Figure 23

Using the angle of strike (S) this (i,j,k) system can be orientated in the geographic graticule with the i-j horizontal plane. The trend of the lineation L on map will then be equal to s±d.

According to Elliot (1965) rake is accurately and easily measured if the lineation surface is fairly steep, whereas deflection (d) is more sensitive over wider areas and particularly when lineation-surfaces exhibit gentle dips.

In actual practice combination 5 is recommended whenever its parameters are exposed. Since this would be a minimum specification, additional measurements of dips of the axial or lineation planes and trend of the lineation could be added in order to supply geometric control to the three-dimensional picture of the tectonite defined by combination 5.

REFERENCES CITED

ATHERTON, M.P. (1965). The composition of garnet in regionally metamorphosed rocks. In: Pitcher, W.S. and Flinn, G.W. (eds.), Control Metamorphism, pp.281-291.

AUBOUIN, J. (1965). Geosynclines. Dev. in Geotectonics 1, Elsevier Publ. Co., Amsterdam, 335 p.

BADGLEY, P.C. (1965). Structural and tectonic principles. Harper and Row, New York, 521 p.

, PENTILLA, W.C. and TRIMBLE, J.K. (1960). Geologic aspects of fractured reservoirs. Unpubl. Pap. Ann. Mtg. Soc. Petrol. Engs. Amer. Inst. Min. Eng., Denver, Colorado.

BAILEY, E.B. and McCALLIEN, W.J. (1937). Perthshire tectonics: Schichallion to Glen Lyon. Trans. roy. Soc. Edinb. 50, pp.79-117.

BARKER, F. (1958). Precambrian and Tertiary geology of Las Tables Quadrangle, New Mexico. New Mexico Bur. Min. Miner. Res. Bull. 45, Socorra, New Mexico.

BARTH, T.F.W. (1959). Principle of classification and norm calculations of metamorphic rocks. J. Geol. 67, pp.135-152.

BEETZ, P.F.W. (1933). Geology of South West Angola, between Cunene and Lunda axis. Trans. geol. Soc. S. Afr. 36, pp.137-176.

BELOUSSOV, V.V. (1959). Types of folding and their origin. Int. geol. Rev. 1, pp.1-21.

(1963). Basic problems in geotectonics. McGraw-Hill Book Co. Inc., New York, 816 p.

BILLINGS, M.P. (1954). Structural geology. Prentice-Hall Inc., 514 p.

(1960). Diastrophism and mountain building. Bull. geol. Soc. Amer. 71, pp.363-398.

BINNS, R.A. (1964). Zones of progressive regional metamorphism in the Willyama Complex Broken Hill district, New South Wales. J. geol. Soc. Austr. 11, pp.283-330.

——— (1965). The mineralogy of metamorphosed basic rocks from the Willyama Complex Broken Hill district, New South Wales. Miner. Mag. 35, pp.306-326.

BIRCH, F. (1961). Role of fluid pressure in mechanics of overthrust faulting (discussion). Bull. geol. Soc. Amer. 72, pp.1441-1443.

BISSEL, H.L. (1959). Silica in sediments of the Upper Paleozoic of the Cordilleran area. In: Silica in Sediments, Soc. econ. Paleontologists Mineralogists spec. Publ. 7, pp.150-185.

BROWN, E.H. (1967). The greenschist facies in part of eastern Otago, New Zealand. Contr. Miner. Pet. 14, pp.259-292.

BUDDINGTON, A.F. (1963). Isograds and the role of H_2O in metamorphic facies of orthogneisses of the north-west Adirondack area, New York. Bull. geol. Soc. Amer. 74, pp.1155-1182.

BÜSCH, W. (1966). Petrographie und Abfolge der Granitisation im Schwarzwald, 5. Neues Jb. Mineral. Abh. 104, pp.190-258.

CAREY, S.W. (1954). The rheid concept in geotectonics. J. geol. Soc. Austr. 1, pp.67-117.

——— (1958). Continental drift: A symposium. Geol. Dept. Univ. Tasmania.

——— (1962). Scale of geotectonic phenomena. J. geol. Soc.India 3, pp.97-105.

CARPENTER, J.R. (1968). Apparent retrograde metamorphism: Another example of the influence of structural deformation on metamorphic differentiation. Miner. Pet. 17, pp.173-186.

CLARK, R.H. and McINTYRE, D.B. (1951). The use of the terms pitch and plunge. Amer. J. Sci. 249, pp.591-599.

CLARK, S.P. (1961). A redetermination of equilibrium relations between kyanite and sillimanite. Amer. J. Sci. 259, pp.641-650.

CLIFFORD, P. (1960). The geological structure of the Loch Luichart area, Rosshire. Q. J. geol. Soc. Lond. 115, pp.365-388.

CLIFFORD, T.N. (1960). Spessartine and magnesium biotite in coticule-bearing rocks from Mill Hollow, Alstead Township, New Hampshire, U.S.A.. Neues. Jb. Miner. Geol. Abh. 94, pp.1369-1394.

——— (1967). The Damaran episode in the Upper Proterozoic-Lower Paleozoic structural history of southern Africa. Spec. Pap. geol. Soc. Amer. 92, 100 p.

CONYBEARE, C.E.B. and CROOK, K.A.W. (1968). Manual of sedimentary structures. Bull. Bur. Min. Res. Geol. Geophys. Austr., Canberra 102, 327 p.

DANIELSSON, A. (1950). Das Calcit-Wollastonitgleichgewicht. Geochim. Cosmochim. Acta 1, pp.55-69.

DE MARTONNE, E. (1929). Traité de geographie physique. Librairie Armand Colin, Paris, 3 vols.

DE SITTER, L.U. (1956). Structural geology. McGraw-Hill Publ. Co. Ltd., London, 552 p.

DE VILLIERS, J. (1968). Ann. Rep. P.R.U. Dept. Geol., Univ. Cape Town, 6, (in press).

—— and SIMPSON, E.S.W. (1967). Late Precambrian tectonic patterns in south-western Africa. UNESCO-IUGS Symp. Cont. Drift, Montevideo, (in press).

—— and SOHNGE, P.G. (1959). The geology of the Richtersveld. Mem. geol. Surv. 48, Gov. Printer, Pretoria, 295 p.

ELLIOTT, D. (1965). The quantitative mapping of directional minor structures. J. Geol. 73, pp.865-880.

ENGEL, A.E.J. and ENGEL, C.E. (1958). Progressive metamorphism and granitisation of the major paragneiss, north-west Adirondack Mountains, New York : Part I. Bull. geol. Soc. Amer. 69, pp.1369-1414.

—— (1960). Progressive metamorphism and granitisation of the major paragneiss, north-west Adirondack Mountains, New York : Part II. Bull geol. Soc. Amer. 71, pp.1-58.

EVANS, B.W. (1965). Application of a reaction-rate method to the breakdown equilibria of muscovite and muscovite plus quartz. Amer. J. Sci. 263, pp.647-667.

FAIRBRIDGE, R.W. (1966). Phases of diagenesis and authigenesis. In: Larsen, G. and Chillingar, G.V. (eds.): Diagenesis in sediments. Elsevier Publ. Co., Amsterdam, pp.19-89.

FOLK, R.L. (1962). Spectral subdivision of limestone types. In: Ham, W.E. (Ed.), Classification of carbonate rocks. Mem. Amer. Assoc. Petrol. Geologists 1, pp.62-85.

FRETS, C.D. (1969). Geology and structure of the Huab-Welwitschia area, South West Africa. Bull. P.R.U. Geol. Dept., Univ. Cape Town, 5, 235 p.

FRIEDMAN, G.M. and SANDERS, J.E. (1967). Origin and occurrence of dolostones. In: Chillingar, G.V., Bissel, H.J. and Fairbridge, R.W. (eds.), Carbonate rocks. Elsevier Publ. Co., Amsterdam, A: pp.267-348.

FYFE, W.S. and TURNER, F.J. (1966). Reappraisal of the metamorphic facies concept. Contr. Miner. Pet. 12, pp.354-364.

——, TURNER, F.J. and VERHOOGEN, J. (1958). Metamorphic reactions and metamorphic facies. Mem. geol. Soc. Amer. 73, 259 p.

GALLITELLI, P. (1959). Elementi di mineralogia. Nistri-Lischi (eds.), Pisa, 650 p.

GEOLOGICAL MAP OF SOUTH WEST AFRICA, (1963). Gov. Printer, Pretoria.

GEVERS, T.W. (1931). An ancient tillite in South West Africa. Trans. geol. Soc. S. Afr. 34, pp.1-17.

—— (1932). Kaoko-eruptives and alkali rocks at Cape Cross, South West Africa. Trans. geol. Soc. S. Afr. 35, pp.85-96.

—— (1934). The geology of the Windhoek district in South West

Africa. Trans. geol. Soc. S. Afr. 37, pp.221-251.

——— (1936). The morphology of the western Damaraland and the adjoining Namib Desert of South West Africa. Trans. geol. Soc. S. Afr. 32, pp.111-149.

——— (1963). Geology along the north-western margin of the Khomas Highlands, between Otjimbingwe-Karibib and Okahandja, South West Africa. Trans. geol. Soc. S. Afr. 65, pp.199-258.

——— and FROMMURZE, H.F. (1929). The geology of north-western Damaraland, in South West Africa. Trans. geol. Soc. S. Afr. 32, pp.31-55.

GILLULY, J., WATERS, A.C. and WOODFORD, A.O. (1958). Principles of geology. Freeman & Co., San Francisco, 534 p.

GINSBURG, R.N. (1957). Early diagenesis and lithification of shallow-water carbonate sediments in south Florida. In: Le Blanc, R.J. and Breeding, J.G. (eds.), Regional aspects of carbonate deposition. Soc. econ. Paleontologists Mineralogists, spec. Publ. 5, pp.80-99.

GOLDSCHMIDT, V.M. (1921). Die Injektionsmetamorphose im Stavanger Gebiet. Skr. Vidensk. Selsk. Christ. 1, Mat.-naturv. Kl.10.

GREENWOOD, H.J. (1962). Metamorphic petrology: Metamorphic reactions involving two volatile components. Carneg. Instn. Wash. 61, pp.82-85.

GUJ, P. (1967). Structural geology of the Auas mountains Windhoek district, South West Africa. Ann. Rep. geol. Surv. S. Afr. (in press).

——— (1968). Preliminary report on the geology of areas 1913A&B and 1813C (Sesfontein Reserve, Kaokoveld, South West Africa). Ann. Rep. P.R.U. Dept. Geol., Univ. Cape Town, 6.

——— (1969). The springs of Sesfontein and Warmquelle, Kaokoveld, South West Africa. Unpubl. Rep. geol. Surv. S. Afr.

HALLER, J. (1956). Der zentrale metamorphe Komplex von NE Grønland, Teil I. Meddel. om Grønland 73.

HANDIN, J. and HAGER, R.V. Jr. (1957). Experimental deformation of sedimentary rocks under confining pressure : Tests at room temperature on dry samples. Bull. Amer. Assoc. Petrol. Geol. 41, pp.1-50.

———, HAGER, R.V., FRIEDMAN, M. and FEATHER, J.N. (1963). Experimental deformation of sedimentary rocks under confining pressure : pore pressure tests. Amer. Assoc. Petroleum Geologists Bull. 47, pp.717-755.

HARKER, R.I. and TUTTLE, O.F. (1955). Studies in the system $CaO-MgO-CO_2$; Part I. Amer. J. Sci. 253, pp.209-224.

HARRISON, J.V. and FALCON, N.L. (1934). Collapse structures.

Geol. Mag. 71, pp.529-539.

——— (1936). Gravity collapse structures and mountain ranges, as exemplified in south-western Iran. Q. J. geol. Soc. Lond. 92, pp.91-102.

HARTE, B. and JOHNSON, M.R.W. (1969). Metamorphic history of Dalradian rocks in Glens Clova, Esk and Lethnot, Angus, Scotland. Scott. J. Geol. 5, pp.54-80.

HARTNADY, C.J.H. (1969). Structural analysis of some pre-Cape formations in the Western Province. Bull. P.R.U. Geol. Dept., Univ. Cape Town, 5, 70 p.

HAUGHTON, S.H. (1969). Geological history of Southern Africa. The geol. Soc. S. Afr., 535 p.

HEARD, H.C. and RUBEY, W.W. (1966). Tectonic implications of gypsum dehydration. Bull. geol. Soc. Amer. 77, pp.741-760.

HEIM, A. (1932). Bergsturz und Menschenleben. Fretz & Wasmuth Verlag, Zürich, 218 p.

HERMANN, P. (1908). Beitrag zur Geologie von Deutsch-Südwestafrika. Mber. dt. geol. Ges., pp.259-298.

HILLS, E.S. (1963). Elements of structural geology. John Wiley & Sons Inc., New York, 483 p.

HODGSON, R.A. (1961). Regional study of jointing in Comb Ridge-Navajo Mountain area, Arizona and Utah. Bull. Amer. Ass. Petrol. Geol. 45, pp.1-38.

HOLLAND, J.G. and LAMBERT, R. St.J. (1969). Structural regimes and metamorphic facies. Tectonophys. 7, pp.197-217.

HSU, K.J. (1955). Granulites and mylonites of San Gabriel mountains, California. Univ. Calif. Publ. geol. Sci. 30, pp. 223-253.

——— (1969). Role of cohesive strength in the mechanics of overthrust faulting and of landsliding. Bull. geol. Soc. Amer. 80, pp.927-952.

——— (1969a). Reply to Hubbert, M.K. and Rubey, W.W. discussion. Bull. geol. Soc. Amer. 80, pp.955-960.

HUBBERT, M.K. and RUBEY, W.W. (1959). Role of fluid pressure in mechanics of overthrust faulting. Bull. geol. Soc. Amer. 70, pp.115-206.

JOHANNSEN, A. (1948). A descriptive petrography of the igneous rocks. Univ. Chicago Press,Chicago, Illinois, 4 vols.

JOHNSON, J.H. (1961). Limestone-building algae and algae limestones. Johnson, Boulder, Colorado, 297 p.

KAHLE, C.F. (1965). Possible role of clay minerals in the formation of dolomite. J. sediment. Pet. 35, pp.448-453.

KATZ, M.B. (1969). The nature and origin of the granulites of Mont Tremblant Park, Quebec. Bull. geol. Soc. Amer. 80, pp. 2019-2037.

KAY, H. (1951). North-American geosynclines. Mem. geol. Soc. Amer. 48.

KELLEY, V.C. and CLINTON, N.J. (1960). Fracture systems and tectonic elements of the Colorado Plateau. Univ. New Mexico Publ. Geol. 6.

KNILL, J.L. (1960). A classification of cleavages, with special references to the Craignish district of the Scottish Highlands. Int. geol. Congr. 21(18), Copenhagen, pp.339-364.

KORN, H. and MARTIN, H. (1959). Gravity tectonics in the Naukluft Mountains, S.W.A. Bull. geol. Soc. Amer. 70, pp.1047-1070.

KRÖNER, A. (1968). The gneiss-sediment relationships north-west of Vanrhynsdorp, Cape Province. Bull. P.R.U. Geol. Dept., Univ. Cape Town, 3, 233 p.

KRSMANOVIC, D. and LANGOF, Z. (1964). Large scale laboratory tests of the shear strength of rocky material. Felsmechanik u. Ingenieurgeologie, Suppl. 1, pp. 20-30.

KRUMBEIN, W.C. and SLOSS, L.L. (1963). Stratigraphy and sedimentation. Freeman, W.H. and Co., San Francisco, 497 p.

KUNTZ, J. (1913). Geologische Übersichtskarte des Kaokoveldes, (Deutsch-Südwestafrika) mit Karte 1:800,000. Z. prakt. Geol. 21.

LAMBERT, I.B., ROBERTSON, J.K. and WYLLIE, P.J. (1969). Melting reactions in the system $KAlSi_3O_8$-SiO_2-H_2O at 18.5 Kb. Amer. J. Sci. 267, pp.609-626.

LARSEN, G. and CHILLINGAR, G.V. (1967). Diagenesis in sediments. Elsevier Publ. Co., Amsterdam, 551 p.

LAUBSCHER, H.P. (1961). Die Fernschubhypothese der Jurafaltung. Ecl. Geol. Helvetiae 54, pp.221-282.

LE ROEX, H.D. (1941). A tillite in the Otavi Mountains, S.W.A. Trans. geol. Soc. S. Afr. 44, pp.207-218.

LEUBE, A. (1965). Report on the geology of the area west of Welwitschia and Fransfontein, South West Africa. Unpubl. Rep. geol. Surv. S. Afr., 36 p.

MABBUTT, J.A. (1952). The evolution of the middle Ugab valley, Damaraland, South West Africa. Trans. roy. Soc. S. Afr. 33, pp.333-365.

MacCARTHY, G.R. (1926). Colours produced by iron in minerals and sediments. Amer. J. Sci. 12, pp.17-36.

MARMO, V. (1967). On granites: a revised study. Bull. Comm. geol. Finl. 227, 83 p.

MARTIN, H. (1950). Südwestafrika. Geol. Rdsch. 38, pp.6-14.

——— (1965). The Precambrian geology of South West Africa and Namaqualand. P.R.U. Univ. Cape Town, Rustica Press, Wynberg, 159 p.

——— (1968). Paläomorphologische Formelemente in den Landschaften Südwestafrika. Geol. Rdsch. 58, pp.121-128.

——— (1969). Problems of age relations and structure in some metamorphic belts of southern Africa. Geol. Ass. Canad. spec. Num. 5, pp.17-26.

MASON, B.H. (1962). Metamorphism in the southern Alps of New Zealand. Amer. Mus. Nat. Hist. Bull. 123, pp.211-248.

MATHIAS, M. (1956). Petrology of the Messum igneous complex, South West Africa. Trans. geol. Soc. S. Afr. 59, pp.23-59.

MEHNERT, K.R. (1962). Zur Systemitik der Migmatite. Krystallinikum 1, pp.95-110.

(1969). Migmatites. Elsevier Publ. Co., Amsterdam, 393 p.

MELLIS, O. (1942). Gefügediagramme in stereographischer Projektion. Zeitschr. Miner. Pet. Mitt. 53, pp.330-353.

METZ, P.W. and WINKLER, H.G.F. (1963). Experimentelle Gesteimsmetamorphose-VII: Die Bildung von Talk aus kieseligem Dolomit. Geochim. Cosmochim. Acta 27, pp.431-457.

MISCH, P. (1964). Stable association wollastonite-anorthite, and other calc-silicate assemblages in amphibolite-facies crystalline schists of Nanga Parbat, north-west Himalayas. Beitr. Miner. Pet. 10, pp.315-356.

MIYASHIRO, A. (1953). Calcium poor garnet in relation to metamorphism. Geochim. Cosmochim. Acta 4, pp.179-208.

NEL, L.T. (1954). Ann. Rep. geol. Surv. Dept. Min. S. Afr. pp.141-142.

NEVIN, C.H. (1936). Principles of structural geology. John Wiley and Sons, New York, 348 p.

NEWTON, A.R. (1968). Correlation and nomenclature in the Precambrian. Trans. geol. Soc. S. Afr. Annex. 71, pp.215-224.

NORRISH, K. and HUTTON, J.T. (1969). An accurate X-ray spectrographic method for the analysis of a wide range of geological samples. Geochim. Cosmochim. Acta 33, pp.431-453.

NORTH, F.K. (1964). Gravitational tectonics. Bull. Canad. Petrol. Geol. 12, pp.185-225.

POTAPOV, I.I. (1960). Skhema Klassifikatsii tectoniche-skiku form. Sovetsk. geolog. 8, pp.66-74. (English Transl.: Int. geol. Rev., 1961, 3, pp.1168-1173).

POWERS, S. (1926). Reflected buried hills. Bull. Amer. Ass. Petrol.

Geol. 10, pp.422-422.

RABIE, L.P. (1954). Unpubl. Map Bethlehem Steel Corp.

——, BRANDT, J.W. et al. (1949). Unpubl. Maps and Rep. Kaokoveld Explor. Co.

RALEIGH, C.B. and GRIGGS, D.T. (1963). Effect of the toe in the mechanics of overthrust faulting. Bull. geol. Soc. Amer. 74, pp.819-830.

RAMSAY, J.G. (1963). Structure and metamorphism of the Moine and Lewisian rocks of the north-west Caledonides. In: Johnson, H.R.W. and Steward, F.H. (eds.), British Caledonides. Oliver & Boyd, Edinburgh.

—— (1967). Folding and fracturing of rocks. McGraw-Hill Book Co., 568 p.

RAST, N. (1958). Metamorphic history of the Schichallion Complex. Trans. roy. Soc. Edinb. 63, pp.413-427.

RODGERS, J. (1953). The folds and faults of the Appalachian valley and ridge Province. Southeastern Miner. Symp. 1950, Kentucky geol. Surv., Ser. 9, spec. Publ.1, pp.150-166.

SANDER, B. (1948). Einführung in die Gefügekunde der geologischen Körper, Teil 1, Springer Verlag, Vienna.

SCHALK, P.K. and HÄLBICH, I.W. (1965). The geology of the area around Windhoek, Rehoboth and Dordabis. Unpubl. Rep. geol. Surv. S. Afr.

SHATSKI, N.S. and BOGDANOV, A.A. (1959). Explanatory notes on the tectonic map of the U.S.S.R. and adjoining countries. Int. geol. Rev. 1, pp.1-49, (orig. Russian, 1957).

SHREVE, R.L. (1966). Sherman landslide, Alaska. Sci. 154, pp. 1639-1643.

—— (1968). The Blackhawk landslide. Geol. Soc. Amer. spec. Pap. 108, 47 p.

SIEDNER, G. and MILLER, J.A. (1968). K-Ar age determinations on basaltic rocks from South West Africa and their bearing on continental drift. Earth Plan. Sci. 4, pp.451-458.

SMIT, J.M.v.d.M. (1962). Stratigraphy and metamorphism of the Otavi Series south-east of Otavi, South West Africa. Trans. geol. Soc. S. Afr. 65, pp.63-78.

SMITH, D.A.M. (1965). The geology of the area around the Khan and Swakop Rivers in South West Africa. Mem. geol. Surv. S. Afr. 3 (S.W.A. Series), 113 p.

SÖHNGE, P.G. (1961). The geology of the Tsumeb Mine. Trans. geol. Soc. S. Afr. 64, pp.367-382.

SPRY, A. (1963). Chronological analysis of crystallisation and deformation of some Tasmanian Precambrian rocks. J. geol.

Soc. Austr. 10, pp.193-207.

——— (1969). Metamorphic textures. Pergamon Press, Oxford, 350 p.

SPÖRLI, B. (1968). Syntectonic dolomitisation in the Helvetic nappes of Central Switzerland. Bull. geol. Soc. Amer. 79, pp.1839-1846.

STAHL, A. (1926). Geologische Grundzüge des nördlichen Südwestafrika und Erzlagerstätten des Otaviberglandes. Z. prakt. Geol. 34, pp.145-160.

——— (1940). Die Otaviformation des Etoschabogens, (Südwestafrika). Beitr. geol. Erf. Dtsch. Schutzgeb. 22, pp.1-66.

STILLE, H. (1940). Einführung in den Bau Nordamerikas. Borntraeger, Berlin, 717 p.

SUTTON, J. and WATSON, J. (1951). The pre-Torridonian metamorphic history of the Loch Torridon and Scouric areas in the northwest highlands. Q. J. geol. Soc. Lond. 106, pp.241-307.

TURNER, F.J. (1968). Metamorphic petrology. McGraw-Hill Book Co., New York, 403 p.

——— and WEISS, L.E. (1963). Structural analysis of metamorphic tectonites. McGraw-Hill Book Co. Inc., 545 p.

TRÜMPY, R. and HERB, R. (1962). Eastern and northern Alps. In: Lombard, A. (ed.), Guidebook for the international field institute, Alps. Rep. Amer. geol. Inst., pp.86-130.

TYRRELL, G.W. (1926). Principles of petrology. Methuen & Co., London, 349 p.

VAN BEMMELEN, R.W. (1960). New views on east-Alpine orogenesis. Rep. 21st Sess. Int. geol. Cong. 18, pp.99-116.

VELDE, B. (1964). Low-grade metamorphism of micas in pelitic rocks. Carneg. Instn. Wash. Yearb. 63, pp.142-147.

VERWOERD, W.J. (1964). Stratigraphic classification: A critical review. Trans. Proc. geol. Soc. S. Afr. 67, pp.263-286.

VISTELIUS, A.B. (1966). Structural diagrams, (translated from Russian). Pergamon Press, Oxford, 178 p.

VON ENGELHARDT, W. (1961). Zum Chemismus der Porenlösung der Sedimente. Bull. geol. Inst. Univ. Uppsala 40, pp.189-204.

VON PLATEN, H. (1965). Experimental anatexis and genesis of migmatites. In: Pitcher, W.S. and Flinn, G.W. (eds.), Controls of metamorphism. Oliver & Boyd, Edinburgh, pp.203-218.

WENK, E. (1962). Plagioklas als Indexmineral in den Zentralpen. Schweiz. Miner. Pet. Mitt. 42, pp.139-152.

WERNER, F. (1961). Zu Verkittungsvorgaengen an Psammiten. Geol. Rdsch. 51, pp.507-517.

WHITTEN, E.H.T. (1966). Structural geology of folded rocks. Rand McNally & Co., Chicago, 663 p.

WILLIAMS, H., TURNER, J.F. and GILBERT, C.H. (1954). Petrography. Freeman, W.H. & Co., San Francisco, 406 p.

WINCHELL, N.H. and WINCHELL, A.N. (1927). Elements of optical mineralogy. Wiley J. and Sons Inc., New York, 2 vols.

WINKLER, H.G.F. (1967). Petrogenesis of metamorphic rocks. Springer-Verlag. Berlin, 237 p.

——— and VON PLATEN, H. (1957-62). Experimentelle Gesteinmetamorphose: I-VI. Geochim. Cosmochim. Acta 13 (1957), pp. 48-69; 15 (1958), pp.91-112; 18 (1960), pp.294-316; 24 (1961), pp.48-69, 250-259 and 26 (1962), pp.145-180.

ZEN, E-an (1960). Metamorphism of lower paleozoic rocks in the vicinity of the Taconic range in West-central Vermont. Amer. Mineralogist 45, pp.129-175.

ZWART, H.J. (1961). The chronological succession of folding and metamorphism in the Central Pyrenees. Geol. Rndsch. 50, pp. 203-218.

——— (1962). On the determination of polymetamorphic mineral associations and its application to the Bosost Area (Central Pyrenees). Geol. Rndsch. 52, pp.38-65.

STRUCTURAL SECTIONS

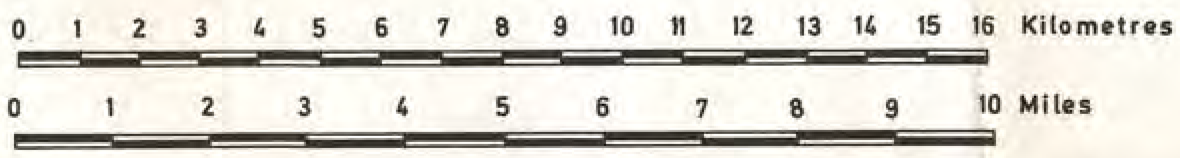

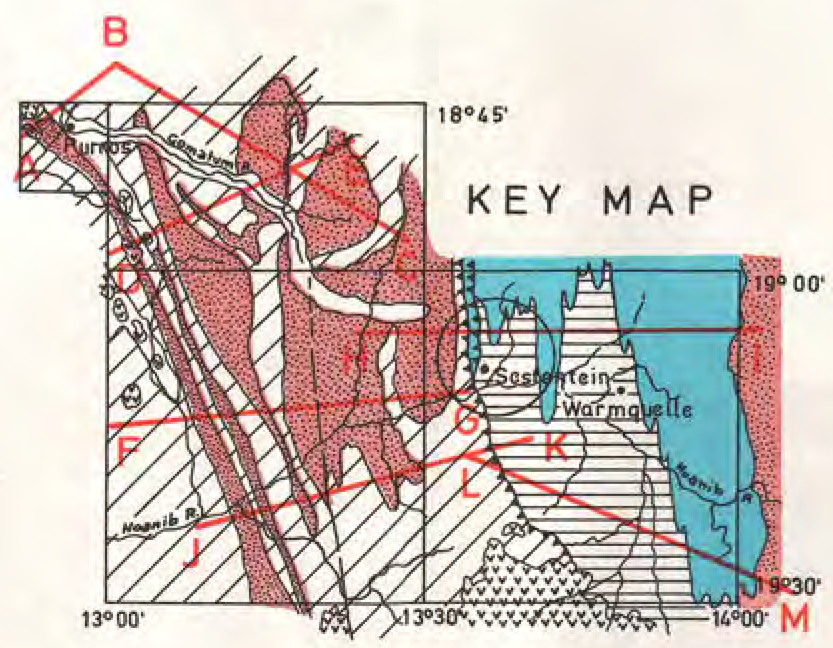

SECTIONS EXTEND ACROSS ADJOINING SHEETS. SEE KEY MAP.

VERTICAL SCALE = HORIZONTAL SCALE. ALTITUDES IN METRES.

GOTHIC

SHEET 1813 C

GOMATUM

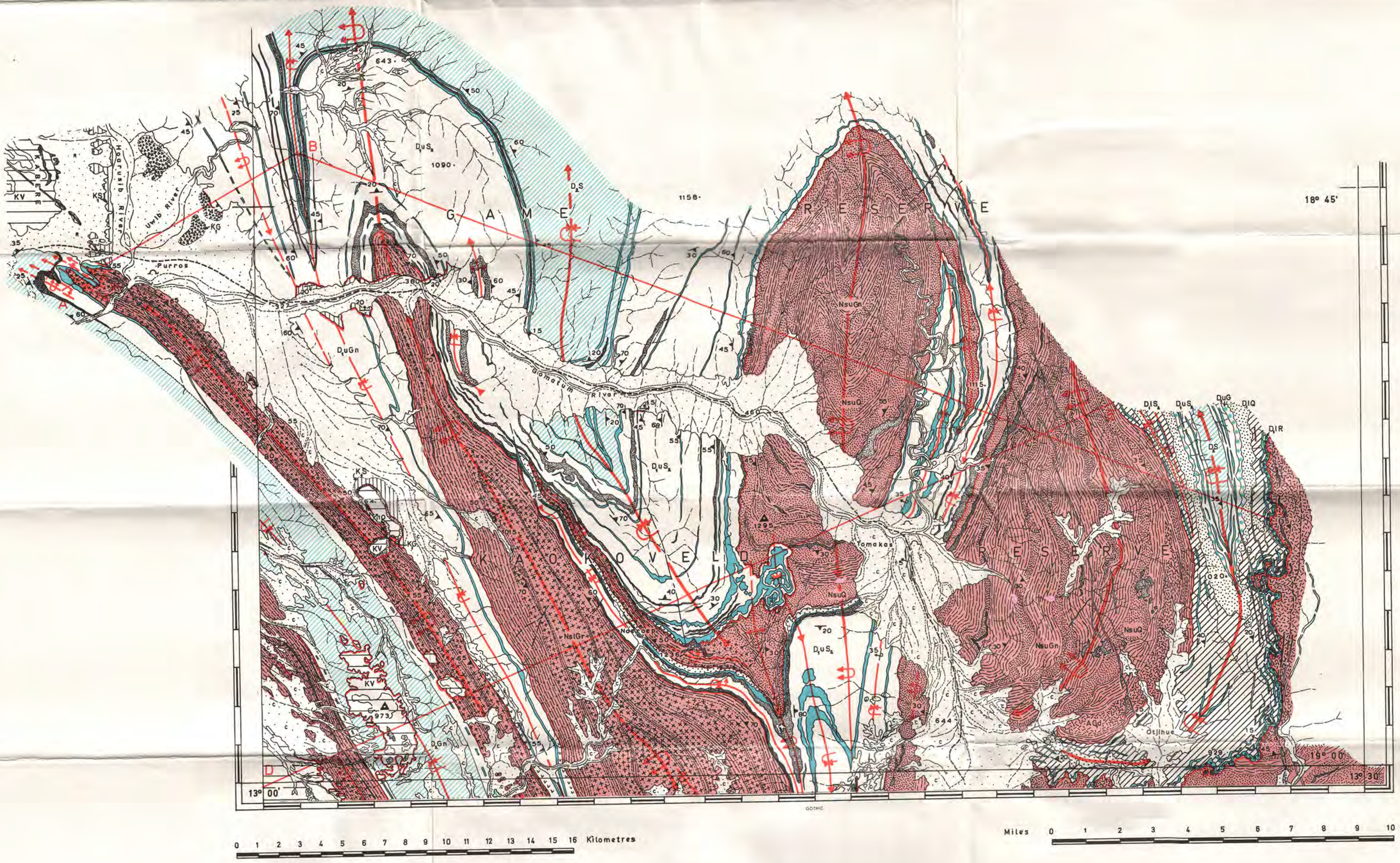

GEOLOGICAL SHEETS 1813 C - 1913 A - 1913 B

SURVEYED AND DRAWN BY P. GUJ (1969)

LEGEND

GOMATUM - HOANIB - SESFONTEIN AREA

KAOKOVELD, SOUTH WEST AFRICA

- Track
- Stream (1), pan (2)
- Settlement (1), vegetable garden (2)
- DRIES 1176 — Trigonometrical beacon with altitude in metres
- Horizontal (1), inclined (2), vertical (3) and inverted (4) bedding
- Slaty cleavage
- Horizontal (1), inclined (2) and vertical (3) foliation
- U — Unconformity

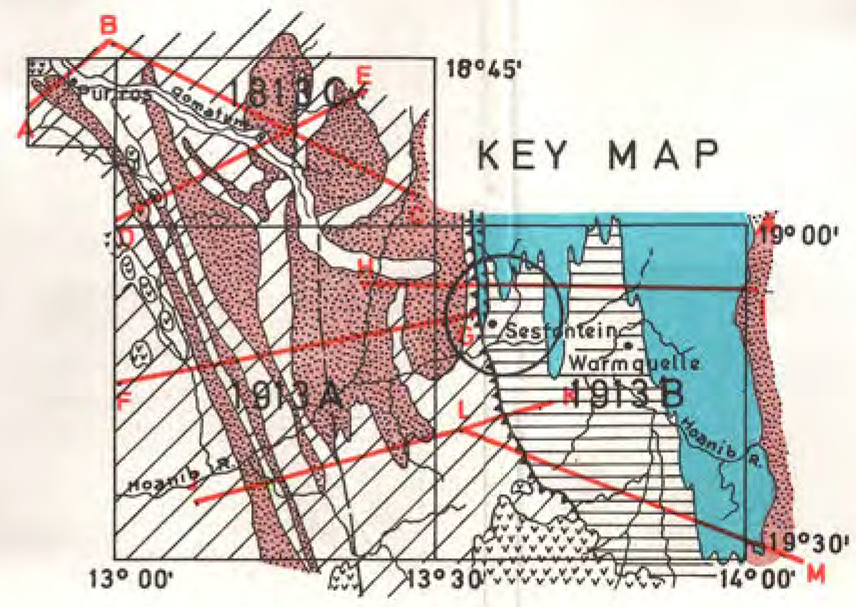

- D P — Disconformity (D) or paraconformity (P)
- Upright to inclined (1), overturned (2) anticline, axial-plane dip (3), plunge (4)
- Upright to inclined (1), overturned (2) syncline
- Anticlinorium (1), synclinorium (2): nappe
- Normal fault
- Wrench fault
- Thrust (1), intense shearing and syntectonic dolomitisation (2)
- A — B Trace of section
- Structural form-lines

SCALE (ALL MAPS AND SECTIONS)

0 1 2 3 4 5 6 7 8 9 10 11 12 13 14 15 16 Kilometres

0 1 2 3 4 5 6 7 8 9 10 Miles

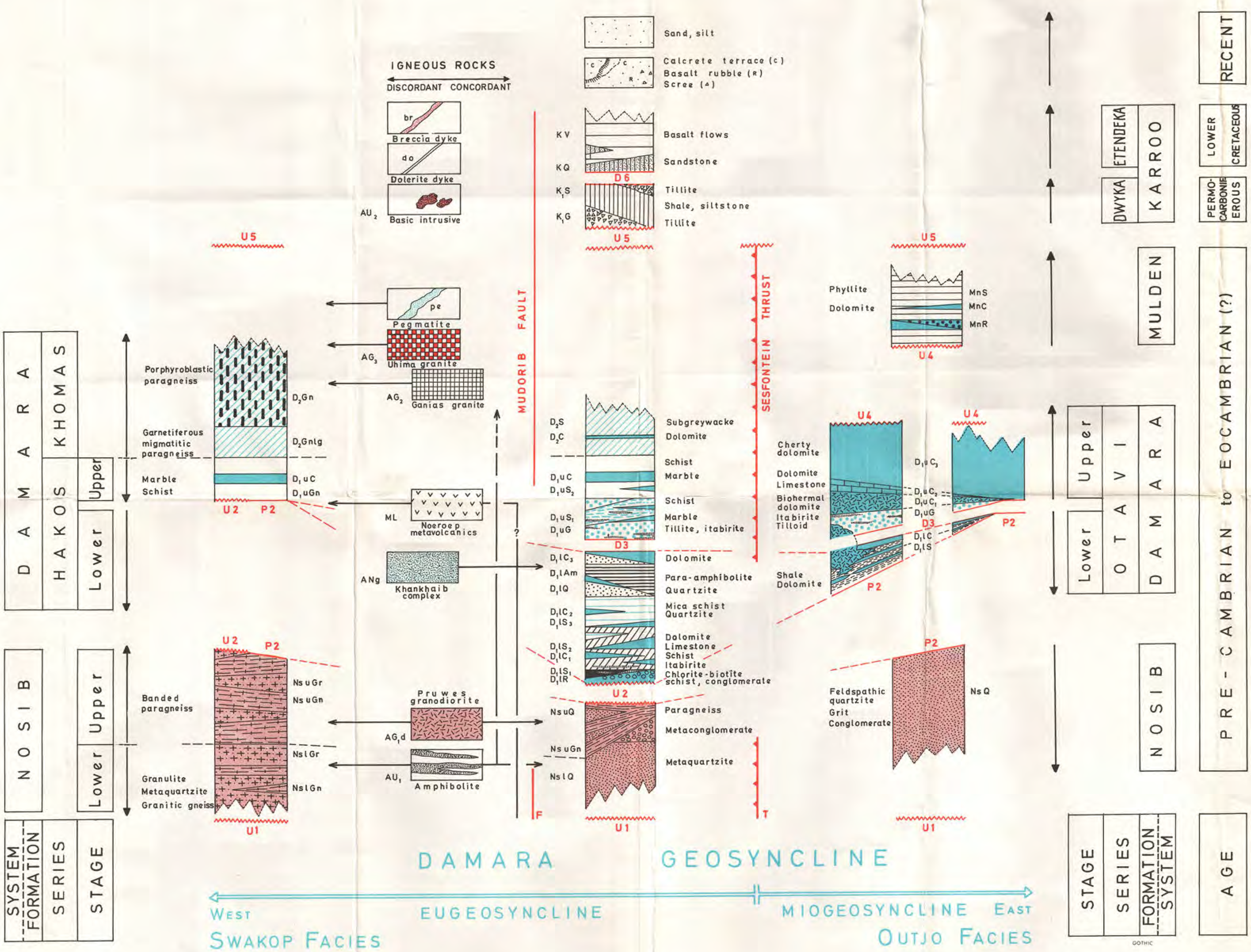

SHEET 1913 A

HOANIB

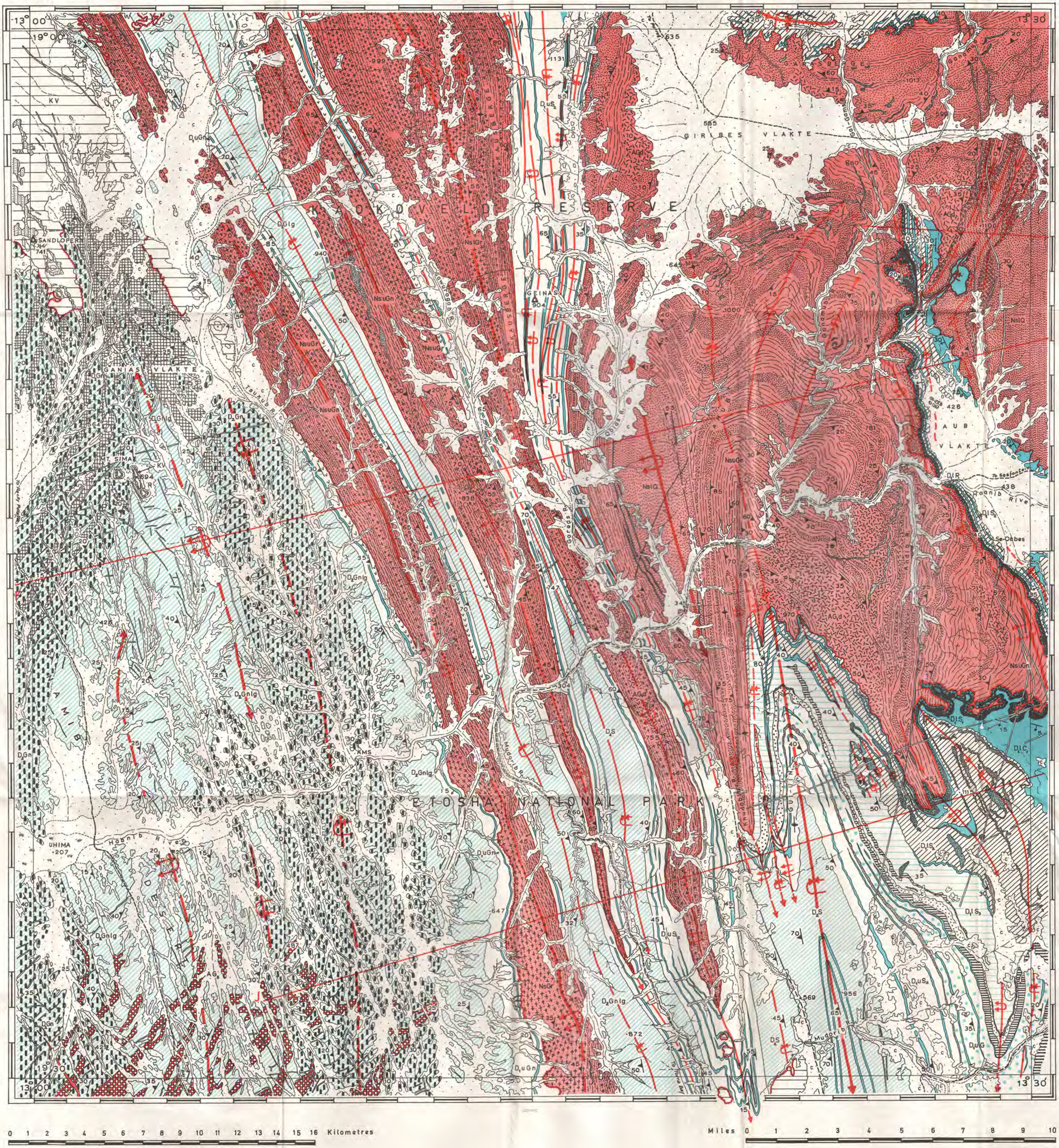

SHEET 1913 B

SESFONTEIN